THE FORMATION, ASSESSMENT AND APPLICATION

OF PRECISION SURFACES

by

Gholam-Hassan Hemmaty, B.Sc., M.Sc.

A THESIS SUBMITTED AS PARTIAL REQUIREMENTS
FOR THE DEGREE OF DOCTOR OF PHILOSOPHY (C.N.A.A.)

Leicester Polytechnic

September 1988

SUMMARY

The Formation, Assessment and Application of Precision Surfaces

G. H. Hemmaty

This work investigates formation of precision surfaces by grinding and abrasive processes and their subsequent functional behaviour during running-in under marginal lubrication and levelling during electroplating. Techniques of surface assessment and characterisation using stylus profilometry is discussed. Slope parameters which have been neglected in the past have been shown to be a particularly useful predictor of surface behaviour.

It is suggested that the reduction in wear rate observed in abrasive processes is mainly due to formation of flat lands on grits. A theory has been developed taking into account the area of these flats which results in considerable improvement in wear prediction. Using a single grit approach, a mathematical model is also obtained for R_a and compared with the experimental data using percentage of zero slope to represent the area of flats.

Grinding process and significance of dressing is discussed, it is shown that both micro-milling and abrasive wear approaches to grinding converge to the same results. By applying the abrasive wear model to a grinding situation a model is derived to predict the normal grinding force and its changes by dulling of the grains. Grinding experiments were performed and the results are compared with the model.

The functional behaviour of ground surfaces during running-in has been investigated. An experimental pin and ring test rig interfaced with a digital computer was used which confirmed that the wear prior to running-in is related to initial R_a. It is further shown, however, that this dependence is conditioned by other surface characteristics and in particular the "area of zero slope".

Finally, a number of computer models have been developed to give a graphic simulation of the changes in surface topography associated with electrochemical processes. It is suggested that the variation in levelling performance can be explained in terms of a levelling (plating) coefficient.

ACKNOWLEDGEMENTS

The author wishes to express his deep gratitude to Dr. T.C. Buttery of Leicester Polytechnic for his valuable supervision and continuous encouragement and support throughout this project.

Acknowledgement is additionally due to Rod Coppell and other members of the staff at Leicester Polytechnic for their practical assistance and advice.

Finally, I wish to thank Mrs Angie Hing and Mrs Valerie French for the typing of this thesis.

CONTENTS

CHAPTER ONE

SURFACE CHARACTERISATION

Chapter 1 - Surface Characterisation

1.1 Introduction

Recent years have seen a growing expansion in measurement and assessment of surface characteristics. The manufacturing industries spend considerable time and effort on the production of suitable surface finishes for consumer products, engineering products and components. Two pressures have been dominant. First, there is the need to improve control of the manufacturing process and second, there has been the need for a better understanding of the role which the geometry of a part plays during its working life. More recently, the replacement of operators by robots in remote manufacturing and the necessity for controlling the manufacturing costs have made it preferable that exact finish requirements be specified on the drawing board.

Whitehouse (1974) mentions three major developments in surface metrology:

1. an increase in the use of digital techniques.
2. development of surface metrology instruments having more than one accurate degree of movement.
3. the use of relocation profilometry.

The driving force behind these developments has been the need for a better understanding of the characteristics of surface geometry. Surface geometry is generally divided arbitrarily into different

classifications according to its scale. Consideration of the manufacturing processes reveal that there are four orders of geometrical irregularities which are recognized in standards (BS 1134 : 1972). These are:

First order. Those arising out of inaccuracies in the machine tool, deformation of the work under the cutting forces, or the weight of the material itself.

Second order. Those caused by vibrations of the machine or workpiece (for example, chatter marks).

Third order. Those caused by the machining itself and characteristics of the process.

Fourth order. Those arising from the rupture of the material during the chip removal.

In practice, it is accepted that the first and second orders of irregularities produce waviness, while the third and fourth orders produce true surface roughness. It usually happens that a surface consists of many different wavelengths, some resulting from the feed of the tool and others caused by the actual cutting action. In addition there may be others produced by vibration. The complete texture of the surface may thus be very complex and in general it is not possible to separate each contributing cause by instrument.

1.2 Formation of Surfaces

The surfaces found in modern engineering may show the marks of any of a great variety of formative processes. Sometimes they are left with the texture created by a major operation which formed the bulk shape: milled, rolled, extruded and cast surfaces are common. However, when a surface is intended to interact with another solid, for example in sliding contact, it is often prepared with a further treatment which affects the surface layer only, e.g. plating which adds material and grinding in which material is removed from the surface.

The texture of the surface is the result of a very large number of separate events, each affecting only a small region of the surface (such as deposition of an ion in plating or a single contact with a grit in grinding). Williamson et al (1969) consider the elemental mechanism of the common techniques of preparing surfaces and show that they can be divided into three broad categories: cumulative (in which the shape of every small region is the cumulative result of all the events happening over that area) such as plating, extreme value e.g. grinding (the final surface reflects only the most extreme of the events which occurs at each point) and transitional where the surface shows the evidence of more than one preparation process. Plateau honing is an example of a secondary (finishing) process showing the effects of two machining processes. Light wear "running-in" is another example which frequently occurs in engineering.

The "transitional" topography can be thought of as being in two parts: a lower section, which is the original topography unchanged, and an upper one which reflects the secondary process. Pure surface texture in which every part of the surface has been created by the same process occurs only when a treatment acts on the entire surface and also obliterates the marks of all previous treatments. Depending on the tribological situation the behaviour of such a "composite" surface may be determined predominantly by either of the surface 'strata'. The entire complexity of surface is presented by "surface texture". It is those irregularities with regular or irregular spacing which tend to form a pattern or "texture" on the surface.

1.3 Surface Examination Methods

The techniques of surface measurement can be divided into two main groups:

1. Contacting (stylus) methods.
2. Non contacting methods.

The development of contacting methods goes back some fifty years when the German engineer Gustav Schmalz produced some profile graphs of roughness texture (Reason, 1979). Electrical capacitance and pneumatic devices, both of which involve contact with

surface but not movement across it received early attention, Graneek et al (1952) and Sherwood et al (1967-68). Devices of this nature have difficulty in distinguishing between the effect of roughness and the changes in overall curvature. Some successful non-contact methods have also been developed,e.g.a small spot of light to trace the surface instead of stylus, oblique sectioning and non contact assessment based on optical diffusion have attracted a number of workers, Trumpold (1967), Rabinowicz (1950) and Church (1979).

A number of these techniques are briefly explained here. It is worth mentioning that some of these methods give quantitative measures of surface finish whereas others provide purely qualitative assessment.

1.3.1 Air Gauging

In this method the rate of flow of air between a gauge head and the specimen surface is an index of the surface finish. The gauge head may be formed to match the form of the specimen surface. The pressure measured in the gauge head is a function of the flow of escaping air around its rim and therefore a measure of the texture of a narrow band of the surface in the shape of the gauge head. This method is not suitable for a detailed computerized assessment of surface geometry, but is well adapted for use on a production line. Also there are difficulties in distinguishing between the effects of roughness and longer wavelength effects such as overall specimen curvature to which the gauge is very sensitive.

1.3.2 Capacitance Method

The capacitance between two conducting surfaces is directly proportional to their area and the dielectric constant of the medium between them and inversely proportional to their separation. If a rough surface is regarded as the sum of a number of small elemental areas at different heights it is fairly easy to work out the effective capacitance between it and a smooth detector. Sherwood et al (1967/68). For a rough surface with random height distribution p(z) the value of capacitance would be proportional to

$$\int_{-\infty}^{+\infty} \frac{P(z)dz}{h-z}$$

where h is the separation of the mean plane.

An instrument for measuring surface roughness based on a capacitance principle has recently become commercially available. Fromson et al (1976).

1.3.3 Optical Reflectivity

This method of measurement attempts to quantify surface finish by means of measurements of diffuse and/or specular reflection of light from the specimen surface. Instruments providing a single numeric measure on this basis are often termed 'glossmeter'.

More recently, the increased availability of low powered lasers has generated a lot of interest in optical surface finish assessment techniques. In some applications like wood machining, with its high level of vibration, the in-process monitoring of surface quality using stylus instruments is impossible; their response (400 Hz bandwidth) would be inadequate to track surface profiles traversing at 140m/min as the required bandwidth is 2.3KHz for 1mm wavelength. A fast-response, non-contact method of measuring is required. The technique currently being investigated and showing much promise, is the use of laser light to highlight the apexes at the intersection of the surface arcs, Maycock (1986). A broad beam of laser light is directed at grazing incidence (θ<1.5 degree) to the surface being machined, and in the same plane as the traversing workpiece. This has the effect of highlighting the leading slope of each cusp in the beams path and produces a pattern of light and dark on the surface of the workpiece. This pattern which contains the periodic information of interest, is traversed past a single photodiode. The output voltage is sampled, digitised and stored in a computer memory for subsequent analysis. The data captured is not prone to distortion due to vibration as the plane of vibration is almost perpendicular to the broad incident beam.

1.3.4 Electron Microscopy

This technique offers very high magnification of the horizontal scale. In transmission electron microscopy direct examination of

surface is not possible. This introduces uncertainty as to the fidelity of the image which is also difficult to interpret. Reflection electron microscopy allows direct surface examination but as with transmission microscope have limited depth of field. The more recently developed scanning electron microscope is a reflection instrument with great depth of field and is thus more suited to metal surface examinations.

1.3.5 Taper Sectioning

This involves cutting through the specimen at a shallow angle to the surface. The section is polished and examined microscopically. The result is a profile with a vertical scale exaggerated. The technique has the disadvantage of being destructive and also the picture seen is not a true section but is in effect an integration over a final length of the surface at right angles to the section, hence features of small scale may be ignored or distorted. The method also has the same criticisms of a single stylus trace.

1.3.6 Profile Examination by Stylus Technique

This is the principle of operation of a widely used class of surface measuring instruments. A fine stylus is drawn at a constant speed over an irregular surface and the variations of its vertical displacement with time will represent the variation of height of a section of the surface with horizontal displacement. As the average

slope of surface is small, the vertical movement of the stylus requires some amplification. In the early stylus instruments this was achieved by means of a mechanical linkage. In modern versions the amplification is electrical. The stylus is attached to a transducer, a resonating piezo-electric crystal whose natural frequency is modulated by the vertical motion. The signal generated by the transducer is proportional to the instantaneous difference in height between the stylus and some reference datum. This may be fixed, as an accurately flat or curved gauge along which the pick-up is constrained to move, or it may be relative, in the form of a skid or shoe which travels over the surface before or behind the stylus. The disadvantages of the stylus instruments are its bulk, complexity, relative fragility, high initial cost and the limitation to a single section of a surface at any given time. The single advantage which outweights all these is the availability of an electrical signal, which can be subjected to all the conditioning processes of modern electronics to yield any desired parameter. Information in this form is also suitable for acceptance analysis by computers. Radhakrishnan (1971).

1.4 Surface Measurement by Stylus

Stylus profilometry has become by far the most commonly employed technique for surface topography examination. In early instruments the stylus was often a phonograph needle (Abbott and Goldschmidt, 1937). These were too large and heavily loaded. Diamond styli are now universally employed. They are usually cones

of 90° included angle and tip radius of 4-12μm. A truncated pyramid with 90° included angles between opposite surfaces however has been used by Taylor and Hobson manufacturers (fig.1.1).

Although these two types of styli appear to be quite different, in practice, due to wear in use their differences can become almost negligible. The slope of most real surfaces are so gentle that the penetration of valleys is not usually a problem.

The vertical movement of stylus is translated by a transducer to an electrical signal. Moving coil transducers have sometimes been used, but their output depends on the velocity of the stylus rather than its position and must be integrated to give an amplitude. Most widely used, is a linear variable differential transformer (LVDT). The movement of stylus causes a differential change in the air gap of a pair of coils, causing a differential change in the air gap which forms part of the magnetic circuit of the coils. This causes a differential change in the inductance depending on the position of stylus (fig.1.2). The change in inductance alters the output of a bridge circuit excited by an oscillator at a frequency much higher than the maximum anticipated frequency of stylus displacement. The carrier frequency must subsequently be removed from the signal by demodulation.

1.4.1 Reference Line

Analysis of the surface profile requires preprocessing of the

signal which is contaminated with the set-up errors. The roughness component of the surface is then required to be extracted from this signal. This involves positioning in some ways a reference line within the profile from which the roughness parameters can be measured to the exclusion of all else. In the case of roughness measurement for instance, the tilt of the part, error of form and the waviness would have to be removed.

Schmalz conceived the reference as a straight line engaging the lowest valleys so that the irregularities appeared as hills rising above it. Hence it became usual to speak of the height of the irregularities (Reason, 1979). Some of the reference lines used today are polynomials, mean line, filter line and envelopes. A best fit straight line for instance has been used to remove the tilt by Whitehouse (1974).

The M- or mean line system is now specified in most national profile standards. It is defined as a line parallel to the geometrical profile such that the area of solid above it is equal to the area of void below it. Alternatively, it is a line parallel to the geometrical profile such that the sum of squares of the deviations from it of the effective profile is a minimum. To eliminate the effect of secondary texture the profile is split into a number of "sampling lengths" for each of which a separate mean line is computed. The mean lines of adjacent sampling lengths need not meet. The sample length is described as just that length of surface over which a meaningful reading can be made. A typical value often used is 0.8mm (0.03 in). Usually about five consecutive sample length are traversed by commercial instruments to get a good average.

In the E- or envelope system proposed by Weingraber (1957) and others the reference lines are defined by the loci of centers of circles of different radii rolled along the profile. These produce the contacting profile (smaller circle) and curve of form (larger circle). The contacting profile and curve of form can be obtained mechanically by using skids of appropriate shape.

1.4.2 Filtering

Fundamentally the centre line is a graphical method. Instrumentally a similar effect is achieved by passing the profile signal through a high-pass 2-CR filter, whose cut-off is nominally equal to sample length. Filtering is now the most common preprocessing technique and most instruments use a standard filter which has 75% transmission at the cut-off. The waviness separation can be changed by altering the cut-off. In the E-system this is achieved by changing the skid radius.

Although the accepted graphical and electrical methods of determination of the mean line are nominally equivalent, the difference in the shape of their mean lines, the one straight and the other tending to undulate, can lead to residual differences in Ra and other parameters. These are generally small however and are sometimes referred to by the term "method divergence".

The problem often encountered in practice is in fixing a value which decides the boundary between the roughness and waviness.

Frequency selective filtering is used to remove some components of the profile. This could be done on the basis of assumption about their source of origin, e.g. in studying the nature of the grinding process, frequency components in the range comparable with the vibration frequency of the machine may mask the effects of cutting and rubbing action of the grits and therefore may be removed. It should be noted, however, that this makes the parameter values derived from the filtered profile dependent on the transmission characteristics and cut-off of the filter used. Since the frequency spectra of different aspects and mechanisms usually overlap, the problem arises when distinguishing between these profile components on a purely frequency selective basis and some vital information may be removed during filtering.

The characteristic of a high-pass analog filter poses another problem in this respect. Ideally the filter should transmit without attenuation all sinusoidal components of the waveform with wavelengths less than the sampling length and should then rapidly attenuate to those of greater wavelengths. Simple filters, however, tend to attenuate gradually, the attenuation being independent of amplitude. This is accompanied by a phase shift of the low frequencies relative to the high frequencies which leads to distortion of the waveform. Analogue filters with sharper cut tend to distort the phase around the cut-off even more.

To overcome these problems, an improved type of filter with good amplitude and phase characteristics was developed by

Whitehouse (1967-68) for analysis of surface profiles. This filter has not been used, however, because of practical problems in implementation. Shunmugam et al (1976) presented a method based on fitting single frequency sinusoidal curves to the profile which is independent of the instrument characteristics.

One of the important benefits of using digital computers in surface assessment has been the increase in the accuracy using digital filter rather than analogue which does not rely on the accuracy of the equipment.

1.4.3 Defects of Stylus Method

Some of the sources of error inherent in the stylus technique are mentioned briefly.

- Effect of stylus size.

Since stylus tip is of a finite dimension it fails to follow peaks and valleys faithfully and hence produces a distorted record of the surface. The so called "effective profile" (BS 1134 : 1972) recorded by the stylus will be the locus of some point on the stylus. It would seem therefore that a profile containing many peaks and valleys of radius of curvature smaller than the stylus tip or many slopes steeper than 45° would be likely to be significantly misinterpreted by a stylus instrument with 90° included angle.

Thomas and Sayles (1978) show, however, that the spectral density of many machined surfaces falls off as the square of the

wavelength. The roughness associated with smallest and shortest features is therefore a negligible fraction of the total measured roughness.

- Effect of stylus load.

Although stylus load is small, not more than 70mg force for the finest stylus (ISO 3274) the area of contact is also small and the local pressure may be sufficiently high to cause significant local elastic downward or plastic deformation of the surface being measured.

The stylus generally does make a visible scratch. It is believed, nevertheless that this is acceptable. Williamson (1967-68) in a series of careful experiments could find no evidence of stylus measurement being affected by plastic deformation. Nakamura (1966) has considered the effect of stylus geometry on its dynamic response. His results indicate that with typical surface conditions the errors incurred are negligible.

Another possibility of error lies in the lateral deflection of the stylus by asperities. A deflection of up to 1μm has been reported by Agullo and Pages-Fita (1974). Nevertheless the standard Talysurf stylus with a tip of 8μm makes this kind of error negligible.

- Effect of skid.

For many purposes and particularly at high vertical magnifications, a skid is used. The transducer in this case does not give the instantaneous height difference between the stylus and the datumn,

but the difference in level between the stylus and the skid. The skid itself can damage the surface. Here the same argument can be applied as in the case of stylus deforming the surface. The amount is usually so small that it seems unlikely to be an important source of error on hard surfaces. More importantly, the skid acts as a mechanical high-pass filter. This has two consequences. Firstly, information about longer wavelengths is lost and if these wavelengths are relevant to the problem under investigation then a skid must not be used. Secondly, the skid introduces a phase lag which might be supposed to distort the appearance of the surface. Reason (1944).

Experiments suggest, however, that this distortion is not obtrusive Nara (1966). His results also suggest that mechanical filter has quite a sharp cut-off and that the power spectrum, which of course contains no phase information, is relatively unaffected at shorter wavelengths (fig.1.3).

More recently Ishigaki and Kawaguchi (1981) studied the effect of skid theoretically. They concluded that the effect of skid can be expressed by a function of the tip radius of the skid and that the effect of skid for unidirectional surface roughness is larger than that for a non-directional surface roughness.

1.5 Application of Digital Computers in Surface Assessment

Exploitation of digital computers in profilometry has created a revolution in measurement and analysis of surface characteristics.

Computerising the measuring process allows any parameter of the surface texture to be checked in a fraction of time that was required by earlier generations of the measuring instruments with their more limited electronics. The major disadvantage with analogue computers is that they are not capable of differentiating the profile accurately. There is evidence that the first and second derivatives are important in determining the nature of problems like contacting surfaces and wear process, Archard (1961) and Greenwood and Trip (1965). With digital computation facilities any parameter may be evaluated providing realistic formulae are available. The system is much more versatile and it is possible to reprocess the data to give a number of surface parameters. Figure 1.4 shows a computerized surface measuring equipment, Kaliszer et al (1972). Many of the functions previously carried out by conventional mechanics or the operator may now be taken over by computer, for example filtering, magnification and switching. By minimizing the number of operator interventions and adjustments, the system further increases the accuracy of the measurement.

Amongst the first experimenters to use the digital method in the early 1960's were Greenwood and Williamson (1966) who were able to show that many surfaces had a distribution of height and peak values which were nominally Gaussian.

The increasing dependence of surface roughness analysis upon digital computation causes a consequential need to specify conditions for digitizing the data. Mathematical models of surfaces have

suggested that the values of many parameters of tribological significance will vary with the sampling interval. Whitehouse and Archard (1970).

Some of the problems involved in digital assessment of surface profiles are listed here.

1. Sampling.

The first consideration in sampling is the frequency content of the waveform to be digitized. If the highest frequency is f, then according to Nyquist the minimum rate of sampling to completely define the waveform is 2f. Under these conditions the samples are uncorrelated. In practice no signal cuts-off sharply at a frequency f, so that the usual procedure is to sample at about three times faster than the smallest wavelength likely to be of interest.

Sampling too often results in highly correlated and redundant information, whereas sampling too rarely can result in aliaising which basically means that frequencies in the waveform higher than the sampling frequency can actually appear to be low frequencies. Aliaising can be removed either by sampling faster or by smoothing the data prior to evaluation usually by high-cut filtering. The latter solution is preferred although it is important to know where to position the filter cut, Whitehouse (1974).

In surface texture measurement, the signal representing the roughness waveform has already been smoothed relative to the true surface profile because of the finite tip of the stylus which act as a

mechanical filter. So the problem of trying to decide the highest frequency present in the waveform has, to some extent already been solved before the digitisation.

In practical instruments, the tip of the stylus is about 2.5μm which implies that sampling should take place at about every one micrometre. If flaws or freak events such as maximum peaks are being looked for, then this must be the order of sampling, but if only averaging parameters are being assessed, then about 5μm is good enough.

2. Quantisation.

This refers to the accuracy to digitisation of each individual measurement. In a typical analogue to digital convertor four or five decimal places are usually used, but the accuracy ultimately depends on the input. Errors produced by other effects have usually been larger than these quantization errors.

1.5.1 Computation of Parameters

Frequently the results from different researches are not in complete agreement (assuming the true roughness data is available). There are to main reasons for this:

a) lack of definition of parameters.

b) numerical analysis errors.

In calculating the value of slope for instance, one researcher may use three points definition while the other employs five points.

Even within the confines of one definition different results can be obtained. The digitised data from a A-D convertor depends on the degree of quantization interval. If the accuracy is changed then different values for the parameters will be obtained. Fundamentally, the sampling, quantization and the definition of parameters must all be linked together before realistic comparison can be made.

1.6 Surface Assessment

King and Spedding (1983) classify three approaches to surface characterization:

Process Specification. Which gives a measure of roughness scale with the specification of manufacturing process. It provides some degree of control over the overall form of the surface topography for a fixed condition of a specified manufacturing process.

Functional Parameters. These attempt to remedy the deficiency of characterization based on scale alone by devising new parameters of the surface which are supposed to describe its suitability for a specific application. This method has a drawback by making comparison between different applications difficult.

Statistical Characterization. This attempts to define the surface topographical characteristics in a general sense by describing its profile height and spatial properties. The statistical descriptors employed in this way may have no individual significance to any functional property, nevertheless, taken together they contain the

required information. One of the advantages of this approach is that it should be possible, given values of these (primary) parameters, to derive good estimate of all the other (secondary) parameters used in surface metrology.

Attempts to design functional surface parameters, e.g. Hydell (1967-68), tends to generate a rash of surface finish parameters, Whitehouse (1982), each of limited applicability. A complete statistical description of a profile can be given, however, in terms of two basic statistical functions, i.e. its ordinate height distribution and a suitable spatial function such as autocorrelation function or slope distribution.

1.6.1 Statistical Methods

Statistical methods were effectively first introduced into surface metrology by Abbot and Firestone (1933) when they proposed the bearing area curve as a method of surface profile specification. Although it seems obvious now that this is in fact the cumulative probability density function for the surface heights, the problem is not straightforward. This is because the heights on surfaces are not independent events.

1.6.1.1 Profile Amplitude Distribution

This is in fact statistical distribution of profile ordinate heights, or amplitude density function. Many popular surface finish

parameters such as Ra and Rq are in fact measures of the scale of the distribution of amplitude heights (fig.1.5). For a profile represented by a series of N discrete height observations y this is given by:

$$f(y) = \lim_{\substack{N \to \infty \\ \Delta y \to 0}} \frac{1}{\Delta y} \frac{n_y}{N}$$

where n_y is the number of ordinates between $y - \frac{\Delta y}{2}$ and $y + \frac{\Delta y}{2}$.

A typical graphical representation of this function is shown in figure 1.6 together with the corresponding bearing ratio curve which is an alternative form of the probability density function of the amplitudes.

$$B(y) = \int_y^{\infty} f(y)dy$$

Amplitude distribution contains all the height information in the profile but it can only be easily represented graphically and thus some way of describing it numerically is required. Its general scale of size is usually represented in such parameters as Ra, Rq, etc. Ra is also termed the centre line average (CLA) or arithmetic average (AA) roughness and is probably the most widely used surface finish parameter.

$$R_a = \frac{1}{L}\int_0^L |y - \bar{y}| \, .dx.$$

where $\bar{y}$ is the mean line and L is the sampling length along the horizontal axis x. Rq, the RMS roughness is less commonly used than Ra in practice. It is defined for the profile as

$$R_q = RMS = \left(\frac{1}{L}\int_0^L (y-\bar{y})^2 dx \right)^{\frac{1}{2}}$$

It corresponds to the statistical standard deviation 's' of the profile ordinates.

$$R_q = \left[\int_{-\infty}^{+\infty} (y-\bar{y})^2 \, f(y)dy \right]^{\frac{1}{2}} = \left[E(y-\bar{y})^2 \right]^{\frac{1}{2}}$$

Geary (1935) investigated the ratio of Ra/Rq as a measure of the departure of a distribution from the Gaussian form. For an amplitude distribution of a defined shape simple numeric relationships exist between the commonly used height parameters. For example, it can be shown that for a sinusiodal profile

$$\frac{R_a}{R_q} = \frac{2\sqrt{2}}{\pi} = .9003$$

and for a profile with normal amplitude distribution this ratio is

$$\frac{R_a}{R_q} = \sqrt{\frac{2}{\pi}} \simeq .7979$$

One can, in fact, consider the ratios of different scale parameters as dimensionless 'shape factors' of the height distribution.

A statistically more unified approach to describe the scale and shape of the distribution is to use its general moments as proposed by Peklenik (1967-68) for surface metrology applications.

$$\mu n = \int_{-\infty}^{+\infty} (y-\bar{y})^n \, f(y) \, dy = E\left[(y-\bar{y})^n\right]$$

μn is the nth central moment of the distribution. The second central moment of the height distribution, RMS, provides a scale of size of the distribution while higher moments can yield dimensionless coefficients describing the shape of the distribution. The ratio $\mu_3/\mu_2^{3/2}$ is often termed the 'normal coefficient of skewness' and is a measure of the symmetry of the profile (or its amplitude distribution) about its mean line. $\frac{\mu_4}{\mu_2^2}$ is the 'moment coefficient of Kurtosis' and is a measure of the 'scratchiness' or 'spikiness' of the profile (or the spikiness of the profile height distribution with respect to the length of its tail), (fig.1.7). They were first introduced by Al Salihi (1967). Their functional significance has been investigated since by Ostvik and Christensen (1969), Stout et al (1977), Buttery (1981) and King et al (1978). King and Spedding (1982) showed that reliable estimates of the general surface profile height parameters can be made given a knowledge of the r.m.s. roughness, skew and Kurtosis of the profile.

It should be noted that surface roughness values, in general, vary a little owing to the measuring position on a surface. Tadao Tsukada (1986) investigated the scatter of the specific values of Rmax, Rz, Ra and r.m.s. roughness measured at different positions

on a surface and the confidence interval of these values. He observed that two-dimensional roughness value of these parameters fluctuate according to a Gaussian distribution. A method to obtain the confidence interval of the sample roughness value was also given.

1.6.1.2 Description of Spatial Characteristics

The spatial properties of a surface profile may be statistically characterized by its autocorrelation function or power spectrum (power spectral density function). Although a fine-turned surface possesses some degree of periodicity, for instance, nevertheless it is impossible to distinguish it from a ground surface which is highly random by visual inspection. Autocorrelation and power spectra are able to bring out the differences more clearly by showing the periodic components. Sayles and Thomas (1976) proposed the structure function as an alternative to autocorrelation.

All of these functions are, essentially, different ways of expressing the same information and are therefore mathematically related. The autocorrelation function and power spectrum, for example, being a Fourier transform pair. Autocorrelation function is the dimensionless value of the covariance of the profile heights. This may be given as

$$\alpha(\lambda) = \text{Lim}\ \frac{1}{L}\int_0^L y'(x)\ y'(x+\lambda)\ dx$$

$$L \longrightarrow \infty$$

where $y' = y - \bar{y}$

For a sample of N equispaced discrete observations of profile heights this will be estimated

$$A(K) = \frac{1}{N-K} \sum_{i=1}^{N-K} y'_i \cdot y'_{i+k}$$

λ and K are separation or (lag).

The autocorrelation is then defined as

$$\rho(\lambda) = \frac{\alpha(\lambda)}{\alpha(0)} \qquad \text{or} \qquad R(K) = \frac{A(K)}{A(0)}$$

$\alpha(0)$ and A(0), autocovariance at zero lag are variance and sample variance of the profile respectively. They contain the total power of the profile and so they are equal to the area below power spectral density function.

Power spectral density function is the frequency domain representation of the autocovariance and the two functions form a Fourier transform pair.

$$P(w) = \frac{1}{2\pi} \int_{-\infty}^{+\infty} \alpha(\lambda)\ e^{-iw\lambda}\ d\lambda$$

$$\alpha(\lambda) = \int_{-\infty}^{+\infty} P(w)\ e^{iw\lambda}\ dw$$

power spectrum density may also be expressed in terms of the Fourier

transform of the profile y = f(x), i.e. F(w).

$$P(w) = \underset{L \longrightarrow \infty}{\text{Lim}} \frac{1}{L} \left| F(w) \right|^2$$

Here F(w) is double sided transformation of profile heights i.e.

$$F(w) = \int_{-\infty}^{+\infty} f(x) \cdot e^{iwx} \, dx$$

1.6.1.3 Combined Amplitude and Spatial Parameters

An alternative parametric description of the spatial properties of a random profile may be made in terms of its slope and curvature of peaks and valleys. Many surface properties are directly dependent on its derivatives, mainly the first and second. Kaliszer et al (1972), Spragg and Whitehouse (1972) and Peklenik (1965).

Estimation of curvature and slope needs differentiation of the profile. It should be noted that if this is done by digital technique as is usually the case, the results will depend on the form of the numerical differentiation procedure employed. Chetwynd (1978) has examined the use of differential formulae in the context of surface texture profile analysis. He concludes that a seven

point formula is adequately accurate for real surfaces profiles.

$$h \frac{dyo}{dx} = \frac{1}{60} (y_3 - 9y_2 + 45y_1 - 45y_{-1} + 9y_{-2} - y_{-3})$$

The derivation of slope information involves measuring the slope at each point along the surface profile. The slope calculated may be arranged in the form of a distribution curve. This distribution may then be characterized by its mean deviation and other parameters.

The mean of the slopes at all points in the profile within the sampling length is the average slope. Certain information may be deduced from slope parameters. For example, the steeper the average slope, the longer the actual length of the surface compared with its nominal length. This parameter may have advantages in painting and plating applications where the length of the surface for keying is of significance. Other areas are contact mechanics and friction contact, Stout (1981).

Other hybrid parameters have been defined including average wavelength which is a measure of power spectrum. It is defined as

$$\lambda q = \frac{2}{\pi} \sqrt{\frac{m_0}{m_2}} = \frac{2}{\pi} \left[\frac{\int_{-\infty}^{+\infty} p(w)\,dw}{\int_{-\infty}^{+\infty} w^2 P(w)\,dw} \right]^{\frac{1}{2}}$$

This can therefore be conveniently determined directly from the profile as

$$\lambda_q = 2\pi \frac{Rq}{\Delta q}$$

Δq is the standard deviation of the profile gradients.

A similar parameter based on the mean deviation has also been used.

$$\lambda_a = 2\pi \frac{Ra}{\Delta a}$$

where Δa is the mean deviation of the prifile gradients.

For a truly sinusoidal profile these parameters take the value of the wavelength of the sinusoid, while for random profiles they provide a useful measure of the general scale of irregularity spacing (similar to autocorrelation length).

Thomsen et al (1965) have proposed the use of the standard deviation of the slope and the mean deviation of the profile for a complete characterization of a stationary random profile. Peklenik (1963) suggested using the standard deviation of the slope as an estimate of the correlation function. Kubo (1965) and Nara (1962) have both advocated the use of the slope distribution. The profile true length which is a function of the irregularities present, was considered by Radhakrishnan (1973) as an additional parameter for surface roughness measurement. It was found that by

itself the profile length did not show any appreciable correlation with the conventional roughness value, but together with the roughness value, it identified the profile much better than the methods usually employed.

1.7 Surface Texture, Manufacture and Function

For a successful optimization of systems involving surfaces, a comprehensive characterization of the surface texture is a prerequisite. Problems in design such as wear, lubrication,strength of parts, paintability, etc. cannot be satisfactorily approached without information about the surface geometry that exhibit a profound random character.

Moreover, geometrical surface configuration indicate the specific characteristics of the manufacturing process in which the surface was generated. This is possible because the texture is in effect 'finger print' of the whole of the manufacturing process. So it can be said that surface texture serves two main purposes: (i) in the production process it serves as a method for controlling the quality of the products and an indication of any variation in the process parameters, (ii) surface texture can also give an indication of the subsequent performance of the product under service conditions. Thus, surface texture plays an important role by providing a link between manufacturing and performance.

It is known that manufacturing costs goes up exponentially as surface roughness goes down, Eberhardt (1965). This has led to

extensive efforts to develop less expensive manufacturing methods to reduce the cost of obtaining fine surface finishes. But this is treating the symptoms rather than the disease itself; significant saving is possible by a proper specification of the finish.

If the generated surface is considered as the output of the manufacturing system, it is concievable that the surface also reflects the dynamic behaviour of the machine tool, i.e. the relative movement between the tool and the workpiece. The study of workpiece surface topography as a method of monitoring the changes in the action of abrasive, for example, has been investigated by Peklenik (1964) and Buttery et al (1977). The abrasive process was also considered by Whitehouse (1971) using autocorrelation function. Hamed et al (1978) related the autocorrelation function to different grit sizes of coated abrasive.

1.7.1 Quality Control

To achieve the required quality of surfaces which would have an important influence on the operation of the component, the control of the manufacturing process is essential. In the past, this control has been an overall link without monitoring any specific process parameter and based on a single parameter of the surface. The link could break if the production process was changed. The same could happen with a change in function or the monitoring parameter. Obviously, more parameters are needed for a fuller and stronger link

which allows a degree of control which is not upset by these changes. A minimum number of parameters has to be sought, however, since any correlation between them would be wasteful and a large number of parameters will simply not get put on the drawing board. Statistical techniques can be used to determine which parameters of the surface are best to use. Amplitude distribution and a measure of spatial characteristics like slope distribution or autocorrelation function are now known to contain most of the information, nevertheless it is necessary to condense them in order to be able to make practical use of them. Two minimum factors which are needed from them are a unit of size and some estimation of the shape. For amplitude distribution CLA value or any of the peak height parameters such as R_t, R_z, etc. plus a shape factor such as skewness can be used. Similar units of size and shape are recommended for spatial functions. Another reliable parameter is the average wavelength. The shape factor for autocorrelation is still open to discussion.

When an appropriate surface finish has been established for a specific function, it is desirable to use the most economical method possible to fabricate the component. Establishing the machining conditions for a finishing process to obtain the specified topography is not straightforward. For example, the manufacturing process usually consists of at least two machining operations, the first being bulk metal removal to shape the component, and the second to produce the desired finish and achieve dimensional precision. The production engineer must determine which combination of operations achieve the desired finish most economically. The problem arises when the "shadows" of the earlier operation remain evident in the topography of the finishing process. Chetwynd et al (1982).

In an ideal situation the factors to be considered would involve only the operational setting of the machine, e.g. the geometric characteristics of the cutting tool, feed rate, and the type of cutting fluid used. Under these ideal conditions it has been possible to calculate the theoretical roughness developed in a machining operation of simple processes like single point tool cutting. Some typical examples are given by Dickinson (1967-68). Relationship for less traditional metal shaping processes such as electro-discharge machining (EDM), electrochemical machining (ECM) and ultrasonic machining (USM) have also been investigated. Ghabrial et al (1982).

For complex cutting operations such as grinding and milling expressions which describe the relationships between the operating conditions and the surface roughness are not available. Manufacturers usually follow their own guidelines acquired through experience. Factors such as built-up tool edge, discontinuous chip formation, chatter and many others contribute to non-ideal surface finish arising under practical machining conditions.

Despite these problems useful information about the manufacture can be obtained from a post process examination of the surface. The general tool shape and the wear marks on the tool are imprinted into the surface profile which are not easily detected by eye even at high magnifications. Using random process theory, however, it is possible to detect and quantify these effects. Whitehouse (1978). Useful information can also be found about the machine itself. Surface examination techniques can be used to control the tool wear,

machine conditions and surface conditons without interference in the process itself.

1.7.2 Prediction of Functional Behaviour

Sherrington and Smith (1986) recently investigated a wide range of examples in which the surface topography of the component has been found to bear a significant effect on function and cost of a part. The finish affects the appearance, fatigue life, hardness, dimensional tolerances, friction and wear of a part. Surface finish specification therefore is a design responsibility. It is the designer who must optimise the surface finish with respect to performance and cost.

Despite the extensiveness of the studies being done on the subject, the relationship between topography of the component and its performance is frequently not understood. Even in instances where the relations are clear, they may be ignored and overlooked by designer. As a consequence the surface finish of a component may be overspecified or may not be specified at all, Stout (1980). The choice of parameters for specification of the surface finish strongly depends on the intended function. In optical reflectivity, for example, the slope of the texture is critical. In wear and contact mechanisms the relation is less clear, although some parameters like per cent zero slopes has been found to be useful, Buttery et al (1984). The texture must have some effect in tribological situations because it is via the surface that stresses

are transmitted to the body of material. The central point to any investigation of tribological surface function has been recognised to be the contact of the surfaces.

In contact mechanics the two main important issues are the mode of deformation under load and the real area of contact. Surface characteristics were first brought into contact and wear studies in the works of Archard (1957) and Greenwood and Williamson (1966). Whitehouse and Archard (1970) produced the next breakthrough when they developed an important link between the random process theory and those parameters significant in contact and wear. Williamson (1968) used a computer to plot complete contour maps of surfaces and demonstrated that the surfaces contact rarely at the peaks. Buttery (1981) gives an overview of models of both surface formation and surface performance in relation to abrasive processes in the light of information made available by changes in surface topography.

1.8 Conclusion

Stylus instrument is the only really effective method in general surface characterization. Its strength is based on producing a signal which is suitable for processing by conventional analogue and digital electronic circuitry. A lot of disadvantages and limitations of stylus profilometry like the effect of flank angle which imposes a limit on the steepest slope that may be measured, damage to the surface and giving a two-dimensional representation of a real surface are much less serious than they appear.

The processing of surface data from a profilometer by digital computer has been a major advance in the measurement and assessment of the surface texture since it allows a greater number of parameters and statistical functions more readily available.

Surface texture is a highly complex reflection of the manufacturing process and an indicator for predicting the functional behaviour. Although this has been known in general, only with the application of digital methods and random process theory has it acquired significance. Optimization of manufacturing process with respect to surface texture and prediction of functional behaviour of components is nevertheless still very complex and any advancement in these areas therefore is subject to a better, and more thorough characterization of surface texture and relevant parameters. The centre-line-average, Ra, appears to be the most used of these parameters containing height information about the profile. The average slope is a convenient spatial parameter which has been neglected in preference to more stylish functions such as auto-correlation function and power spectral density. Unlike these functions slope can often be related directly to the mechanism of surface formation (cutting tool profile) or to interactive processes such as running-in. In this thesis a number of mechanism models of surface formation and surface function are developed which directly involve average slope or its derivatives.

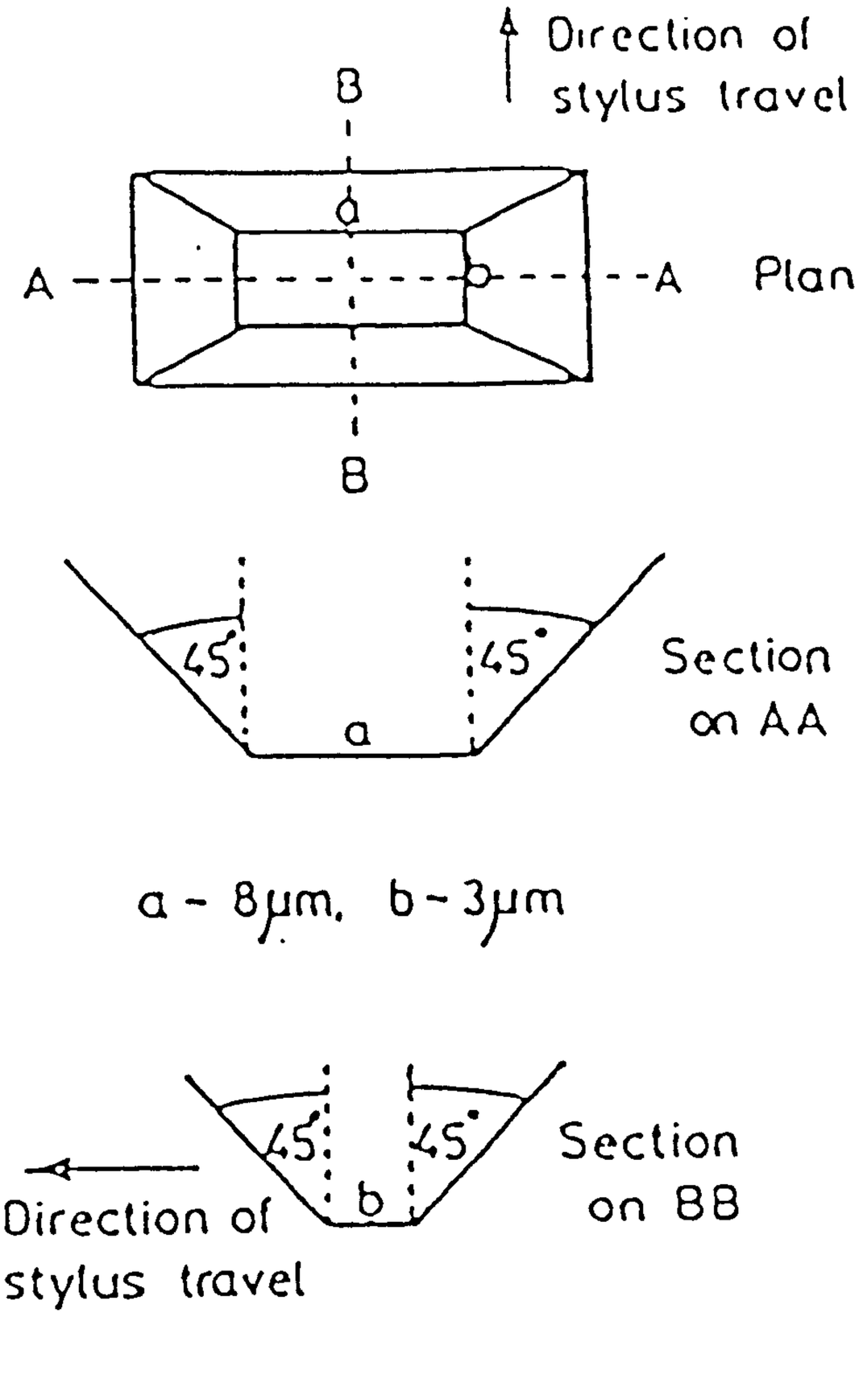

Figure 1.1 Geometry of the Talysurf Standard Stylus.

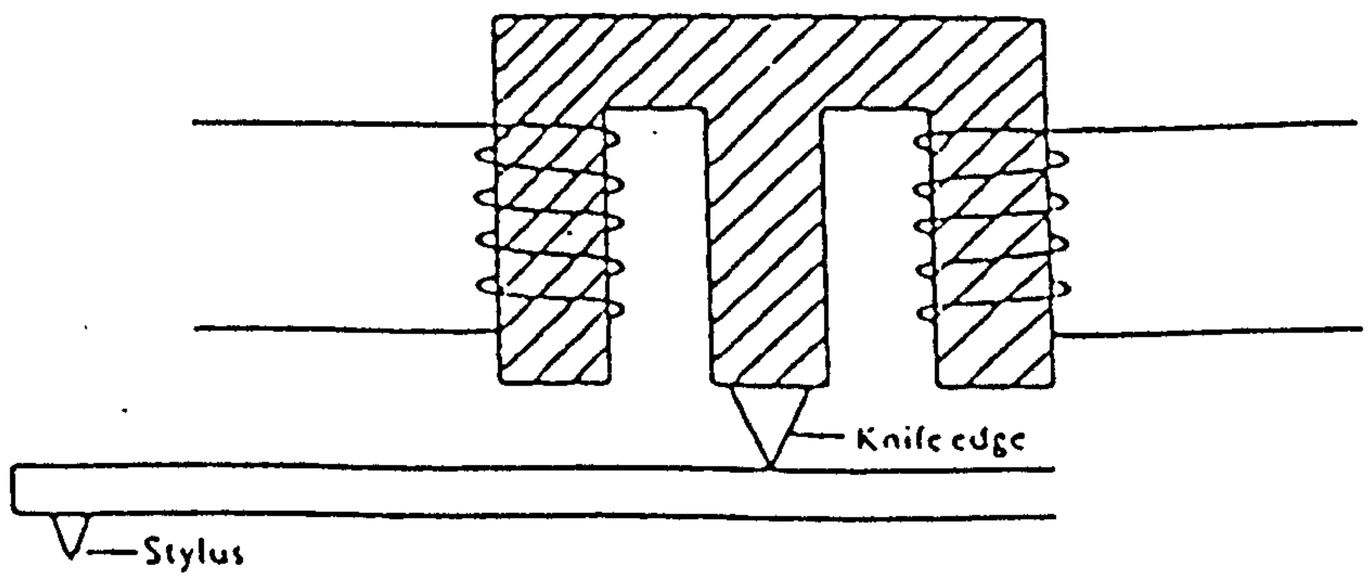

Figure 1.2 Schematic of LVDT Transducer.

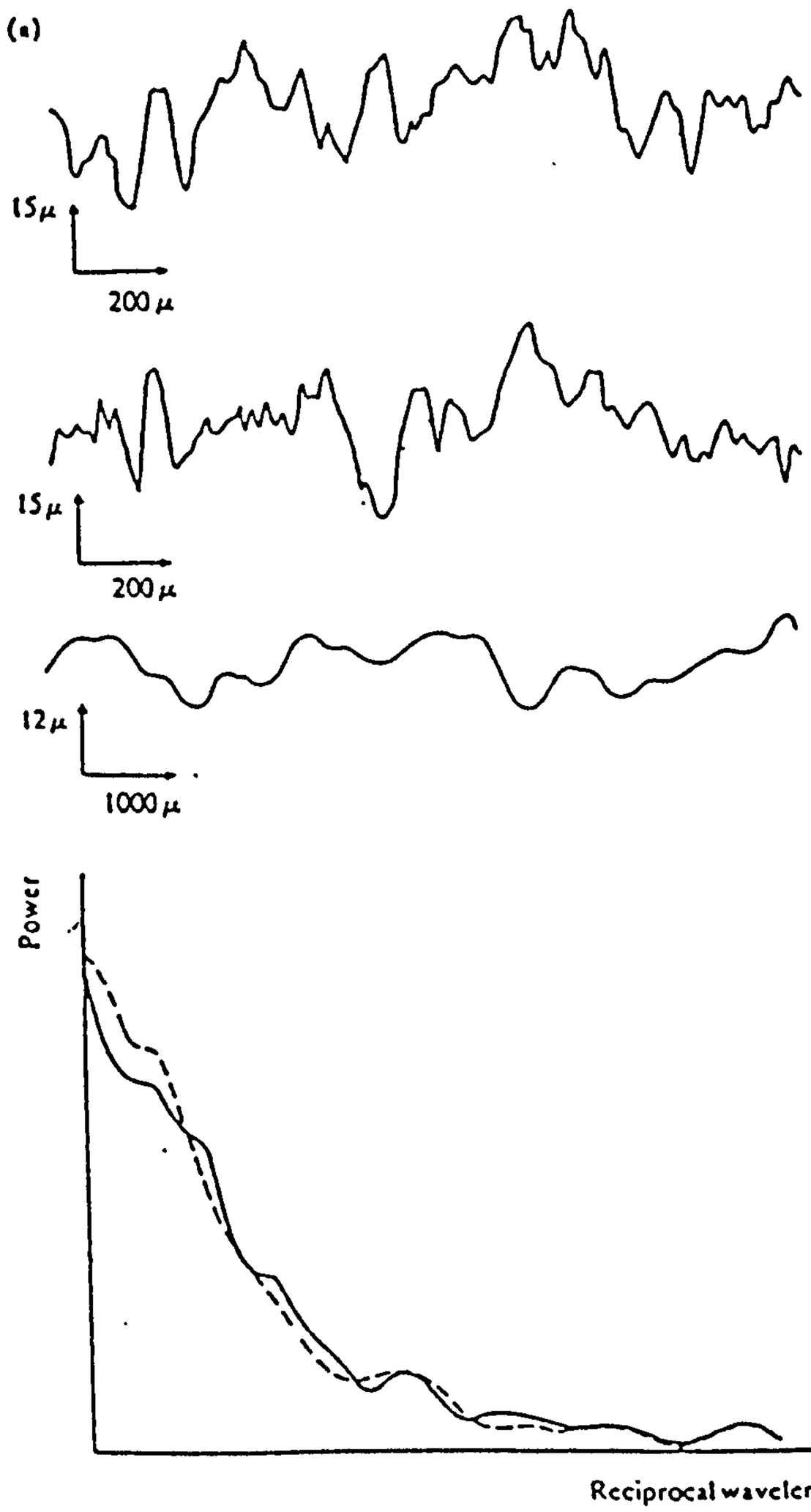

Figure 1.3 Effect os skid (Nara 1966).

(a) Profile as seen by (top to bottom) stylus with absolute datum; stylus with skid, skid with absolute datum.

(b) Power spectra of (a):
solid line, stylus with absolute datum
broken line, stylus with skid.

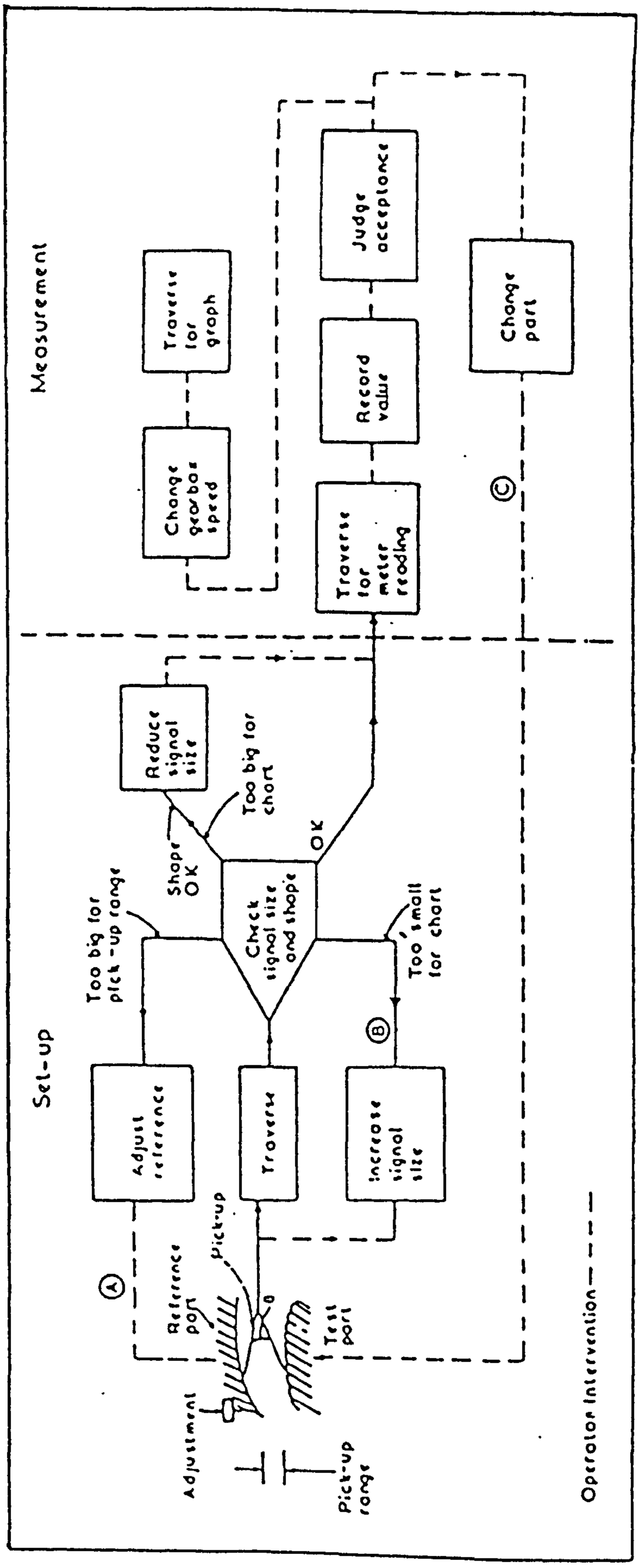

Figure 1.4 Advantages of computation (Kaliszer et al 1972).
(1) Loops A, B and C can be automatic, (2) Judgement of acceptance can be made objective,
(3) The shape of the reference part is not critical (but needs to be known and repeatable).

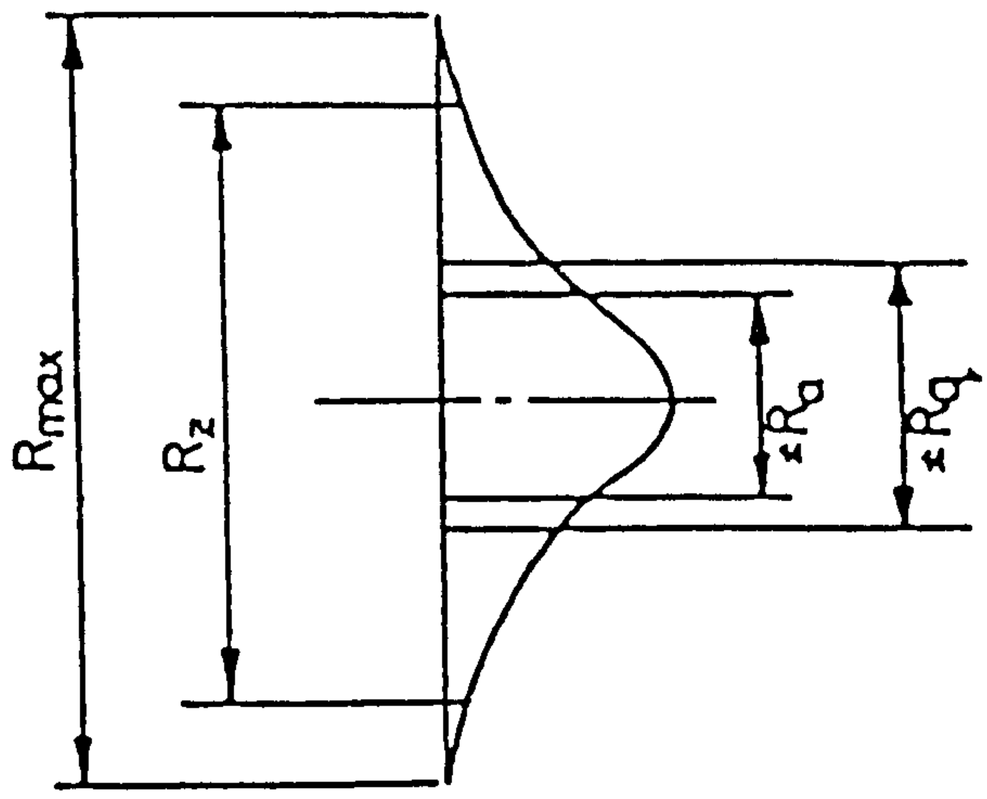

Figure 1.5 Some common parameters defining Amplitude Distribution.

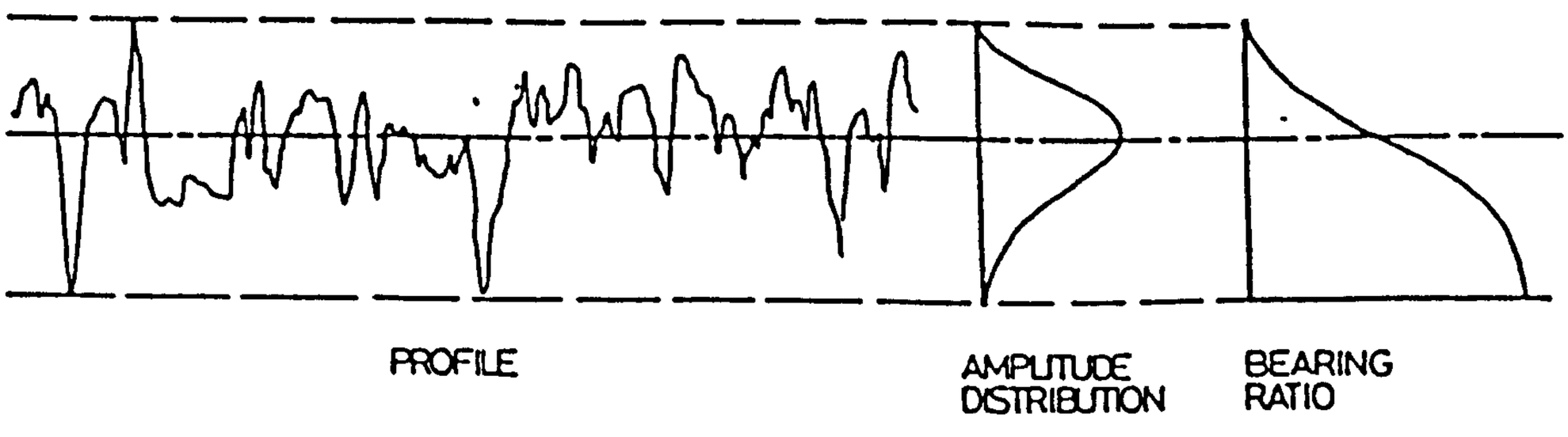

Figure 1.6 Amplitude distribution and Bearing ratio curve for a surface profile.

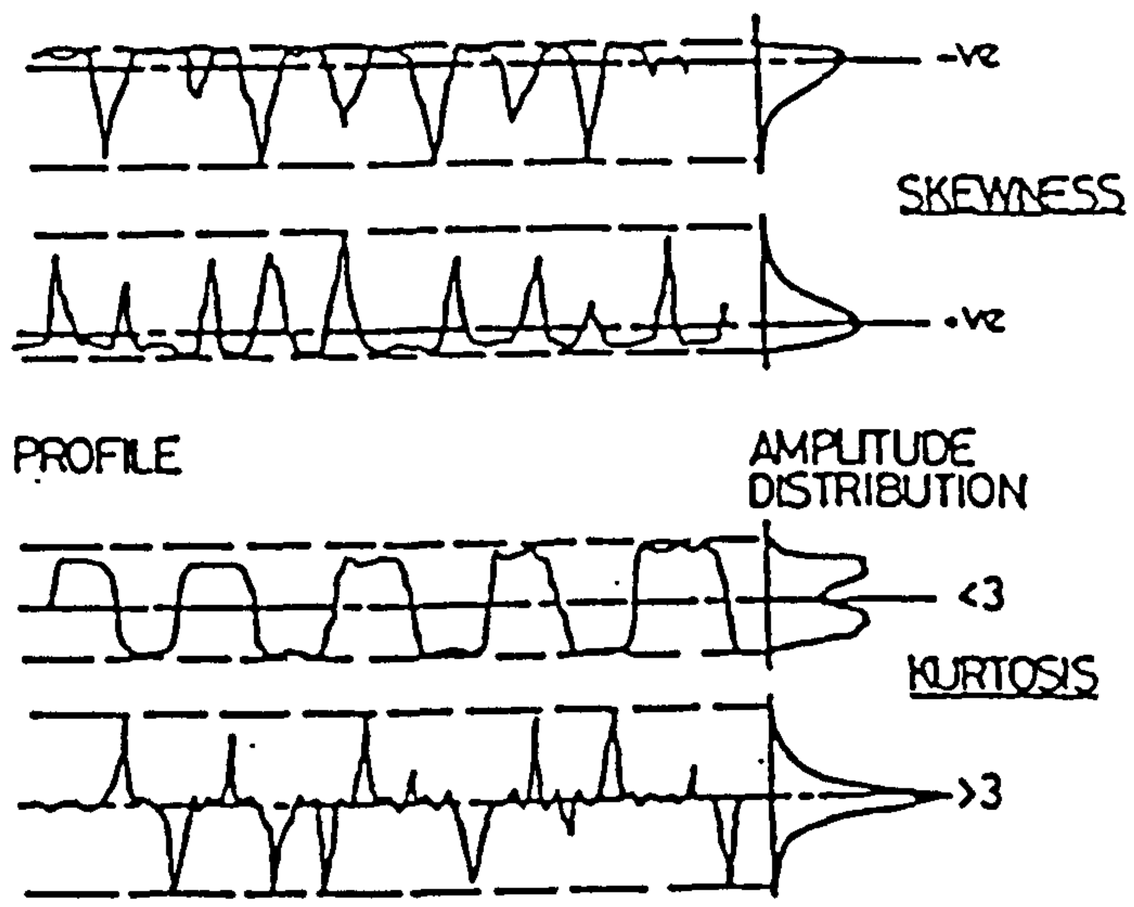

Figure 1.7 Some profiles illustrating skewness and Kurtosis in their Amplitude distribution.

CHAPTER TWO

ABRASIVE WEAR, A REVIEW

Chapter 2 - Abrasive Wear, a Review

2.1 Introduction

The abrasive process is important not only as a major cause of wear in the bearings of machines, but also as a mean for removing and shaping material. Abrasive coated papers and solid discs are used as means of removing material, mainly for smoothing the surface. Grits used in the manufacture of belts and discs are generally acicular in shape and are aligned by electrostatic methods with their major axis normal to the backing material. This should result in a sharper cutting profile and a reduction in negative rake angles much in evidence with the randomly oriented "blocky" grains used in grinding wheels, with an improved ability to abrade metal. In abrasive processes it is assumed that the abrasive surface is harder than the material being braded. The action of abrading the material produces grooves in its surface the content of which ultimately becomes the wear product. The resulting surface is therefore related to the characteristics of the indenting tips of the abrasive.

Quantitative expressions for abrasive wear have been developed by considering the abrasive particles to have simple geometrical shapes. These expressions are generally of the form

$$\frac{V}{L} = K\frac{W}{P_m} \qquad (2.1)$$

where V is the volume loss

L the sliding distance

W the normal load

P_m the flow pressure of the material.

The value of K varies with abrasive particle geometry. In general the theory predicts the wear volume to be inversely proportional to the hardness of the material being abraded and directly proportional to sliding distance and applied load.

2.2 Experimental Observation of Abrasive Wear

Hardness:

The pioneer investigations by Kruschov and Babichev (1960) showed that, for a large range of annealed pure metals the wear resistance (inverse of wear rate per unit sliding distance) was directly proportional to hardness, (fig.2.1). Their experimental conditions were chosen to eliminate the effects of such factors as speed of sliding, frictional heating and deterioration of abrasives during service. For cold worked materials, however, they found that wear resistance was largely independent of the amount of cold working to which the material had been subjected. Since cold working increases hardness, Kruschov and Babichev suggested that this apparently anomalous behaviour was due to the intense work hardening which

occurs during the abrasive process. They claimed that the resistance to abrasive wear depends on the hardness of the material in its maximum work hardened state, and as this is attained during the course of the test, preliminary work hardening will have no effect. This observation also supports the view that the material may undergo considerable disturbance such as ploughing before being removed as wear debris. Other investigators have since confirmed the effect of hardness to be linear with respect to wear resistance. Buttery (1969) and Goddard (1961) for example.

Particle Size:

Effect of grit size on its ability to remove material has been investigated by a number of researchers. Nathan and Jones (1966) established that there is a certain critical particle size, for each material - abrasive combination, which determines the exact nature of wear process. Above the critical value the wear rate is independent of the particle size, but below the critical value the wear rate is dependent on particle size. Figure 2.2 shows a typical set of result due to Goddard and Wilman.

Nathan and Jones arranged their experimental procedure in such a way that any deterioration effect in the abrasives were minimised by causing the specimen to traverse across the width of a rotating abrasive belt to follow a helical path thus ensuring that fresh abrasive was being continuously met by the specimen. This is similar to the approach used by Kruschov (1957) who used a rotating abrasive disc. Kruschov's procedure had the disadvantage that effective cutting speed on such a disc would change gradually.

Larsen-Bades (1968) catalogues three possible explanations for this "knee" or critical grain size.

(1) Avient, Goodard and Wilman (1960) suggested that chip removed by the abrasives clogged the paper by filling all, or part, of spaces between the grits. This limits the cutting action, and would be specially effective in the case of the fine grits and specimens of large contact area.

(2) Mulhearn and Samuel (1962) found that the finer grains of silicon carbide appeared to contain a large number of cracks which would make them break easily and thus reducd their ability to remove material.

(3) Larsen-Badse (1968) in his studies on the influence of the grit size concluded that some of the abrasive grains are in contact with the abrasive only elastically. These grains did not contribute to the cutting of metal, and the effect was strongly grit size dependant, being very pronounced for fine grits and negligible for grit diameter above the critical value.

Effect of Load:

The applied load has been found to have a linear relation with wear rate by a number of workers. Nathan and Jones (1966), for instance, established a linear relationship whilst testing coarse grit silicon carbide paper, but the load had to be kept below 2kg for this linear relationship to apply to the smaller grit sizes. Kruschov and Babichev (1960) confirmed that abrasive wear is directly proportional to the load when limiting the applied load to 1kg during the testing of fine grit Al_2O_3. By restricting the force involved and ensuring a fresh supply of abrasives these

two groups of researchers have minimised the effect of deterioration of abrasive which happens under normal conditions. In practical situations the abrasive is repeatedly used and therefore deteriorates gradually. The combined effects of the level of applied force and the hardness of the specimen are a major influence on the rate of deterioration of the coated abrasive, and thus the wear rate and the surface texture of the specimen. Larsen-Badse (1972) emphasises that if grit wear could be eliminated then the volumetric wear of the material would be directly proportional to the applied load.

Most of the investigators have, in the main, concentrated their studies of the process on fairly soft metals. The experimental equipment used by the majority was designed to ensure that each grit was only actively engaged with metal on one occasion. One exception to these comments are Mulhearn and Samuel (1962) who studied the effect of repeated traverses over the same strip of coated abrasive, these conditions being more relevant to the industrial situation where, with few exceptions, it is not practical, or economic to use only virgin papers. A study of the effect of the deterioration of the abrasive under repeated use is thought to be more relevant to the industrial applications of metal removal by coated abrasives.

Grit Geometry:

A number of workers have reported on scratch tests involving both idealised tools and single abrasive grits. The main object of such experiments has been to provide more information concerning the basic mechanism by which the material is removed during abrasion.

One of the most significant differences between cutting using abrasives and single point cutting is the rake angle of the cutting tool. This is usually negative for most abrasive grits, whilst it is generally positive in single point cutting. Kruschov and Babichev (1960), using idealised indentors, showed that the tangential force depends on the material being scratched and it decreased with increase in the scratching angle. As a result of their experiments they concluded that two types of scratch were possible, one involves the formation of a groove by a ploughing action which displaces the material, the other a cutting mechanism, the groove volume being removed as in turning. Their results indicate that the transition from ploughing to cutting depends on the material being scratched, the cutting angle of the indentor and its orientation relative to the surface.

Mulhearn and Samuel (1962) proposed a critical 'attack angle'; the attack angle being the angle between the cutting facet of indentor and the work material surface; to explain the existence of cutting and non cutting grits. Grits with attack angle less than critical value plough a groove without removing material, grits with a greater attack angle remove a chip. They found that only 10% of the grits on their abrasive paper had attack angles exceeding the critical value. They concluded that only 10% of the grits were cutting and that the remainder plough a groove without removing material.

Sedriks and Mulhearn (1963 and 1964) have used pyramidal tools of known geometry and orientation to simulate scratching by abrasive

particles. They point out that for particles with attack angles greater than 90° there is no frontal facet to support the load and the tool would dig into the work material. Obviously in this situation conventional wear theory is not applicable, since in abrasive wear theories the load is considered to be supported by one or more of the inclined faces which stays in contact with the work.

It is generally agreed that only a small percentage of the total number of grits present on the surface of an abrasive tool are sufficiently prominent to contact the surface.

These prominent grits are considered to have three possible roles, namely:

(1) They are "active" because their geometry is such that they engage with the workpiece and result in the removal of a chip of metal.

(2) They provide "bearing" surfaces which support some of the applied load, and a grit may have such a role, because it has developed a wear flat, or it is said to be glazed.

(3) An intermediate condition can exist in which a grit can deform the surface by a ploughing action without actually removing metal, and at the same time participating in supporting the applied load. In experiments carried out by Buttery and Archard (1971), they found that a grit can plough and remove some of the material being displaced at the same time.

2.3 Abrasive Wear Theory

Abrasive wear theory is based on the assumption that the groove geometry is closely similar to the geometry of the grit producing it. The general form of the abrasive wear equation can be represented as:

$$\frac{\Delta V}{\Delta L} = C \frac{\Delta W.\cot\theta}{H} \qquad (2.2)$$

(Rabinowicz, 1965).

For a total load W and assuming all the grits have the same geometry we can write

$$\frac{V}{L} = C \frac{W.\cot\theta}{H} \qquad (2.3)$$

In these equations θ is the half angle of the scratch formed on the abraded surface. W is the load, H hardness, L sliding distance and V is the volume of wear.

For a process with 100% efficiency, the constant C is a function of the assumed geometry of the abrasive particle. No allowance is made here for the build-up at the front of indentor or ploughing ridges at the edges of the scratch. The existence of these phenomena, however, is well known. Figure 2.3 shows the scratches made by a Vickers diamond tracked on a SKF steel (Hamed, 1977). With edge configuration first there is little evidence of build-up, whereas with the Vickers diamond facet

configuration, the chip runs up the face roughly doubling the area of contact. This was also observed by Sedricks and Mulhearn (1963) when they tracked idealised tools across a flat surface facet first. Tests carried out by Kruschov and Babichev (1960) and Buttery (1969) on the other hand show that scratching with edge first configuration plough the surface forming ridges at the sides of the scratch. Therefore, only part of the material displaced can be removed. Buttery (1969) calculated the value of C for a number of idealised indentors and proposed a value of 0.5 based on the above considerations as a representative value in the general form of wear equation. The general behaviour of the wear equation can best be demonstrated by referring to figure 2.4 which shows the volume of wear, (a) and the wear rate, (b) against sliding distance.

Even when a representative value of width to depth ratio (θ) is taken into account, abrasive wear theory has been found to be in error when applied to the actual wear situation, as the predicted figures are greater than the observed values. Two possible explanations of this discrepency are (1) only a proportion of the grits are cutting at any time, or alternatively, (2) only a proportion of the scratch volume is actually removed. The modified form of the wear equation can thus be written as

$$\frac{V}{L} = \frac{0.5 \alpha \beta \ W \ Cot\theta}{H} \qquad (2.4)$$

where

α = the proportion of the grits actually cutting.

β = the proportion of the groove volume removed.

Hamed, M.S. (1977) showed that for idealised indentors β varies with hardness and for a given indentor it increases with increase in hardness.

Figure 2.5 shows the results of abrasive wheel experiments made by Buttery and Archard (1971). This kind of behaviour is in total agreement with the abrasive wear theory and is usually encountered in a stable condition where the deterioration of the abrasive is negligible or there exist a self-sharpening process which compensates for any dulling effect of the abrasives.

A second type of behaviour can also be observed. Mulhearn and Samuel (1962) carried out abrasive wear tests where the surface of the abrasive was used repeatedly. They used silicon carbide papers, the work material being fully cold-worked mild steel. Their results showed the rate of wear gradually fell with sliding distance. As a result of their experimental work Mulhearn and Samuel developed an expression for the mass loss M_n of the form

$$M_n = M_o(1 - e^{-\eta n}) \qquad (2.5)$$

where

n = number of revolutions (slideing distance)

M_o = mass loss after an infinite number of revolutions

η = a constant.

They showed that this expression was in good agreement with their practical observations and associated the decline in the wear rate to the clogging of the abrasive paper.

Buttery and Archard (1971) produced similar results (fig.2.6) but they related the change in the wear rate to glazing rather than clogging. In their experiments with abrasive pin against steel ring they showed a reduction in wear rate with sliding distance in every case. The gradual change in the rate of metal removal, which occurs with abrasives, indicates a progressively changing wear situation. At the outset, sharp grits cause removal of metalic fragments. At the end the grits are blunt and highly polished. This glazing can be accompanied by clogging with oxide debris; a condition which is clearly deviated from the abrasive wear theory based on sharp grit geometry (fig.2.7). Further evidence of the glazing grits was found in a pin on disc abrasive wear test made by Mashloosh et al (1984). The pin was made to rub on the same track continuously throughout the test. The degradation of the abrasive paper resulted in the production of two different types of wear debries, which have been identified as spiral-shaped, indicating a cutting mechanism, and plate-like, indicating a rubbing mechanism.

Scanning electron microscopy has been used to observe the change in the wear mechanism, Buttery and Archard (1971). These observations confirmed that initially the grits were seen to be sharp and they produced a rough 'ploughed field' surface. After 180 min. running, the wheel had glazed considerably and the tips of many of the grits consisted of flat highly polished plateaux.

(fig.2.8). The corresponding steel surface was smooth and polished.

Published descriptions of the surface finish results suggest close similarities with the process described above. Buttery et al (1977) experimenting with a pin on disc machine under a load of 5N and a sliding speed of 90.5 $m.min.^{-1}$ and using aluminium oxide grits size 36, 60 and 100 with SKF steel found that the surface characteristics of the steel pin changed as the wear rate reduced and it was suggested that similar changes were taking place on the surface of the abrasive. The surface finish Ra of the pin showed a rapid improvement at the beginning of each experiment. The rate of reduction in Ra however gradually decreased. When the wear approached a steady state condition, the surface finish Ra also approached an almost constant value.

Figure 2.9 shows the values of average slope recorded by the same authors. Although the abrasive wear theory is highly dependent on average slope (θ = 90 - average slope), these changes in the average slope alone are insufficient to explain the marked reduction in wear rate and the accompanied improvement in surface finish. Allowance must be made for the wear flats formed on the abrasive surface. Table 2.1 is the summary of test results by Mackie (1982) on grade 60 Al_2O_3 disc at a speed of 90.5 m/min running against SKF steel. When the changes observed in the value of θ (θ = 90 - average slope) are taken into account, the predicted values of weight loss by the theory is still considerably larger than the experimental results. This is shown in Figure 2.10 for

the load of 2N. This deviation is thought to be due to the fact that abrasive wear theory is only applicable to sharp grits. Mulhearn and Samuel attributed the changes in the wear rate to the clogging of the abrasive paper since they used fine grades of abrasive. Buttery et al using both optical and S.E.M. showed that the reduction in the wear rate is due to the formation of wear flats on the abrasive grits analogous to glazing in grinding. They found no evidence to show that all the abrasive had been used up or that the abrasive had been loaded.

2.4 Discussion

The main parameters involved in abrasive wear are well established and their effects have been shown experimentally. The relation between these parameters is demonstrated in the sharp grit abrasive model (abrasive wear theory of sharp grit). Under certain circumstances, i.e. when the effective sharpness of the abrasives remains unchanged this model can predict the wear rate. In general, however, like many cutting processes the abrasive action of grits brings about a condition which reduces their effectiveness and slows down the cutting action. Flat lands appear on the grits which results in only a proportion of the load contributing to cutting. This in turn reduces the wear rate and affects the surface roughness of the product. Although the experimental evidence of these changes are plentiful and the importance of glazing has been underlined by a number of researchers, nevertheless, no attempt has been made to incorporate this parameter into the wear model. This is important not only for a correct assessment of wear rate but also in relation to other factors involved like surface roughness and forces.

Although clogging has been suggested as being responsible for the reduction in wear rate, it cannot explain other changes which occurs in the wear process such as reduction in surface roughness and a change in the shape of the chips produced. Moreover a reduction in wear rate has been observed in conditions where no clogging has taken place. These observations serve to underline the importance of the alternative factor namely formation of wear lands on grits and the need to incorporate it in the abrasive wear model.

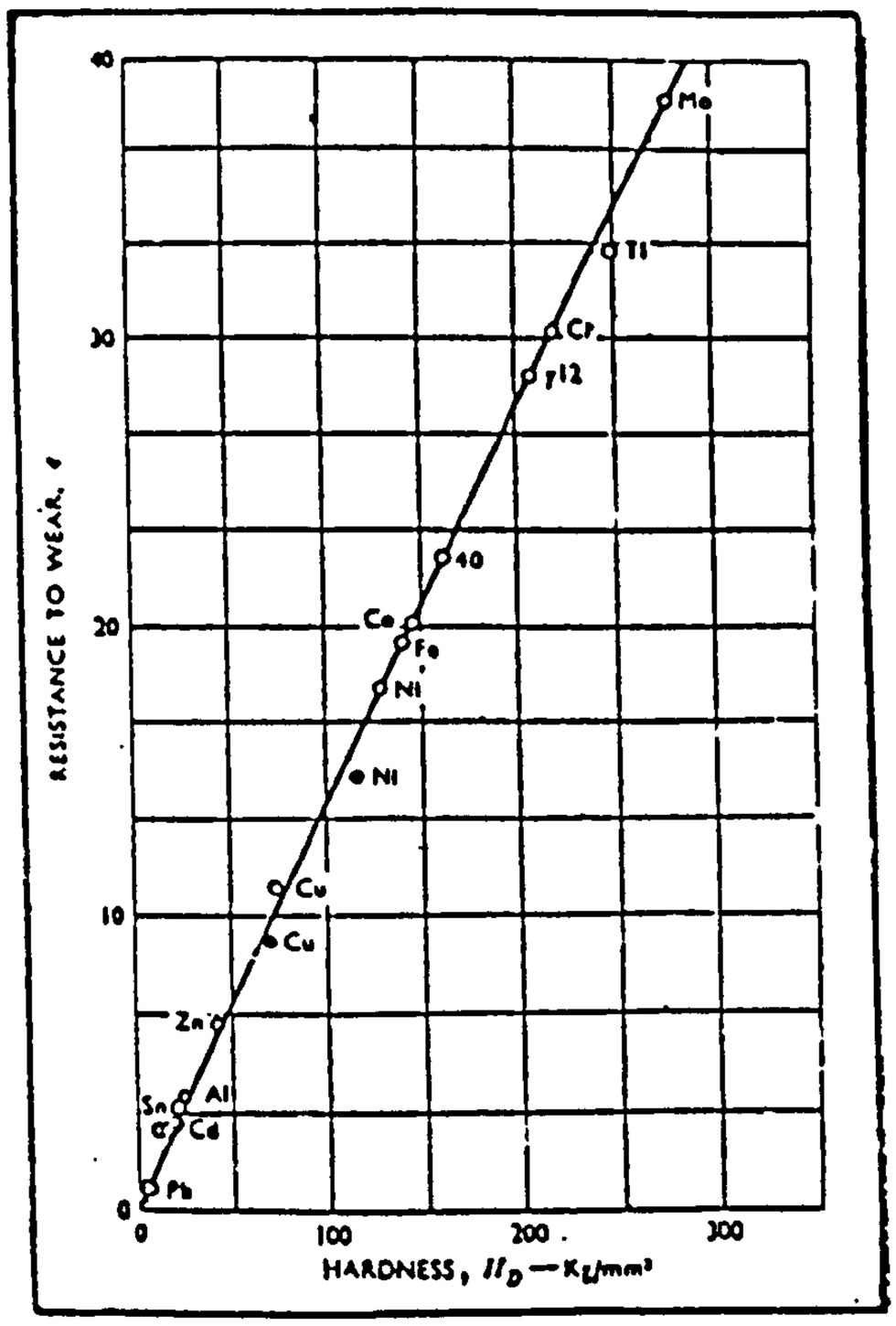

Figure 2.1 Wear resistance against Sliding distance for commercially pure metals. (Kruschov and Babichev 1957).

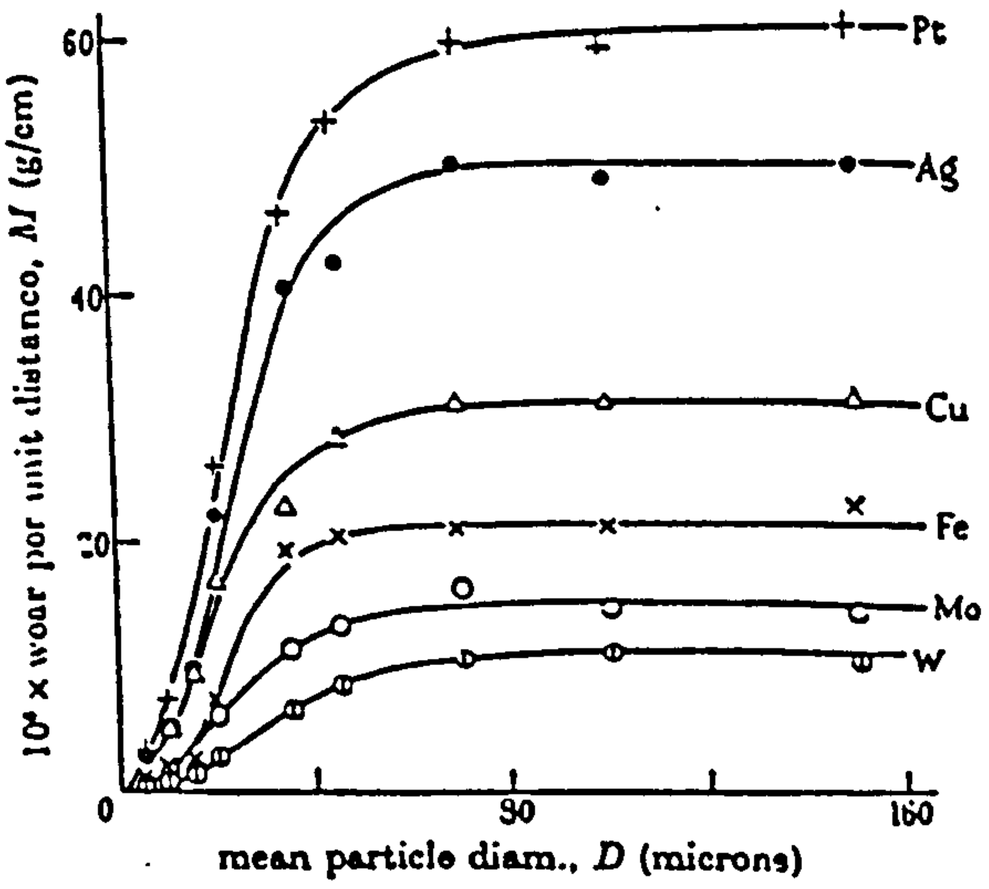

Figure 2.2 Variation of wear rate with mean particle diameter of abrasive for various metals at the equilibrium stage of pick-up of abrasive, on dry emery paper at 1 Kg Load. (Goddard and Willman, 1962).

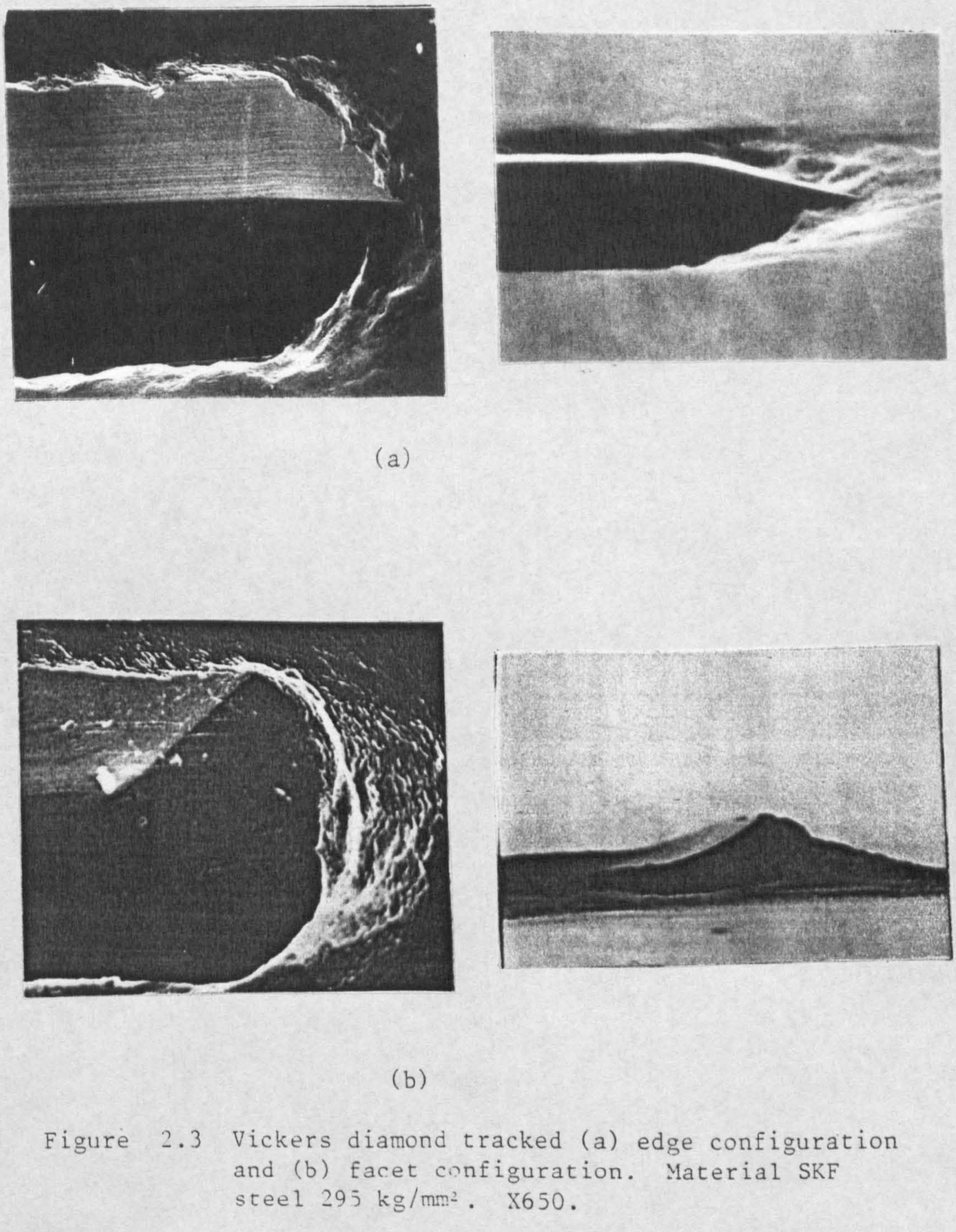

(a)

(b)

Figure 2.3 Vickers diamond tracked (a) edge configuration and (b) facet configuration. Material SKF steel 295 kg/mm². X650.

(Hamed, 1977)

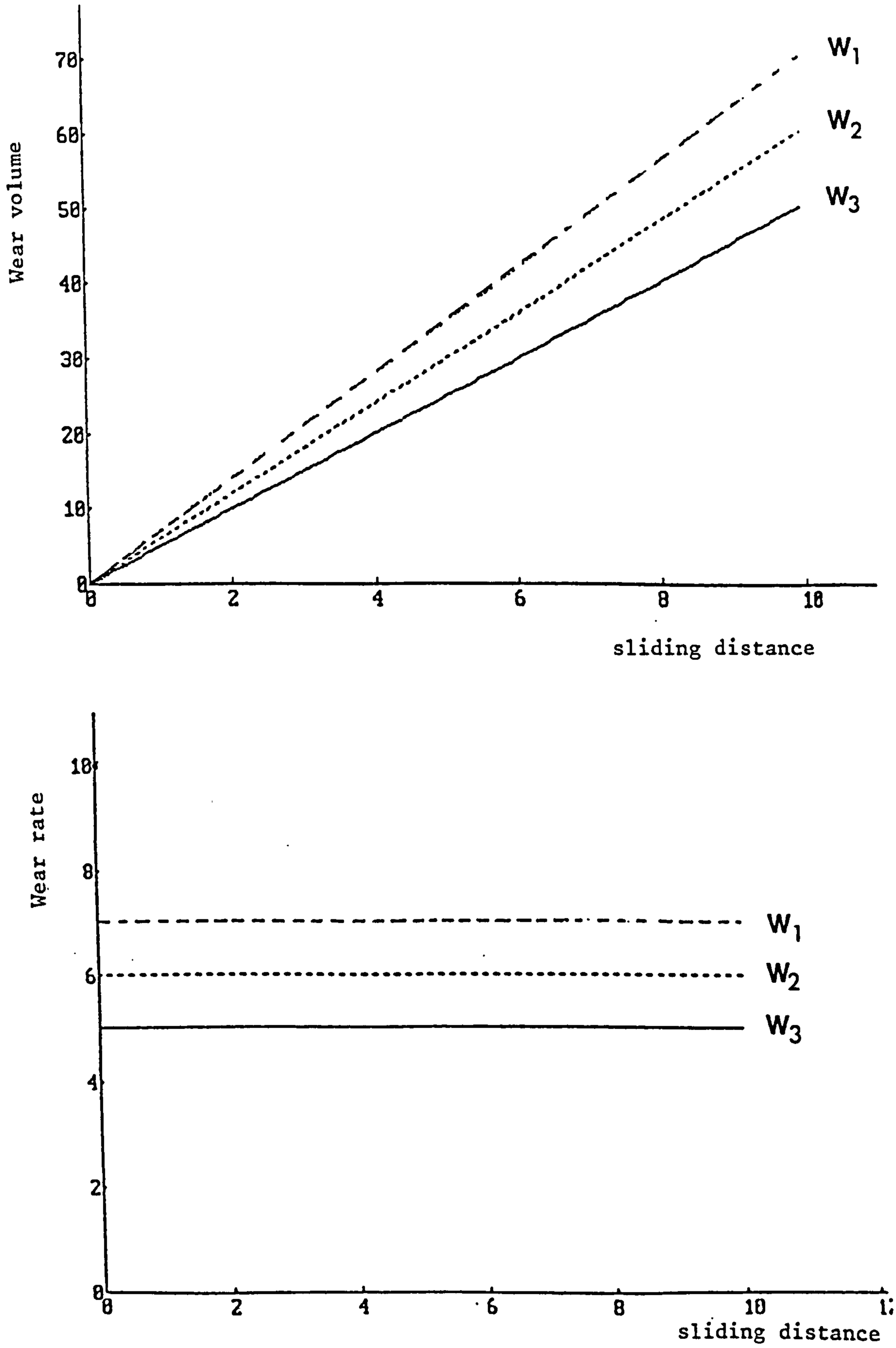

Figure 2.4 Schematic representation of sharp grit model.

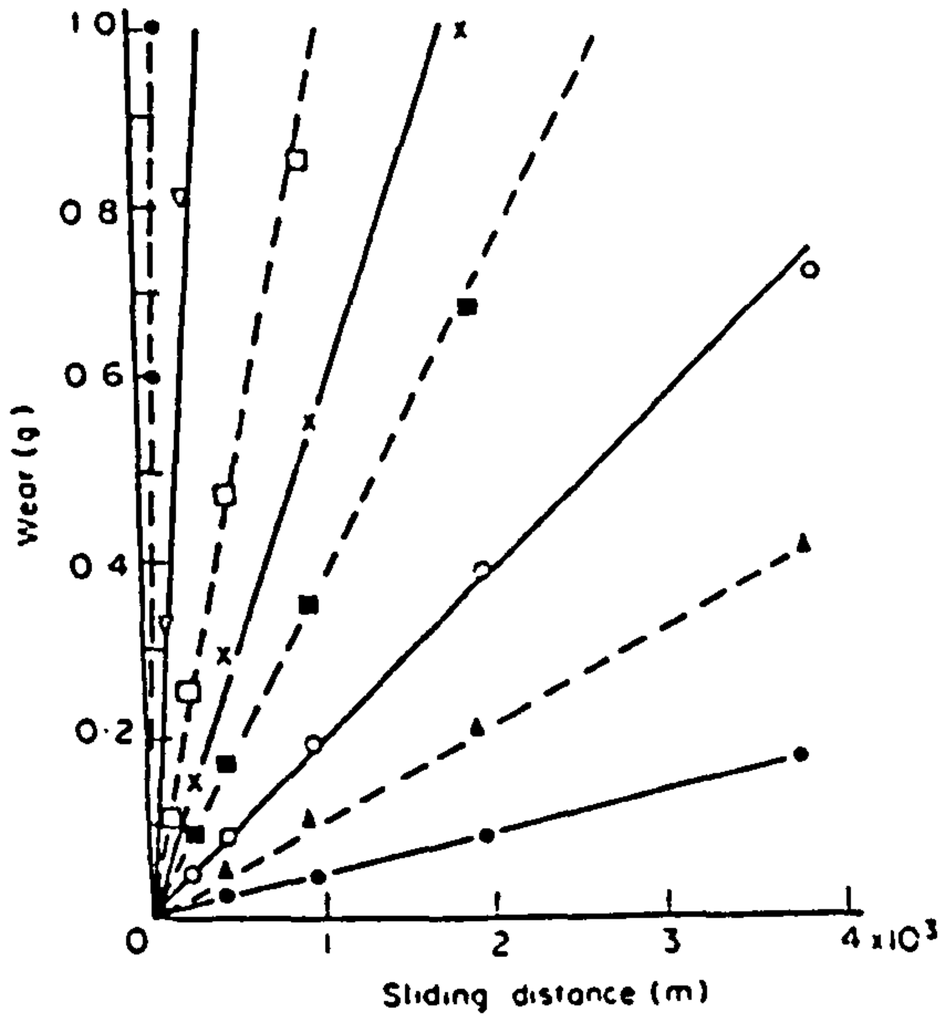

Figure 2.5 Wear as a function of sliding distance for a range of conditions. Pin, 28"„ Cr steel; ring, 1 in. diameter sixty-grit wheel, speed 750 rev/min. Loads (kg): ●——●, 0·04; ▲---▲, 0·10; ·——·, 0·20; ■---■, 0·375; ×——×, 0·75; □---□, 1·25; △——△, 2·50; ●---●, 5·0.

(Buttery and Archard, 1971)

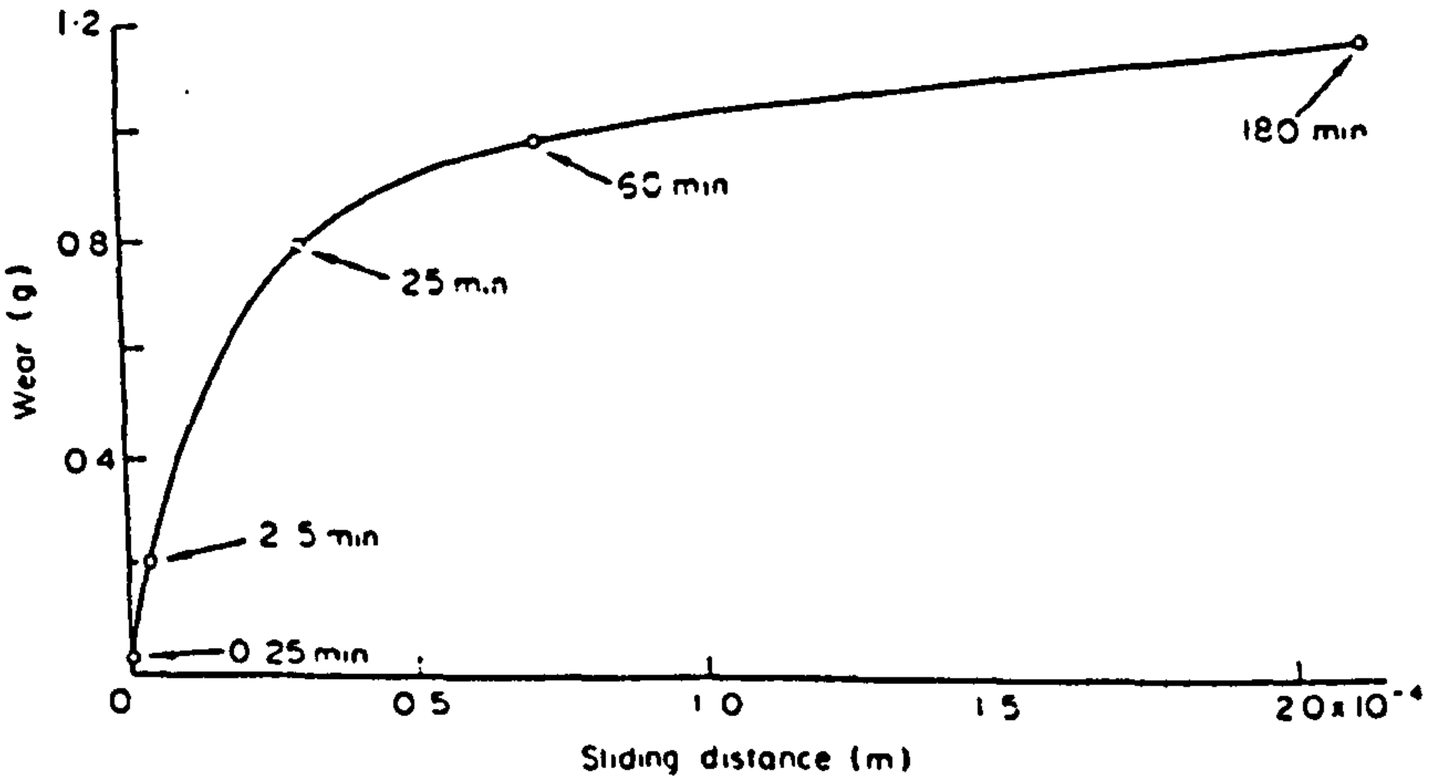

Figure 2.6 Wear as a function of sliding distance for an experiment in which a transition in wear behaviour occurred. The times indicated are those at which the surfaces were examined by scanning electron microscopy. The pin was of a 1"„ C steel (350 DPN) rubbing on a 1 in. diameter sixty-grit wheel running at 1500 rev/min.

(Buttery and Archard, 1971)

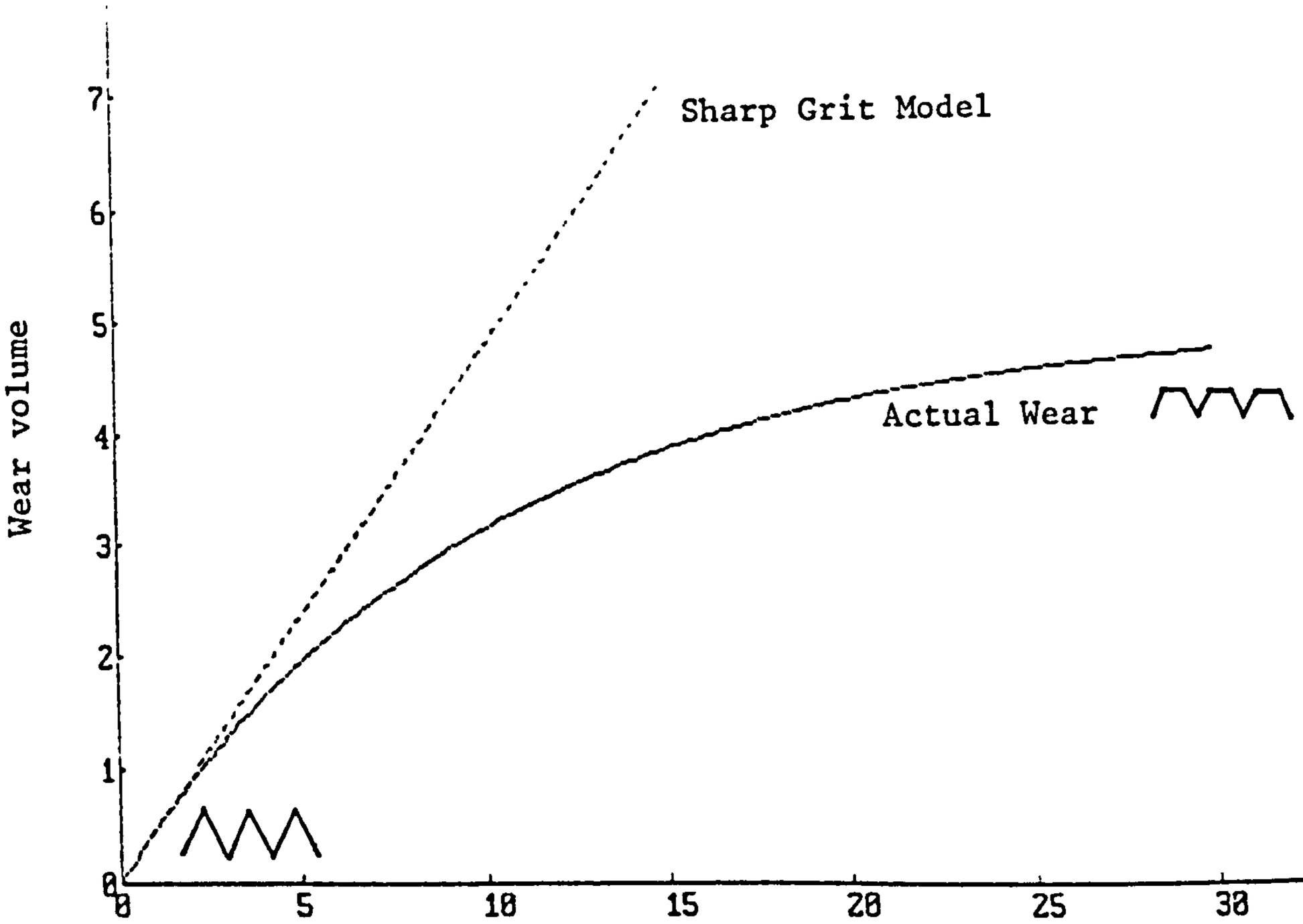

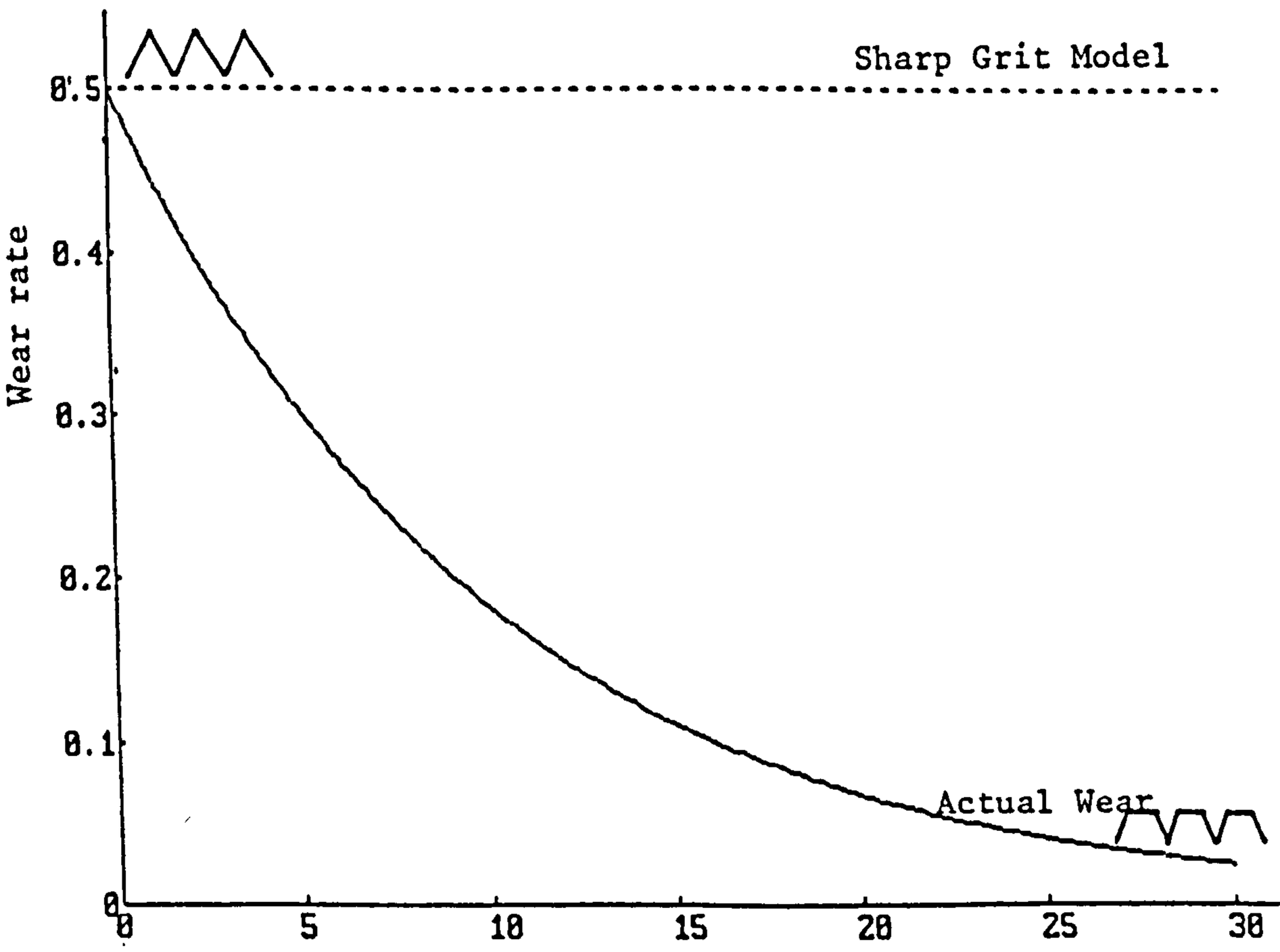

Figure 2.7 Deviation from sharp grit model due to blunting of grits.

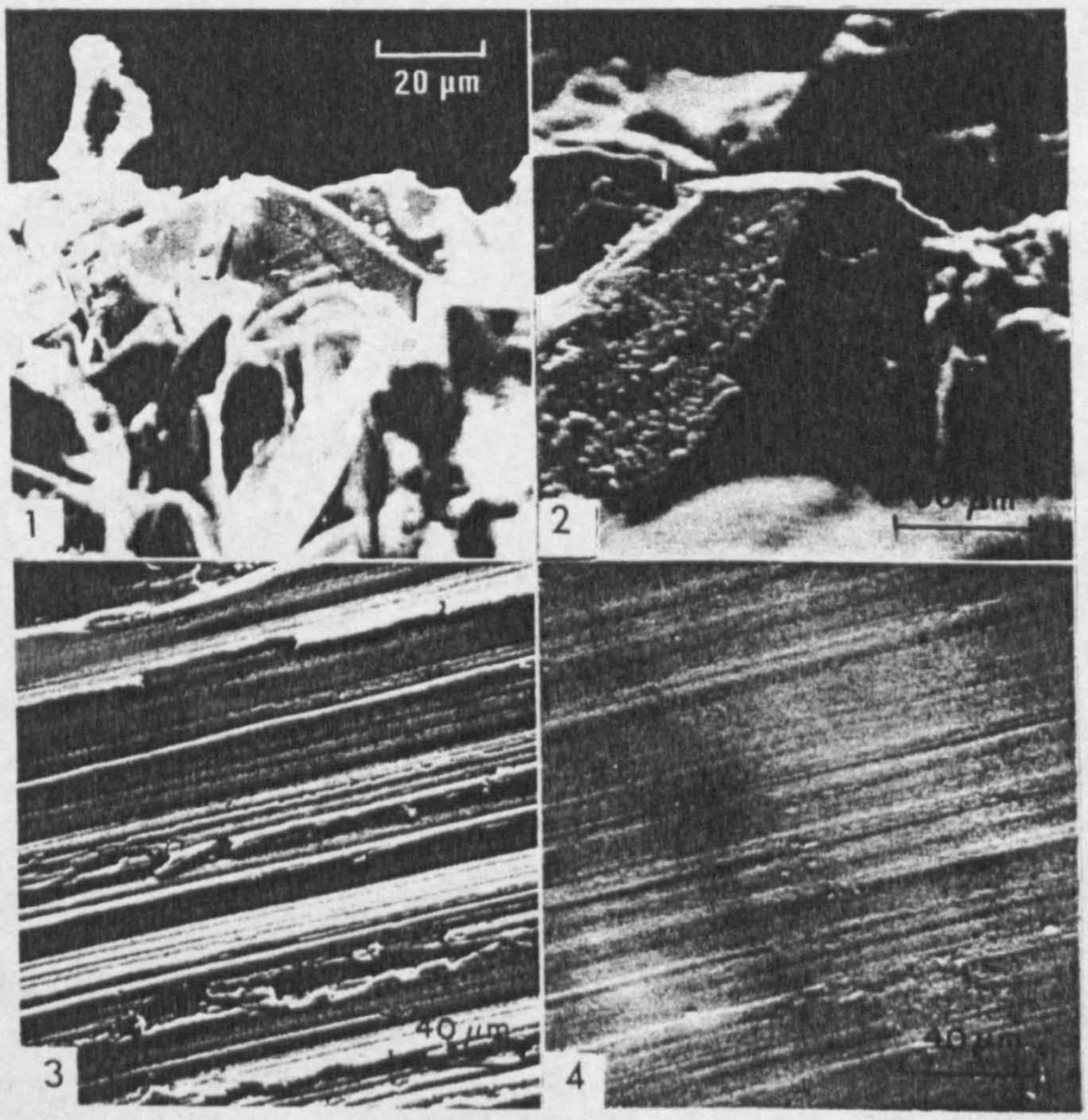

Figure 2.8 1 Scanning electron micrograph of sharp grit viewed horizontally. × 550.

2 Scanning electron micrograph of glazed grit viewed horizontally. × 300.

3 Steel pin which has run for 0·25 min viewed at 77° to the horizontal. × 375.

4 Steel pin which has run for 180 min viewed at 77° to the horizontal. × 375.

(Buttery and Archard, 1971).

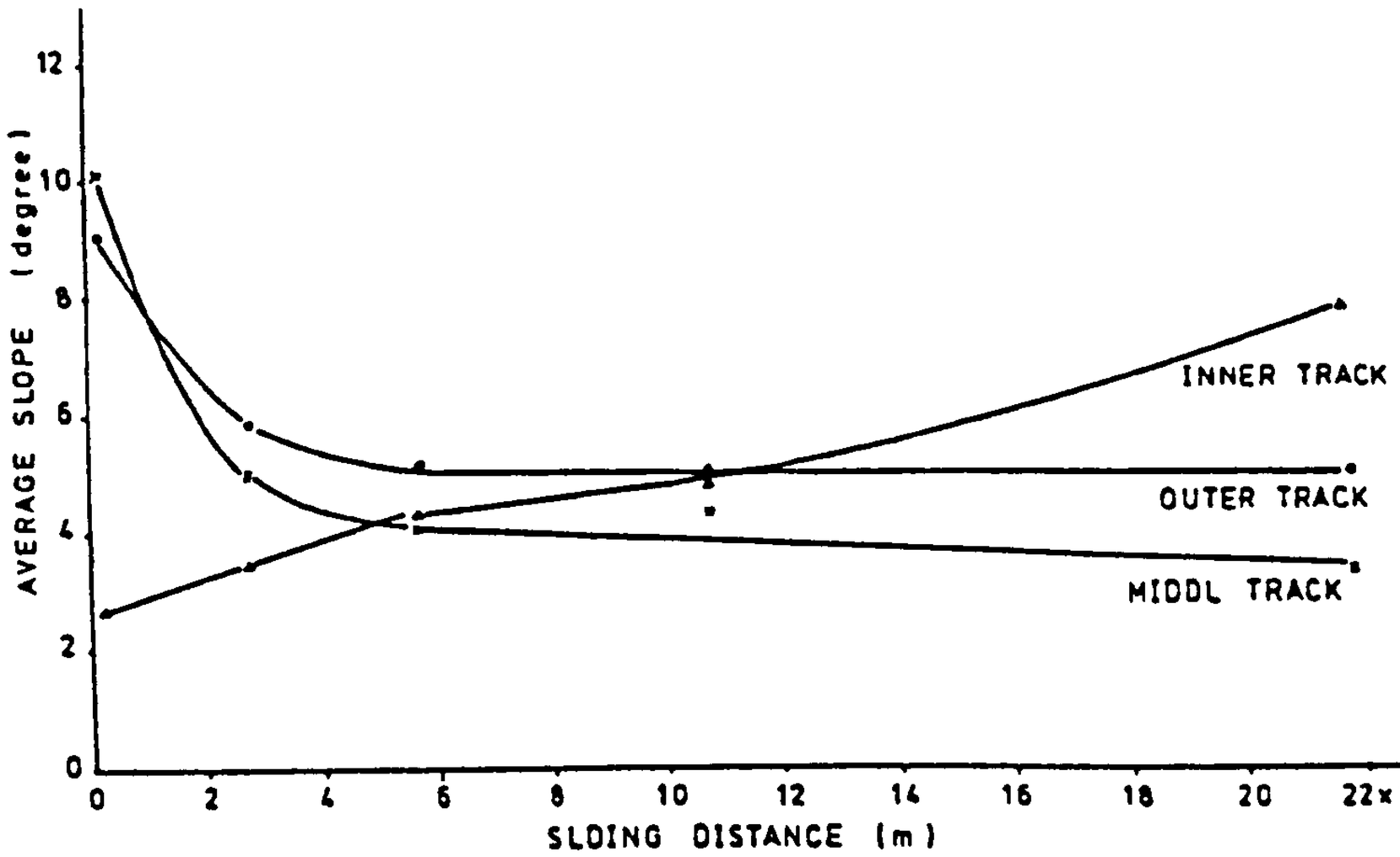

Figure 2.9 Variation of average slope as sliding distance increases. (Buttery et al, 1977).

3.2a :- Hard Specimens

APPLIED FORCE (N)	TEST TIME (min)	WEIGHT LOSS (g)	COMPUTER RESULTS			
			h max (μm)	Ra (μm)	RMS (μm)	Av. Sl. (degrees)
2	2	0.0112	29.871	3.138	4.110	9.92
	240	0.0619	9.246	1.275	1.615	3.49
5	2	0.0329	23.571	3.901	4.733	9.32
	240	0.2530	9.042	1.143	1.557	2.20
7	2	0.0681	30.023	3.528	4.658	9.87
	240	0.3467	13.564	1.622	2.294	2.74
10	2	0.1057	17.069	2.399	2.986	8.53
	240	0.6476	11.176	1.086	1.412	3.16
15	2	0.1961	16.002	2.364	2.958	8.67
	240	1.0719	8.534	1.124	1.477	3.04
18	2	0.2587	17.628	2.282	2.911	8.61
	240	1.5931	7.010	0.941	1.231	3.06

Table 2.1 Changes in average slope and other surface parameters with wear. (Mackie, 1982).

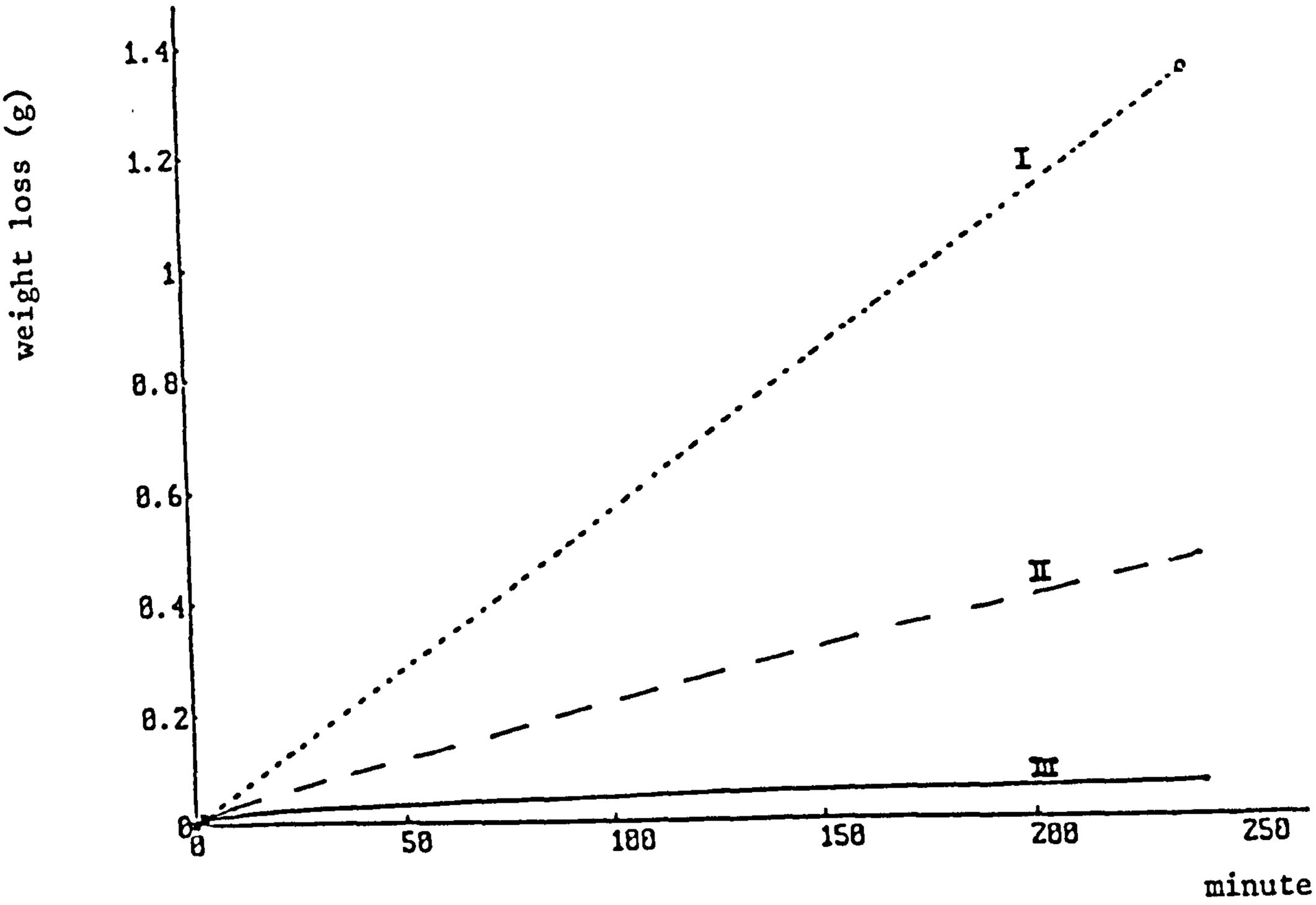

Figure 2.10 I - Sharp Grit model.
II - Modified Sharp Grit model.
III - Real data.

CHAPTER THREE

BLUNT GRIT THEORY

Chapter 3 - Blunt Grit Theory

3.1 Introduction

A theory has been developed here for grits of known geometry abrading a surface which takes into account the progressive blunting of the grits as the wear proceeds. The theory is based on the assumption of plastic deformation of the material surface. Wear theories forecasting the magnitude of wear rate are generally based on the concept of real area of contact, that is they argue that the surfaces will wear at those places where they touch and relate the worn volume V produced in a sliding distance L to the true area of contact of a unit event. A similar attitude has been taken here. Previous wear theories however, have ignored the changes that may occur during the interaction of the surfaces to the geometry of the unit event. In the case of abrasive wear this change is mainly the appearance of the wear flats at the tip of sharp asperities.

3.2 Theory

Consider a blunted Vickers indentor abrading a flat surface under a normal load ΔW in the facet first configuration. Figure (3.1) describes the geometry of the grit and the ideal scratch produced by it.

At the start, when the indentor is at rest the grit is sharp and the projection of the area supporting the load is $4a^2$. Therefore

$$4a^2 = \frac{\Delta W}{P_m} \qquad (3.1)$$

where P_m is the flow pressure of the material in Kg/mm^2. Since the flow pressure of the metal is proportional to its hardness (P_m = 1.08H for a Vickers indentor), P_m in the above equation can be approximated by hardness. This is particularly true for the abrasive grits which have apex angles larger than that of a Vickers indentor (68°).

The indentor then starts tracking along the surface and produces a scratch. It can now be assumed that the load is supported by only the front facets of the indentor since there is no material behind it. Buttery (1969) made a series of scratch tests with pyramidal and conical indentors using specimens of different hardness. The scratch widths (2a) were measured from the Talysurf traces. In each case the deduced scratch width assuming the frontal facets were supporting the load was in good agreement with the experimental observations.

Furthermore, by tracking along the specimen the sharp indentor gradually develops a flat area on its tip (Blunt grit). The projection of the area which support the load has now changed to:

$$A_f = A_1 + A'_1 = 4b^2 + \tfrac{1}{2}[2(a+b)(a-b)]$$

$$A_f = a^2 - b^2 + 4b^2$$

The indentor penetrates further into the surface to support the load so that:

$$\frac{\Delta W}{P_m} = a^2 - b^2 + 4b^2 \qquad (3.2)$$

The area of the scratch produced (figure 3.1) is

$$A_3 = (a^2 - b^2)\ \mathrm{Cot}\theta \qquad (3.3)$$

Assuming 100% efficiency the wear volume ΔV produced at a sliding distance ΔL is given by

$$\Delta V = A_3 . \Delta L \qquad (3.4)$$

Therefore:

$$\frac{\Delta V}{\Delta L} = A_3 = (a^2 - b^2)\ \mathrm{Cot}\theta \qquad (3.5)$$

Substituting for $(a^2 - b^2)$ from equation (3.2) into the above relationship, we have

$$\frac{\Delta V}{\Delta L} = (\frac{\Delta W}{P_m} - 4b^2)\ \mathrm{Cot}\theta \qquad (3.6)$$

This is similar to the expression for a sharp abrasive but it includes an extra term $(4b^2)$ expressing the area of the wear flat developed during abrasion. This area changes with sliding distance and as the wear progresses it increases.

The volume of abrasive loss v related to the flat $(4b^2)$ is given by:

$$v = 4/3\ b^3\ \mathrm{Cot}\theta \qquad (3.7)$$

The equation for the wear rate (3.6) can be modified as

$$\frac{\Delta V}{\Delta L} = (\frac{\Delta W}{P_m} - 4b^2)\ Cot\theta = \frac{\Delta W}{P_m} Cot\theta - 3\frac{v}{b} \qquad (3.8)$$

By introducing a ratio $G = \frac{V}{v}$ as the ratio of the wear volume to the volume of the abrasive loss,(3.8) can be written as:

$$\frac{\Delta V}{\Delta L} = \frac{\Delta W}{P_m} Cot\theta - 3\frac{V}{G.b} \qquad (3.9)$$

For a given kind of abrasive and material hardness, b and G are functions of the sliding distance. A general equation of the form

$$\frac{\Delta V}{\Delta L} = [C\frac{\Delta W}{P_m} - \gamma b^2]\ Cot\theta \qquad (3.10)$$

can be obtained for indentors of different shape where the values of C and γ depends on the geometry of the indentor:

$$\frac{\Delta V}{\Delta L} = (\frac{\Delta W}{P_m} - 2b^2)\ Cot\theta \qquad \text{Vickers edge first}$$

$$\frac{\Delta V}{\Delta L} = (\frac{\Delta W}{\pi/2 P_m} - 2b^2)\ Cot\theta \quad \text{Conical indentor}$$

$$\frac{\Delta V}{\Delta L} = (\sqrt{3}\frac{\Delta W}{P_m} - 3b^2)\ Cot\theta \quad \text{Triangular facet first}$$

$$\frac{\Delta V}{\Delta L} = (\frac{\sqrt{3}}{2}\frac{\Delta W}{P_m} - 3/2b^2)\ Cot\theta \qquad \text{Triangular edge first}$$

A value of $\gamma = 2$ can be chosen as a representative to give an average effect of the flat area in general. The value of C is chosen as C=0.5 as proposed by Buttery (1969). We can write therefore an equation in general as:

$$\frac{\Delta V}{\Delta L} = (0.5\frac{\Delta W}{P_m} - 2b^2)\ Cot\theta \qquad (3.11)$$

Where,

ΔV = volume change mm^3

ΔL = sliding distance mm

ΔW = load per grit Kg

P_m = hardness (flow pressure) Kg/mm^2

2b = dimension of the flat (scratch width) mm

Similarly, from equation (3.9) we have:

$$\frac{\Delta V}{\Delta L} = 0.5\frac{\Delta W}{P_m} \cot\theta - 2\frac{V}{Gb} \qquad (3.12)$$

A model of the form

$$V = V_o(1-e^{-\eta' L'}) \qquad (3.13a)$$

is chosen for volume of the wear produced. This has been shown by Mulhearn and Samuel (1962) in a pin on disc situation to represent the abrasive wear data well. L' here is the sliding distance of the disc relative to the pin and is related to L, the distance each grit slides along the surface by

$$L' = \frac{\pi D}{l} L$$

l in the above is the specimen length and D=2r where r is pin distance from the centre of the disc. The wear model can therefore be written in an identical form in term of L.

$$V = V_o(1 - e^{-\eta L}) \qquad (3.13b)$$

where $\eta = \eta'\frac{\pi D}{L}$

Differentiating with respect to L, the wear rate $\frac{\Delta V}{\Delta L}$ can be written as

$$\frac{\Delta V}{\Delta L} = \eta V_o\, e^{-\eta L} \qquad (3.14)$$

If the abrasive action of the indentor (equations 3.11 and 3.12) is to match this rate of wear then the volumes of wear flat (b) and G ratio are controlled accordingly. Applying the boundary conditions of the model to equation (3.11) we have:

At very large sliding distances (i.e. when the blunted abrasive grit is no longer producing any abrasive wear)

$$\frac{\Delta V}{\Delta L} = 0, \quad L = \infty$$

$$(0.5\frac{\Delta W}{P_m} - 2b^2)\ \mathrm{Cot}\theta = 0$$

or

$$b = b_o = \tfrac{1}{2}(\frac{\Delta W}{P_m})^{\frac{1}{2}} = \tfrac{1}{2}p_s^{\frac{1}{2}} \qquad (3.15)$$

where $p_s = \frac{\Delta W}{P_m}$ and

b_o = flat dimension at $L = \infty$

At this stage of wear the area of flat on the grit is large enough to support the load without any plastic deformation and the grit is mainly rubbing the surface.

$4b_o^2 = \frac{\Delta W}{P_m}$ which is in agreement with (3.15).

Also from equation (3.12) we have, at very large sliding distances,

i.e. $L = \infty$

$$\frac{\Delta V}{\Delta L} = \tfrac{1}{2}\ (\frac{\Delta W}{P_m})\ \mathrm{Cot}\theta - 2\frac{V}{Gb} = 0$$

which gives

$$V = V_o = \frac{G_o}{8}\ \mathrm{Cot}\theta\ (\frac{\Delta W}{P_m})^{3/2} = \frac{G_o}{8}\ \mathrm{Cot}\theta\ p_s^{3/2} \qquad (3.16)$$

Where V_o and G_o are V and G at $L = \infty$

At the start of tracking (L = 0), the grit is sharp therefore b = 0 and the wear rate equation (3.11) reduces to:

$$\frac{\Delta V}{\Delta L}) = 0.5\frac{\Delta W}{P_m} \text{Cot}\theta \qquad (3.17)$$

$$L = 0$$

Comparing this with (3.14) and replacing for V_o from (3.16), η can be deduced as

$$\eta = \frac{4}{G_o}\left(\frac{\Delta W}{P_m}\right)^{-\frac{1}{2}} = \frac{4}{G_o} p_s^{-\frac{1}{2}} \qquad (3.18a)$$

or

$$\eta' = \frac{4}{G_o}\left(\frac{\Delta W}{P_m}\right)^{-\frac{1}{2}} \cdot \frac{l}{\pi D} = \frac{4}{G_o}\left(\frac{l}{\pi D}\right) p_s^{-\frac{1}{2}} \qquad (3.18b)$$

The wear model is therefore completely defined in terms of the following parameters:

$$G_o = \frac{V}{v})_{L=\infty}$$

$$P_s = \frac{\Delta W}{P_m}$$

θ = half angle of the scratch

Therefore

$$V = \frac{G_o}{8} \text{Cot}\theta \left(\frac{\Delta W}{P_m}\right)^{3/2} \left[1 - e^{-\frac{4}{G_o}\left(\frac{\Delta W}{P_m}\right)^{-\frac{1}{2}} .L}\right] \qquad (3.19a)$$

or

$$V = \frac{G_o}{8} \text{Cot}\theta \left(\frac{\Delta W}{P_m}\right)^{3/2} \left[1 - e^{-\frac{4}{G_o}\left(\frac{\Delta W}{P_m}\right)^{-\frac{1}{2}} \cdot \frac{l}{\pi D} L'}\right] \qquad (3.19b)$$

The final wear volume V_o depends on G_o, p_s and θ whereas the form of the wear curve (η) depends on p_s and G_o and is independent of the grit geometry (θ). The wear rate $\frac{\Delta V}{\Delta L}$ can be expressed as a function of sliding distance by differentiating (3.19) to give:

$$\frac{\Delta V}{\Delta L} = \tfrac{1}{2}\left(\frac{\Delta W}{P_m}\right) \text{Cot}\theta \; e^{-\frac{4}{G_o}\left(\frac{\Delta W}{P_m}\right)^{-\frac{1}{2}} L} \qquad (3.20a)$$

$$\frac{\Delta V}{\Delta L'} = \tfrac{1}{2}\left(\frac{\Delta W}{P_m}\right) \text{Cot}\theta \; \frac{l}{\pi D} \; e^{-\frac{4}{G_o}\left(\frac{\Delta W}{P_m}\right)^{-\frac{1}{2}} \cdot \frac{l}{\pi D} L'} \qquad (3.20b)$$

Using equations (3.11) and (3.20), the area of flat can be expressed as

$$4b^2 = \left(\frac{\Delta W}{P_m}\right) \left(1 - e^{-\eta L}\right) \qquad (3.21)$$

Considering $v = b^3 \text{Cot}\theta$ in general, since v and V are both functions of sliding distance, G can be expressed as

$$G = G_o \left(1 - e^{-\eta L}\right)^{-\frac{1}{2}} \qquad (3.22)$$

where $G_o = 4/\eta \; p_s^{-\frac{1}{2}}$

Although G depends on sliding distance, the model depends on the constant G_o only. There is no independent test to measure this parameter directly and therefore measurement of a single point is initially required to calculate G_o factor which determines the model.

3.3 Application to Abrasive Paper

To apply the theory developed so far for a single grit to the

conditions of abrasive paper it is assumed that the abrading action of abrasive grits on the paper produces independent events with no interaction on each other. It is further assumed that the grits are of the same geometry, aligned with their major axis perpendicular to the surface of the paper and are at the same height. The volume of wear produced by the abrasive paper is then equal to simple addition of the wear of single grits. For a pin on disc situation each section of the abrasive disc having an area equal to the pin contacting surface A and along a ring of diameter D (D = 2r where r is pin distance from the centre of the disc) will have a wear rate equal to:

$$\frac{\Delta V_1}{\Delta L} = C.A.\left(\frac{0.5\Delta W}{P_m} - 2b^2\right) \text{Cot}\theta$$

where

C = number of cutting points on the paper per mm^2.

A = apparent area of contact (area of the specimen).

If the load on the pin W is equally shared by the grits,

$W = C.A.\ \Delta W$

and we have

$$\frac{\Delta V_1}{\Delta L} = \left(0.5\frac{W}{P_m} - 2ACb^2\right) \text{Cot}\theta$$

and similarly , from equation (3.12)

$$\frac{\Delta V_1}{\Delta L} = 0.5\ \frac{W}{P_m}\ \text{Cot}\theta - 2\frac{V_1}{Gb}$$

Since there are $\frac{\pi D}{l}$ sections each of an area A around the disc the total wear rate $\frac{\Delta V}{\Delta L}$ can be written as

$$\frac{\Delta V}{\Delta L} = \frac{\pi D}{l}\left(0.5\frac{W}{P_m} - 2ACb^2\right) Cot\theta \qquad (3.23)$$

or

$$\frac{\Delta V}{\Delta L} = 0.5\frac{\pi D}{l} \cdot \frac{W}{P_m} Cot\theta - 2\frac{V}{Gb} \qquad (3.24)$$

Again by applying the boundary conditions the following equation can be obtained similar to those derived for a single grit, or alternatively the wear model may be obtained by summation of equation (3.19), the wear model of a single grit ($\frac{\pi D}{l}$.A.C.) times.

$$b_o = \tfrac{1}{2}(AC)^{-\frac{1}{2}} p^{\frac{1}{2}} \qquad (3.25)$$

$$V_o = \frac{G_o}{8}(AC)^{-\frac{1}{2}} Cot\theta \frac{\pi D}{l} p^{3/2} \qquad (3.26)$$

$$\eta = \frac{4}{G_o}(AC)^{\frac{1}{2}} p^{-\frac{1}{2}} \qquad (3.27a)$$

$$\eta' = \frac{4}{G_o}(AC)^{\frac{1}{2}} \frac{1}{\pi D} p^{-\frac{1}{2}} \qquad (3.27b)$$

where $p = \frac{W}{P_m}$ in these equations.

The wear model is given by

$$V = \frac{G_o}{8}(AC)^{-\frac{1}{2}} Cot\theta \frac{\pi D}{l} p^{3/2} \left[1 - e^{-\frac{4}{G_o}(AC)^{\frac{1}{2}} . p^{-\frac{1}{2}} L}\right] \qquad (3.28a)$$

$$V = \frac{G_o}{8}(AC)^{-\frac{1}{2}} Cot\theta \frac{\pi D}{l} p^{3/2} \left[1 - e^{-\frac{4}{G_o}(AC)^{\frac{1}{2}} \frac{1}{\pi D} . p^{-\frac{1}{2}} . L'}\right] \qquad (3.28b)$$

And the wear rate can be written as:

$$\frac{\Delta V}{\Delta L} = \tfrac{1}{2}\left(\frac{\pi D}{l}\right) p\ Cot\theta\ e^{-\eta L} \qquad (3.29a)$$

or

$$\frac{\Delta V}{\Delta L'} = \tfrac{1}{2}p \, \mathrm{Cot}\theta \, e^{-\eta' L'} \qquad (3.29b)$$

In wear studies the discrepency between the theoretical and practical wear rates are usually accounted for by introducing two factors:

α - probability of grits which are cutting at any one time.

β - proportion of the scratch volume removed.

In developing the blunt grit theory, however, so far it has been assumed that every grit produces a wear particle and that the efficiency of material removal for each event is 100%. A further source of discrepency could lie in the assumption by the theory that the only change taking place by the abrasive grit is due to attricious wear which results in wear flats at the tip of cutting points. In practice grits can pull out of their bonds, fracture or glaze. The fracture (and pull out in grinding wheel) results in sharp and fresh cutting points to be introduced to the metal; a process known as self sharpening. Although the flat area caused by attricious wear is an important factor in controlling the wear rate, the process of self sharpening can increase the wear rate which results in the prediction by the theory to be under estimated.

If va is volume of abrasive being lost due to attricious wear, then we have

$$G = \frac{V}{v_a}$$

In general, the abrasive loss, v, can be thought of as

$$v = v_a + v_f$$

where $v_f = v_{fracture} + v_{pull-out}$

The ratio of metal to abrasive loss $\frac{V}{v}$ can therefore be written as:

$$\frac{V}{v} = \frac{V}{v_a + v_f} = \frac{V}{v_a(1+\frac{v_a}{v_f})} = \frac{V}{v_a} \times \frac{1}{1+\frac{v_a}{v_f}} = G \times \frac{1}{1+\frac{v_a}{v_f}}$$

Where $\frac{1}{1+v_a/v_f}$ can be viewed as a measure of self-sharpening. Equations (3.25 to 3.31) derived for the model should therefore be modified to incorporate these new parameters. Combining the three parameters α, β and $\frac{1}{1+v_a/v_f}$ into a single parameter f, we have:

$$b_o = \tfrac{1}{2}(AC)^{-\frac{1}{2}} p^{\frac{1}{2}} \qquad (3.30)$$

$$V_o = \frac{G_o}{8} f (AC)^{-\frac{1}{2}} \cot\theta \frac{\pi D}{l} p^{3/2} \qquad (3.31)$$

$$\eta = \frac{4}{G_o} (AC)^{\frac{1}{2}} p^{-\frac{1}{2}} \qquad (3.32a)$$

$$\eta' = \frac{4}{G_o} (AC)^{\frac{1}{2}} \frac{l}{\pi D} p^{-\frac{1}{2}} \qquad (3.32b)$$

$$V = \frac{G_o}{8} f (AC)^{-\frac{1}{2}} \cot\theta \frac{\pi D}{l} \left(\frac{W}{P_m}\right)^{3/2} \left[1 - e^{-\frac{4}{G_o}(AC)^{\frac{1}{2}}\left(\frac{W}{P_m}\right)^{-\frac{1}{2}}.L}\right] \qquad (3.33a)$$

or

$$V = \frac{G_o}{8} f (AC)^{-\frac{1}{2}} \cot\theta \frac{\pi D}{l} \left(\frac{W}{P_m}\right)^{3/2} \left[1 - e^{-\frac{4}{G_o}(AC)^{\frac{1}{2}}\left(\frac{W}{P_m}\right)^{-\frac{1}{2}} \cdot \frac{l}{\pi D}.L'}\right] \qquad (3.33b)$$

$$\frac{\Delta V}{\Delta L} = \tfrac{1}{2}\, f\, \frac{\pi D}{l}\left(\frac{W}{P_m}\right)\, \mathrm{Cot}\theta\, e^{-\eta L} \qquad (3.34a)$$

or

$$\frac{\Delta V}{\Delta L} = \tfrac{1}{2}\, f\, \left(\frac{W}{P_m}\right)\, \mathrm{Cot}\theta\, e^{-\eta' L'} \qquad (3.34b)$$

Figure (3.2) shows schematically the characteristics of abrasive wear process according to the blunt grit and sharp grit models.

3.4 Verification of the theory

Before performing any experiment it was decided to check the theory using available data from the literature. Table (3.1) shows the results of an experiment with grade 60 aluminium oxide abrasive paper rubbing against SKF steel at hardened condition (900 VH), Mackie (1982). The final values of wear after 4 hours of run are recorded for different levels of force. The table also includes the corresponding values of M_o as predicted by the theory. A good degree of agreement can be observed. Figure (3.3) is a plot of the experimental data and the values of M_o as predicted by the theory. In calculating M_o by the model the first point of the experimental data (Force = 2N, M_o = 0.0619) has been used to calculate G_o. Values of M_o at different levels of force are then calculated using the relationship $M_o = \frac{1}{8} \rho\, G_o\, \mathrm{Cot}\theta\, (CA)^{-\frac{1}{2}} \cdot \frac{\pi D}{l}\, p^{3/2}$ and assuming

$\rho = 0.0079$ gr/mm^3

$\mathrm{Cot}\theta = 0.158$

$CA = 7$ Mackie (1982)

The variation of wear with sliding distance is shown in table (3.2) and figure (3.4) for both the experimental (Mackie 1982) and the blunt grit model in the case of 18N applied load. Other conditions being similar to those of previous test. The model was determined using the last point of the experimental data as M_o to calculate (G_o) parameter. This was then used to calculate the wear at different sliding distances using equation (3.33) and assuming f=1.

3.5 Experimental procedure

A number of tests were carried out which involved rubbing steel pins against abrasive discs. The same area on the disc was used in each test to observe the changes in the wear rate with the deterioration of abrasive grits. The main parameters influencing the abrasive wear process which also appear in the abrasive wear models are:

1 - Load

2 - Abrasive (its type, relative hardness, and shape and size of the grits)

3 - Sliding distance

4 - Specimen material (its metallurgical structure and hardness, and the size of the specimen).

The less important factors such as the velocity of the abrasive, humidity and the temperature have little or no influence on wear process. According to Nathan and Jones (1966) the variations in the atmosphere temperature and humidity would have little effect; these views also being held by Kruschov and Babichev (1960). The velocity of

the abrasive surface has been shown to affect the degree of frictional heating induced in the abraded material. Temperatures in the range of 320-900°C have been observed at the grit chip interface, Moore (1971). According to Moore, however, the overall effect on abrasive wear is likely to be small.

Load

The combined effect of the level of applied force and the hardness of the specimen is a major influence on the wear rate and the rate of deterioration of abrasive. In the test reported here a load of 1.536 Kg was employed.

Specimen

These were 6x6 mm square sectioned pins, 30 mm long and approximately 8 gr in weight (density 7.71×10^{-3} g/mm^3). A ball bearing steel, SKF, 1%C, 1.5% Cr was selected as test material which is known to respond well to heat treatment. The square section chosen for the pin ensured that each grit experienced the same degree of contact with the specimen. Whilst a small area for the pin is desirable to avoid clogging of the abrasive surface, this is on the other hand restricted by a minimum area required for an accurate assessment of the surface texture. A 6x6 mm^2 dimension was therefore decided to allow traces from the pin surfaces to be taken.

Abrasive

Aluminium oxide abrasive discs grade 60 were used for these experiments. Aluminium oxide is widely used in the form of coated abrasives for the removal of materials. The grits used in a grade 60 abrasive paper are

large enough to reveal the formation of any flat on them during wear at normal degrees of magnification, (x100).

Test Rig

Figure (3.5) shows the pin on disc configuration used for these tests. A lathe cross-slide mechanism is adapted to carry a specimen holder which would provide a relocatable pin on disc configuration. The load is applied through a lever and by changing the weights and their positions on the lever a variety of loads can be applied. A variable speed system is incorporated to give a wide range of r.p.m. which can be set and monitored.

Experiments

The tests involved rubbing a steel pin under a load of 1.536 Kg at a fixed position against abrasive discs of grade 60. The pin was polished and positioned at 5 cm from the centre of the disc at a constant r.p.m. (288) to give a sliding speed of 90.5 m/min. The disc was stopped at certain intervals for measurements to be taken.

The change in the specimen weight (wear) was measured using a Sartorius balance to an accuracy of 0.00001 gr.

Surface texture of the pin was measured using a Talydata 2010 system. This is a Talysurf 10 interfaced to a microcomputer with special software which provides a wide range of surface parameters.

At each interval the abrasive disc was removed carefully to be monitored under a microscope for observation and measurement of the area of flats

formed on the cutting grit tips. Assessment was made by dividing the circular track of the pin on disc into four equal regions. Nine random position from each region were monitored under a microscope at a (x100) magnification. This magnification gave a 1 mm^2 field of view; the area of any flat within which was measured. A value for the flat area was then obtained by averaging the 36 recorded sample values. A similar procedure was adapted to estimate the number of active grits at the final stage of the wear process. In this case, however, 25 random positions were chosen within each region on the track; the number of polished cutting points being counted each time within 1 mm square field of view. A value for C the number of cutting points per mm square of the abrasive was estimated by averaging the number of cutting points for the 100 random samples.

3.6 Results

Table (3.3) contains the summary of the results of a typical experiment. Generally the abrasive wear experiments gave a reduction in the rate of wear with increase in sliding distance. The value of Ra and average slope of the surface of the pin also fell as sliding distance increased, Table (3.3). The table also contains the measured area of flats and shows that this parameter increases with sliding distance. These changes are plotted in figure (3.6) to (3.9).

To apply the results to theory an average value of θ (the half apex angle of a typical grit) is required. This was estimated by averaging the values obtained for average slope (Δa) at different stages during the wear process. The half apex angle of the grit could

then be calculated as

$$\theta_{ave} = 90 - (\Delta a)_{ave} = 90 - 12 = 78^{\circ}$$

The last value for Δa at the sliding distance of 27150 m, however, was disregarded since at this stage the process is mainly of rubbing rather than cutting on which the theoretical model is based. Other values used in the model are

$C = 0.2$ number of cutting points per mm^2.

$P_m = 720$ Kg per mm^2.

Table (3.4) shows the prediction by the sharp grit theory and blunt grit theory compared with the experimental values obtained for wear at several sliding distances. The large deviation between the sharp grit model and the experimental values is to some extent reduced when the value of θ_{ave} is replaced by the value of θ obtained at each stage of the wear (Modified Sharp Grit). Figure (3.10) shows the modified values of sharp grit theory (Table 3.4) compared with the experimental data.

The prediction by the blunt grit model taking into account the estimated values for the area of flats at the tip of cutting points and using equation (3.23) is also included in Table (3.4). At sliding distances of 16290 m or more a negative value is obtained indicating that the wear has already reached the rubbing stage where according to the model any further sliding would not result in wear by cutting and only increase the rubbing flat areas. (Figure 3.11).

The blunt grit model is also capable of predicting the wear process without any knowledge of the wear flats (equation 3.33). In this form, however, the value of the parameter G_o is required. Using equation (3.34) at 90.5 m sliding distance since the wear at this stage is almost linear we can replace $\frac{\Delta V}{\Delta L}$ by $\frac{V}{L}$. G_o can now be calculated using the experimental value of wear at this point as:

$G_o = 6897 \times 10^3$

The values for M_o and η can then be calculated from equations (3.31) and (3.32) as

$M_o = 2.72$ gr

$\eta' = 6.4 \times 10^{-7}$

By using equation (3.33) it is now possible to predict the amount of wear at any sliding distance, Table (3.4) and figure (3.12). Figure (3.13) shows a comparison between the modified version of sharp grit theory, blunt grit theory and the actual values.

It should be mentioned here that had the last point of the experimental values been used as M_o to calculate G_o, then different values would have been derived for G_o and η. This is shown in figure (3.14).

3.7 Discussion

The experimental results showed, as expected, a gradual reduction in wear rate as wear proceeds. At the same time as the severity of the wear reduced the surface roughness of the pin improved and this was

accompanied by a reduction in the average slope, figures (3.7) and (3.8); these changes being in line with the blunt grit model. The wear rate although very small at prolonged running was somewhat greater than the values predicted by the theory. Unlike the model which assumes a zero rate of wear once the area of flats is large enough to support the load without any plastic deformation, the experimental values always showed some degree of wear even at very large sliding distances, figure (3.6). The increase in the actual area of flats at grit tips, figure (3.9) was also found to be somewhat higher than expected by the theory specially at the latter stages of wear. As a result the prediction of wear by theory, equation (3.23) taking into account the estimated actual plateaux areas resulted in negative values at later stages of the wear, Table (3.4) and figure (3.11). This high value obtained for the area of flats could be due to several reasons:

- The model assumes that the plateaux produced are rubbing against a flat surface parallel to the area of flats. This leads to the assumption that the contact area between the grit and the surface which support the load is equal to the plateaux area. Such condition does not happen in practice. The work-surface is rough and consequently only part of the flat land area rubs against the surface and supports the load. As the wear proceeds and the flat area grows with respect to the average wavelength of the surface this portion which is of relevance to the blunt grit model reduces to smaller percentage of the total area of flat and therefore higher values expected to be observed in practice.

- It is assumed by the theory that the reduction in wear rate during the process is brought about solely by the formation of flats at grit tips which support the load. The model, therefore, neglects other factors such as temperature, work hardening and the effect of clogging. It can be argued for instance that the worn part of the abrasive grains increases the heat generation by rubbing mechanism and results in an increase in the cutting resistance of the workpiece. The combined effect of these factors can contribute to a change in the wear rate and therefore the values assumed by the model for flat areas would be different from the actual results.

- During the test runs slight vibration was present. It is therefore expected to observe larger flat areas due to the extra dynamic load on the pin which was not accounted for by the model.

- Finally since the theory is concerned with the effect of flat area on wear rate and not their values it assumes that when the area is large enough to support the load the wear rate becomes zero and further growth in the plateaux area is neglected. In reality, however, they carry on growing, their rate of growth could even increase at this stage due to extensive rubbing and three body abrasion.

Figure (3.3) shows M_o, the final amount of wear, against different loads. The good match between the theory and the experimental values is due to one of the outcomes of the theory, namely the wear is proportional to the $W^{3/2}$ rather than W as suggested by the sharp grit model. The prediction of the actual values of wear by the model equation

(3.28) at different sliding distances is reasonably well assuming f=1 as shown in figures (3.12) and (3.14). This is clearly shown in figure (3.13) in comparison with the modified sharp grit model. As can be seen from figures (3.12) and (3.14) however, the form of the model differs depending which point of the experimental results was used to calculate the constant G_o of the model. If the value of wear at the sliding distance 90.5m is used to calculate G_o, Table (3.4), then at large values of sliding distance the theory overestimates the actual values, figure (3.12). On the other hand, if the last point in Table (3.4), i.e. the wear at sliding distance 27150m is taken as M_o to deduce G_o then the model tends to deviate from the actual values at the initial stages of wear, figure (3.14). This rigidity in the model arises from the fact that the exponential form used for blunt grit is determined, mathematically, by two independent parameters, namely η and M_o, equation (3.13). These parameters in the model however, are not independent. The relationship between them can be expressed as

$$M_o \eta = \frac{p}{2} \left(\frac{W}{P_m}\right) \cot\theta$$

This is the consequence of the assumption by the theory that the area of the flat is the only parameter affecting the wear rate and as a result the model is defined by the parameter G_o only; M_o and η are both defined by G_o, equation (3.26) and (3.27). The introduction of the parameter f into the model suggests that other factors are also responsible in the change of wear rate and mathematically allows the parameters η and M_o to be independent which makes the model more flexible. Figure (3.15) shows the improved model taking into account the factor f.

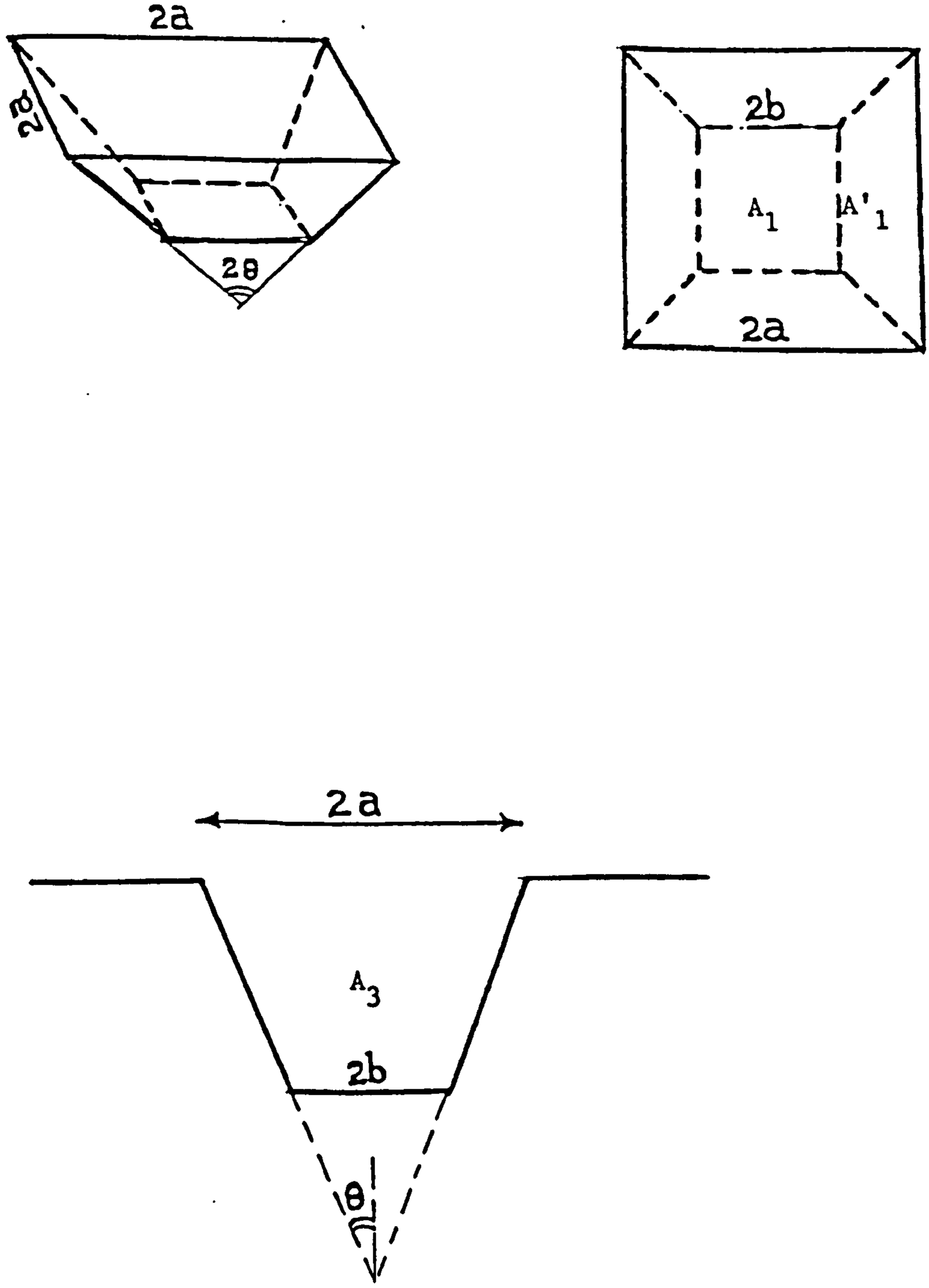

Figure 3.1 Geometry of a blunted grit and the idel scratch produced by it.

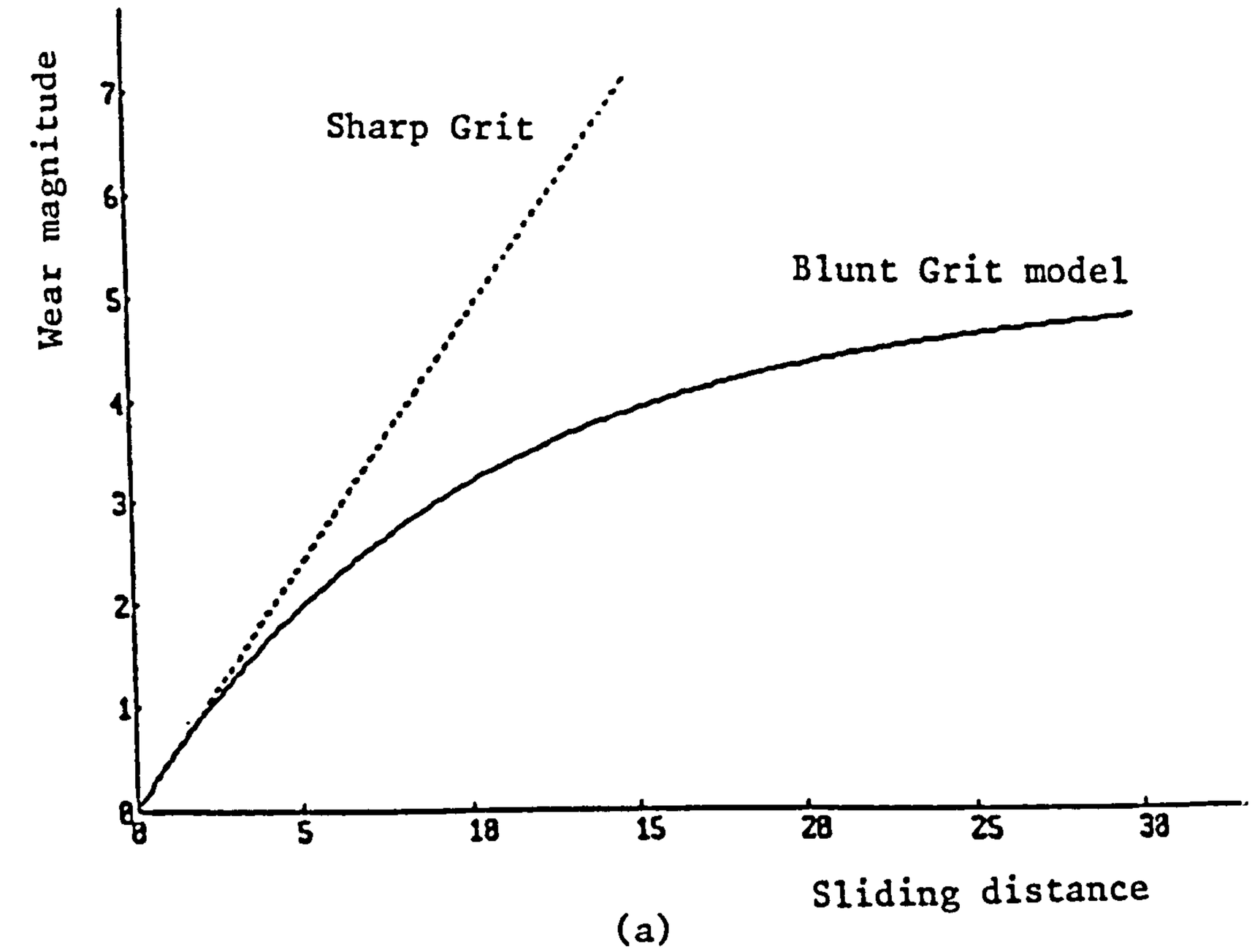

(a)

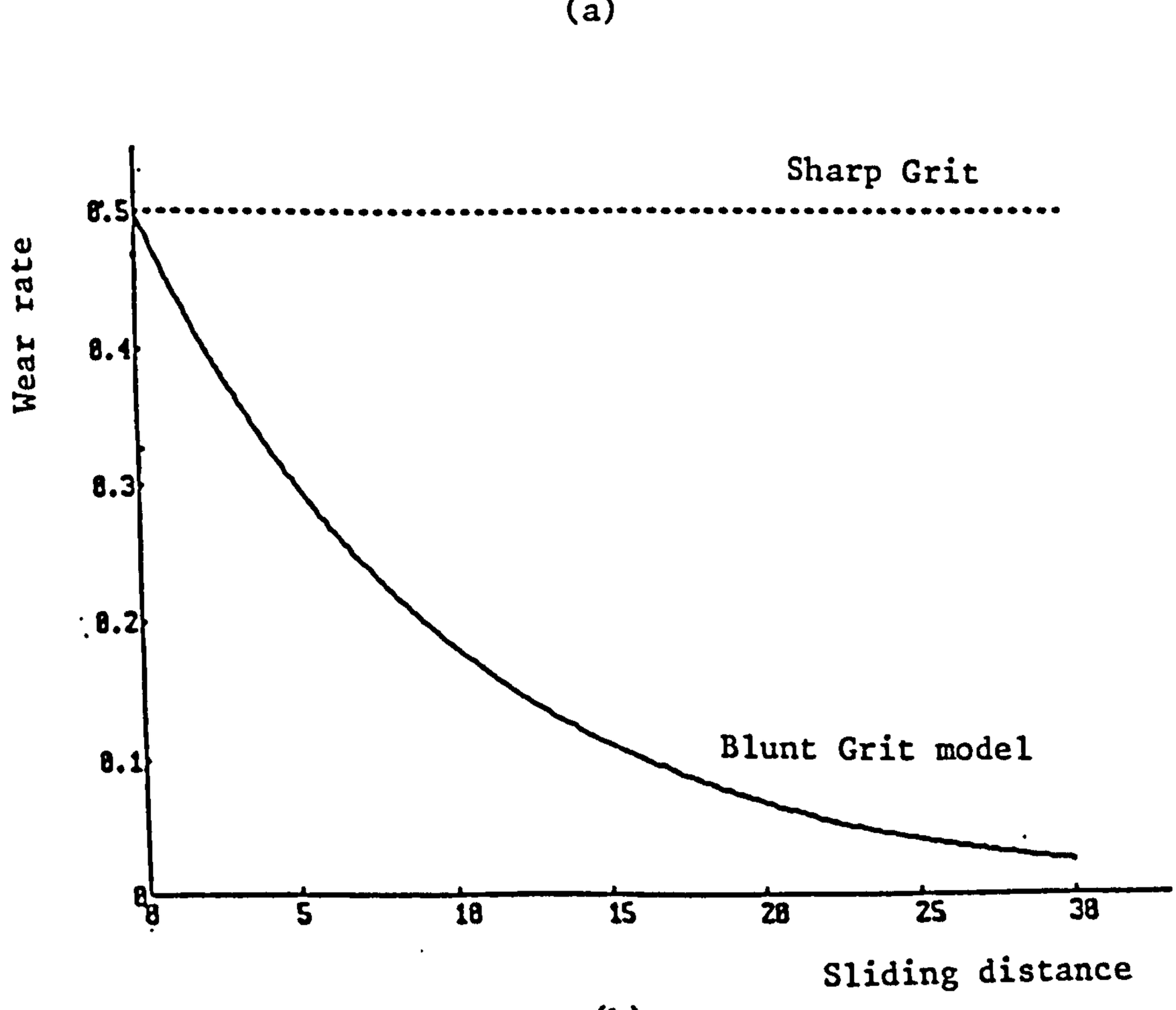

(b)

Figure 3.2 Schematic representation of the Blunt Grit model; (a) wear against sliding distance, (b) wear rate against sliding distance.

Load (N)	2	5	7	10	15	18
M_o Experiment	0.0619	0.253	0.346	0.647	1.071	1.593
M_o Theory	0.0619	0.244	0.405	0.692	1.271	1.671

Table 3.1 Final values of wear M_o (g) produced after 4 hour at different Levels of Load, Mackie (1982), and the corresponding values of M_o predicted by the Blunt Grit model.

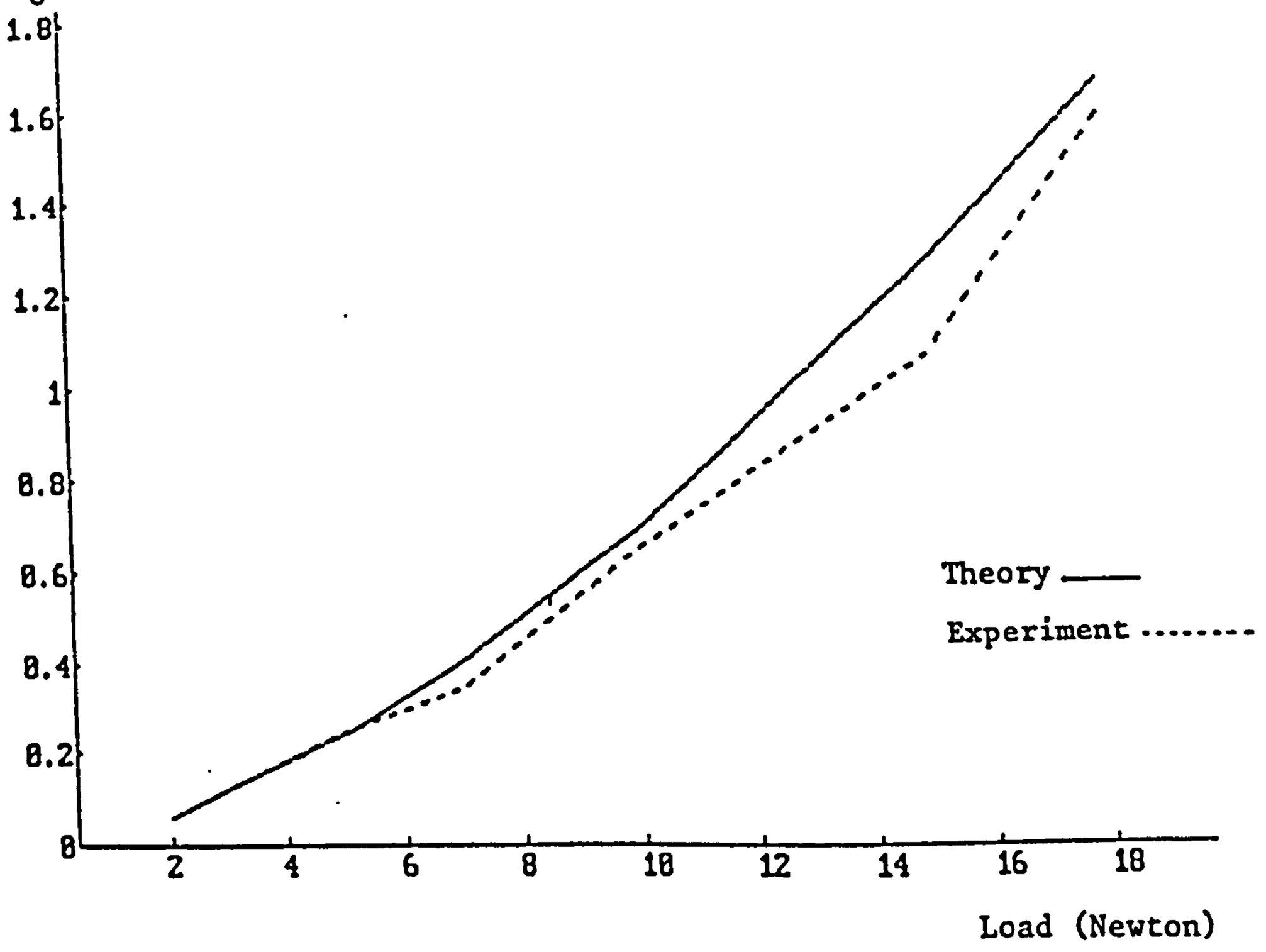

Figure 3.3 Comparison of the model with the experimental data, Table 3.1.

Sliding Distance (m)	180	2655	10665	21510
Weight Loss Experiment	0.258	0.9	1.4	1.593
Weight Loss Theory	0.208	1.39	1.59	1.593

Table 3.2 Wear against sliding distance. Experimental results by Mackie (1982); and the Blunt Grit prediction.

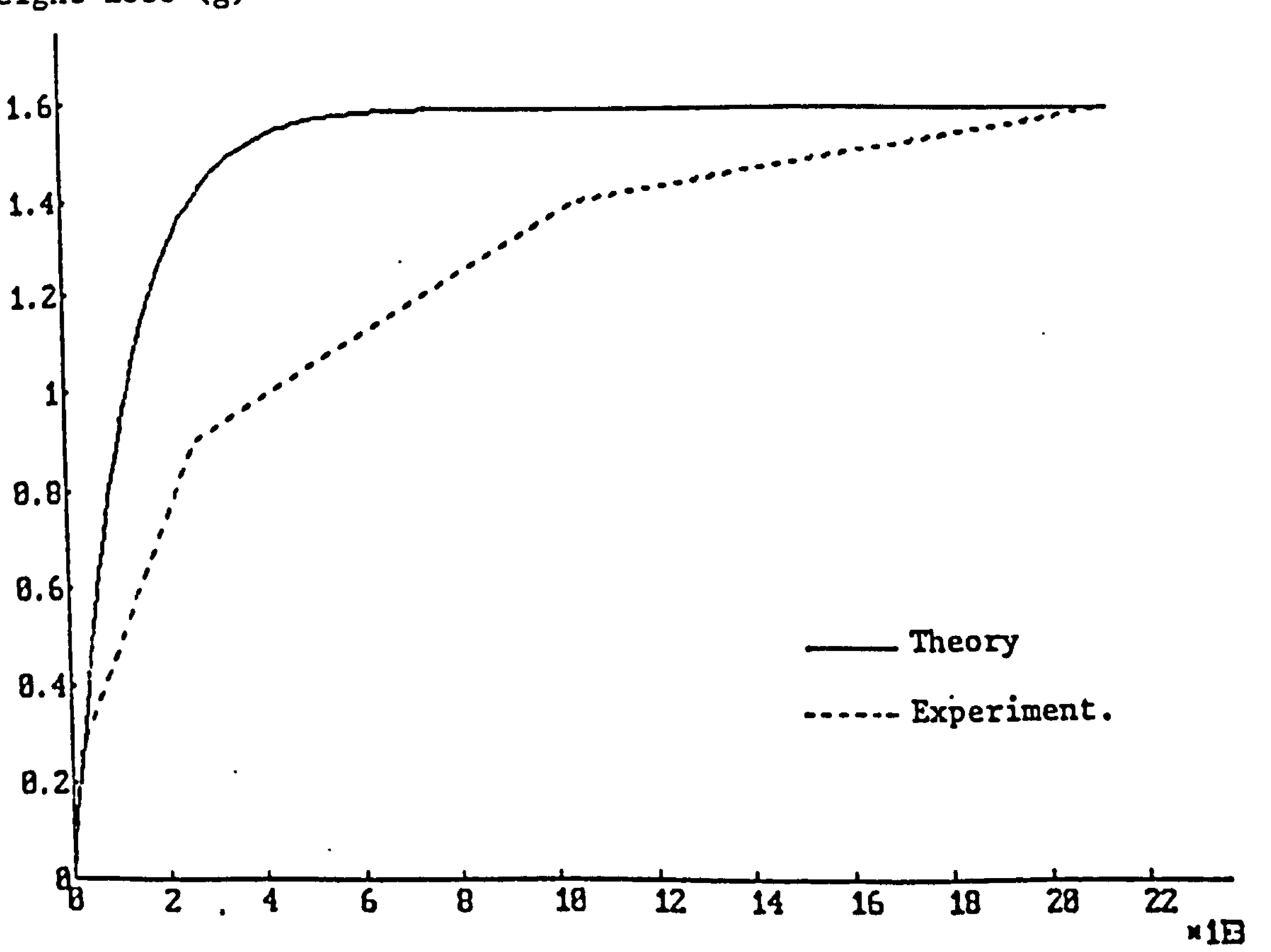

Figure 3.4 Comparison of the model with the experimental data Table 3.2.

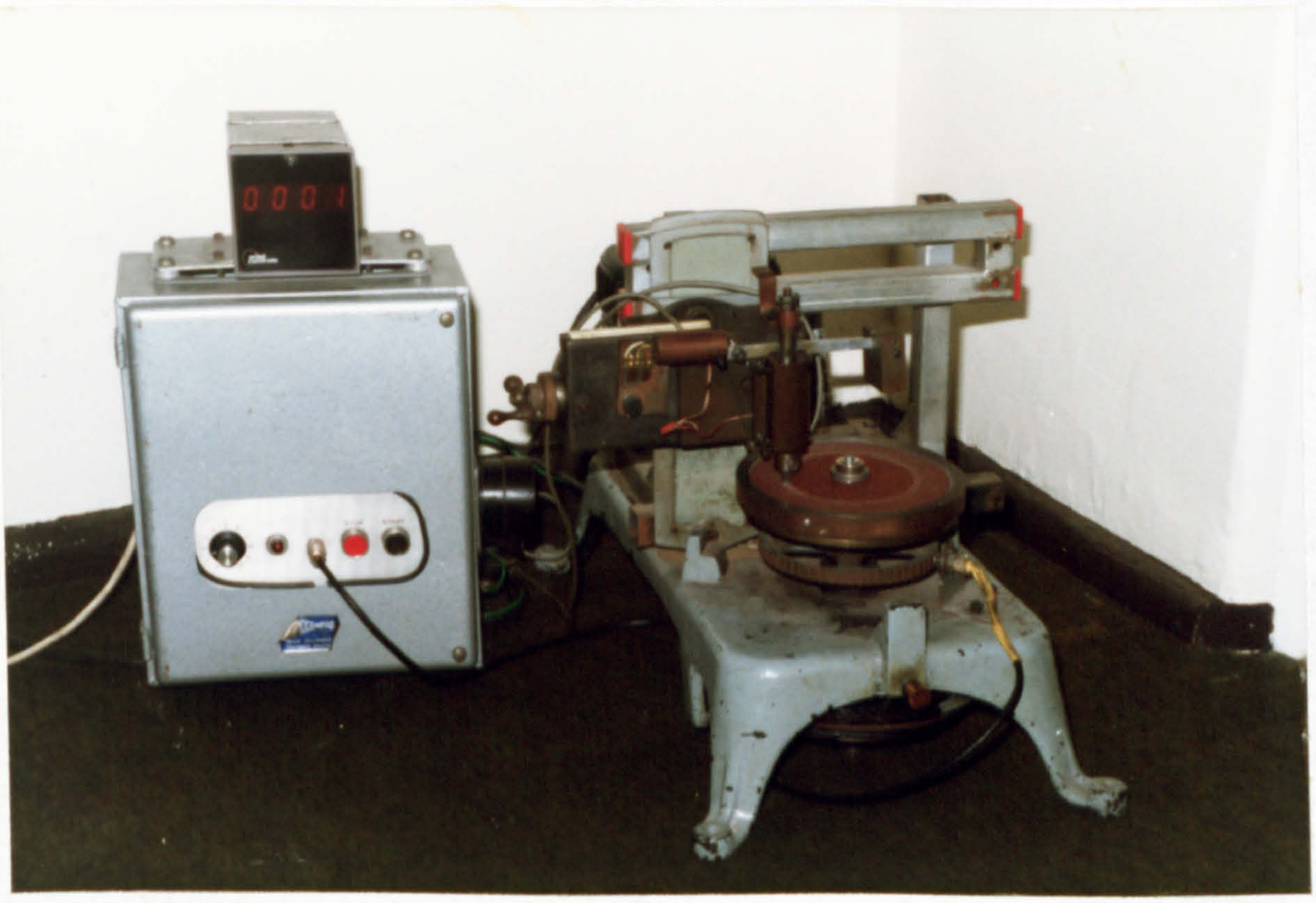

Figure 3.5 Pin on disc test rig.

Sliding Distance (m)	Weight Loss (g)	Surface Roughness μm	Average Slope	Area of Flat per mm^2
90.5	0.1489	3.94	16.1	Negligible
452.5	0.5827	2.20	14.3	4.37×10^{-6}
2262.5	1.0204	2.32	13.8	2.36×10^{-5}
6787.5	1.521	1.80	8.6	2.35×10^{-5}
16290	1.6914	1.67	7.2	1.16×10^{-4}
27150	1.78405	1.45	5.2	5.43×10^{-4}

Table 3.3 Experimental results of an abrasive test at different sliding distances. Pin hardness 720 V.H.

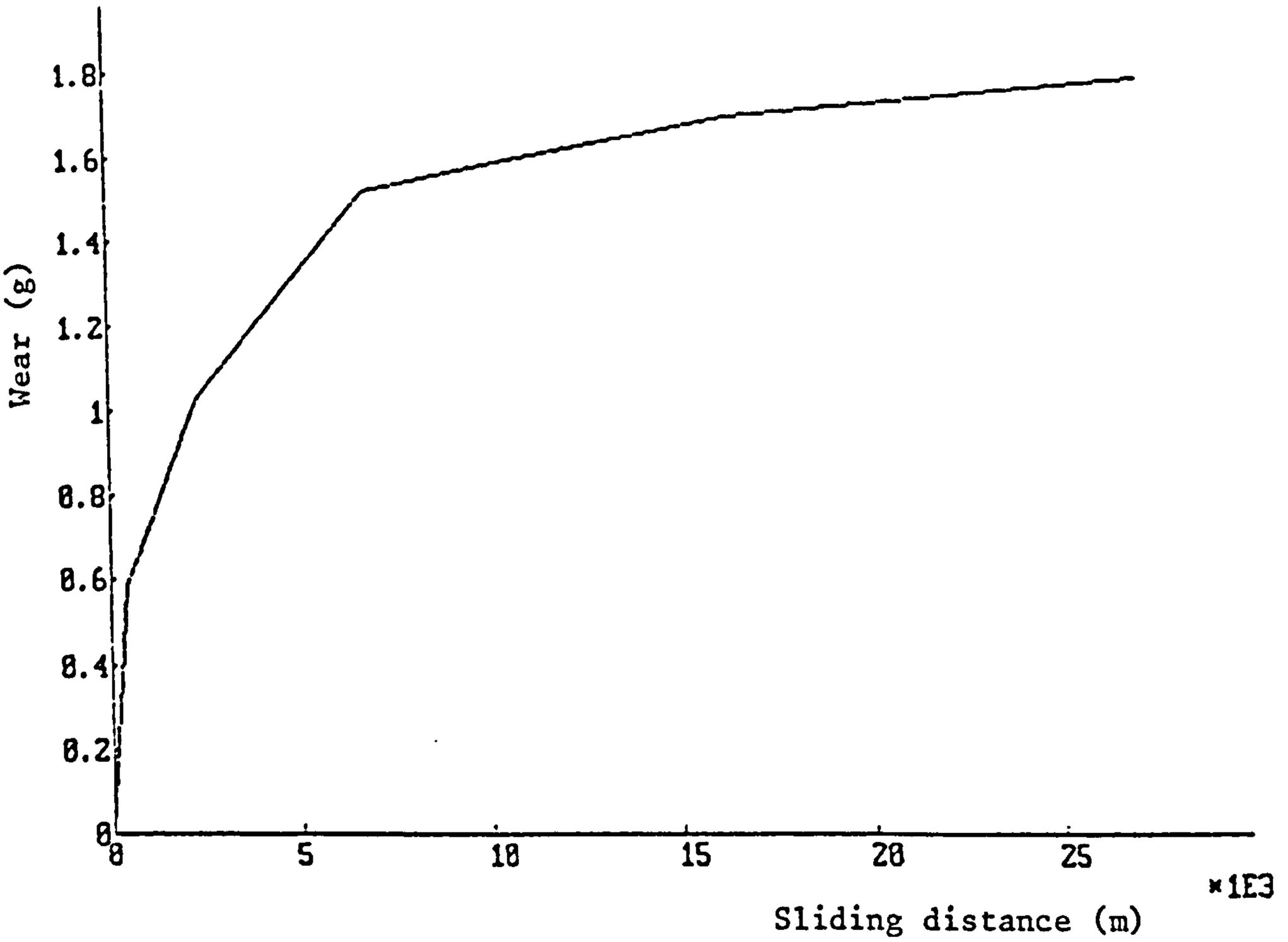

Figure 3.6 Wear against sliding distance. Pin on disc experiment.

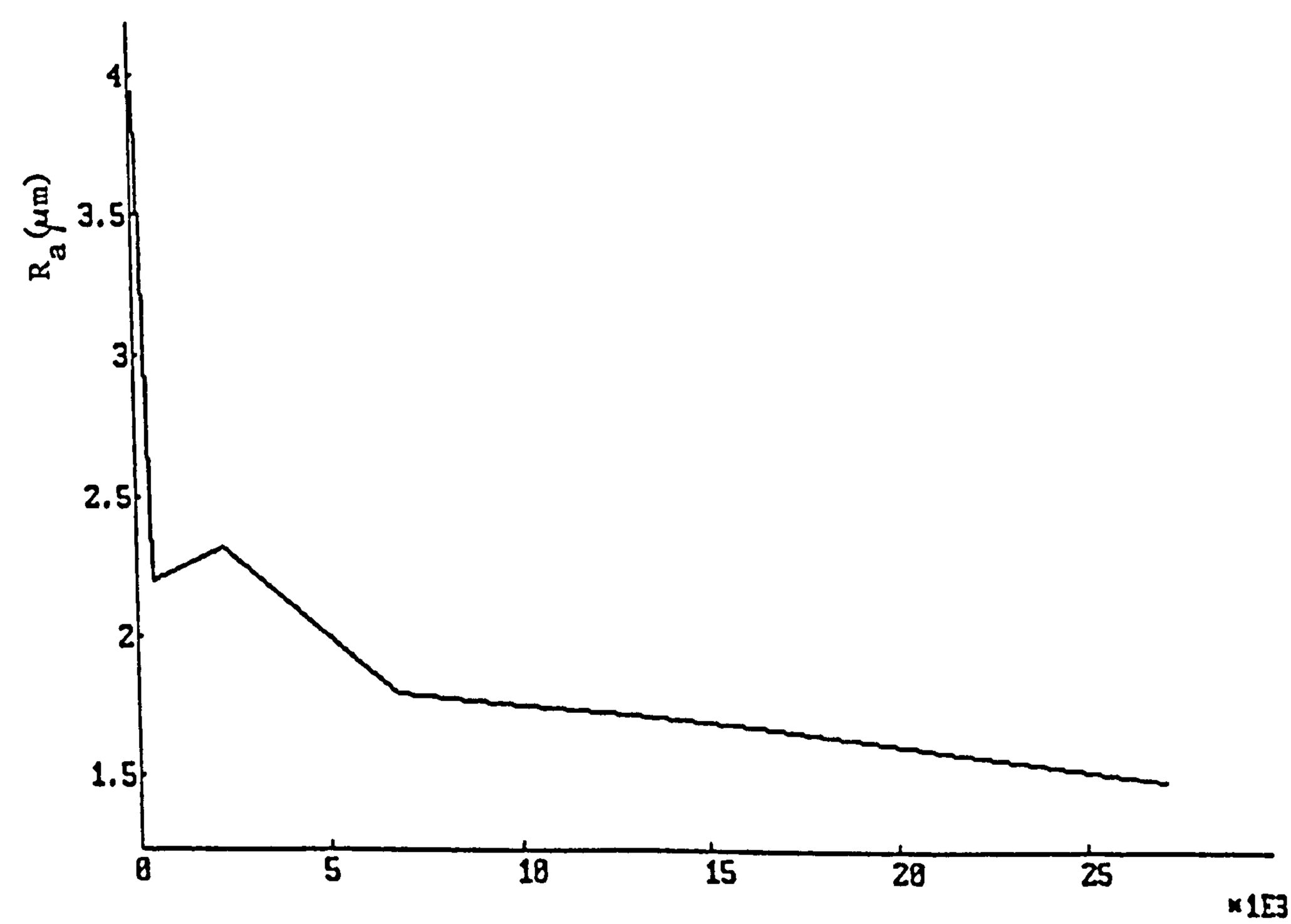

Figure 3.7 Changes in surface roughness of the pin (μm) with sliding distance.

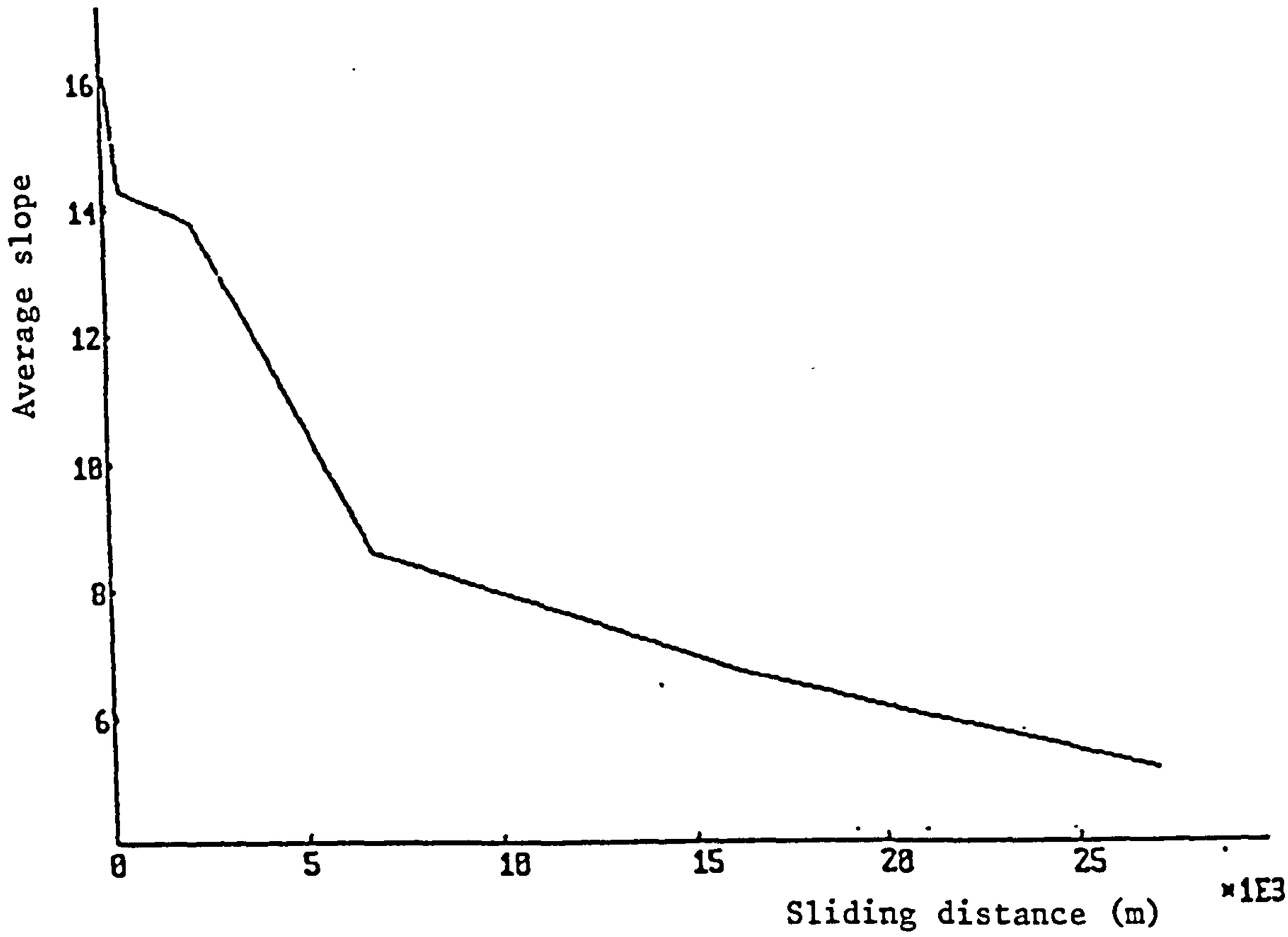

Figure 3.8 Changes in average slope with sliding distance.

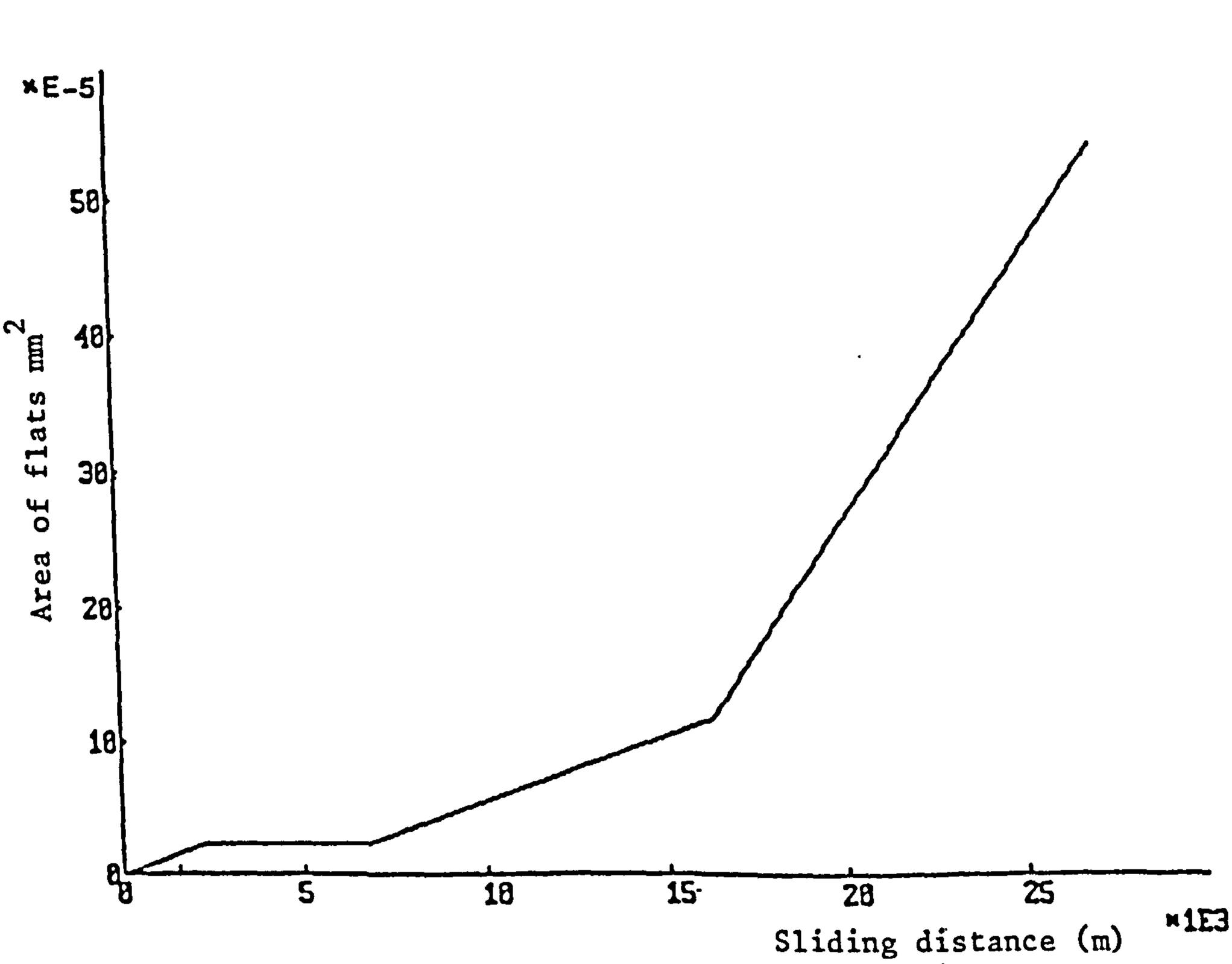

Figure 3.9 Changes in the area of flat (mm^2) per mm^2 of abrasive paper.

Sliding Distance (m)	90.5	452.5	2262.5	6787.5	16290	27150
Experiment	0.1489	0.582	1.020	1.521	1.691	1.784
Sharp Grit Model	0.157	0.788	3.94	11.82	28.37	47.28
Modified Sharp Grit	0.213	0.944	4.55	8.36	15.65	20.07
Blunt Grit Area of Flats	0.157	0.671	0.802	2.43	Negative	Negative
Blunt Grit Model	0.153	0.913	2.08	2.68	2.7	2.719

Table 3.4 Comparison of the experimental wear results (g) with Sharp grit model, Modified Sharp grit, Blunt Grit equation 3.23 and Blunt Grit model equation 3.33.

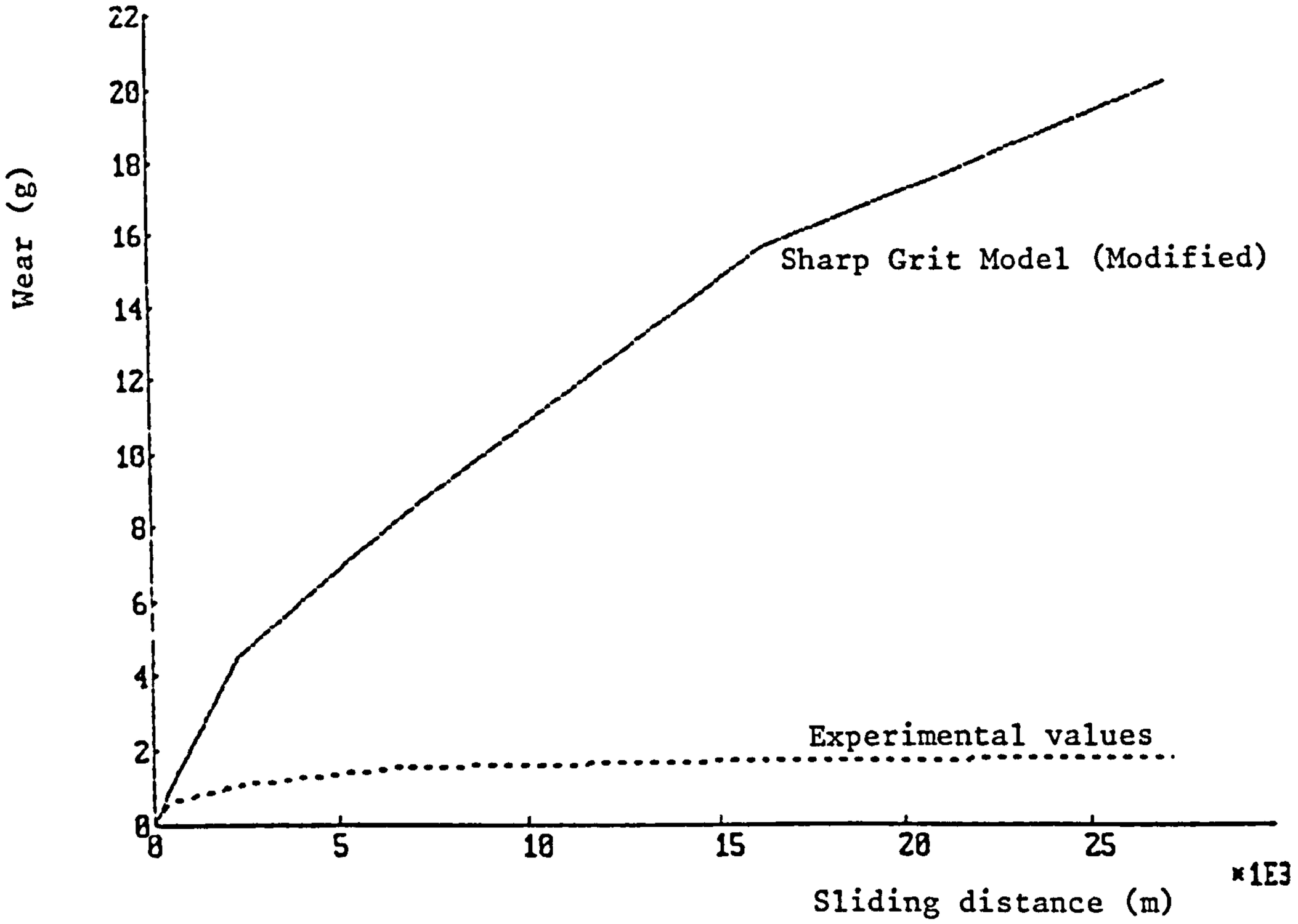

Figure 3.10 Modified Sharp Grit prediction of wear compared with the experimental results.

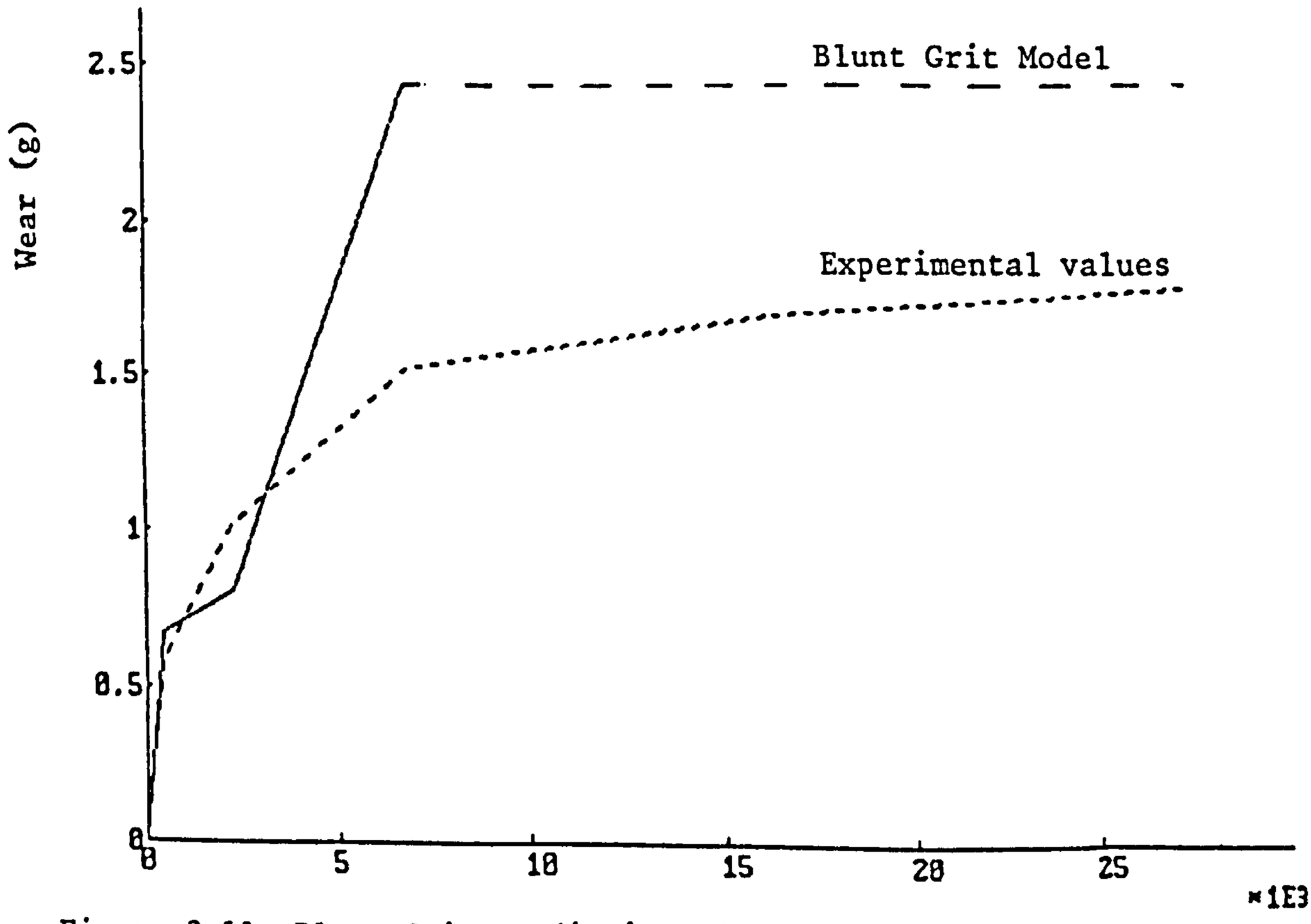

Figure 3.11 Blunt Grit prediction of wear taking into account area of flats compared with experimental results.

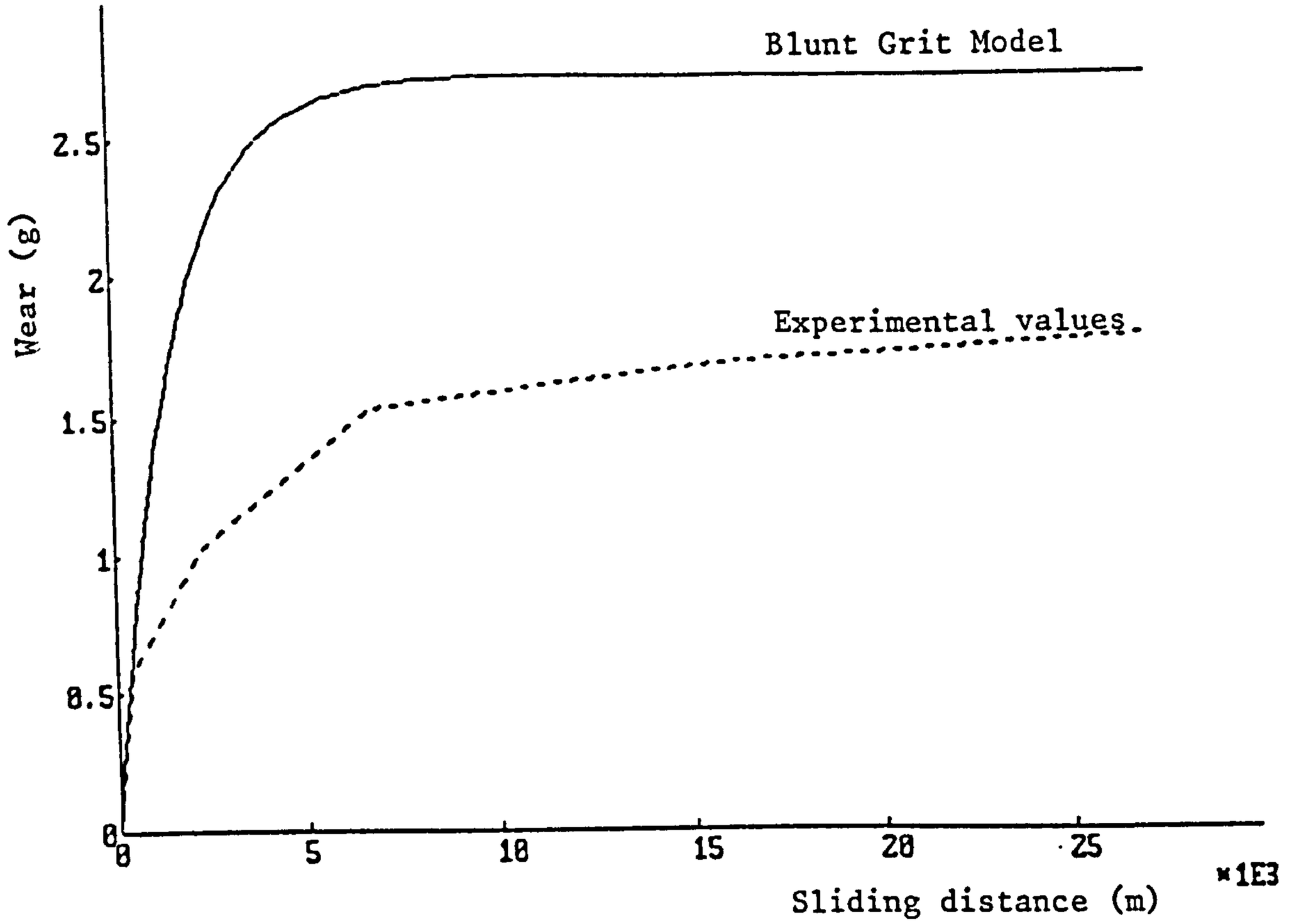

Figure 3.12 Prediction of wear by the Blunt Grit model at different distances of sliding.

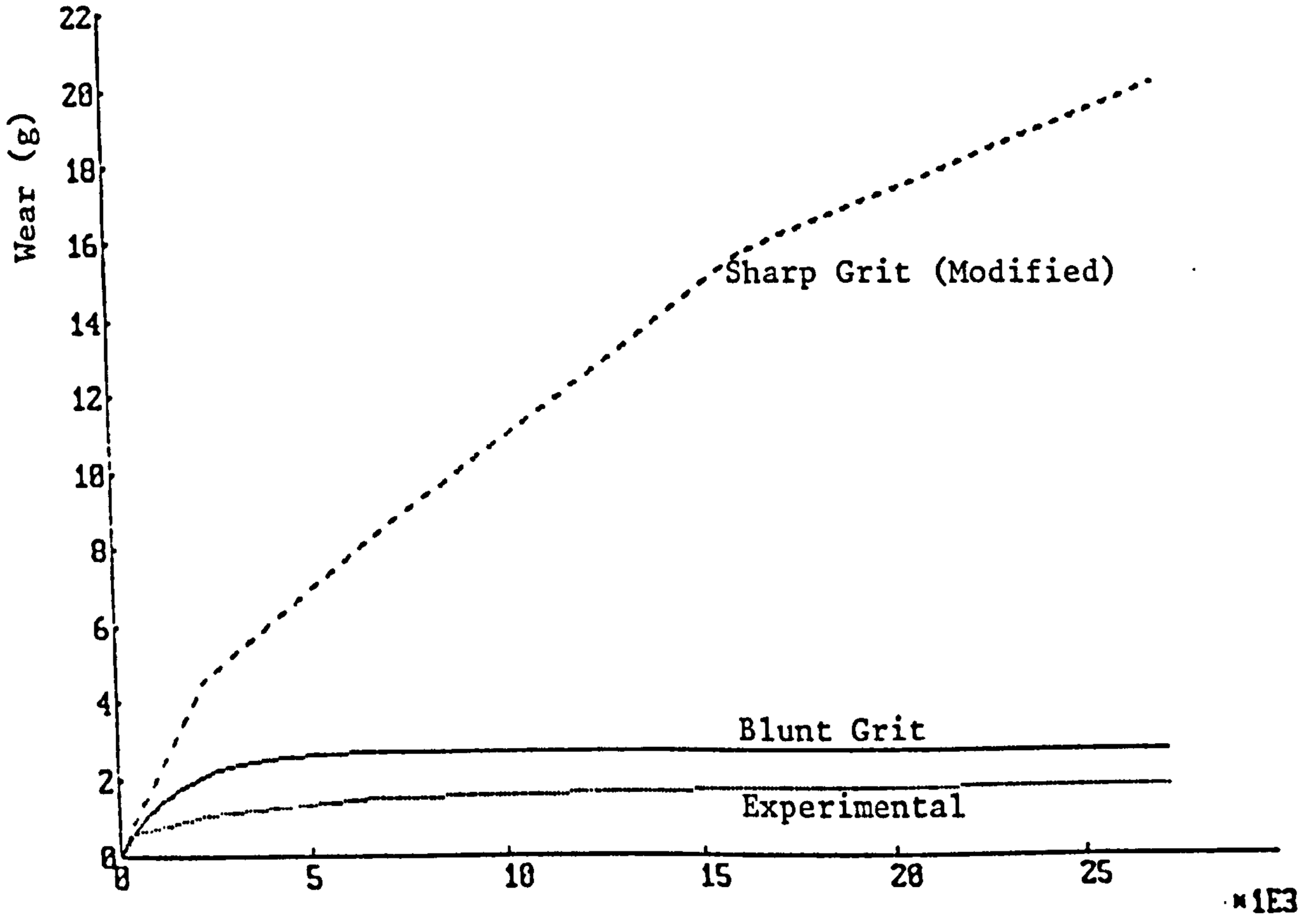

Figure 3.13 Comparison of the wear experiment results with modified sharp grit and the Blunt Grit model.

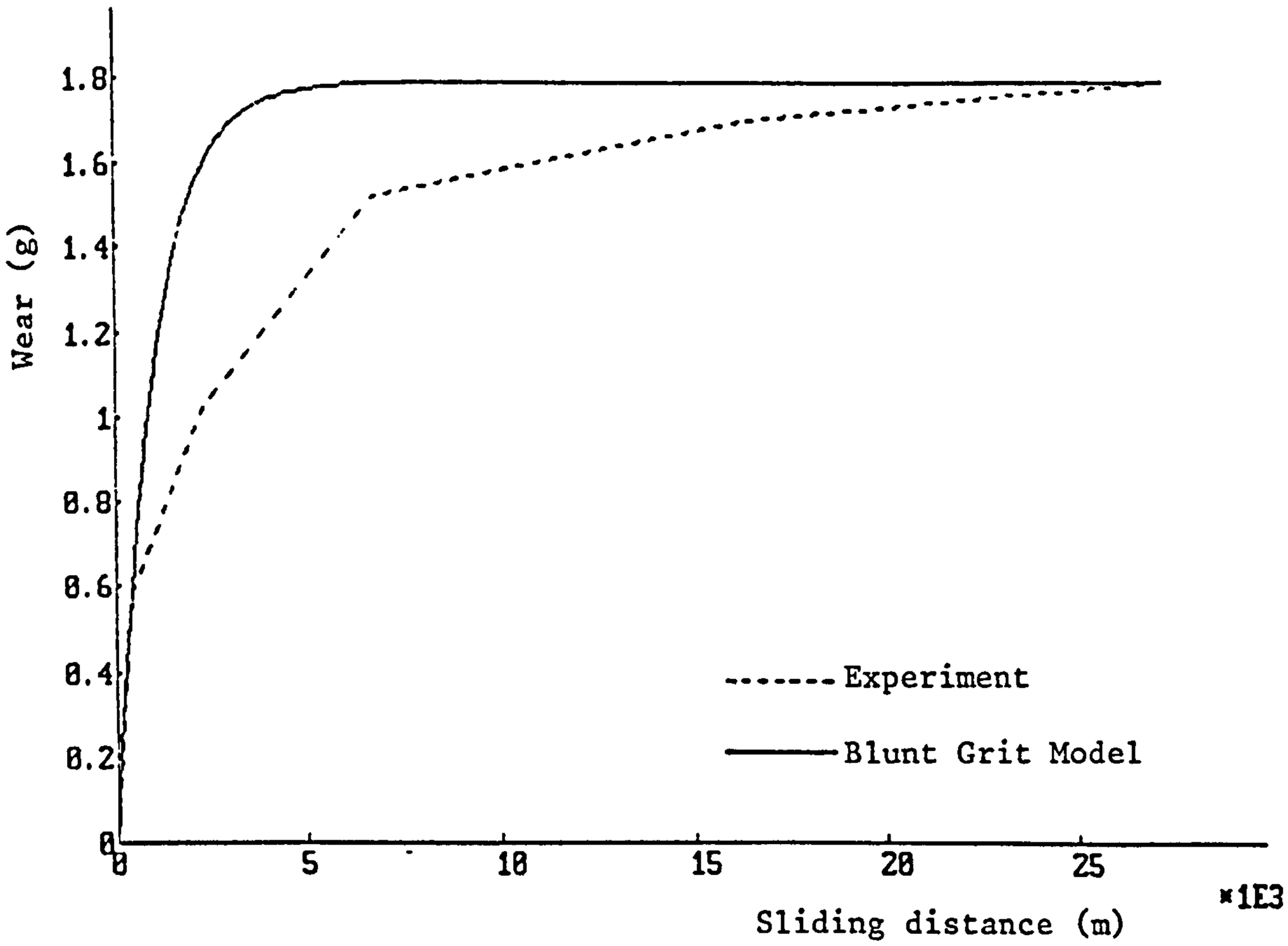

Figure 3.14 Experimental wear results and prediction by the Blunt Grit model assuming f=1 in equation (3.33).

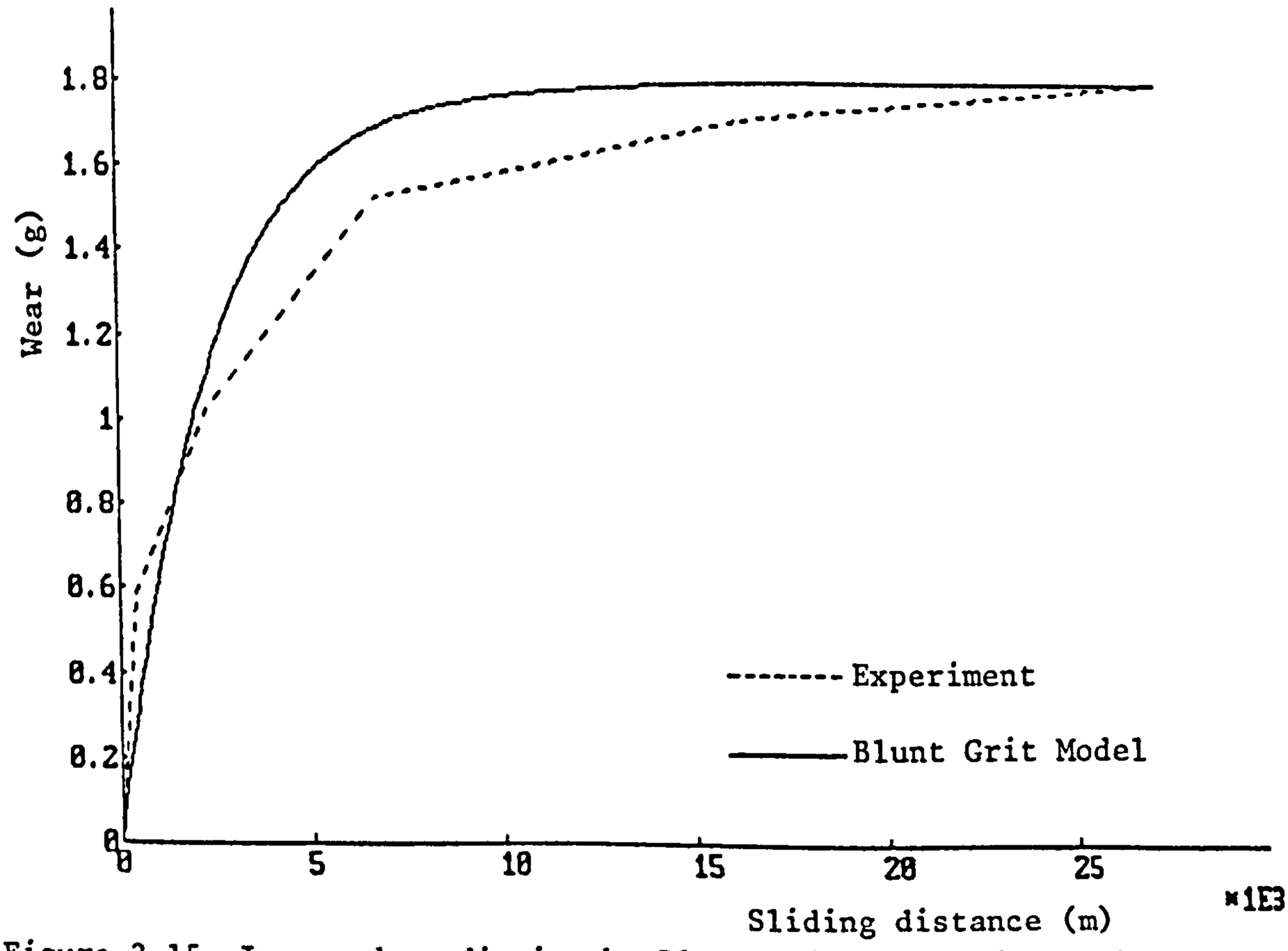

Figure 3.15 Improved prediction by Blunt Grit model, (f=0.65).

CHAPTER FOUR

SURFACE ROUGHNESS PREDICTION

Chapter 4 - Surface Roughness Prediction

4.1 Single Grit Approach

Investigations using single grit or cutters of known geometry have been invaluable in understanding the mechanism of chip formation and the interaction between the work-surface and abrasives in general. Shonozaki et al (1966) measured the normal and tangential components of the cutting force developed during cutting single grooves with a specially designed fly cutter at speeds up to 18 m/min. They observed regions of rubbing, ploughing and microcutting were in evidence at various stages in groove formation and that the rise in the grinding coefficient signified an increase in the extend of ploughing phenomenon.

The results of the test carried out by Crisp et al (1968) at speeds more consistant with grinding condition showed that for a high width to depth ratio, rubbing was a predominant factor, leading to high values of specific energy. They also noticed a decrease in specific energy with an increase in volume of cut which they related to size effect.

A single abrasive grit of random profile was mounted on the periphery of a grinding collet by Grisbrook (1965) to study the formation of groove. He observed the normally expected flow type chip which runs up the rake face of the grit. Metal moved to either side of the groove to form pile up. This lateral movement is the important difference between the action of an abrasive grit and the concept of orthogonal cutting. When this happens in grinding by an abrasive grit, the following grit on the wheel which might be only marginally out of

line, could produce a "combination" type of chip consisting of a flow type combined with the displaced portion of the swell-up formed by the preceding grit. Examining the grinding swarf under a stero-microscope, Grisbrook noticed that apart from spheres which were thought to result from molten chips, the remainder of the swarf consisted of what he considered to be flow type and combination type chips.

Buttery and Archard (1971) used materials having a wide range of hardness in their scratch tests and conditions similar to grinding i.e. width to depth ratio of indentor being 20/1. The Vickers diamond indentor and Rockwell cones were used since as well as being readily available they have the merit of having a width to depth ratio similar to those of grinding grits. They developed an expression for scratch width (2a).

$$2a = 2\left[\frac{W}{2P_m x 10}\right]^{\frac{1}{2}}$$

which showed good agreement width the experimental results. They also expressed the groove geometry in terms of pile-up, figure (4.1) and suggested that the total width of the scratch including pile-up to be taken as a parameter of greatest significance for abrasive theory. Figure (4.2) shows the effect of pile-up on scratch geometry. Generally the softer the material, the greater the degree of pile-up and consequently the smaller the portion of the groove volume removed. As the material hardness increases the efficiency of the scratching process increases, figure (4.3). Using a single grit projecting from an abrasive wheel, they carried out scratching tests similar to those

produced with indentors. The results confirmed the influence of hardness on pile-up and the efficiency of abrasion and showed that a single grit may produce several scratches due to the presence of a number of cutting edges.

Hamed (1977) studied the mechanics of grinding using single grit approach. Idealised cutters and dressing diamond were used to simulate the abrasive grits. Using a dynamometer, forces at speeds up to 37 m/sec. were measured to examine the effect of cutting speed on the efficiency of cutting (β) and specific energy. Based upon the scratch model of Buttery and Archard figure (4.1), Hamed derived an expression for the surface roughness, Ra, of a surface marked with a single scratch having the geometry of a sharp indentor.

$$Ra = K \frac{(W/P_m)^{\frac{1}{2}}}{\tan\theta} \qquad (4.1)$$

Where

$$K = 0.707 \frac{D}{\beta^{\frac{1}{2}}} \qquad (4.2)$$

and D is a function of scratch geometry and pile-up

$$D = \frac{(1+2np-np^2)^2}{4(1+np)^3} \qquad (4.3)$$

β is the scratch efficiency also depending on pile-up, Figure (4.1).

Predicted Ra values were in agreement with experimental results in the initial stages of scratching experiments. However, as the abrasive started to deteriorate the theory predicted higher values

for surface roughness than those observed experimentally. Hamed derived similar expression for a blunted indentor having a certain percentage of flat on its tip. His analysis, however, can be criticized since in order to derive his model Hamed applied the abrasive wear theory of sharp indentor to the geometry of a scratch produced by a blunt grit. The result will be in error since the abrasive wear theory is based on the assumption that the geometry of the scratch conforms to that of the abrasive grit.

4.2 Prediction of Surface Roughness

Using the abrasive wear model of a blunt grit developed in previous chapter an expression is derived for Ra of a single scratch produced by a blunt grit with some degree of wear flat. Referring to figure (4.4) which describes the geometry of a groove produced by a blunt grit of width 2a and flat land 2b, the following definitions can be made, Buttery and Archard (1971).

$$p = \text{pile up} = \frac{R}{H}$$

where R = pile-up height

$$H = \text{scratch total depth} = \frac{p(a-b)}{\tan\theta}$$

n = degree of symmetry of the pile-up (n=1 symmetric)

A_1, A_2 and A_3 can now be calculated in terms of scratch geometry a,b, n and the degree of pile-up, p.

$$A_1 = \frac{p(a-b)[2a-p(a-b)]}{\tan\theta}$$

$$A_2 = \frac{p^2(n+1)(a-b)^2}{\tan\theta}$$

$$A_3 = \frac{(a-b)(a+b-2pa+p^2a-p^2b)}{\tan\theta}$$

Then, since scratch efficiency is given by

$$\beta = \frac{A_3-A_2}{A_1+A_3} \qquad (4.4)$$

We have

$$\beta = \frac{a(1-2p-np^2)+(1+np^2)}{a+b} \qquad (4.5)$$

The volume of material removed per unit sliding distance is given by A_3-A_2.

$$\frac{\Delta V}{\Delta L} = A_3-A_2 = \beta(A_1+A_3)$$

Substituting in terms of scratch parameters we have:

$$\frac{\Delta V}{\Delta L} = \frac{(a-b)(a+b)}{\tan\theta} \cdot \frac{a(1-2p-np^2) + b(1+np^2)}{a+b}$$

Replacing for $\frac{\Delta V}{\Delta L}$ from equation (3.11), the abrasive wear theory for blunt grit

$$\frac{\Delta V}{\Delta L} = \left(\frac{0.5W}{P_m} - 2b^2\right) \cot\theta \qquad (3.11)$$

Then

$$\frac{0.5W}{P_m} = (a-b)\ [a(1-2p-np^2) + b(1+np^2)] + 2b^2$$

Solving for W

$$W = 2P_m(a-b)(a+b)\beta + 4P_mb^2$$

or

$$W = 2P_m a^2[(1 - \frac{b}{a})(1 + \frac{b}{a})\beta + 2(\frac{b}{a})^2] \qquad (4.6)$$

Which gives the normal cutting force (Kg) in terms of the scratch geometry of a blunt grit.

To calculate R_a, the position of a centre line must first be determined. This is a line for which $S_1 = 2S_2$, figure (4.5) and its position can be calculated by expressing the areas S_1 and S_2 in terms of scratch geometry and pile-up as:

$$h = \frac{(a-b)^2 (1+2np-np^2)}{[2a+2np(a-b)] \tan\theta} \qquad \text{Hamed (1977)}$$

R_a can now be calculated with respect to this line. By definition:

$$R_a = \frac{S}{L}$$

Where $S = S_1 + 2S_2$ and L is the total scratch width, figure (4.4).

If S and L are expressed in terms of scratch geometry as

$$S = 2(h^2 \tan\theta + 2bh)$$

$$L = 2a + 2np(a-b)$$

Then we have:

$$R_a = \frac{2(a-b)^2 (1+2np-np^2)}{[2a+2np(a-b)]^3 \tan\theta} \left\{(a-b)^2 (1+2np-np^2) + 2b[2a+2np(a-b)]\right\}$$

or

$$R_a = a/4 \frac{(1-b/a)^2 (1+2np-np^2)}{[1+np(1-b/a)]^3 \tan\theta} \left\{(1-b/a)^2 (1+2np-np^2) + 4b/a[1+np(1-b/a)]\right\} \qquad (4.7)$$

Replacing for 'a' into the above expression of Ra from equation (4.6), we get

$$R_a = K\frac{\left(\frac{W}{P_m}\right)^{\frac{1}{2}}}{\tan\theta} \qquad (4.8)$$

Where

$$K = 0.1767\ \frac{(1-b/a)^2\ (1+2np-np^2)}{[1+np(1-b/a)]^3}\ \times$$

$$\left\{\frac{(1-b/a)^2\ (1+2np-np^2)\ +\ 4b/a[1+np(1-b/a)]}{(1-b/a)\ [(1-2p-np^2)\ +\ b/a(1+np^2)]+2(b/a)^2}\right\}^{\frac{1}{2}} \qquad (4.9)$$

which shows that R_a changes with variation in b/a. The model for sharp grit geometry (4.2) derived by Hamed can be obtained by putting $b/a = 0$ in the above expression.

Surface roughness R_a can therefore be predicted knowing the load W, included angle of the grit $(90 - \Delta_a)$ and pile-up p. It can be shown, Hamed (1977), that the amount of pile-up, p, changes with the material hardness and the relation between them can be approximated to an exponential curve, figure (4.6). Hence, knowing the material hardness, it is possible to estimate pile-up p. For blunt grits a knowledge of b/a is required. A good approximation for this parameter is given by the percentage of the zero slopes of the abraded surface.

4.3 Verification of the Model

The experiments carried out with the pin on disc configuration (chapter 3) can be used to check the model for surface roughness R_a.

The results of applying the model to the conditions of the test reported in (3.5) are shown in Table (4.1) together with the actual values of R_a. The theoretical values are calculated for a symmetric pile-up (n = 1); the degree of pile-up being estimated from figure (4.6). Since the total scratch width (l) changes with the amount of pile-up and its type (symmetric or asymmetric), to remove the effect of variation in the total scratch width on R_a predicted an influence factor is introduced:

$$F = \frac{\text{normalising width}}{\text{total scratch width}}$$

Where the normalising width is the total scratch width at maximum efficiency (i.e. at zero percent pile-up). From high speed scratching experiments on a range of specimens at different hardness, the influence factor for hardened steel has been found to be related to hardness, Hamed (1977).

$$F = 0.3 + 7.77 \times 10^{-4} P_m \qquad (4.10)$$

Where P_m is the hardness in Kg/mm^2 and the equation is valid for small values of n. By dividing the factor K in the model (equation 4.8) by F the effect of total scratch width variability is removed, Table (4.1).

The actual values for R_a were obtained using a Talysurf 3 connected to a Solartron PDP11 computer. The surface profile of the pin was digitised on line and processed by the computer to give a series of surface characteristic parameters including percentage of zero slope, (details of the system in chapter 7). Theoretical

prediction of the surface finish (R_a) using equation (4.8 and considering the percentage of zero slope as the ration $^b/_a$ shows a reasonable agreement with the actual values, figure (4.7). The results of a typical experiment with a soft specimen using a load of 0.5 Kg are shown in Table (4.2) and figure (4.8).

4.4 Discussion

Comparison of the surface roughness values obtained from the model at different sliding distances with the actual results, figures (4.7) and (4.8) shows that the theory underestimates the actual values. In fact the difference between the observed and predicted R_a would probably be greater than that reported since the model does not take into account overlapping of the profiles. Experiments with a single grit (Hamed, 1977) has shown that as the number of scratches increases the surface roughness of the surface is reduced gradually to reach a steady level; its value is not affected by further increase in the number of scratches. It appears, therefore, that the single grit model does not give a reliable estimate of the surface roughness.

A major factor for this discrepency is believed to be the assumption of a levelled surface by the model. Obviously an abrasive paper has only a nominally level surface and the grits are randomly situated at different heights. This results in an uneven distribution of load and alters the value of the number of active grits C ; a condition which has not been dealt with by the model. The application of the single grit model, therefore, requires some statistical averaging of

grit geometry and distribution if a reliable estimation of R_a is required.

The single grit model is useful, however, in demonstrating the effect on surface roughness of grit geometry and pile-up on the surface. The effect of blunting of the grits ($^b/a$) and pile-up (p) on surface roughness is represented in the model by the 'K factor', equation (4.9). Figure (4.9) shows the coefficient K as a function of ($^b/a$) for materials with different hardness (pile-up, p). The plot shows that for hard materials (small p) the effect of blunting ($^b/a$) of cutting points on surface roughness is less than that for the soft materials and as the material become softer its surface roughness become more sensitive to grit blunting. This difference is more pronounced at the smaller values of ($^b/a$) which coincides, in practice, with the initial sliding distances. As ($^b/a$) increases at later stages of run this difference between hard and soft material is reduced and the R_a becomes less sensitive to blunting. These observations demonstrate the importance of hardness with respect to surface roughness. Both pile-up and rate of grit blunting which effect the surface roughness depend on hardness. Soft materials are more sensitive and their surface roughness improve faster with dulling of the grits nevertheless this trend is offset to some degree by the fact that blunting of the grits occurs at a slower rate compared with harder materials.

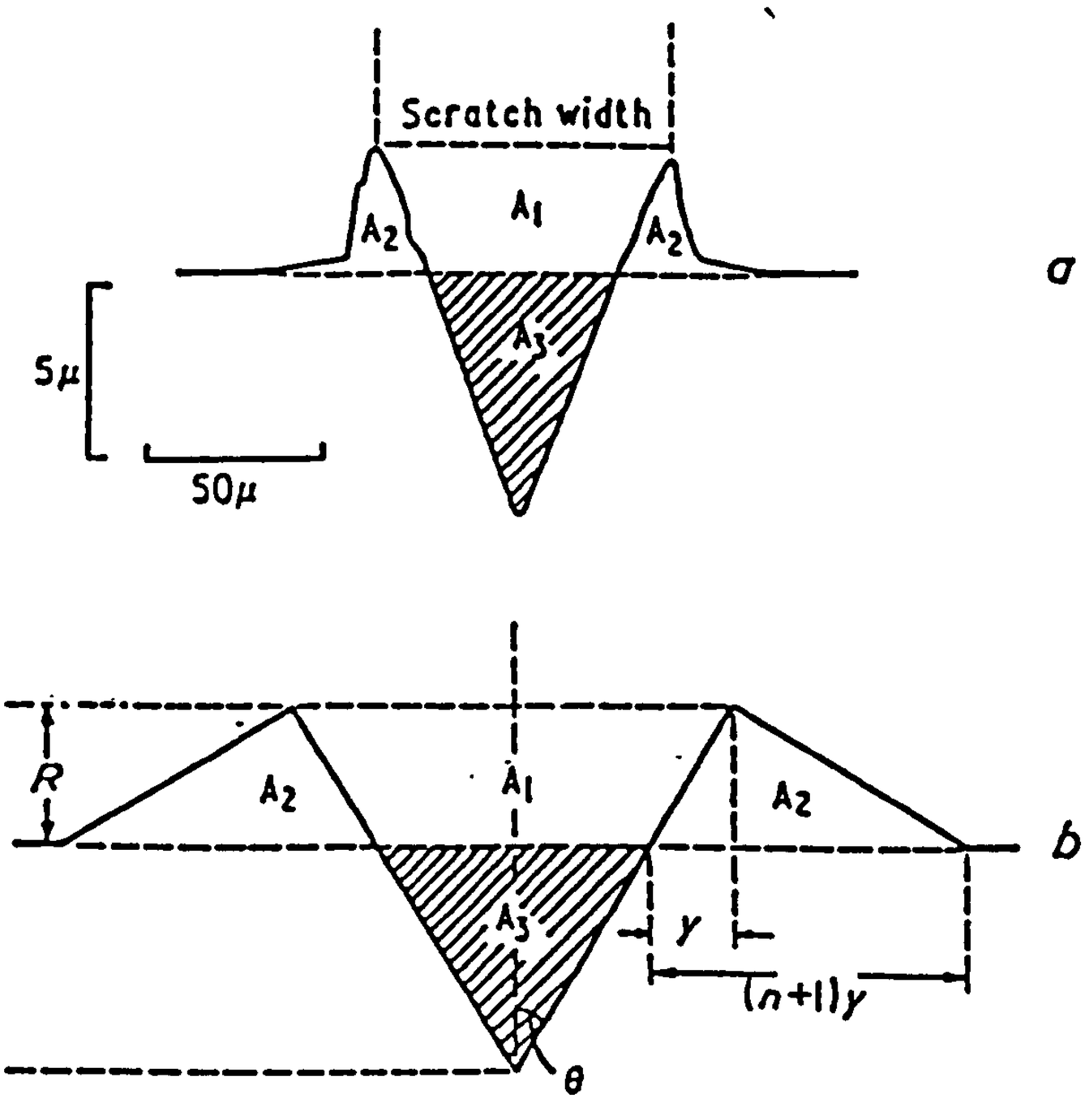

a A typical scratch showing pile-up. Vickers indentor edge-first orientation, Stellite, load 2 kg.
b Idealized representation of the scratch used in the theory.

$$P = R/x$$

$$\text{Volume of pile-up} = A_2 = (n+1)R^2 \tan\theta$$

$$\text{Volume displaced} = A_3 = (x-R)^2 \tan\theta$$

$$\text{Total groove volume} = (A_1+A_3) = x^2 \tan\theta$$

$$\text{Volume removed} = (A_3-A_2) = (x^2-2xR-nR^2)\tan\theta$$

$$\beta = \frac{\text{Volume removed}}{\text{Total groove volume}} = 1-2P-nP^2$$

Figure 4.1 Scratch geometry and proportion of the material removed in term of pile-up, p.

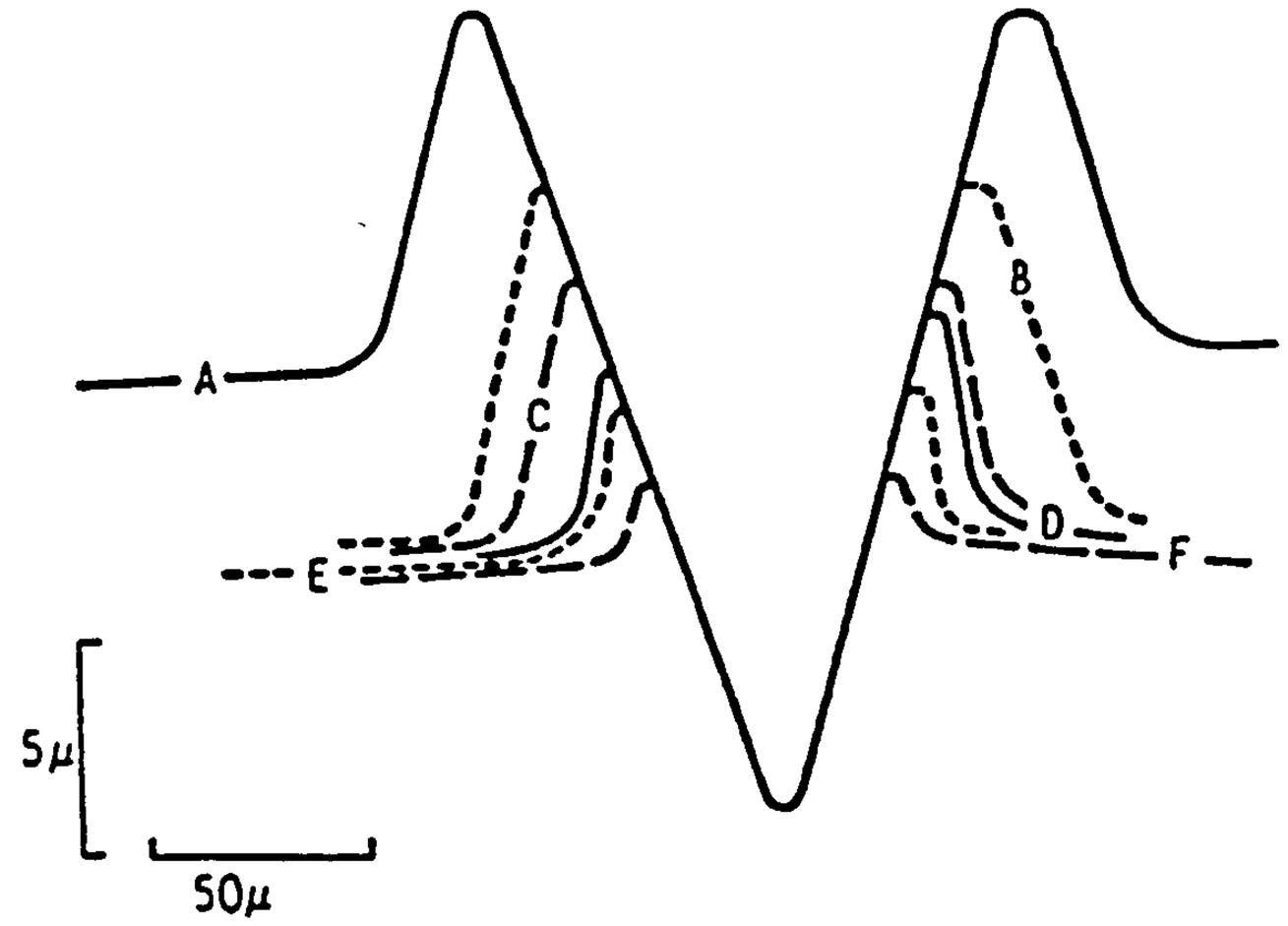

1 per cent C steel hardened and tempered to a range of different values of hardness (D.P.N.) as follows. A, 263; B, 315; C, 441; D, 598; E, 710; F, 890.

Figure 4.2 Composite picture of a series of scratches made with the Vickers indentor in the facet first orientation; load 2 Kg.
Buttery and Archard (1971).

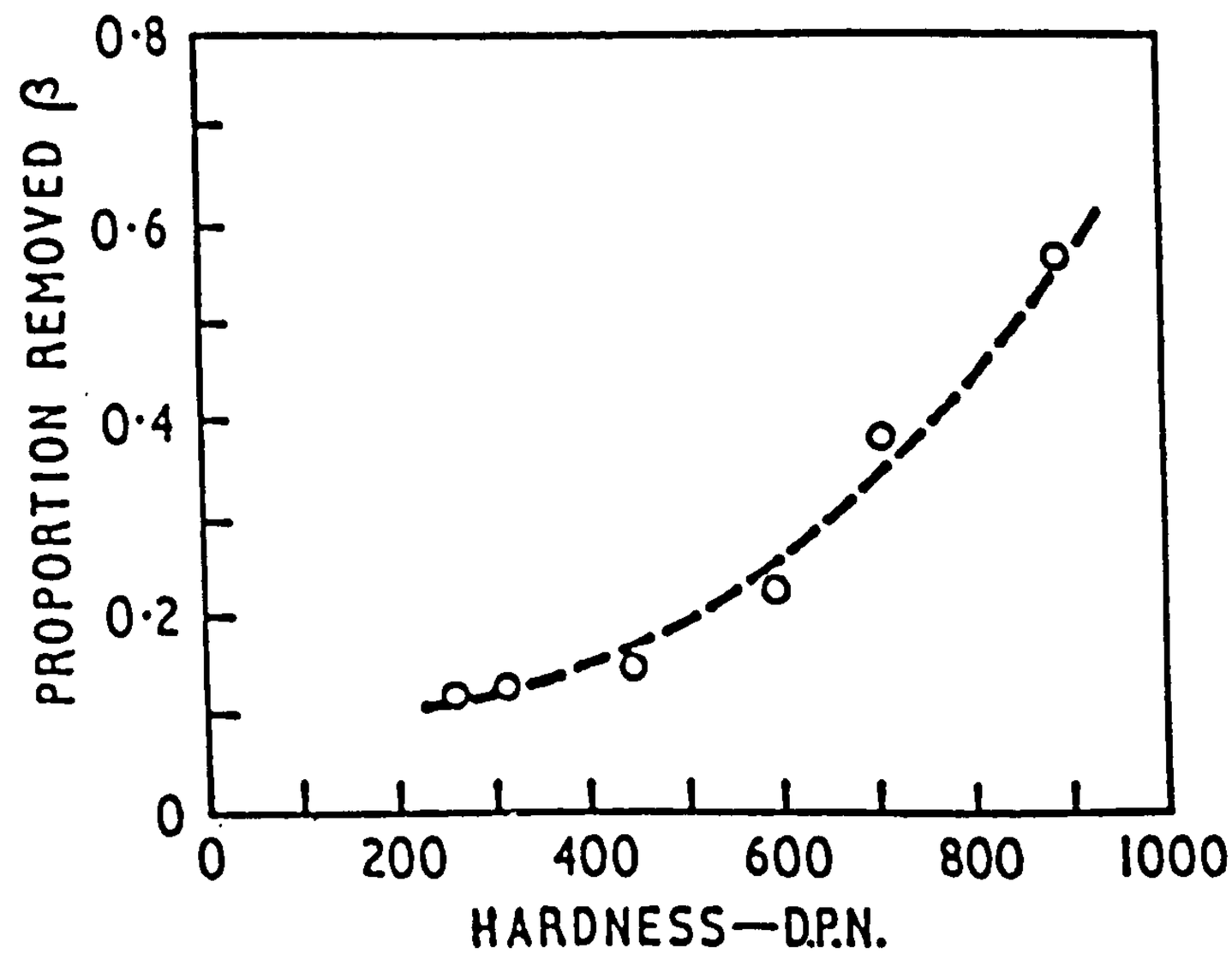

Figure 4.3 Proportion of material removed as a function of hardness for 1 per cent C steel scratched by Rockwell indentor.
Buttery and Archard (1971).

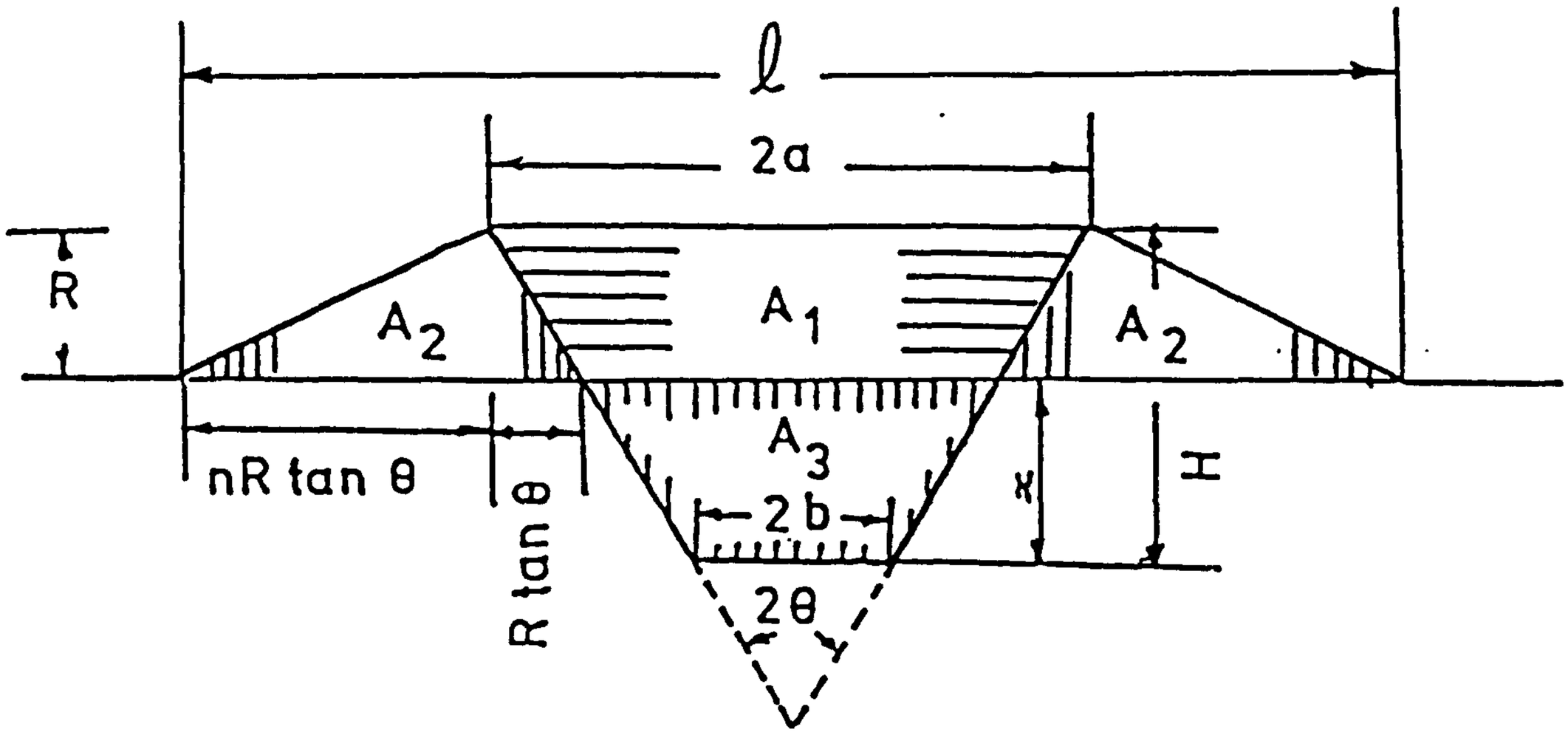

Figure 4.4 Single scratch produced with a blunt grit.

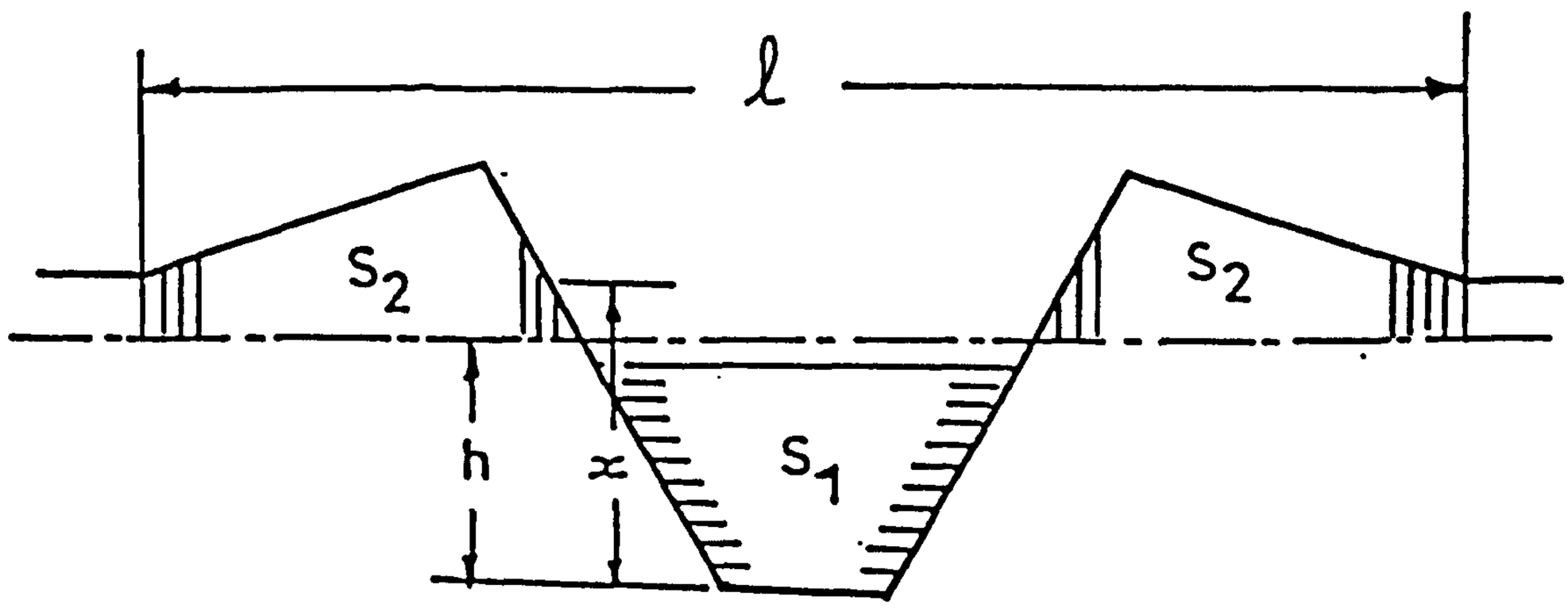

Figure 4.5 Scratch geometry for R_a prediction.

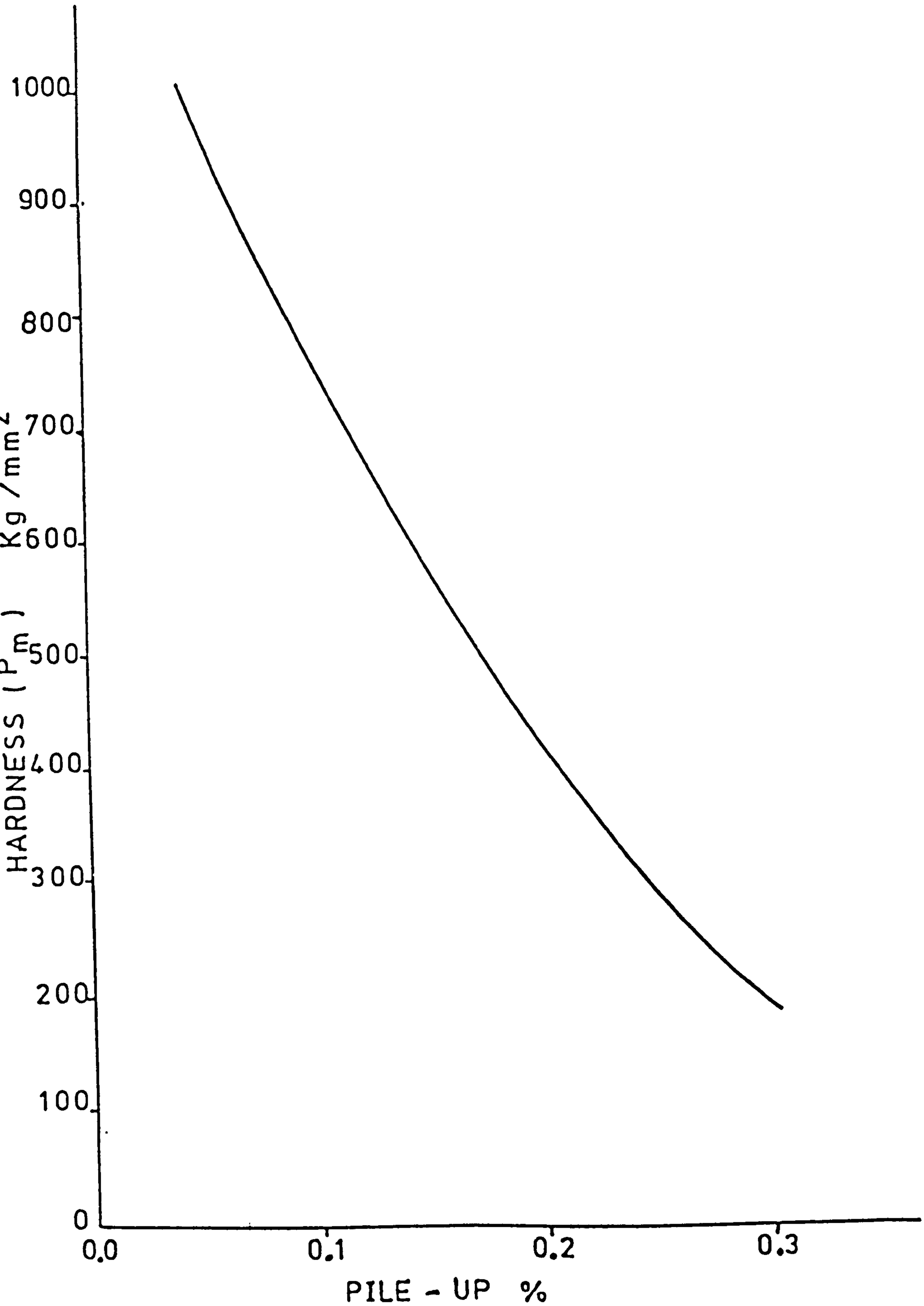

Figure 4.6 Relationship between hardness and % pile-up.

(Hamed, 1977)

Time (min)	1	5	25	75	180	300
Half scratch angle (θ)	73.9	75.7	76.2	81.4	82.8	84.8
% Zero slope	1.4	13.8	18.5	19.2	20.1	23.5
R_a (μm) Experiment	3.94	2.20	2.32	1.80	1.67	1.45
R_a (μm) Theory	0.987	0.789	0.751	0.748	0.74	0.71

Table 4.1 Experimental results of a pin-on-disc test and the prediction of R_a by the Single Grit model. Pin hardness = 720 VPN.

Time (min)	1	5	25	75	180	300
Half scratch angle (θ)	81.3	8.35	84	84.2	85.1	84.8
% Zero slope	2.3	10.1	12.5	14.1	14.9	15.6
R_a (μm) Experiment	3.12	2.42	2.12	2.1	1.92	1.89
R_a (μm) Theory	1.43	1.29	1.24	1.22	1.20	1.19

Table 4.2 Experimental results of a pin-on-disc test and the prediction of R_a by the Single Grit model. Pin hardness = 200 VPN.

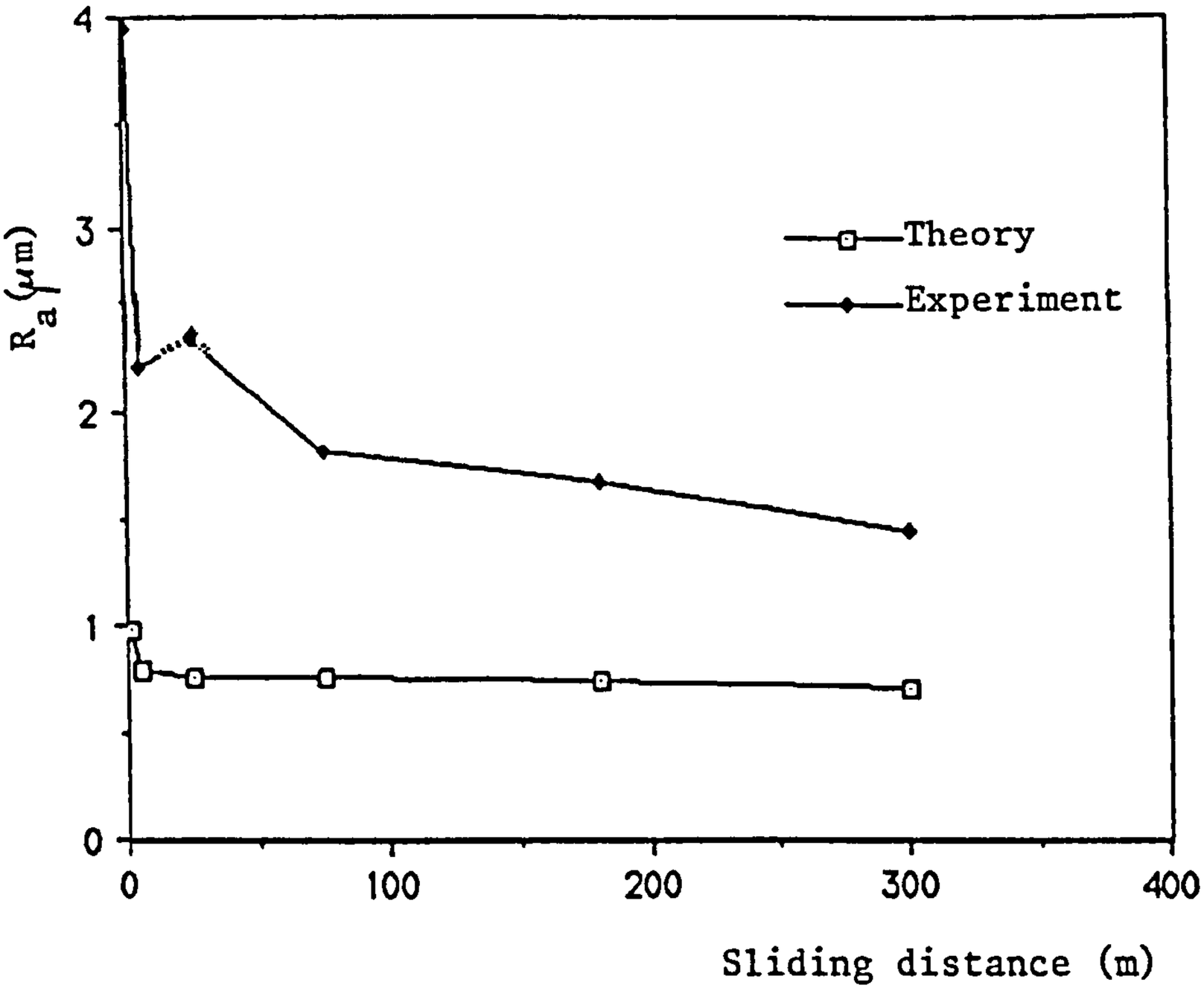

Figure 4.7 The change in surface finish with sliding distance. Hard specimen.

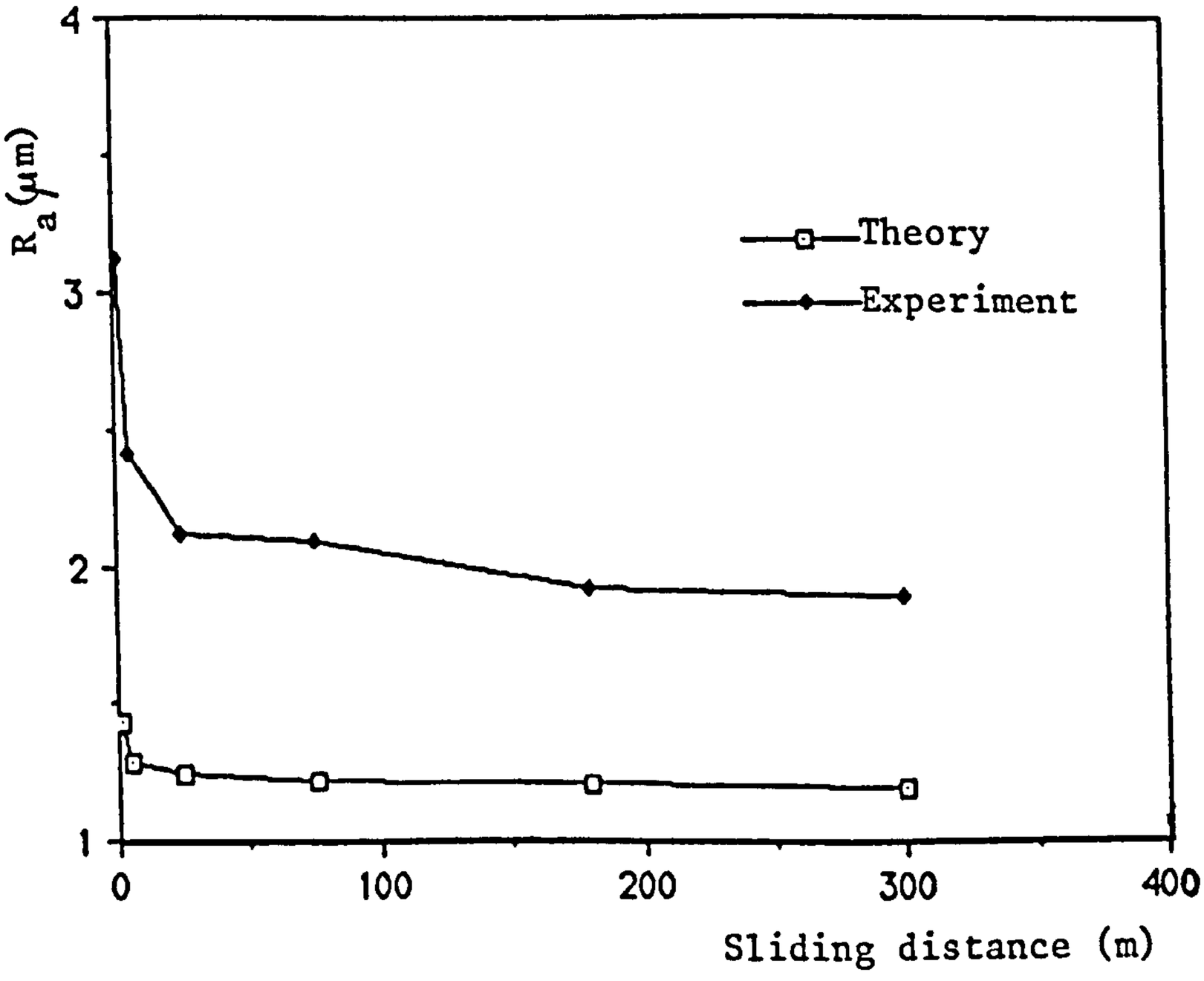

Figure 4.8 The change in surface finish with sliding distance. Soft specimen.

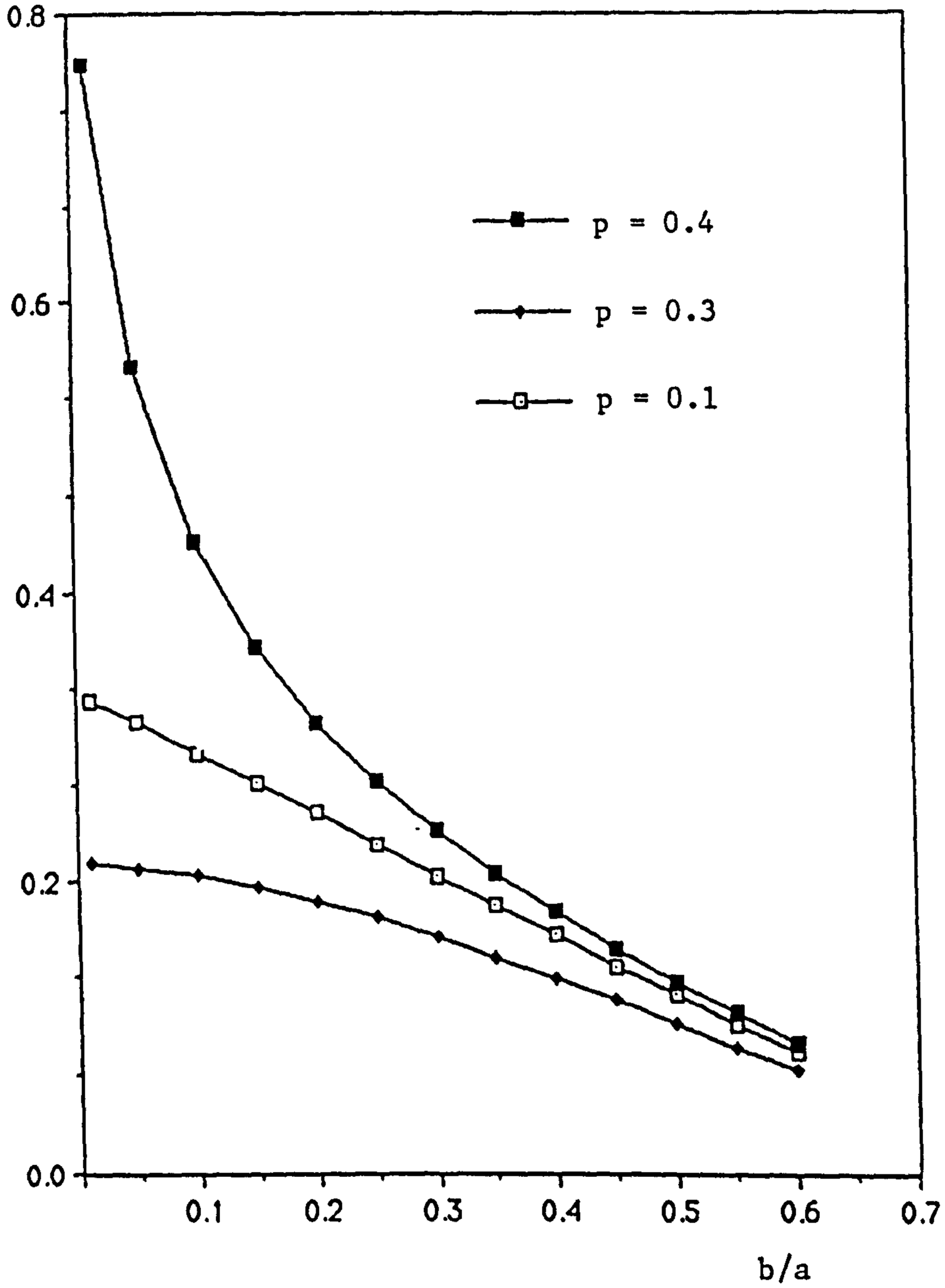

Figure 4.9 Changes in the K factor of the surface roughness model with grit blunting ($^{b}/_{a}$) and pile-up (p).

CHAPTER FIVE

GRINDING PROCESS

Chapter 5 - Grinding Process

5.1 Introduction

The grinding process still remains one of the most important and widely used operations for the precision finishing of components. High metal removal rates while retaining acceptable standards of geometry and surface finish has also become another important application of grinding. Nevertheless grinding is still considered as a process requiring skilled operators and therefore cannot readily fit into the concept of the unmanned factory. Only in exceptional instances has grinding been incorporated within a flexible system and then only to a limited degree, PERA report (1987). This is mainly the result of the complexity of the grinding process which makes it extremely difficult to specify the process. The large number of often inter-dependent parameters, high velocities, and difficulties of measurement are some of the problems associated with grinding. In all the other cutting processes the shape of the cutting tool is well defined and makes up one of the most readily available parameters of the process. The geometry of cutting grits in a grinding wheel is almost infinitely variable and they can only be defined statistically. There are also complications which arise from the inevitable deterioration of the wheel cutting surface during operation. This deterioration can in some cases be so severe as to result in the gross break-down of the wheel surface. This behaviour is generally referred to as "soft" action. Alternatively, the wheel surface may "glaze" which results in higher forces and in this case the wheel is described as "hard".

The result of a survey by PERA of a wide variety of companies engaged in grinding and related industries including end users, manufacturers and suppliers of machine tools show that the grinding wheel is the most important aspect of grinding which requires investigation. Figure (5.1) shows in principle the different factors affecting the grinding operation, Peklenik and Opitz (1962). The quality of the grinding wheel is one of the most important factors with respect to surface roughness, accuracy of size and shape of workpiece and tool life. The outcome of the grinding operation also depends on the right choice of grinding wheel.

5.2 Grinding Wheel

The grinding wheel is a bonded abrasive body consisting usually of Al_2O_3 or SiC abrasive grains in a matrix of ceramic, resinoid or rubber bond. The ceramic bonded (vitrified) wheel is used on the large majority of precision grinding operations. The performance of a grinding wheel is characterized by its components which are the material and size of the grains, the voids and the bond.

The equation describing the volumetric composition of grinding wheel may be written as:

$$V_k + V_b + v_p = 100 \text{ per cent} \qquad (5.1)$$

where V_k = volumetric part of the grain, %.

V_b = volumetric part of the bond, %.

v_p = volumetric part of the pore, %.

By increasing the percentage of bond the bond bridges are reinforced and the hardness of the tool increases. The equation may be written as:

$$V_k + (V_b + \Psi_h) + (v_p - \Psi_h) = 100 \text{ per cent} \qquad (5.2)$$

where Ψ_h = step in the hardness (grade) per cent. Another important factor of grinding tools is their structure. The structure which may be dense or open, is classified by numbers from one to twelve. The volumetric equation for each single step of structure can be written as:

$$(V_k - \Psi_s) + (V_b + \Psi_s) + v_p = 100 \text{ per cent.} \qquad (5.3)$$

where Ψ_s = step in structure, per cent. Peklenik and Opitz (1962).

The grade of wheel is a measure of the tenacity with which the bond material holds the abrasive grits in the wheel. A soft grade of wheel is one from which the grits can easily be dislodged, whereas the removal of grits from a "hard" wheel requires greater force. A harder grade of wheel contains more bonding material. Wheel 'structure' is a measure of the degree and size of the porosity in the wheel. This is effectively the relative spacing of the abrasive grits. An open structure wheel has adequate space, or chip clearance for the material to enter the wheel surface. The surface of the wheel with a 'close' structure can easily become clogged with workpiece material.

The wheels contain grains which are nominally of a certain size, but which in fact are distributed around this nominal size.

5.3 Wheel Wear

In grinding process the grinding wheel removes material from the workpiece but in so doing the workpiece removes material from the grinding wheel so that there is a mutual machining. There appears to be a general consensus of opinion concerning the several mechanisms by which the wheel wear may occur, viz:

(i) attriçious wear by which flat wear areas gradually appear on the grits;

(ii) grit fracture by which fragments of grits become detached.

(iii) grit pull-out in which grits are detached from the wheel as a result of bond-post fracture.

Attricious wear is caused either by the rubbing process between the grit and the workpiece, or by a chemical reaction at the very high temperatures between these materials. In either case the result is a worn flat grit.

Fracture wear is the removal of abrasive particles from the wheel, either by dislodgement from the bond, or by actual fracture within the grit itself. From a practical point of view, neither the structure of a dressed wheel surface nor the detection of any change in its cutting surface during the grinding operation should be ignored.

Figure (5.2) shows the progression of radial wheel wear which has been measured by a number of authors. Krabacher (1959), Koloc (1959) and Pattinson and Chisholm (1967). Wear occurs in three phases:

Phase I - a short period of non-linear rapid wear during which any insecure grits are removed. The amount of wear in this period is related to the dressing technique.

Phase II - a much longer period during which, under a good grinding condition, wear occurs at a constant and relatively slow rate.

Phase III - this phase has not always been identified, but is characterized by a rapid increase in wear rate and severe vibration. In practice grinding will be terminated before wheel enters phase III.

The ratio of the total volume of metal removed to the volume of wheel loss at the end of phase II is known as "Grinding ratio".

Macroscopic measurement of wheel wear does not reveal the microscopic processes that occur during grinding and affect the performance of grinding wheel. The smooth surface of the grits which have sustained attritious wear reflect incident light. Malkin and Cook (1971) used this property to quantify this kind of wear by expressing the reflective areas as a percentage of the wheel surface area. They found that when grinding various types of steel the workpiece surface exhibited grinding 'burn' if a certain percentage

of wear flats was obtained. The glazed wheels are also known to produce smooth workpiece surfaces. When this type of wear is predominant, the grinding ratio is very high.

To detect the microscopic process of the wear, Tsuwa (1960) using a method of light cross section, investigated the change of cutting edges singly and very precisely. His investigations revealed that the plateau area of the edge is easily widened through high-speed and high temperature rubbing with work material. Fracturing and tearing out of the abrasive grains were also observed. Precise measurement of this widening of plateau area was made by Tsuwa (1961), and its importance to the performance of the grinding wheel has been emphasised by Peklenik. Investigations made by Hiroyuki Yoshikawa (1962) showed that a definite relation between the area of plateau and the grinding force exists. They stressed that the performance of a grinding wheel should be interpreted in terms of microsopic structure of the wheel surface which changes during grinding and strongly affects the performance of the grinding wheel. According to these authors the structure change is mainly caused by the three basic mechanisms, attritious wear of the abrasive grains, mechanical fracture and tearing out of grains. The attritious wear widen the plateau area and lower the performance of grinding wheel. On the other hand the latter two decrease the total plateau area and bring out new sharp cutting edges, which improves cutting ability.

5.4 Grinding Forces

Grisbrook (1960) showed that there is a consistant pattern of

change in forces during a normal run in grinding. This is shown in figure (5.3), where it is divided into four regions:

(i) an unstable region where the forces rise to a peak and then fall to a steady value as the dulling effect produced by wheel truing (dressing) wears off. It should be noted that this initial rise of the grinding force has not been identified by other investigators and could therefore be a feature of his dynamometer, i.e. lack of stiffness.

(ii) a region of stable grinding conditions where forces and speeds are constant and heat is in equilibrium.

(iii) in this region there is a progressive build-up of forces and power reflecting the reaction of the wheel to the particular combination of work speed, depth of cut and work material. When grits become dull, overheating may develop and grinding becomes progressively inefficient.

(iv) the rate of increase of forces become less, there is evidence of vibration and as this develops the magnitude of forces commence to fall.

It should be noticed that depending on the kind of wheel and the conditions of grinding the duration of these defined stages in the pattern of force varies.

Grisbrook et al (1962) also investigated the forces developed in surface grinding and they substantiated the values of specific energy and the coefficient of grinding found by Marshall and Shaw. They showed that when used properly, a grinding wheel can behave in

a very stable manner for given wheel and workspeed. The forces remain constant, heat is produced at a steady rate and the wheel is in a free cutting condition; the grits maintaining their sharp cutting points by fracture. Ultimately the grits develop large flats worn upon them and the wheel becomes dull, the cutting conditions become unstable, and forces (and specific energy) rise. Malkin and Cook (1971) also found that grinding forces increased with the incidence of attritious wear. With the correct selection of grit and bond strength and grinding conditions this force increase may be sufficient to fracture or dislodge the worn grit to produce new, sharp cutting edges (self-sharpening).

5.5 Wheel Cutting Points

Theoritecal treatments of grinding have regarded the process essentially as one of cutting using very small single point tools, each grit is assumed to remove a chip. Alden (1914) and Guest (1915) based their determinations of cutting forces on the assumption of one grit one chip and arrived at a grit distribution of the order of 1600 per square inch. Marshall and Shaw (1952) rolled the wheel over smoked glass and from the number of pick-up points obtained a figure of 1930; Sato (1955) by a similar method has a range from 2600 to 3500 for different wheel grades. Examination by a Vickers' projection microscope reveals a much closer spacing than this, Grisbrook (1962).

One grit may have more than one cutting point. Grisbrook suggests that the multi-cutting points merge as the grit wears and

thus for a particular wheel the number of points will depend on grinding conditions and characteristics of the wheel and only when the flats have become so large as to cover the grit will the number approach the figure of the earlier workers.

Whether the cutting points in action each produce a chip at each engagement with the workpiece, as assumed by Shaw and others in simulating grinding by micro-milling, is questionable. Grisbrook argued that it is possible that a grit, having a large contact area, may develop an intensity of pressure too low to rupture the surface of the trochoid left by the preceding grit. This required intensity of pressure must be reached before chip formation can commence and this would account for lack of agreement between the observed chip proportions and the theoretical proportions obtained from the analogy with milling.

5.6 Dressing

As well as the number, shape and the roughness of cutting edges and the amount of wear flats on their tip, grinding operations are affected, to a certain extent, by wheel dressing. Further factors such as machine rigidity, damping characteristics and grinding condition are also important with regard to surface quality.

As with other cutting tools the cutting points on the surface of a grinding wheel gradually loose their sharpness. The cutting ability of the wheel is also reduced by loading of the wheel surface with the ground debries "clogging". Both the functional and

geometric characteristics of the wheel are therefore periodically restored by dressing.

Dressing techniques can be classified broadly, into diamond dressing and crush dressing. The former in which diamond tool is traversed across the wheel face is more common. Tools used include pencil cone, chisel shaped and cluster diamonds (multi-point) tool. Crush dressing is usually associated with form grinding where a hard roller is fed radially into the wheel. In precision grinding the vast majority of wheel dressing operations are carried out using single point diamond tools.

5.6.1 Dressing and Grinding Performance

Dressing imparts its unique characteristics to a grinding wheel so that abrasive surface topography will in general be the resultant of the basic wheel structure and the superimposed effects of the dressing conditions.

Pahlitzsch (1954) and Lindsay (1969) suggest that the diamond actually cuts through the abrasive grit to produce what is effectively a form tool. The dimension of this form are determined by the combination of diamond traverse rate, shape and infeed. The abrasive grits, in turn, transfer their profile to the workpiece during grinding. The passage of a single point diamond has been compared with a truing operation which produces a helical groove on the wheel periphery. Such threaded profile may then be transferred on to the ground surface, Bhateja (1974) and Verkerk (1974). The

depth of the groove formed by a single diamond depends upon the dressing conditions and the shape of the diamond tip. In most cases the depth of the diamond penetration or profile depth can be determined as:

$$R_t = \frac{S^2_d}{8r_d} \qquad (5.4)$$

(Ochiai, 1975)

where

S_d = dress lead mm/rev.

$0.05 \leq s_d \leq 0.2$ mm/rev. and

r_d = radius of the diamond tip (in average $r_d \leq$ 2mm)

Observation of the dressing debries collected from a wheel dressed by a single point diamond dresser by Malkin and Cook (1971) however, showed that the grit size and wheel hardness influence the size distribution of dressing particles. Smaller grits and harder wheels gave smaller dressing particles. They also found that dressing particles for all the wheels used were not much smaller than the grits which went into the wheels. These results suggest that dressing diamond fractures grits to produce relatively large fragments or, possibly, dislodges them from the bond, Vickerstaff (1976).

The passage of a diamond tool across the surface of a rotating wheel is essentially a multi-functional operation. Apart from the two most obvious functions of dressing i.e. truing and sharpening of the wheel, the more subtle influences of diamond dressing are to

affect the wearing action of the wheel during grinding and hence its useful grinding life, Pattinson and Chisholm (1967), and rearrangement of asperities and imposition of a constraint on the radial location of cutting edges in the wheel surface, Bhateja et al (1971). It can be said, therefore, that the wheel profile is directly related to the dressing technique used which in turn can have important effects on the grinding mechanism and work-surface produced. It is now agreed Peklenik (1963), Graham and Baul (1972) and Hamed (1977) for example that the mechanics of the grinding process depends critically on the grit geometry, a condition which is frequently affected by dressing. It has also been shown that the geometry of a grinding wheel surface is at least partially reproduced on the workpiece surface, Vickerstaff (1974).

Investigations, Bhateja et al (1971), Hahn and Lindsay (1971) have shown that for a given dressing technique such as the single point diamond, dressing conditions like diamond geometry, dressing lead and depth of cut influence the wheel grinding performance regarding work surface finish, stock removal capability and wheel wear. With finely dressed wheels (i.e. smaller dressing feed and diamone infeed) the individual asperity peaks tend to be grouped at the same height level, thus the concentration of potential cutting edges at the outermost levels of the wheel surface is high. This is usually equivalent to blunter grits (higher ratios of width to depth of the scratch) which results in less probability of micro-cutting. A fine worksurface is however obtained. With a rough

dressing, grits are sharper and fewer and therefore are able to penetrate more into the work surface. A better stock removal rate is achieved at the expense of obtaining a rougher surface. These observations highlight the critical role of the dressing in the optimization of the grinding process. A successful optimization of the grinding process requires the prediction of the work surface finish under a particular set of grinding conditions. Characteristics of the wheel surface and the effect of wheel dressing on grinding parameters play important role in this respect.

Single point diamond dressing can be defined in terms of a series of controlable variables. These variables can be regarded as the input to the dressing operation.

- Traverse rate of the diamond across the wheel surface.
- Depth of cut or infeed of the diamond.
- Diamond shape.

Other factors such as the approach angle of the diamond only slightly affects the dressing. At most instances the wheel speed is fixed, therefore, no control can be exercised over this factor. Maintaining the dimensions and the shape of the diamond is obviously an important factor if repeatability in grinding is to be achieved Verkerk (1977) and Vickerstaff (1970).

The effect of dressing is usually assessed in terms of variables (output variables) such as

- Wheel surface topography.
- Wheel wear.
- Condition of individual grits.

- Work surface roughness.
- Stock removal rate.
- Grinding forces (grinding ratio).

Because of the random nature of the process, the interrelationship between dressing and these grinding parameters are difficult to establish. Dressing however should not be discussed in isolation since it is an essential part of the grinding process having a profound effect on the mechanism of metal removal and the surface topography of the workpiece.

5.7 Grinding and Abrasive Wear Theory

Earlier investigations into the mechanism of grinding compared grinding with single point cutting operations. Grinding wheel was considered as a multi-toothed milling cutter, each tooth consisting of a small abrasive grain.

When Marshall and Shaw (1952) developed the first dynamometer and measured the tangential and normal grinding forces directly, the fundamental differences between mechanism of grinding and chip forming processes emerged. Although their dynamometer could only be used at relatively slow work speeds, they took measurements over a considerable range of conditions, figures (5.4, 5.5, 5.6). They introduced the important term 'grinding ratio' being defined as the ratio of tangential to normal force similar to the coefficient of friction. Marshall and Shaw showed that grinding coefficient is about 0.5 while the similar ratio in other cutting processes is known to be about 2. This is a considerable difference which suggest

a marked difference between the mechanism of these processes. Another major difference which they observed between grinding and other chip forming processes was the value obtained for the specific energy. This is the energy spent to remove unit volume of material and it was found to be very much greater in grinding operation compared with other chip forming processes, (up to 50 times).

Backer et al (1952) claimed that the differences could be explained largely by 'size effect'. They showed that there is a significance increase in specific energy with decrease in chip size in a micromilling operation, figure (5.7). They concluded that the smallness in chip size in grinding was apparently the most distinguishing characteristics of grinding operation, and the relatively large specific energy and shear stress important effects. This quantitative difference in the cutting dimensions, however, was used by Hahn (1956) to show a different mechanism of chip formation by grinding. In all the other conventional machining processes, the shape of the cutting tool is carefully selected to suit particular requirement. In grinding, the grains which act as cutting tools are of varied and indeterminate geometry, and they usually present a negative rake angle to the work surface. Hahn (1956) pointed out that in single point-theory the assumption is usually made that the tool forces arise from the chip bearing on the rake surface of the tool and that the clearance surface is free from rubbing forces. At very small cuts (0.0004 in), however, this assumption falls down. Using a microturning, Hahn found that for a zero rake angle tool having a $\frac{1}{2}$ degree clearance angle, no chips was formed. Under these conditions the ratio of F_T/F_N was $\frac{1}{2}$ as it

is in grinding. Hahn argues that below the depth of cut of 0.0004" there is no chip, consequently, the assumption that the rubbing forces on the clearance surface in grinding are negligible as in single point cutting is seen to be unrealistic, and on the contrary, because of the relative magnitude of tangential to normal forces and the relative independence of forces from the specimen hardness, a more realistic assumption appears to be that the rubbing forces on the clearance surface of the grain are dominant "rubbing grain hypothesis".

Buttery (1969) stressed the similarities of grinding process and abrasive wear and showed that abrasive wear approach to the grinding can give, to a large extent, a consistant picture of the grinding process. Based on general abrasive wear theory, Buttery derived a model for prediction of grinding forces. For surface grinding this would take the form

$$H = \frac{10830\ T\ d\ w\ Pm}{Dr \alpha \beta\ Cot\theta} \qquad (5.5)$$

where D = wheel diameter, in

r = wheel speed, rev. per min.

T = table speed, feet per min.

d = wheel depth of cut, in.

w = work width, in plunge grinding or cross-feed, in per traverse.

Pm = hardness of material being ground, kg per mm^2.

α = proportion of grits cutting at any time.

β = proportion of scratch volume actually removed.

The model predicts the normal grinding force in terms of grinding parameters and grit geometry by assuming grits of known and fixed shape.

Abrasive wear predictions have assumed, unlike cutting, that the normal force is supported on the frontal facets of the abrasive and that the contents of scratches formed by the abrasion are removed as wear. Buttery showed that the efficiency of the abrasive process is closely linked with the pile up of the material in front and sides of the grit. The percentage of material removed from an abraded track is directly related to the pile-up, which is much higher for softer materials. The major divergence between the earlier results of abrasive wear and grinding tests therefore arises from the simple fact that most abrasive wear experiments had been concerned with soft materials and most grinding experiments with hardened steel. The model developed by Buttery for the prediction of the normal grinding force produced good agreement with the hard specimens but the divergence was big with soft materials.

A further source of divergence between grinding and abrasive wear theory lies in the assumption by the theory of fixed grit geometry whereas the condition in grinding is such that grits change shape with work by the formation of wear lands which consequently alters the width to depth ratio of the unit event. Hahn and Lindsay (1967) performed constant force grinding experiments and monitored the effect of dulling of the grits on grinding forces and grinding performance. They showed that under certain conditions when dulling effects can be observed the plunge velocity, surface finish

and the rate of wheel wear vary with time. It is clear that these changes depend on another variable in addition to the normal force intensity. According to these investigations this variable is the real area of contact. By mounting the wheel under a microscope in such a way that worn grain flats reflected the light up the microscope tube they measured the area of these flats "real area of contact". The relation between grinding force and other grinding characteristics, e.g. wheel wear and surface finish usually established in the wheel characteristic charts is valid, therefore, only as long as the real area of contact is essentially constant.

Figure (5.8) shows the changes in the real area of flats and plunge grinding velocity with time for a specific force. It can be seen that the area of flats increase with time to reach a steady value. The average normal stress between the wheel and work is readily found by the dividing the known grinding force by the real area of contact. Hahn and Lindsay showed that stresses are much lower for the dulled wheels.

5.8 Interrelationship between Grinding and Wear Models for Surface Roughness

Adaptive control of grinding demands the development of a comprehensive theory. Although research workers have developed various theories to explain different aspects of grinding, the approaches to the problem of grinding mechanism has varied, as can be expected from such a complex process. Many investigators have used different simulation techniques, a review of some of these techniques is given by Hamed and Buttery (1977). As a result of

this diversity in techniques, it has been difficult to draw comparisons between these theories since they are often defined in terms of different types of parameter. Backer et al (1952) for instance, based on micro-milling approach to grinding, claimed that grinding process should be interpreted in terms of grit depth of cut (undeformed chip thickness), t, and specific energy. These parameters, however, do not form a part of an abrasive wear treatment of grinding. This makes it difficult to obtain any correlation between these two theories.

By combining the information obtained from different techniques a more complete picture of the process should build up. An attempt has been made here to relate these two theories by expressing the surface roughness (Ra) of a single scratch made by a sharp grit of known geometry, as developed by the abrasive wear treatment of grinding process in chapter 4 in terms of the maximum chip thickness, t, derived by Backer et al in their micromilling simulation of grinding. It should be stressed that investigations have shown that the shape and the number of a few prominent grits dictates the topography of the ground surface and presumably carry the bulk of the force, Hamed (1977).

The expression for maximum chip thickness derived by Backer et al is given by

$$t = \left[\frac{4T}{VC\lambda} \cdot \left(\frac{d}{D}\right)^{\frac{1}{2}}\right]^{\frac{1}{2}} \qquad (5.6)$$

Where

D = wheel diameter in cm.

V = wheel surface speed in cm/min.

T = table speed in cm/min.

λ = width to depth ratio of the undeformed chip.

C = number of cutting edges per mm^2.

d = wheel depth of cut in cm.

t = maximum chip thickness in mm.

Figure (5.9) shows the geometry of the undeformed chip.

A model for surface roughness, Ra, of a single scratch based on the abrasive wear treatment of grinding process was developed in chapter 4 as:

$$R_a = K\frac{(W/P_m)^{\frac{1}{2}}}{\tan\theta} \qquad (4.8)$$

Where

W = load per grit, kg.

P_m = hardness, kg/mm^2.

K is a function of pile-up and grit wear and is given by the expression (4.9).

Application of the abrasive wear theory to grinding provides also a model to predict the normal grinding force. This is shown in chapter 6 equation (6.2) as:

$$W = \frac{2000T\ d\ w\ p_m}{\pi Dr\ \cot\theta} + 4P_mACb^2 \qquad (6.2)$$

For sharp grits b = 0 and the model reduces to the sharp grit

component of the grinding force Wo.

$$Wo = \frac{2000\ T\ d\ w\ P_m}{\pi Dr\ Cot\theta}$$

This is similar to the expression (5.5) derived by Buttery (1969).

$$H = \frac{10830\ T\ d\ w\ P_m}{Dr\ Cot\theta} \qquad (5.5)$$

H = normal grinding force, lb.

D = wheel diameter, in.

r = wheel speed, rpm.

T = table speed, ft/min.

d = wheel depth of cut, in.

P_m = hardness, kg/mm^2.

w = work width, in.

Using this expression, the load per grit in equation (4.8) can be obtained in terms of grinding parameters by dividing the normal grinding force, H, by the number of cutting points:

$$W = \frac{H}{100AC}$$

Where C is the number of cutting points per mm^2 and A is the area of wheel-work contact.

W can therefore be obtained as:

$$W = \frac{H/2.2}{10^2 w(dD)^{\frac{1}{2}}\ C}$$

Replacing for W in the surface roughness model (4.8) from the above expression, we have

$$R_a = \frac{K}{\tan\theta}\left[\frac{H}{2.2\text{x}10^2\ w\ C\ P_m\ (dD)^{\frac{1}{2}}}\right]^{\frac{1}{2}}$$

If H is replaced in the above expression in terms of grinding parameters using equation (5.5) then, allowing for dimensional differences, we have:

$$R_a = \frac{K}{\tan\theta}\left[\frac{10830}{2.2\text{x}12\text{x}10^2\text{x}25.4^2}\right]^{\frac{1}{2}}\left[\frac{T(\frac{d}{D})^{\frac{1}{2}}}{r\ D\ C\ \text{Cot}\theta}\right]^{\frac{1}{2}}$$

Since $\pi Dr = V$

and $\tan\theta = \frac{\lambda}{4}$ (figure 5.9)

We can write

$$R_a = 1.413K\left[\frac{4T(\frac{d}{D})^{\frac{1}{2}}}{\lambda VC}\right]^{\frac{1}{2}}$$

or, from (5.6)

$$R_a = 1.413Kt \qquad (5.7)$$

K is given by (4.9) in general. For a sharp grit b = o and we have

$$K = 0.1767\ \frac{(1+2np-np^2)^2}{(1+np)^3(1-2p-np^2)^{\frac{1}{2}}} \qquad (5.8)$$

Surface roughness, therefore, is a function of the maximum chip thickness t and the pile-up, p. When there is no pile-up (p = o) as in the case of a very hard material we get

$$K = 0.1767 \text{ and}$$

$$R_a = 1.413 \times 0.1767t = 0.25t \qquad (5.9)$$

It should be noted that since the micromilling theory ignores pile-up a surface produced by individual scratches of maximum depth t as shown in figure (5.10) would have a surface roughness $R_a = 0.25t$ which is identical to the expression obtained from the abrasive wear model for hard materials (5.9).

With softer materials pile-up increases and the values of R_a obtained by the two techniques diverge; pile-up is not considered by the micromilling technique and R_a value by this method is always given by $R_a = 0.25t$.

For p = 0.25 (320 VPN) the corrected value for K using equation (4.10) would be

$$K = 0.2826/0.54 = 0.515$$

Therefore

$$R_a = 0.72t$$

which suggests a rougher surface is produced due to pile-up when grinding softer materials.

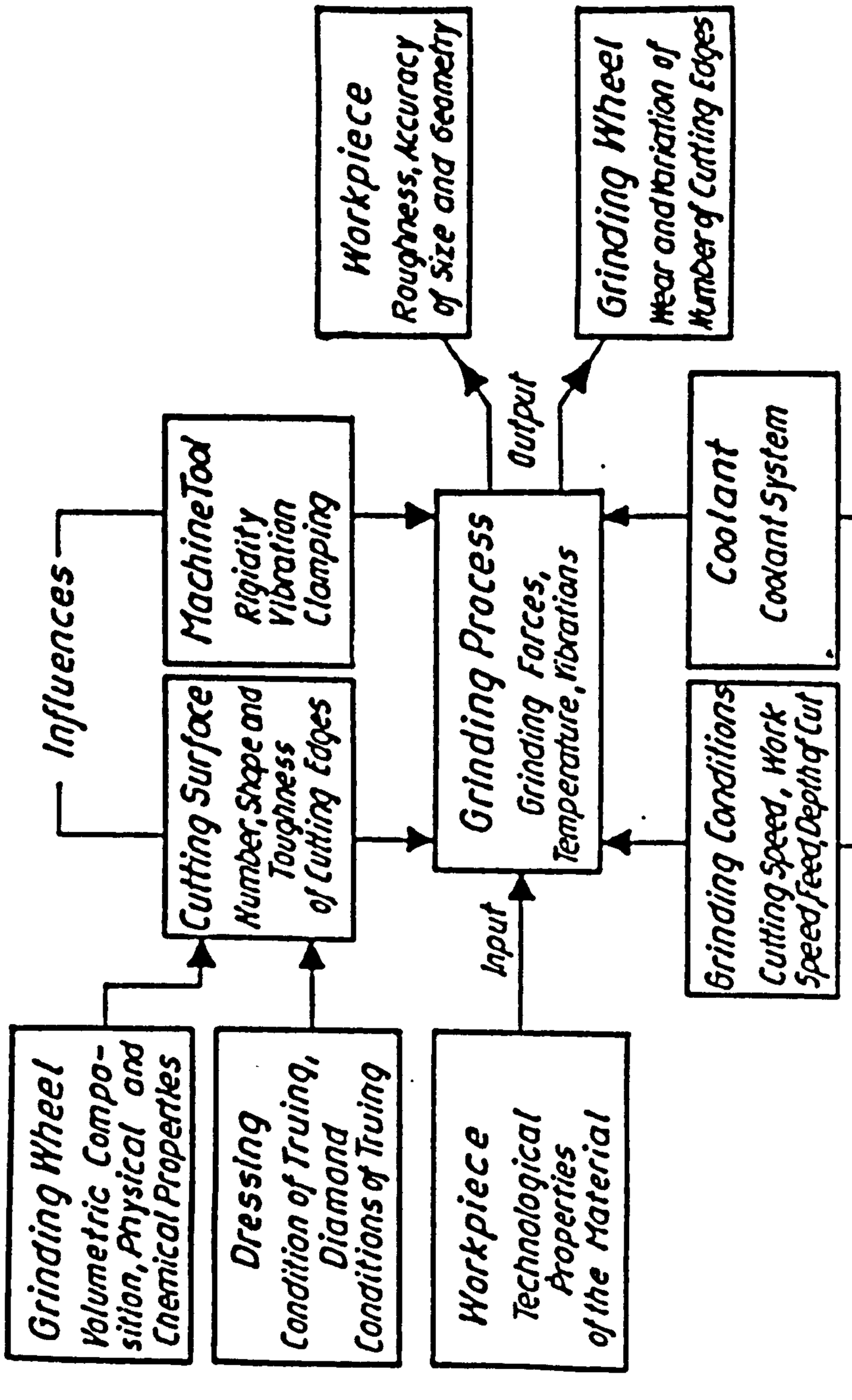

Figure 5.1 Influences on the grinding process.
(Peklenik and Opitz 1962).

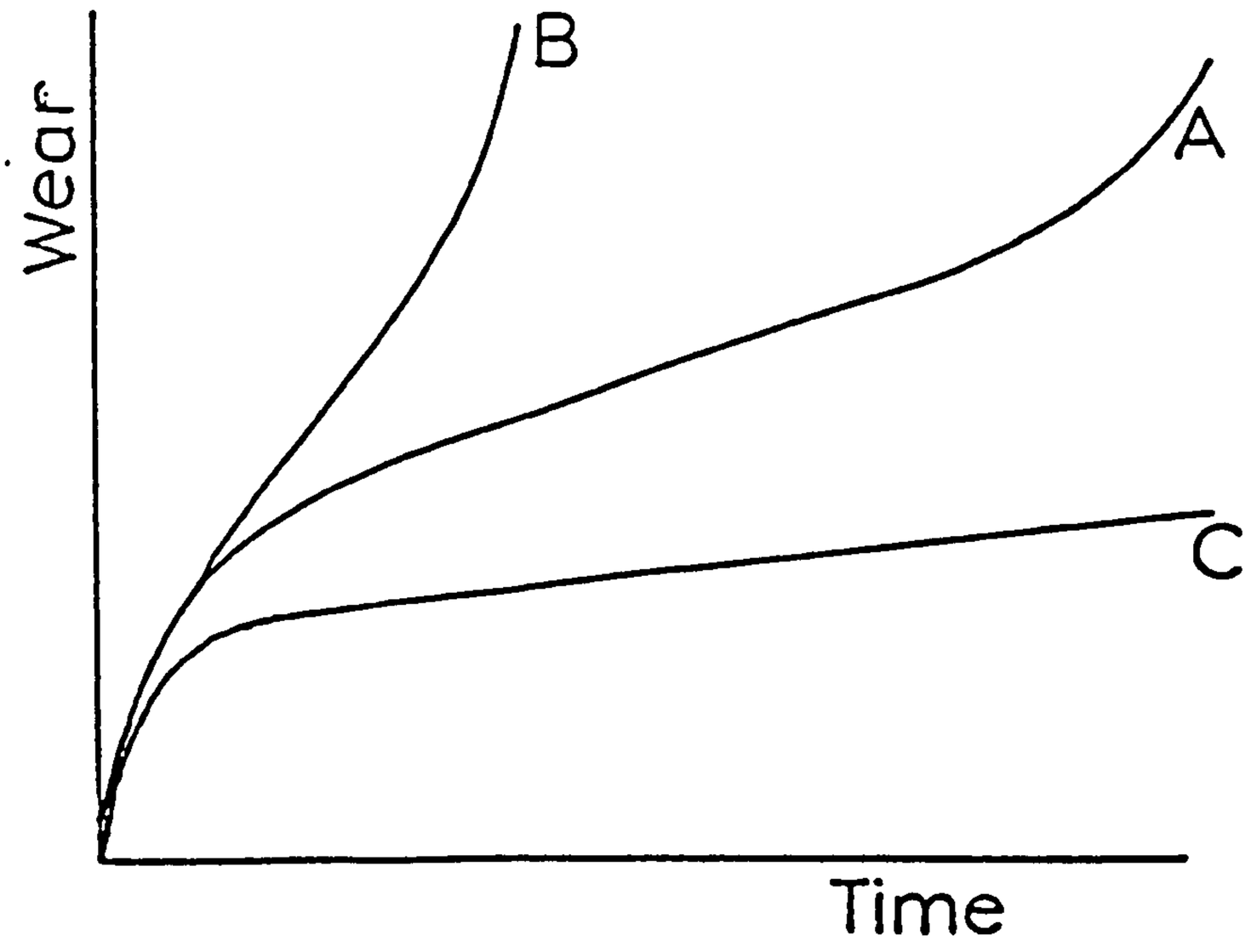

Figure 5.2 Patterns of wheel wear with time.
B - wheel too soft.
C - wheel too hard.

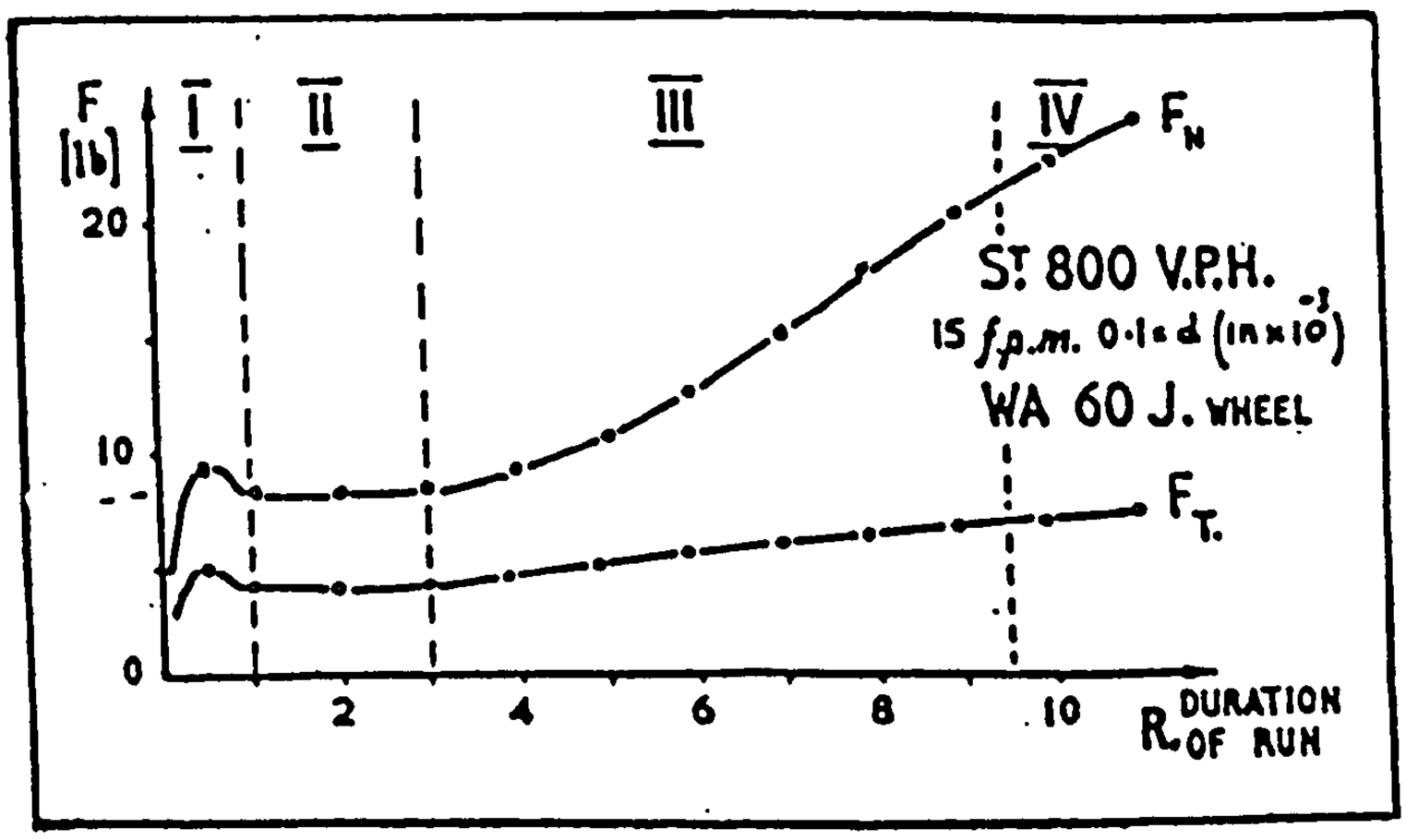

Figure 5.3 Pattern of forces in grinding.
(Grisbrook 1960).

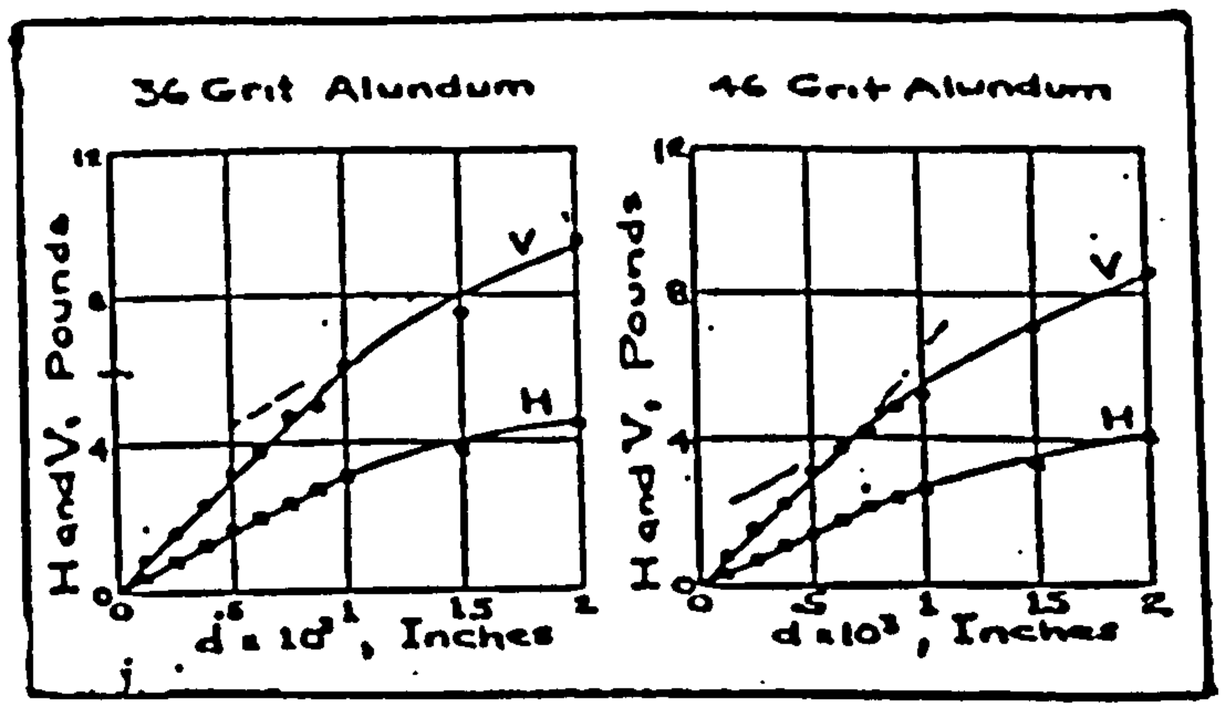

Figure 5.4 Variation of grinding forces with depth of cut.
(Marshall and Shaw 1952).

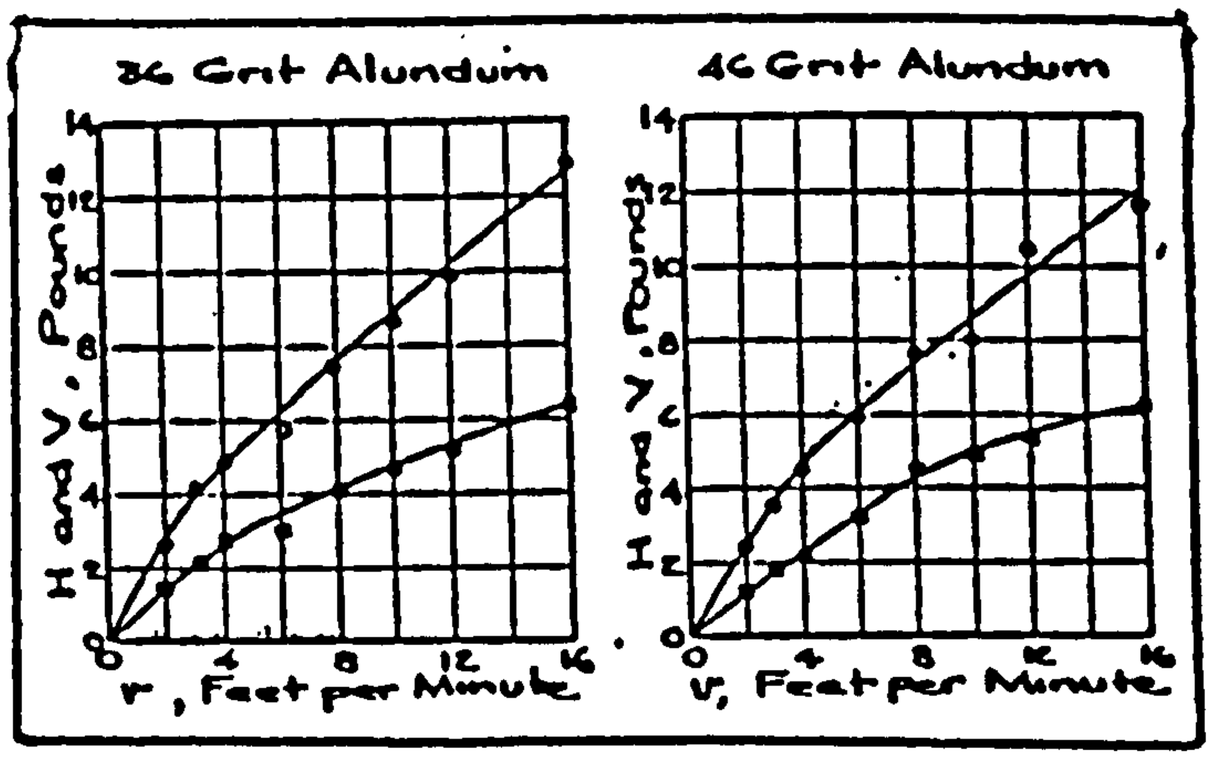

Figure 5.5 Variation of grinding forces with Table speed.
(Marshall and Shaw 1952).

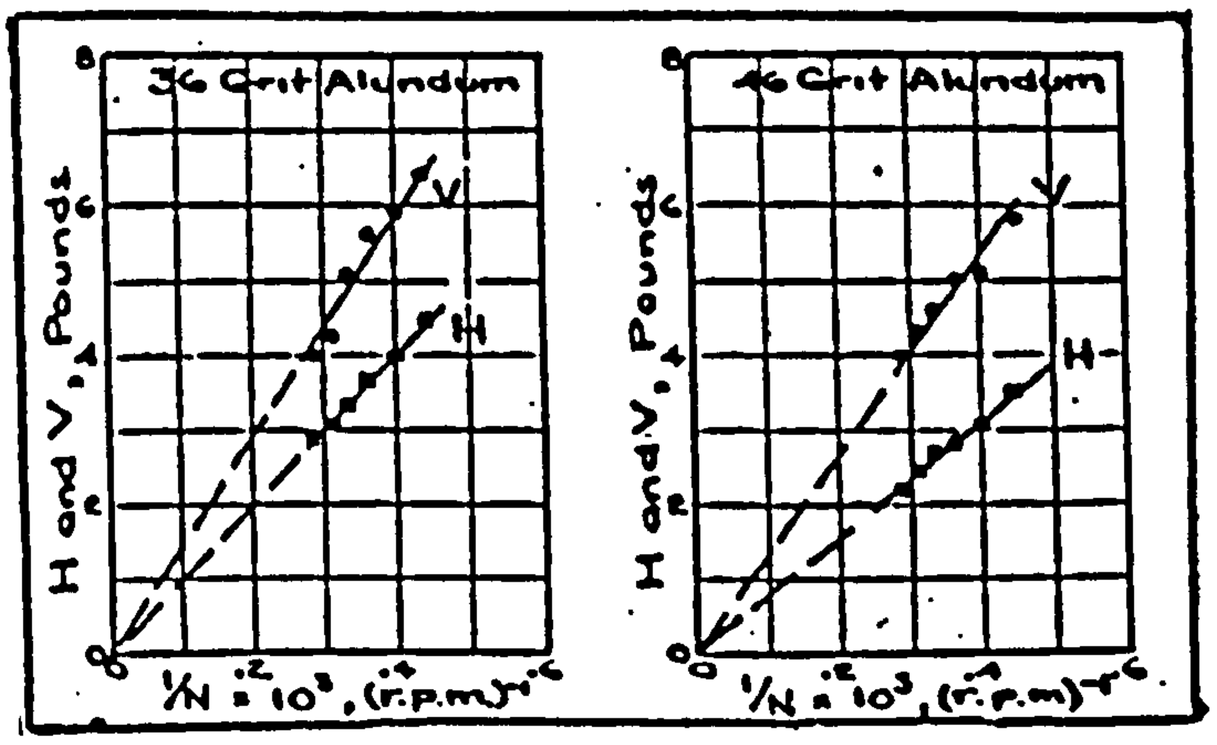

Figure 5.6 Variation of grinding forces with inverse wheel speed.
(Marshall and Shaw 1952).

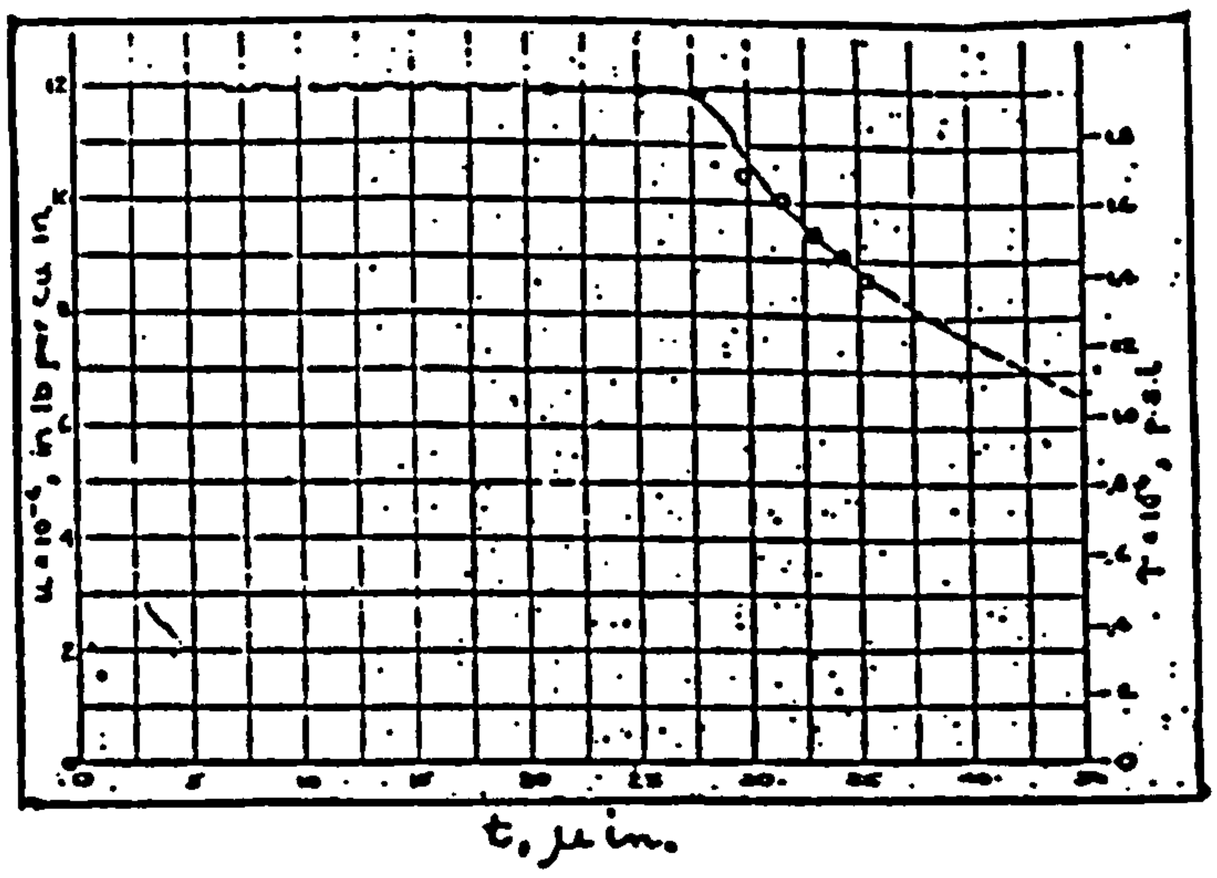

Figure 5.7 Specific energy - depth of cut curve for grinding tests.
(Marshall and Shaw 1952).

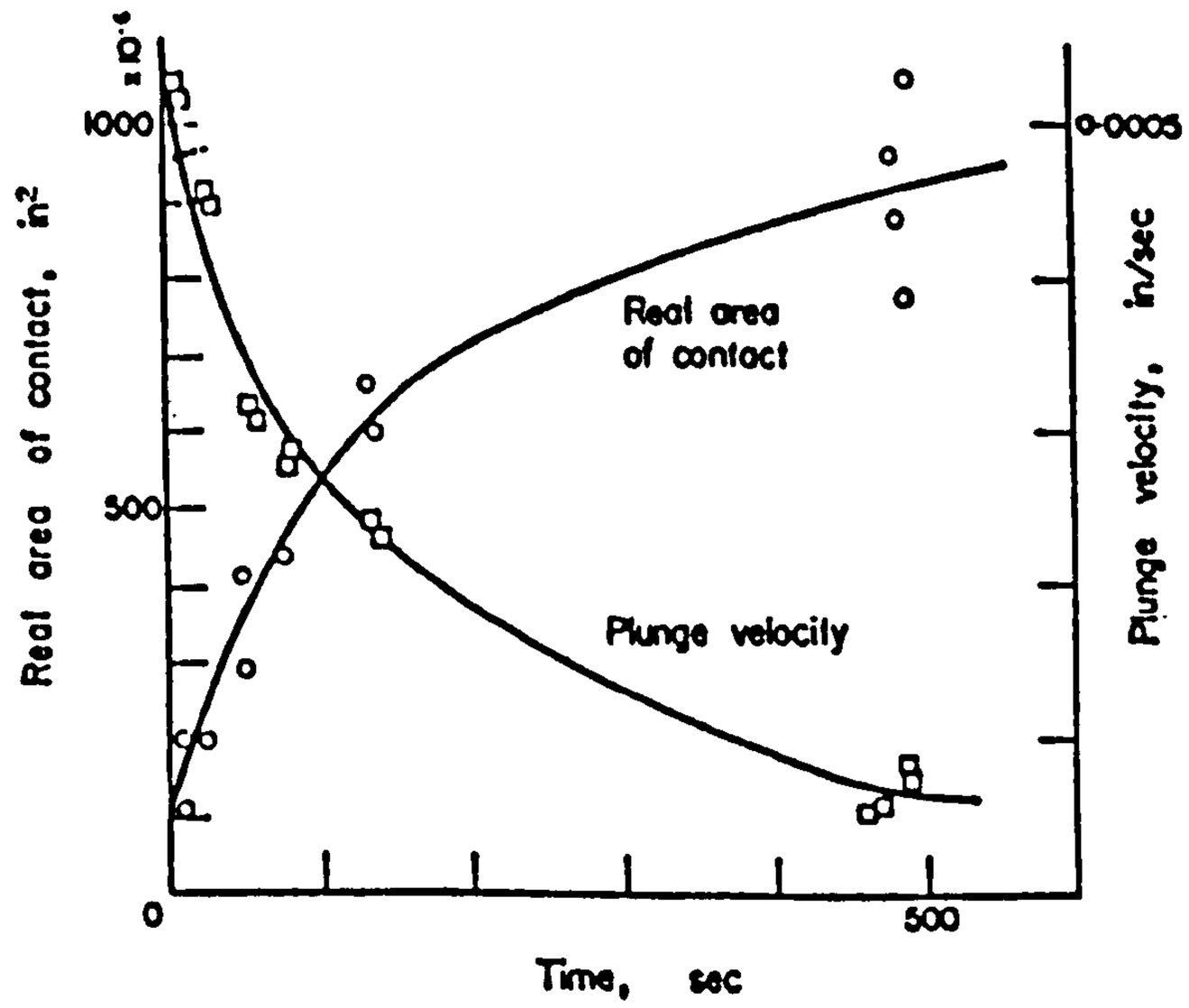

Figure 5.8 Real area of contact and plung grinding velocity vs.time.
(Hahn and Lindsay 1967).

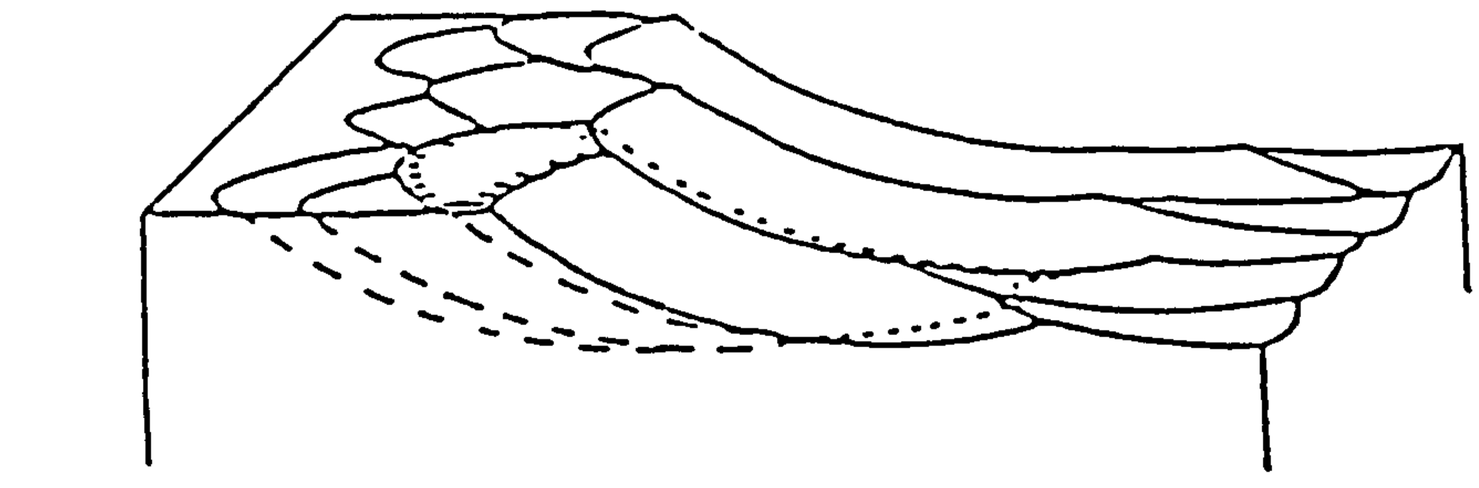

(a)

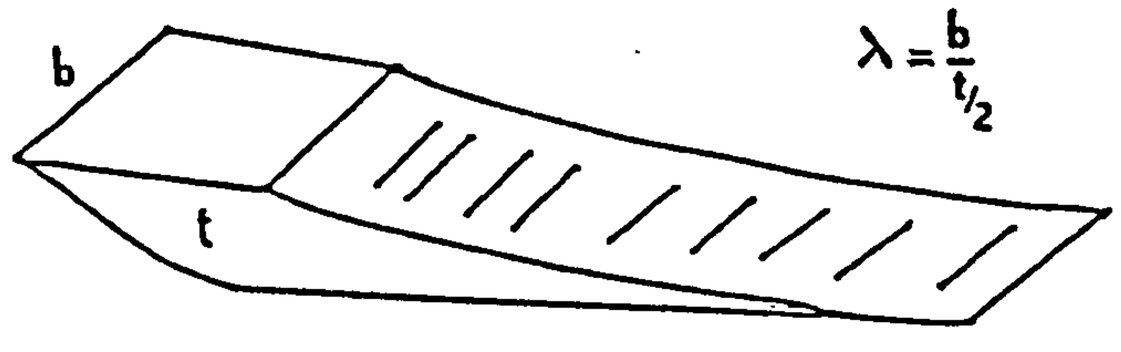

Figure 5.9 Geometry of the undeformed chip.
(a) Actual chip shape.
(b) Shape assumed in analytical studies.

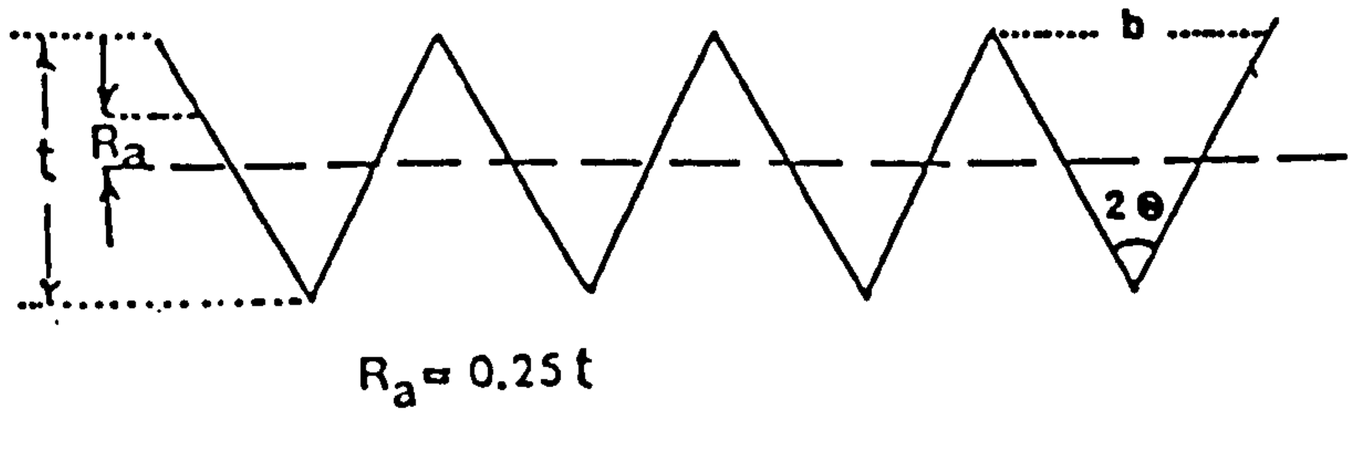

Figure 5.10 Surface produced by individual scratches of depth t.

CHAPTER SIX

FORCE PREDICTION

Chapter 6 - Force Prediction

6.1 Introduction

Under certain grinding conditions for example at high rates of stock removal, the grinding wheel is chosen in such a way that any blunting due to attritions wear of the grits is compensated for by grit fracture. As a result the wheel cutting surface maintains a certain degree of sharpness, the grinding process is more or less in a steady state and since the average grit geometry can be assumed to remain unchanged, the forces are expected to remain constant. Using sharp grit theory of abrasive wear, it is possible to predict the normal grinding force in these conditions, equation (5.5). In precision grinding, however, the fracture wear is kept to a minimum since it is important to keep the dimensions of the wheel constant. Blunter grits are also prefered to produce smoother surfaces. When the grinding conditions are such that the amount of grit fracture is small, the wheel gradually glazes by developing flats on its grains. This is a transient condition in which the forces gradually increase. A different model is then required to predict forces which takes into account the blunting of the grits. Applying the theory developed in chapter (3) to the grinding condition, a model is derived to calculate the normal grinding force with progressive blunting of the grits. The model is obtained by expressing the wear rate per unit sliding distance (equation 3.23) in terms of the parameters of surface grinding.

When applying the expressions developed for the abrasive wear to grinding it is assumed that the same conditions are applicable.

That is to say, the geometry of the groove cut is determined by the shape of the grit, the hardness of the material being ground and the normal force. By keeping the wear rate constant and assuming that forces are related to the grit shape, i.e. width to depth ratio and the amount of wear land b, it is possible to express the rate of metal removal per unit sliding distance in terms of the parameters of grinding. The resulting equation for the wear rate can then be substituted in the expression of wear rate developed for blunt grits, equation (3.23), to obtain the normal grinding force in terms of the grinding parameters.

6.2 Force Prediction (Surface Grinding)

An expression for the normal grinding force in surface grinding is derived as follows:

Let:

D = wheel diameter in cm.

r = wheel speed in revs per minute.

T = table speed in metre per minute.

P_m = hardness of the material being ground in Kg per mm^2.

d = wheel depth of cut in mm.

w = work width in cm. (plunge grinding) or cross feed in cm per traverse.

Then

Wheel surface speed = πDr cm/min.

Work speed = $100T$ cm/min.

Combining the above equations, the relative speed at wheel-work interface is:

Sliding speed (up cut) $= \pi Dr + 100T$ cm/min.

Sliding speed (down cut) $= \pi Dr - 100T$ cm/min.

The rate of metal removal by grinding is given by:

$$\Delta V = \left(\frac{d}{10}\right)(T \times 100).w = 10\ T\ d\ w \quad cm^3/min.$$

Or per unit sliding distance of wheel L'.

$$\frac{\Delta V}{\Delta L'} = \frac{10T\ d\ w}{\pi Dr \pm 100T}$$

Since the table speed in surface grinding is about $^1/_{100}$ of the wheel speed an average value for the rate of metal removal per unit sliding distance will be assumed

$$\frac{\Delta V}{\Delta L'} = \frac{10\ T\ d\ w}{\pi Dr} \quad cm^3/cm \qquad (6.1)$$

From the theory of abrasive wear of blunt grits, equation (3.23) we have;

$$\frac{\Delta V}{\Delta L} = \frac{\pi D}{l}\left(\frac{0.5W}{P_m} - 2AC\ b^2\right) Cot\theta \quad mm^3/mm \qquad (3.23)$$

Using $L' = L \times \frac{D}{l}$ where l is the length of contact between wheel and work, equation (3.23) can be written in terms of L' the wheel sliding distance as

$$\frac{\Delta V}{\Delta L'} = \left(0.5\ \frac{W}{P_m} - 2AC\ b^2\right) Cot\theta \quad mm^2$$

Substituting for wear rate $\frac{\Delta V}{\Delta L'}$, from (6.1) into the above equation, we get

$$\frac{10T\ d\ w}{\pi Dr} \times 100 = \left(0.5\ \frac{W}{P_m} - 2AC\ b^2\right) Cot\theta$$

Re-arranging

$$W = \frac{2000\ T\ d\ w\ P_m}{\pi Dr\ Cot\theta} + 4P_m\ AC\ b^2 \qquad (6.2)$$

Where A in this equation is the apparent area of contact between wheel and worksurface (mm^2). The expression for normal grinding force consists of a term which remains constant during grinding, i.e. $2000T\ d\ w\ P_m/\pi Dr\ Cot\theta$ and an extra term expressing the effect of gradual blunting of the grits, b.

The contact area A can be calculated as

$A = l \times w$

Where l is the arc of wheel in contact with the work surface and is given by

$l = (dD)^{\frac{1}{2}}$. Replacing for A as

$A = (10w)\ (10dD)^{\frac{1}{2}} = 31.62w\ (dD)^{\frac{1}{2}}$ mm^2

We have

$$W = \frac{2000\ T\ d\ w\ P_m}{\pi Dr\ Cot\theta} + 126.5\ Cw(dD)^{\frac{1}{2}}\ P_m\ b^2 \qquad (6.3)$$

Equation (3.21) can be used to express the grinding force in terms of the wheel sliding distance. If ΔW is replaced for by $\frac{W}{AC}$ in this equation, we have

$$4b^2 = \frac{W/AC}{P_m}(1 - e^{-\eta L}) = \frac{W/AC}{P_m}(1 - e^{-\eta' L'}) \qquad (6.4)$$

Replacing for b^2 in the expression of force, equation (6.2) from the above expression we get:

$$W = W_o\ e^{\eta L} = W_o\ e^{\eta' L'} \qquad (6.5)$$

where $W_o = \frac{2000\ T\ d\ w\ P_m}{Dr\ Cot\theta\ f}$ is the sharp grit component of grinding force.

Equation (6.5) could be obtained directly by equating the wear rate, equation (3.34) with equation (6.1).

$$\frac{\Delta V}{\Delta L'} = \frac{1}{2} f \left(\frac{W}{P_m}\right) \text{Cot}\theta \; e^{-\eta' L'} = \frac{10\ T\ d\ w}{Dr} \times 100$$

or

$$W = W_o \, e^{\eta' L'}$$

Furthermore, L' (mm) can be replaced in the above equation (6.5) to express the force in term of V the volume of stock removed. Using equation (6.1), since the rate of metal removal $\frac{\Delta V}{\Delta L'}$ is assumed constant, after integrating (6.1) we have

$$L' = \frac{\pi Dr}{10\ T\ D\ w} V \qquad \text{cm.}$$

Equation (6.5) can now be expressed in term of V, the volume of the stock removed as:

$$W = W_o \, e^{\eta' \frac{\pi Dr}{T\ d\ w} V} \qquad (6.6)$$

Which expresses the normal grinding force as a function of stock removed. It should be noted, however, that η' is dependent on W (equation 3.27)

$$\eta' = \frac{4}{G_o} (AC)^{\frac{1}{2}} \left(\frac{W}{P_m}\right)^{-\frac{1}{2}} \cdot \frac{1}{\pi D} \qquad (3.27)$$

The expression for force can therefore be written as

$$W = W_o \, e^{KW^{-\frac{1}{2}} \cdot V} \qquad (6.7)$$

Where V is the stock removed in cubic centimetre and W the normal grinding force in Kg. The constant K is given by

$$K = \frac{71.13r}{G_o T} \left(\frac{C\ P_m}{w}\right)^{\frac{1}{2}} \frac{D^{3/4}}{d^{I/4}} \qquad (6.8)$$

A straight solution for the model in this form is not possible and W would be obtained by an iterative method.

6.3 Experimental Equipment and Test Procedure

6.3.1 Apparatus

a - Force Measurement equipment

Surface Grinder	Jones & Shipman 1400
Grinding Wheel	A 60 NV (190 x 19 x 32 mm) Universal
Dynamometer	Kiag Swiss 9257 A Kistler
Charge Amplifier	Kistler Type 5001 and 5007
Storage Scope	Gould Advance OS 4000
X-Y plotter	Gould HR 2000

b - Surface Measurement equipment

Computer	Solartron PDP 11
Surface Tracer (1)	Taylor-Hobson Talysurf 3
Surface Tracer (2)	Taylor-Hobson Surtronic 3
Digital Voltmeter	Solartron A 210

Figure (6.1) shows the surface grinder and the equipment used.

6.3.2 Wheel Dressing

A standard commercial diamond was used to dress the wheel prior to each test. The number of passes of the dressing diamond across the wheel has been found to influence the wheel texture (Pahlitzsch and Thoeing, 1959) which in turn has a direct effect on forces and wheel performance. This effect is thought to be due to an increase in the instability of grits on the wheel as the number of passes increases, (Vickerstaff, 1970). Subsequently a standardised dressing procedure was adopted. With the wheel rotating at maximum speed (3500 r.p.m.) several passes of the diamond were made at 0.01 mm depth of cut and a feed rate of 0.0125 mm per wheel revolution to remove the debries until all the previous wear of the wheel were removed. To stabilise the wheel in rim and produce a smooth wheel surface a further two passes at 0.005 mm depth of cut and three passes at 0.003 mm depth of cut was made at a feed rate of 0.48 m/min. Finally, truing operation was terminated by several passes at zero feed to spark out.

The wheel was balanced statically before dressing. Dressing operation was then performed using a new diamond tool; both the feed and the dressing depth of cut were varied to obtain different wheel conditions namely rough, medium and fine.

a) Rough Dressing

Three passes at 0.01 mm. depth of cut;

Three passes at 0.005 mm. depth of cut;

Three passes at 0.003 mm. depth of cut;

Dressing feed = 1.98 $m.min^{-1}$.

b) Medium Dressing

Two passes at 0.01 mm. depth of cut;

Two passes at 0.005 mm. depth of cut;

One pass at 0.002 mm. depth of cut;

One pass at zero down-cut.

Dressing feed = 0.57 $m.min^{-1}$.

c) Fine Dressing

Two passes at 0.01 mm. depth of cut;

Two passes at 0.005 mm. depth of cut;

Two passes at 0.002 mm. depth of cut;

Three passes at 0.001 mm. depth of cut;

Five passes at zero down-cut.

Dressing feed = 0.198 $m.min^{-1}$.

6.3.3 Force Measurement

Grinding forces were measured using a Kiag Swiss 9257A Kistler dynamometer. It has been recommended that the natural frequency of the dynamometer must be at least three times that of the measured event, (Levy and Kroll, 1950). With a natural frequency of 1 KHz, the Kistler dynamometer should therefore be quite capable of responding to any change in grinding forces. Prior to each test the dynamometer was calibrated using static loads. The cross-interference between the force components on the dynamometer was negligible. The workpiece was bolted to the dynamometer by a pair of screws. A tight connection is essential to ensure that the forces are transmitted properly to the dynamometer. A pair of charge amplifiers were used to

amplify the charge representing the grinding force components. Both the amplifiers were fitted with 1 KHz filters. The amplified signals representing the normal and tangential components of grinding forces were relayed to the two channels of the storage scope and a x-y plotter. Forces were measured from the traces obtained from the plotter. Figure (6.2) shows the grinding wheel passing the workpiece attached to the dynamometer and a pair of force traces obtained.

6.3.4 Wheel Cutting Surface Assessment

Traces of the wheel surface were obtained using the surtronic 3 equipped with a chisel-edged stylus of width 1 mm. A cut-off of 2.5 mm was used which gives the longest stroke (12.7 mm). Surface roughness of the wheel and a number of other parameters including peak count were obtained. The value of C, the number of peaks per square mm of the wheel cutting surface was then calculated as

$$C = \frac{n_L}{b.L} = \frac{n_L}{1 \times 25.4}$$

Where

n_L = peak count/in. given by surtronic.

b = stylus width

L = Assessment length.

6.3.5 Experimental Procedure

Experiments were carried out on a Jones & Shipman 1400 horizontal

surface grinder under the following conditions:

Wheel speed, 3500-3000 rpm

Workpiece, a) mild steel, 190 VPN, 79 x 16 x 40 mm.

b) hardened steel, 690 VPN, 79 x 16 x 40 mm.

Width of cut, 16mm.

Table speed, 18 $m.min^{-1}$

Wheel depth of cut, 0.003 (RH,RS) mm per pass

0.002 (MH,MS) mm per pass

0.001 (FH,FS) mm per pass

Grinding fluid, Dry

Grinding was performed under plunge surface grinding condition, that is, the width of the grinding wheel (19 mm) was greater than the workpiece width. Prior to each test both the grinding machine and the measuring equipments were allowed a period of half an hour to warm-up. The dynamometer was calibrated at the start of each test. Surface trace and surface parameters of the wheel were obtained using surtronic 3 fitted with a square skid after wheel being dressed. Due to the random nature of Grinding wheel surface topography, ten readings for each of the wheel surface parameter were taken and an average was calculated in each case to reduce sampling error.

Initial tests indicated that after the wheel had made five complete traverses of the workpiece, grinding force components and the workpiece surface parameters attained stable values and all test measurements were therefore made subsequent to the completion of the fifth traverse. After one pass and then at every successive 250 pass intervals, traces of the force were taken and the wheel surface parameters were obtained. The surface of the ground specimen was measured remote from the grinding environment by means of a Talysurf 3 fitted with a skidless

probe linked to the PDP 11 digital computer programmed to evaluate a range of surface parameters. Details of this system are given in chapter 7. All the workpiece surface parameters were calculated from the digitised traces taken transverse to the cutting lay of the grinding wheel.

Six tests were carried out in this way combining the different wheel dressing (Rough, Medium and Fine) with the Hard and Soft specimens to give:

RH = Rough Dressing, Hard specimen

RS = Rough Dressing, Soft specimen

MH = Medium Dressing, Hard specimen

MS = Medium Dressing, Soft specimen

FH = Fine Dressing, Hard specimen

FS = Fine Dressing, Soft specimen.

Grinding tests where continued until a stage was reached where the wheel condition suggested that its useful operation had terminated.

6.4 Results

Grinding forces and work surface parameters are presented in Table (6.1); wheel surface parameters are shown in Table (6.2). The work surface characteristics produced at different tests varies according to the dressing procedure used. These are shown in figures (6.3) to (6.5). Figure (6.6) shows the initial grinding forces obtained by different dressings.

As the grinding proceeds the work surface parameters change reflecting a change in wheel cutting surface. These can be seen in figures

(6.7) to (6.9).

Variation of grinding force with time: the changes in the normal grinding force as the grinding proceeds can be calculated using equation (6.7) as a function of the material being ground in each case. In the experiments the following values were used:

T = table speed = 18 $m.min^{-1}$

d = wheel depth of cut = 0.003 mm for RH,RS.

= 0.002 mm for MH,MS.

= 0.001 mm for FH,FS.

w = work width = 1.6 cm

P_m = 690 VPN (hard specimen)

= 190 VPN (soft specimen)

D = wheel diameter = 19 cm

r = wheel speed = 3000 r.p.m.

The table speed was obtained from the traces of the force by measuring the time to make a cut and since specimens of known length were used, the average table speed during cutting was calculated. Although the nominal wheel speed was 3500 r.p.m., but it was noticed that during the wheel work engagement the wheel speed dropped considerably. An average value was therefore decided. Figures (6.10) to (6.15) show the changes in normal grinding force with stock removed (cm^3) calculated by the blunt grit model applied to grinding and the actual values obtained for different tests. In calculating the forces using equation (6.7) an average value was used for θ in each case and the parameter f was chosen in such a way that W_o was equal to the actual normal force after one pass. These values for f are shown in each plot.

6.5 Discussion

Examination of tables (6.1) and (6.2) reveals that rougher dressing techniques resulted in wheels with rough cutting surface which in turn produced rougher surfaces. Higher values of average slope, smaller percentage of zero slope and smaller forces were in general associated with rough wheels as shown in figures (6.3) to (6.6). These figures show a noticeable correlation between the pattern of the forces and the percentage of zero slopes for different dressing procedures. This observation suggests that forces in grinding could be strongly influenced by this parameter. With tests RH and MH, for instance, the initial normal forces are equal (5 kg) despite the fact that the cutting surface of the wheels used had quite distinct roughness values. Examination of the table (6.1) shows that the only parameter which is nearly identical in these cases is the percentage of zero slope. Similar observation can be found in tests RS and MS.

As grinding continues and the grits start to blunt a gradual increase is observed in the percentage of zero slopes which is accompanied by a drop in the average slope value, figures (6.8) and (6.9). It is interesting to note that at the same time the grinding coefficient (the ratio of tangential to normal force) gradually decreases, figure (6.16). This reduction in grinding ratio has been identified as being the result of blunting of the grits and the formation of the flats on top of them, Grisbrook (1960), Hahn and Lindsay (1967).

The total area of flats on the wheel surface over an area equal to the wheel-work interface can be deduced. This is given by $2AC\ P_m\ b^2$

and can be calculated from equation (6.2) at each stage during grinding knowing the appropriate values of force. Figure (6.17) shows the variation of this quantity with the number of passes for different tests. Since the apparent contact area between the wheel and the workpiece differ in each case, the values of the total area of flats have been normalised in this figure to give the area of flat per square millimetre of wheel work interface. This area is strongly related to the forces in grinding. According to the blunt grit model the increase in normal grinding force is proportional to the total area of flats.

The prediction of the normal grinding force taking into account the effect of blunting of the grits showed a good agreement with the experimental results, figures (6.10) to (6.15). In calculating the grinding forces only the effect of blunting of the grits were taken into account which was represented by the percentage of zero slope. Although the values of C and Δ_a change with time, these were taken constant in the model. The close agreement between the theory and the experimental values observed emphasises the importance of this factor with relation to forces and justify the use of percentage of zero slopes to represent it.

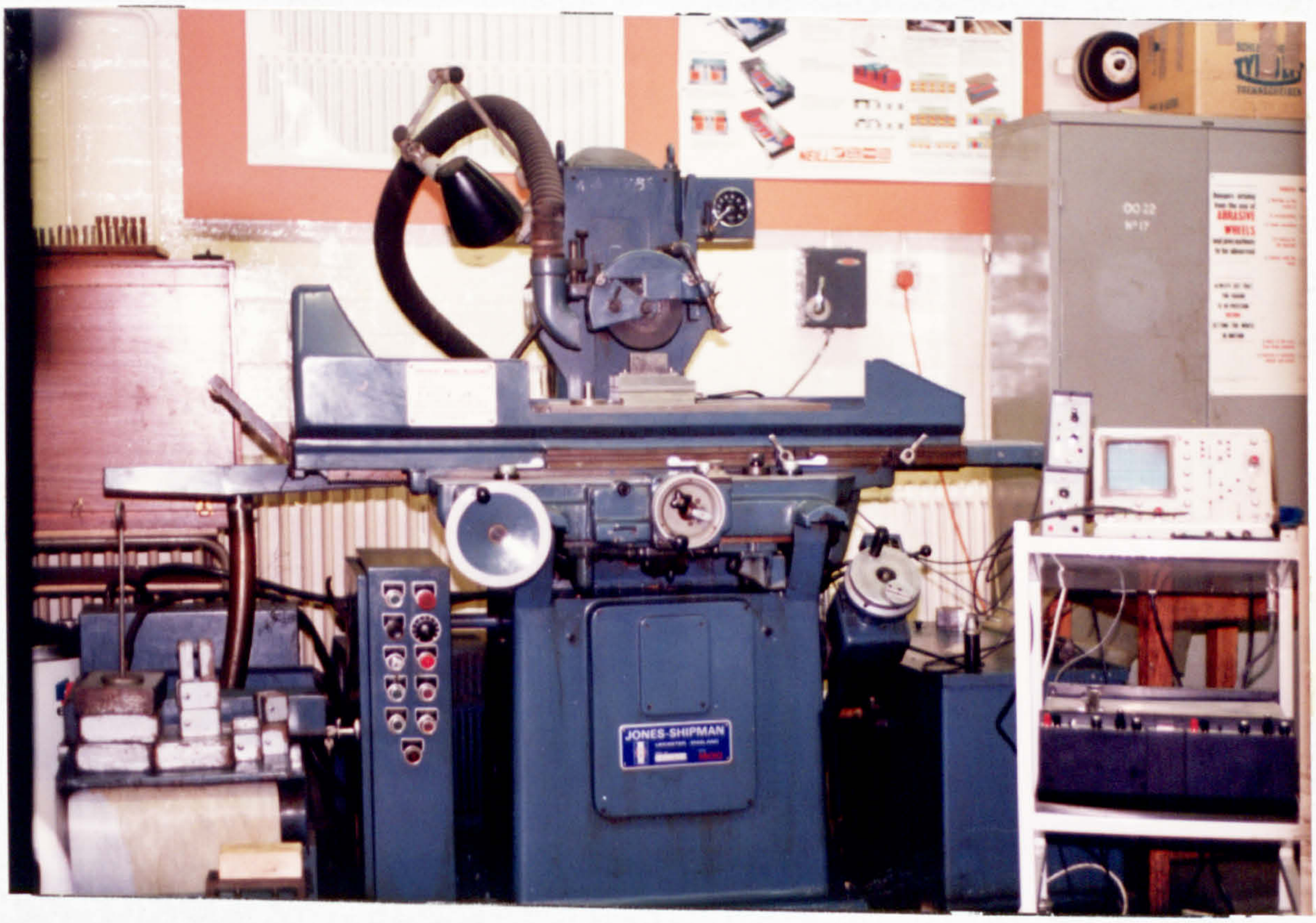

Figure 6.1 Surface grinder and the equipments used.

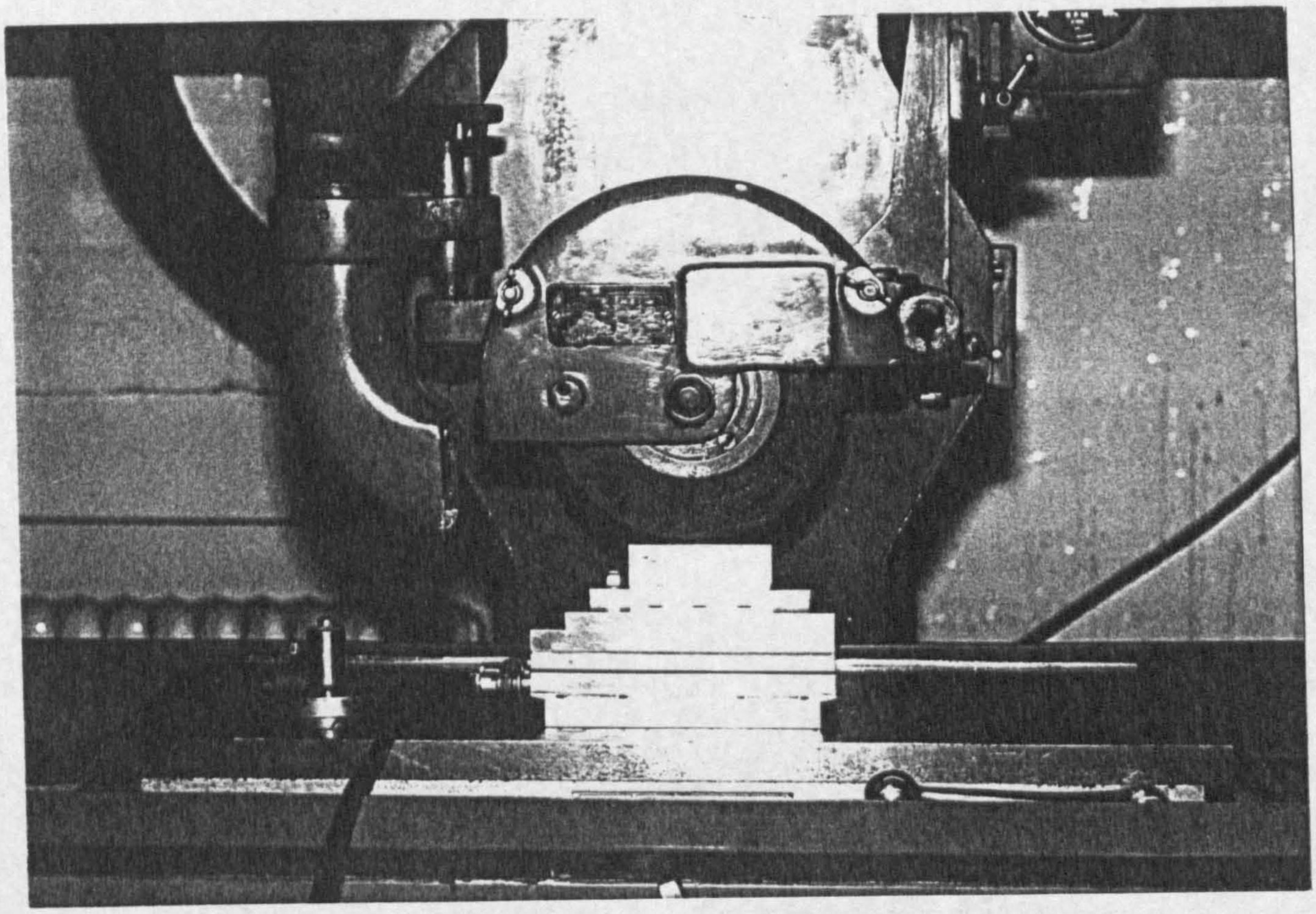

Figure 6.2 Grinding wheel passing the workpiece and the dynamometer and a pair of force traces showing tangential and normal components of grinding force.

Grind. test	F_n(kg)	F_t(kg)	R_a(μm)	% Zero Slope	Δ_a
1RH	5	2.8	3.26	3.6	10.77
250RH	5.8	3.2	2.96	4.5	10.33
500RH	8	4.2	2.42	3.7	10.22
750RH	9	4.6	2.35	4.7	10.29
1000RH	9.5	4.9	1.90	4.2	9.20
1250RH	9.6	4.9	1.89	4.2	8.9
1500RH	10	5	2.0	5	9.73
1750RH	10.8	5.2	1.31	5	8.0
2000RH	14	6.2	1.54	6.4	7.70
1RS	7.0	4.5	4.62	4.8	10.54
250RS	8.0	4.8	3.72	5.4	11.01
500RS	13.5	8.0	3.92	6.0	10.54
750RS	12.0	6.8	3.60	4.4	10.11
1000RS	15.0	7.8	3.41	4.9	8.99
1250RS	18.4	9.2	2.53	6.2	8.3
1500RS	20.0	9.8	2.76	4.9	8.75
1750RS	22.0	10.6	2.78	5.8	7.51
2000RS	27.5	11.5	3.91	6.4	7.32
1FH	6.0	3.0	0.06	9.2	4.59
250FH	6.8	3.3	0.10	15.6	2.96
500FH	8.0	3.9	0.15	15.2	2.24
750FH	8.0	4.1	0.18	13.2	2.24
1000FH	8.0	4.0	0.15	15.6	2.17
1250FH	9.0	3.8	0.14	25.0	1.62
1500FH	10.0	4.0	0.19	23.0	1.28

Table 6.1 - Grinding force and workpiece surface parameters.

Grind. test	F_n(kg)	F_t(kg)	R_a(μm)	% Zero slope	Δ_a
1FS	10.0	5.0	0.39	11.6	3.95
250FS	25.0	12.0	0.64	10.0	3.86
500FS	30.0	14.0	0.98	11.6	3.60
750FS	35.0	15.2	1.46	12.0	2.95
1MH	5.0	2.5	0.57	3.9	9.20
250MH	6.3	3.3	0.72	4.3	10.43
500MH	8.8	4.4	0.72	5.8	9.83
750MH	8.4	4.1	0.77	5.2	8.60
1000MH	10.0	4.2	0.83	5.8	7.88
1250MH	10.0	4.0	1.07	6.0	7.85
1500MH	11.0	4.1	1.17	5.4	7.85
1750MH	12.0	4.3	0.94	6.8	6.25
1MS	6.6	3.5	0.84	5.2	5.53
250MS	7.9	3.9	0.97	9.2	4.49
500MS	9.8	4.5	1.22	7.4	6.0
750MS	12.6	5.3	0.81	9.8	5.29

Table 6.1 continued.

Grind. test	R_a (μm)	n_L	C/mm^2	Grind. coeff.
0RH	10.6	45	1.7	
1RH	15.25	42	1.6	0.56
250RH	16.5	47	1.8	0.55
500RH	14.1	72	2.8	0.52
750RH	13.5	87	3.4	0.51
1000RH	13.0	108	4.2	0.51
1250RH	11.9	108	4.2	0.51
1500RH	8.3	125	4.9	0.5
1750RH	8.2	149	5.8	0.48
2000RH	9.7	158	6.2	0.44
0RS	10.3	39	1.5	
1RS	14.5	35	1.3	0.64
250RS	13.1	38	1.5	0.6
500RS	10.2	82	3.2	0.59
750RS	9.1	86	3.4	0.56
1000RS	9.7	124	4.9	0.52
1250RS	10.1	143	5.6	0.5
1500RS	9.7	162	6.4	0.49
1750RS	9.4	181	7.1	0.48
2000RS	10.5	156	6.1	0.41
0FH	5.4	167	6.5	
1FH	5.7	190	7.5	0.5
250FH	3.7	207	8.1	0.49
500FH	4.7	183	7.2	0.48
750FH	5.1	158	6.2	0.51
1000FH	3.9	207	8.1	0.5
1250FH	6.3	153	6	0.42
1500FH	6.1	127	5	0.4

Table 6.2 - Grinding wheel surface parameters.

Grind. test	R_a (μm)	n_L	C/mm^2	Grind. coeff.
0FS	3.6	82	3.2	
1FS	3.4	210	8.2	0.5
250FS	6.5	120	4.7	0.48
500FS	6.1	149	5.8	0.46
750FS	8.5	65	2.5	0.43
0MH	5.9	142	5.6	
1MH	7.9	172	6.7	0.5
250MH	6.7	175	6.9	0.52
500MH	8.4	190	7.5	0.5
750MH	5.9	215	8.5	0.48
1000MH	6.2	212	8.3	0.42
1250MH	5.3	190	7.5	0.4
1500MH	7.5	143	5.6	0.37
1750MH	7.0	155	6.1	0.35
0MS	6.1	154	6	
1MS	9.4	120	4.7	0.53
250MS	7.0	128	5	0.49
500MS	9.7	102	4	0.45
750MS	9.3	91	3.6	0.42

Table 6.2 continued.

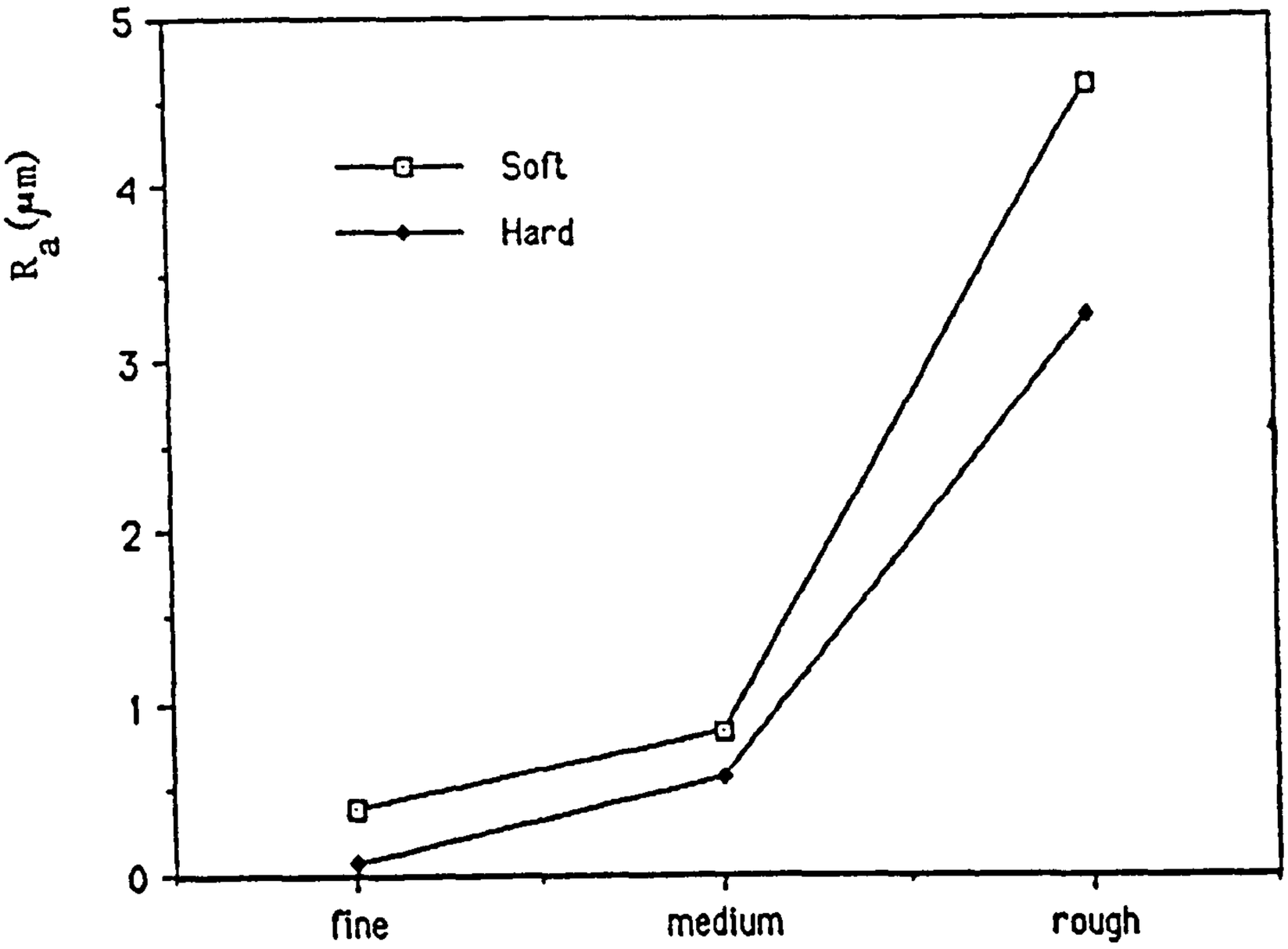

Figure 6.3 Variation of surface roughness R_a with dressing.

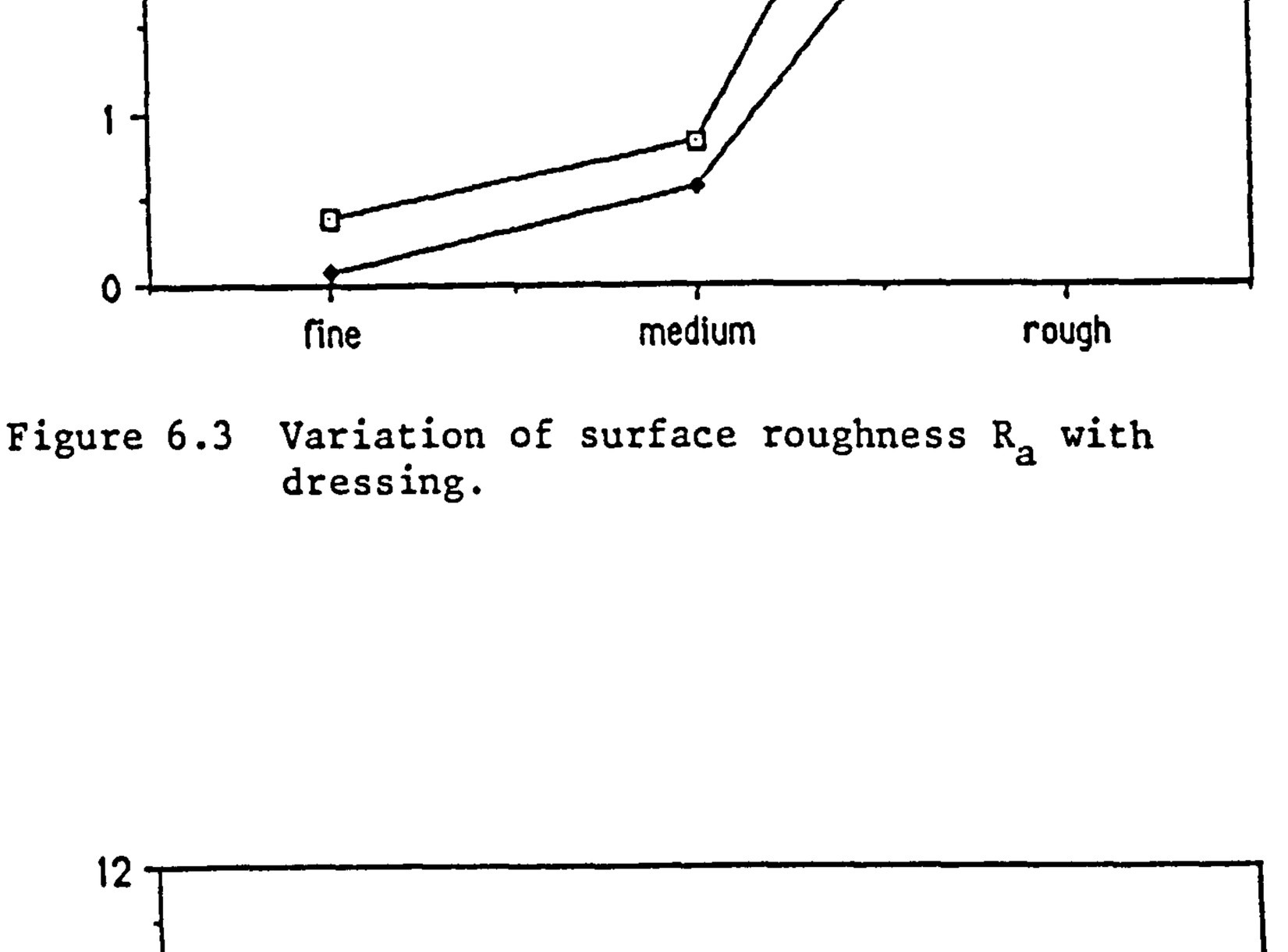

Figure 6.4 Variation of average slope Δ_a with dressing.

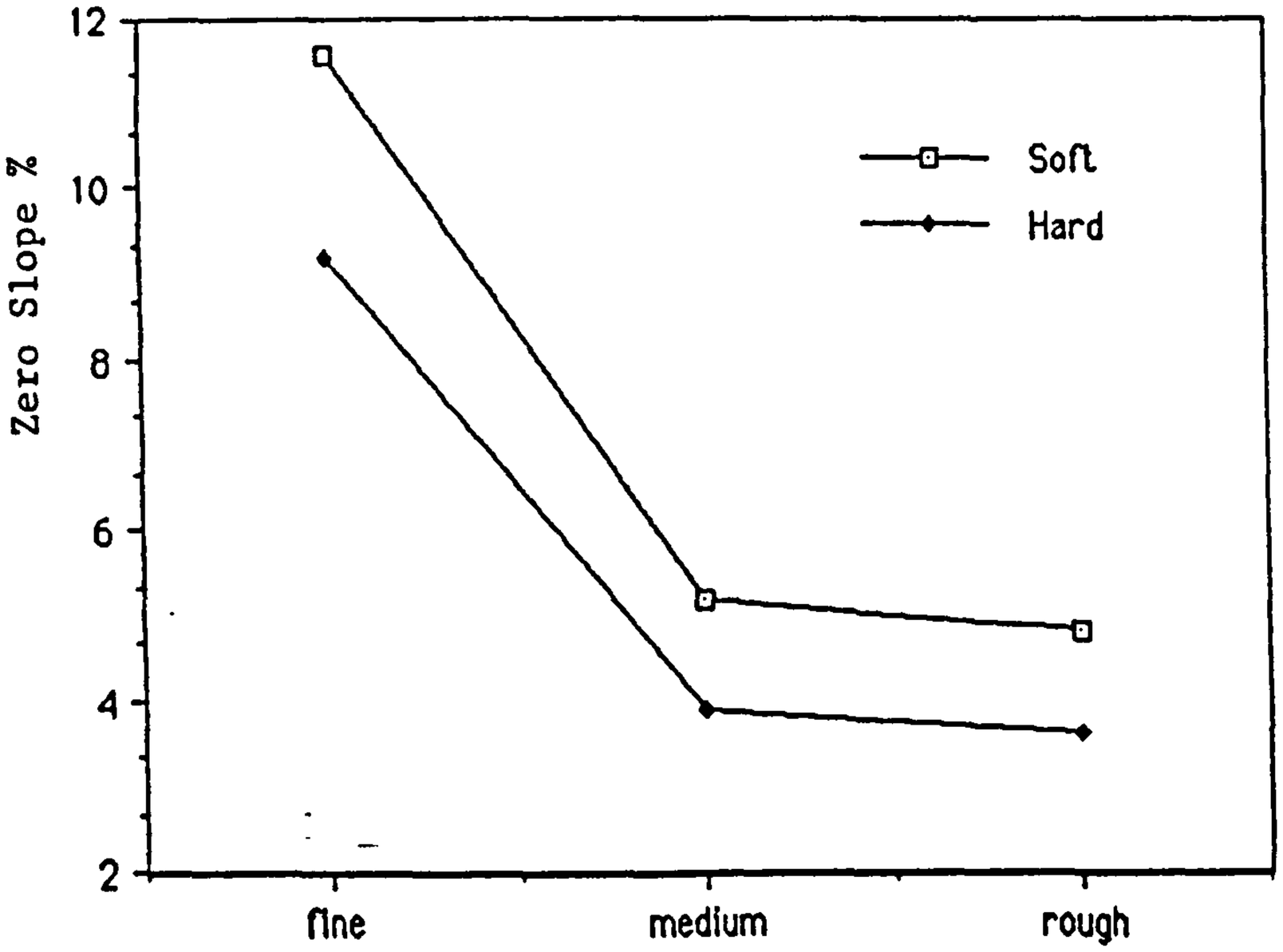

Figure 6.5 Variation of percentage zero slope with dressing.

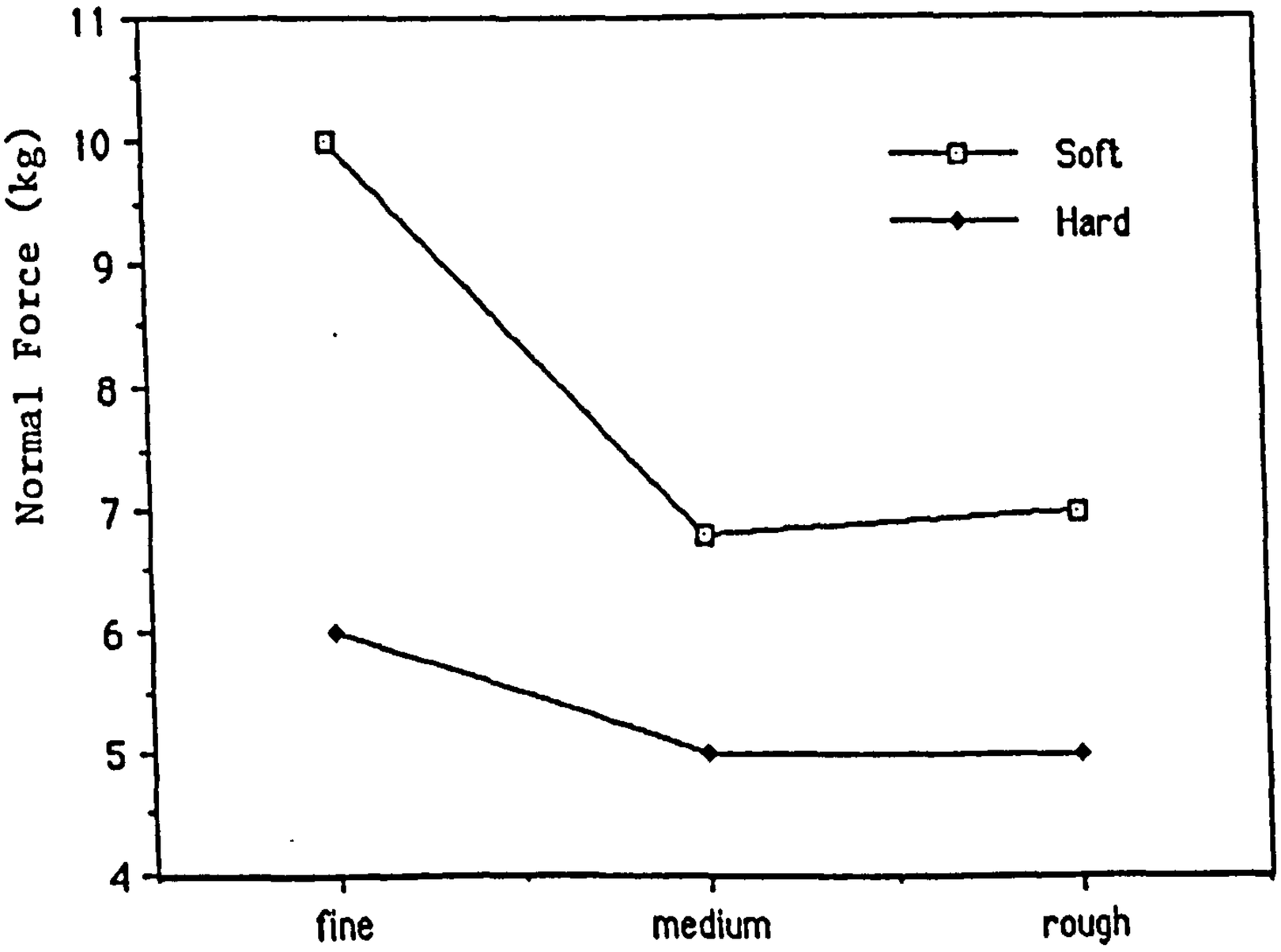

Figure 6.6 Changes in normal grinding force with dressing.

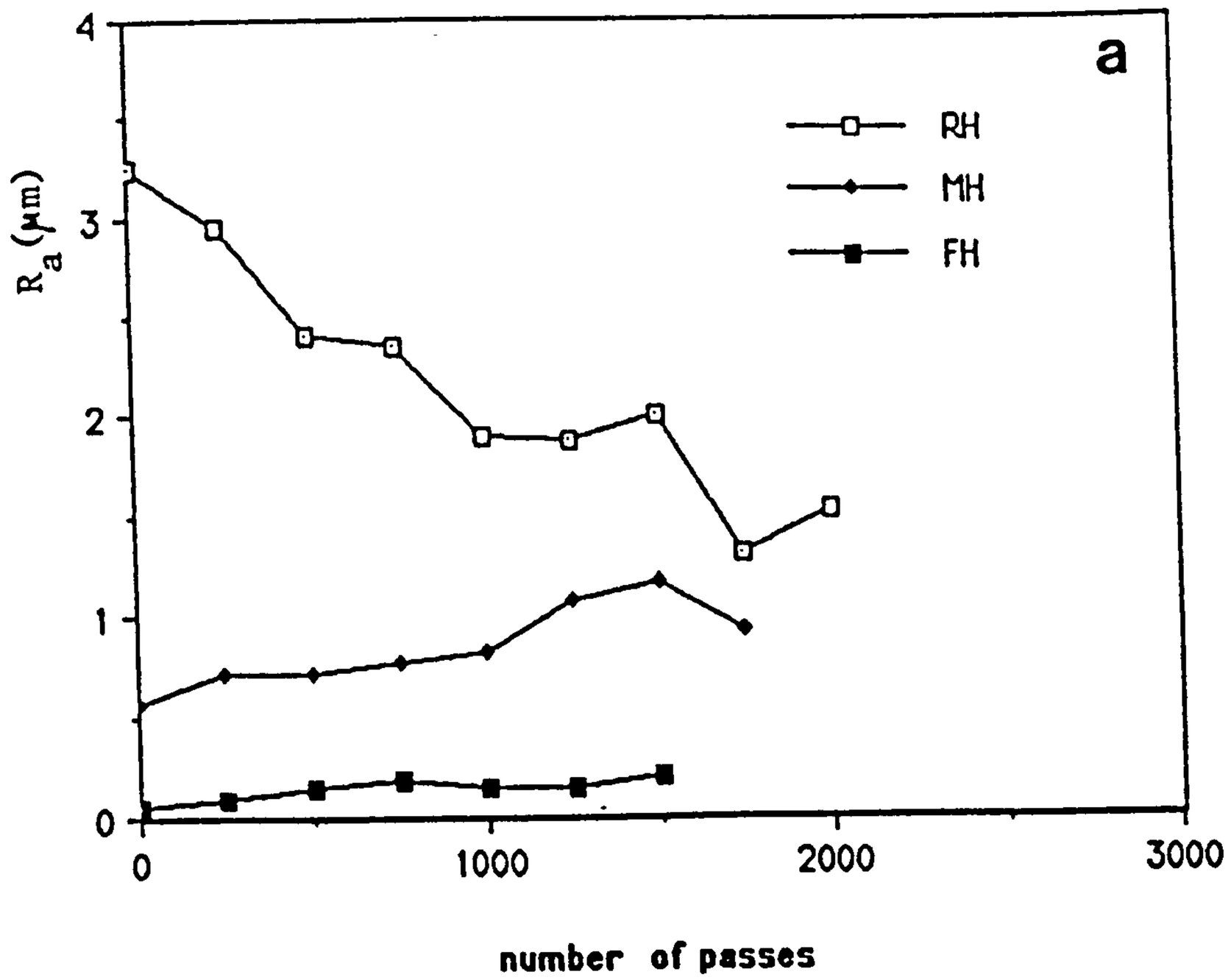

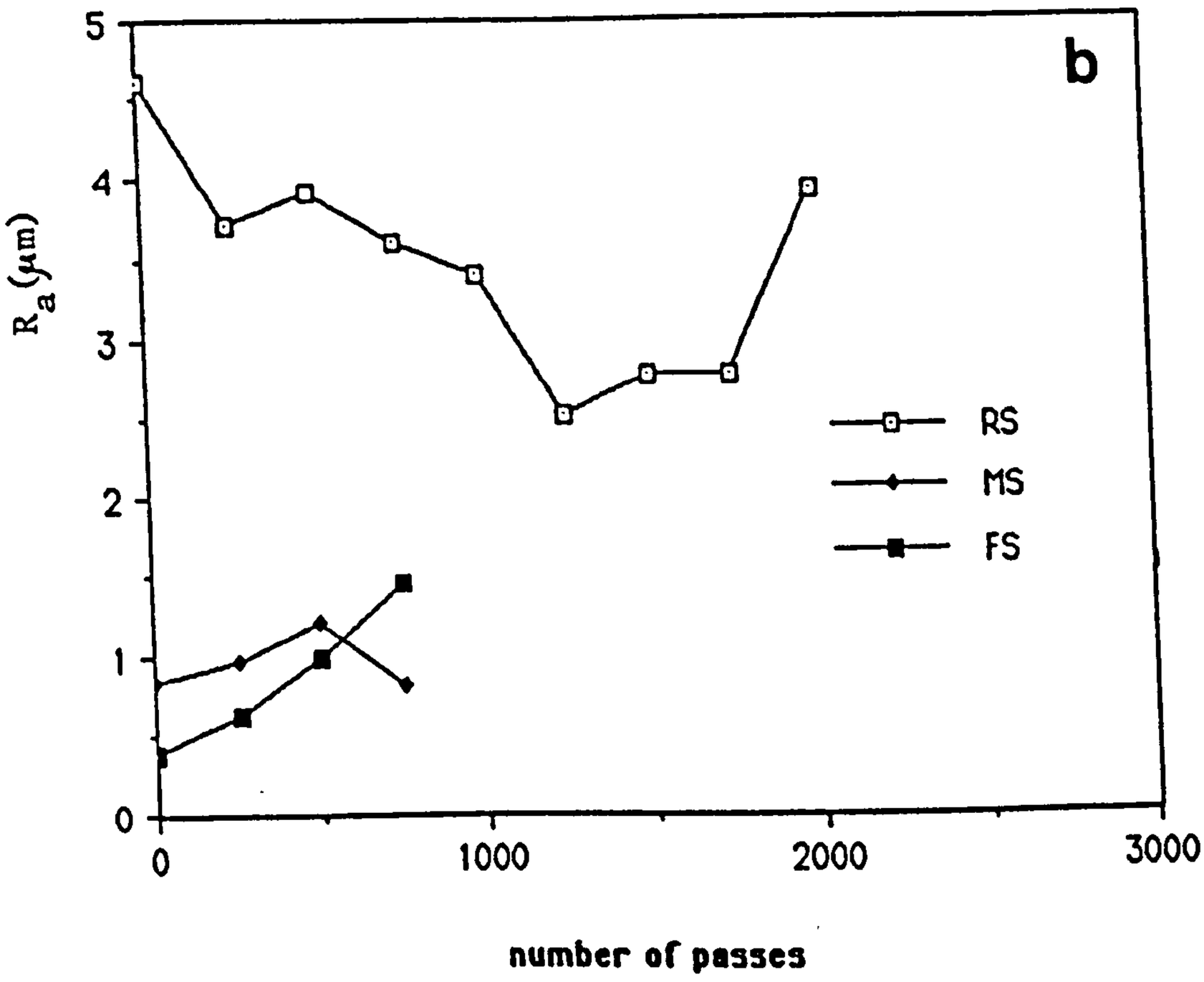

Figure 6.7 Changes in surface roughness with grinding time. (a) Hard, (b) Soft specimen.

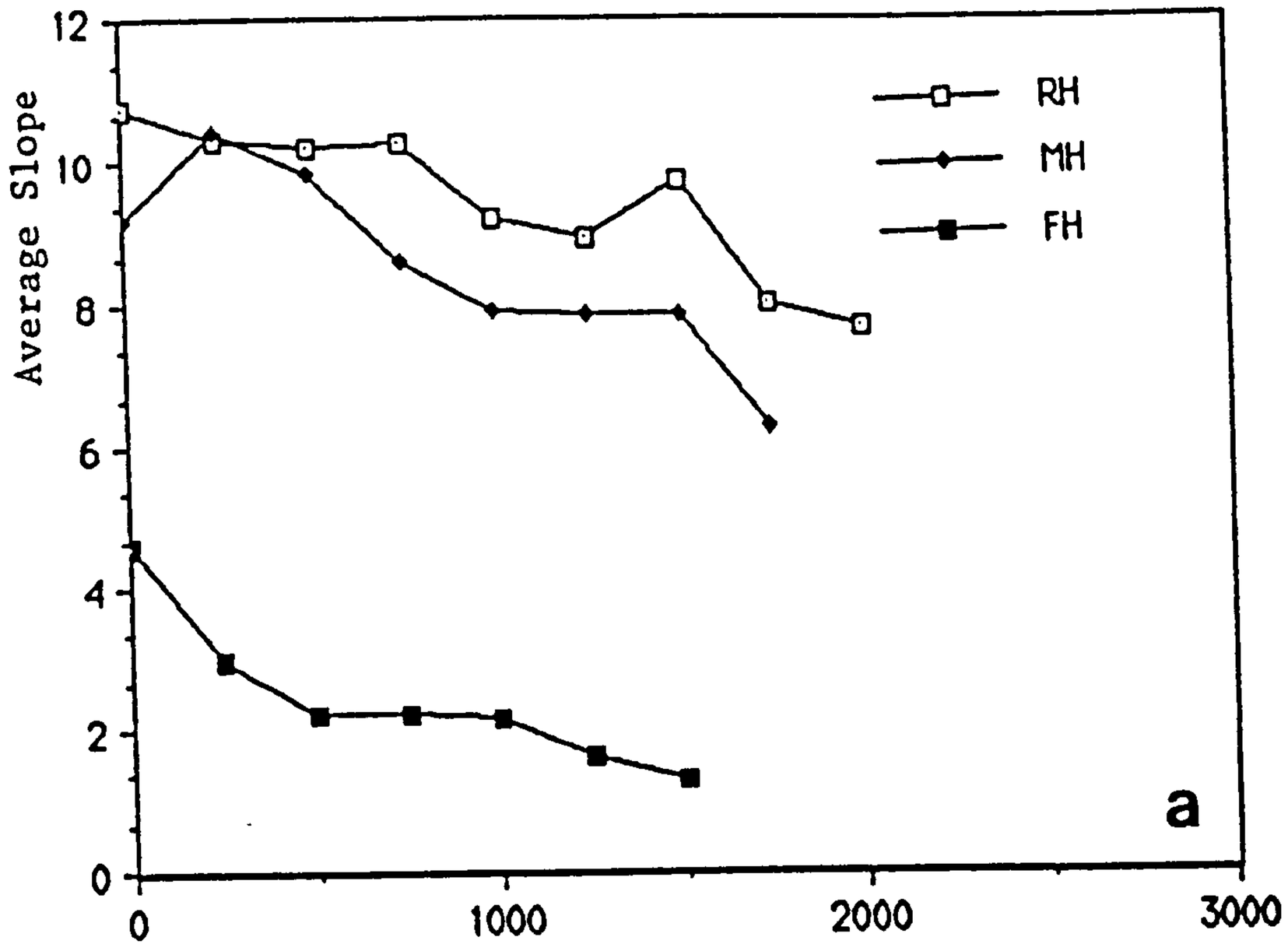

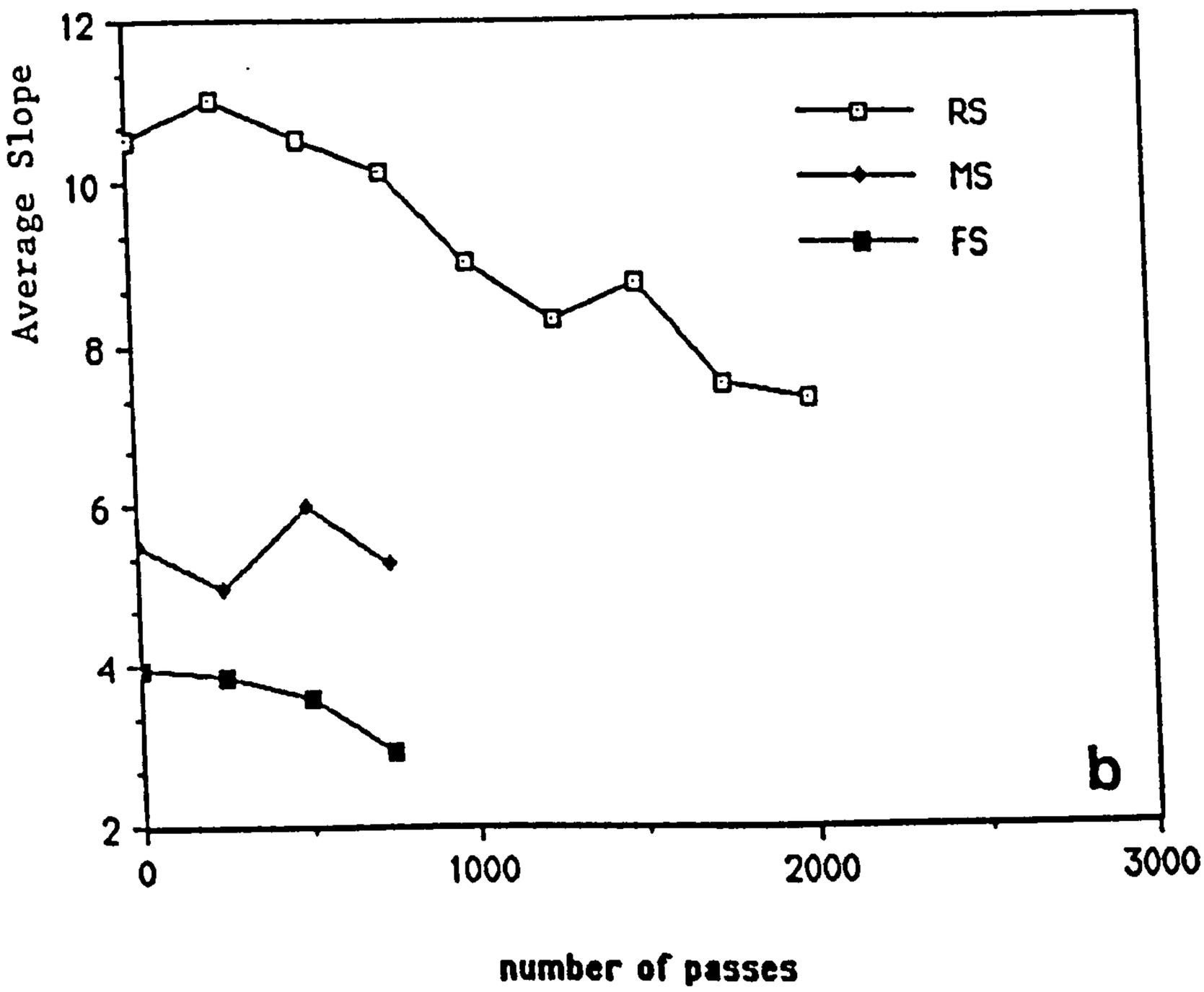

Figure 6.8 Changes in the average slope with grinding time. (a) Hard, (b) Soft specimen.

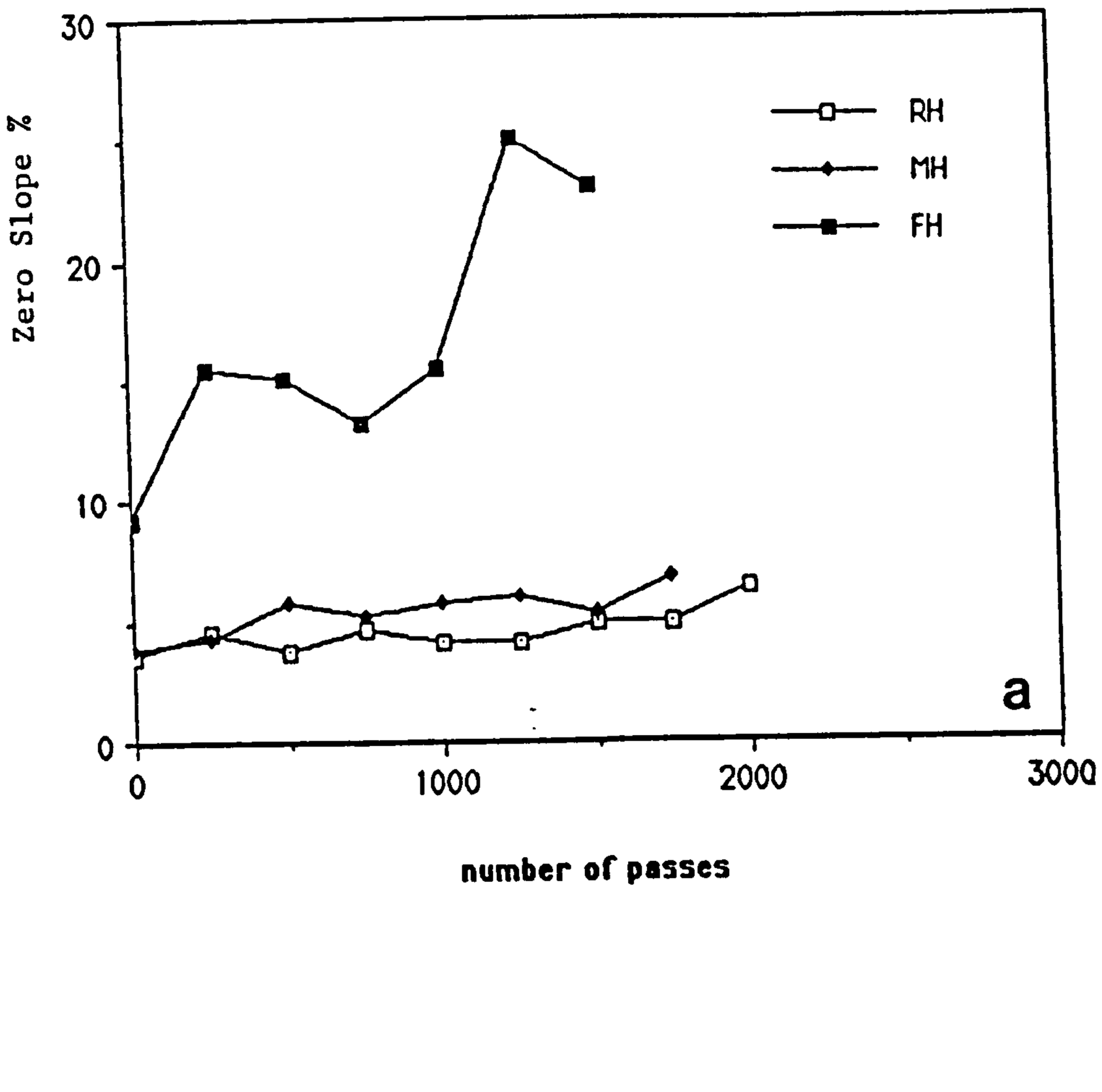

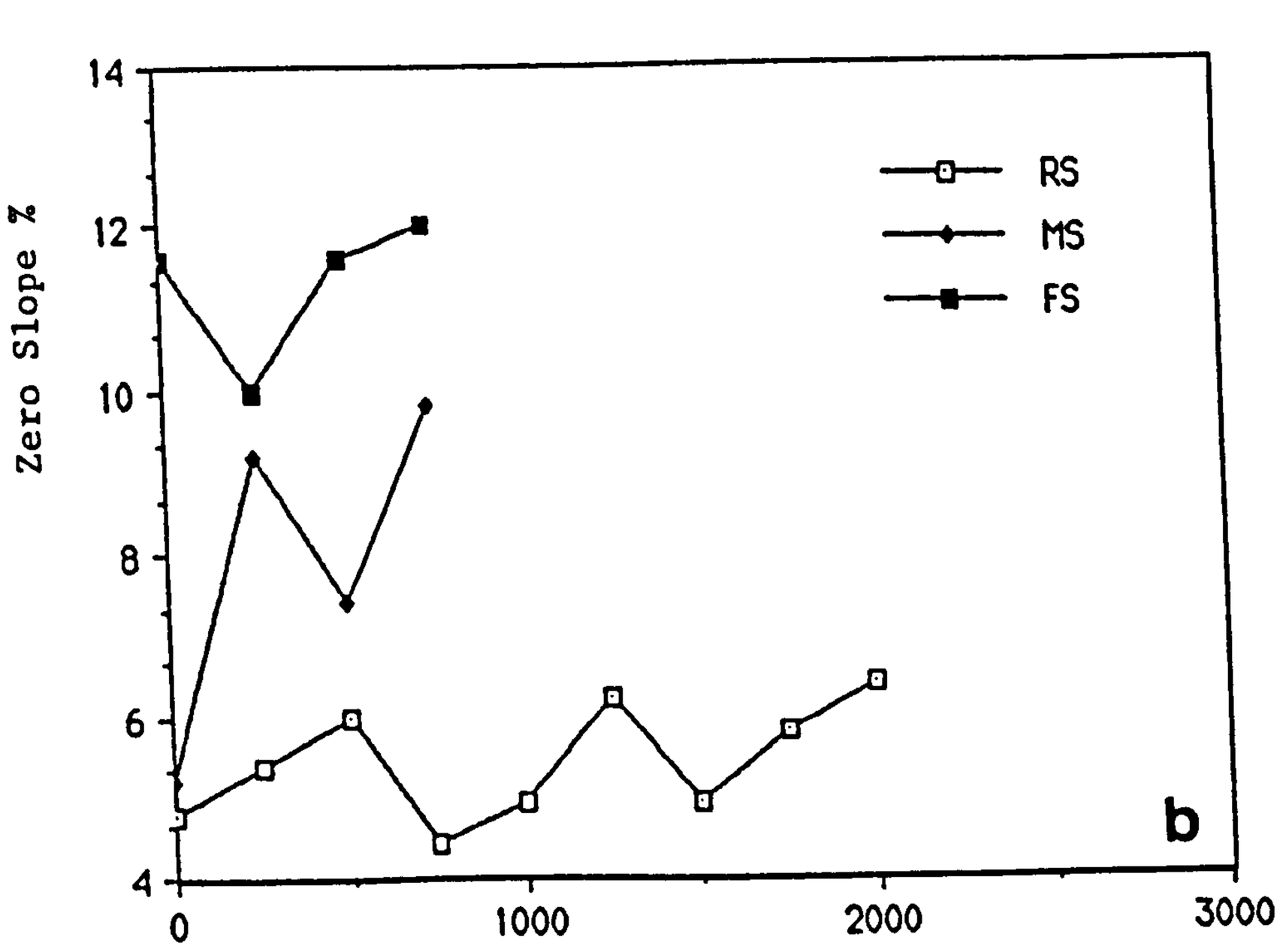

Figure 6.9 Changes in the percentage of zero slope with grinding time. (a) Hard, (b) Soft specimen.

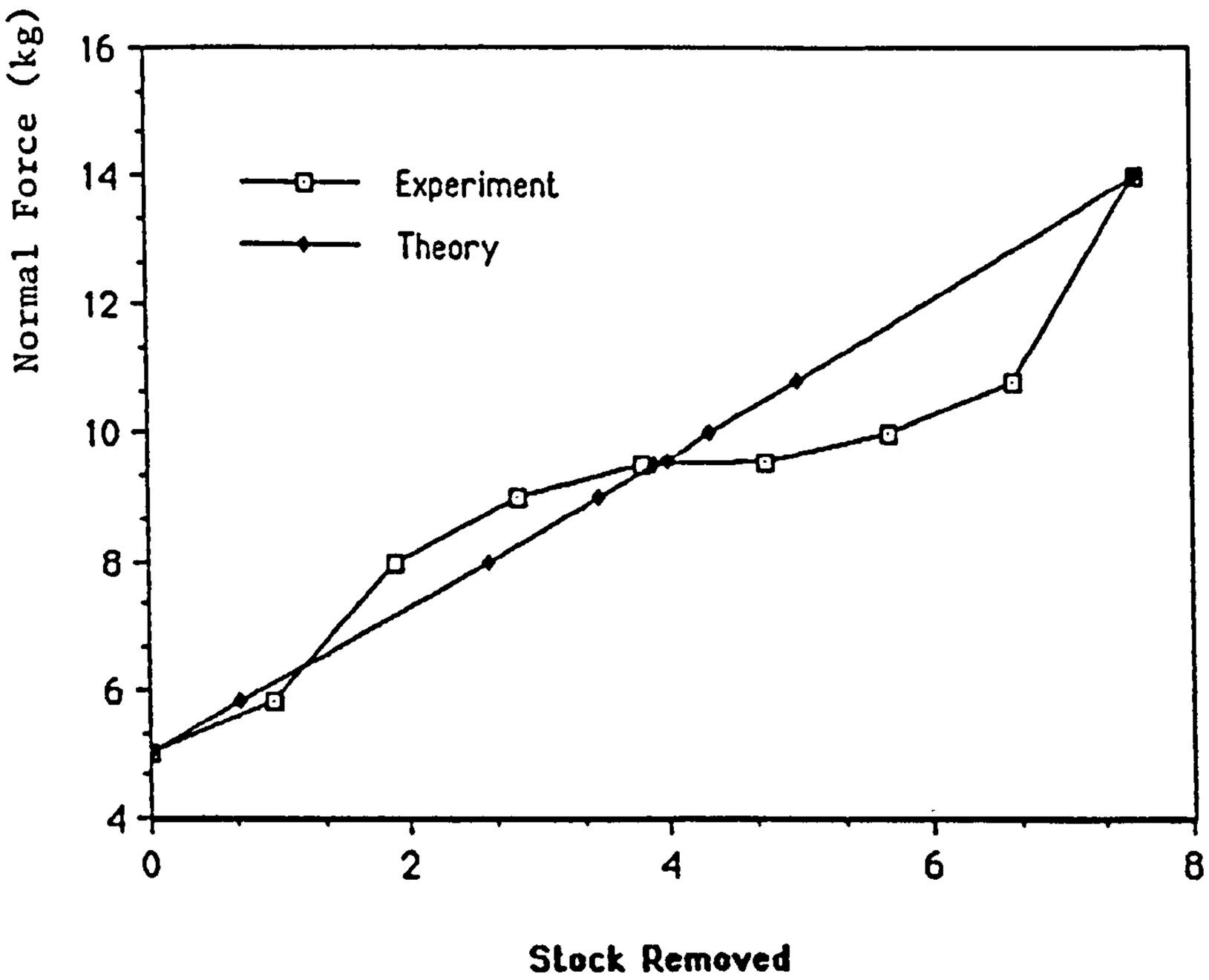

Figure 6.10 Changes in Normal Grinding Force with stock removed (cm^3). Test RH, f = 0.8.

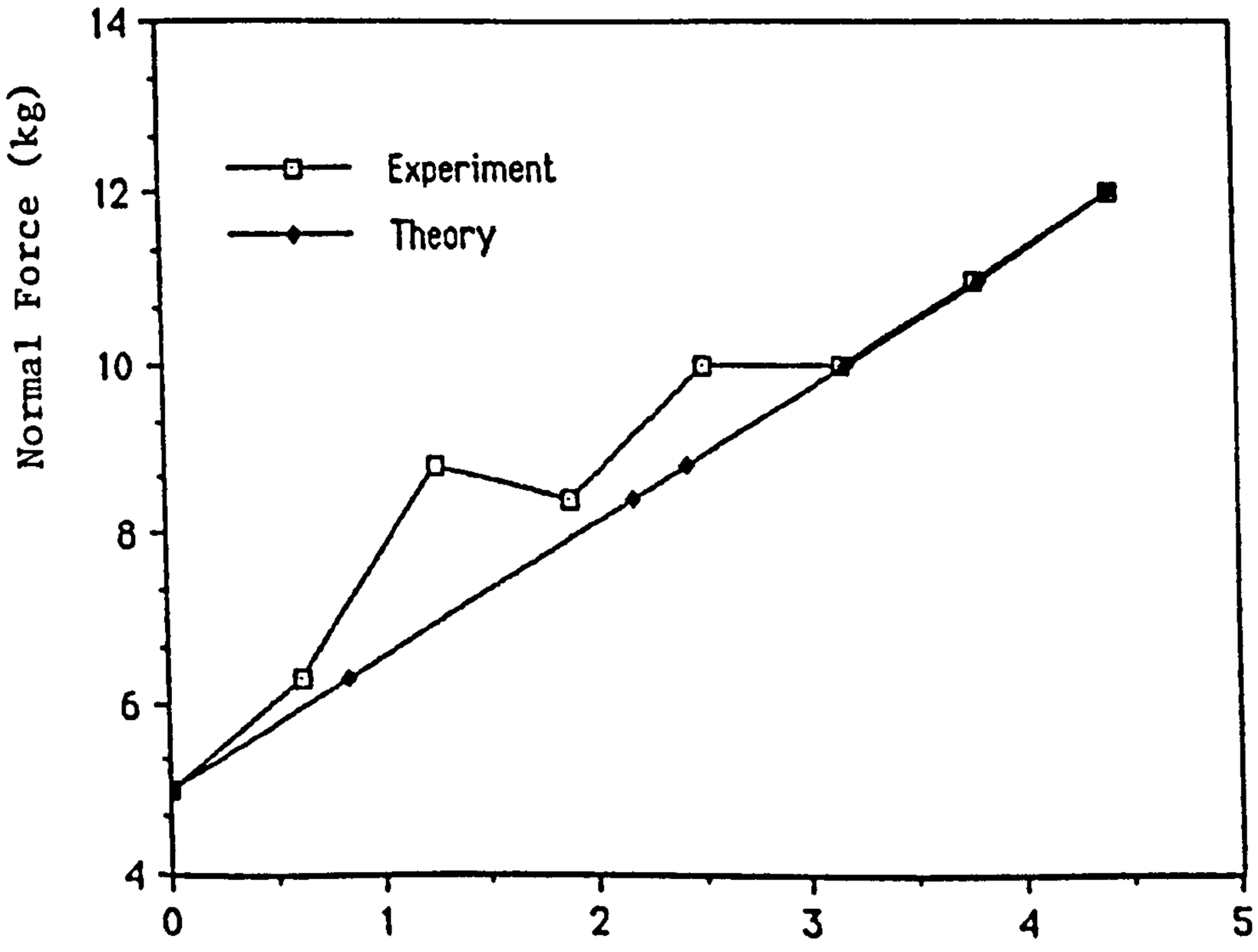

Figure 6.11 Changes in Normal Grinding Force with stock removed (cm^3). Test MH, f = 0.68.

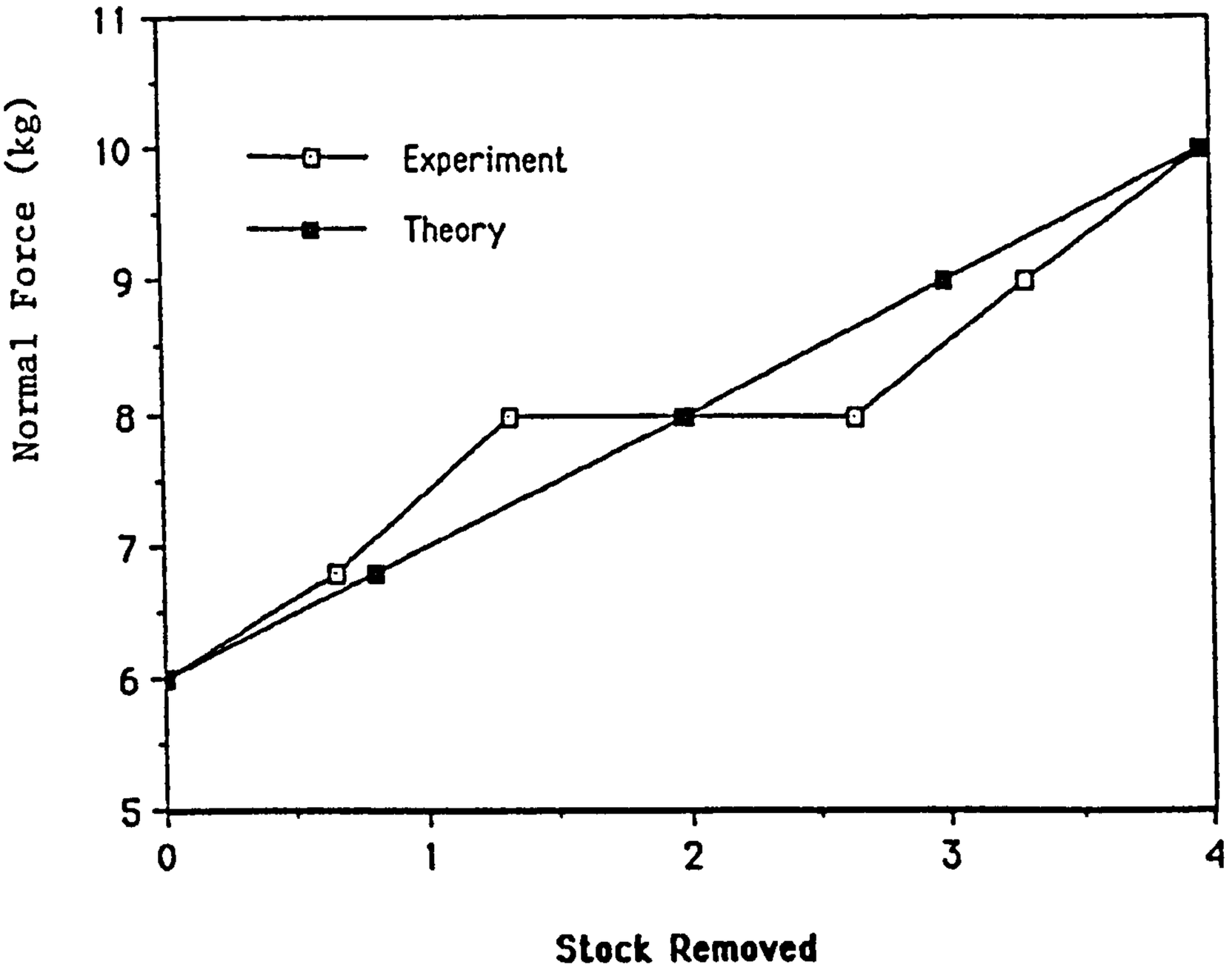

Figure 6.12 Changes in Normal Grinding Force with stock removed (cm^3). Test FH, f = 0.86.

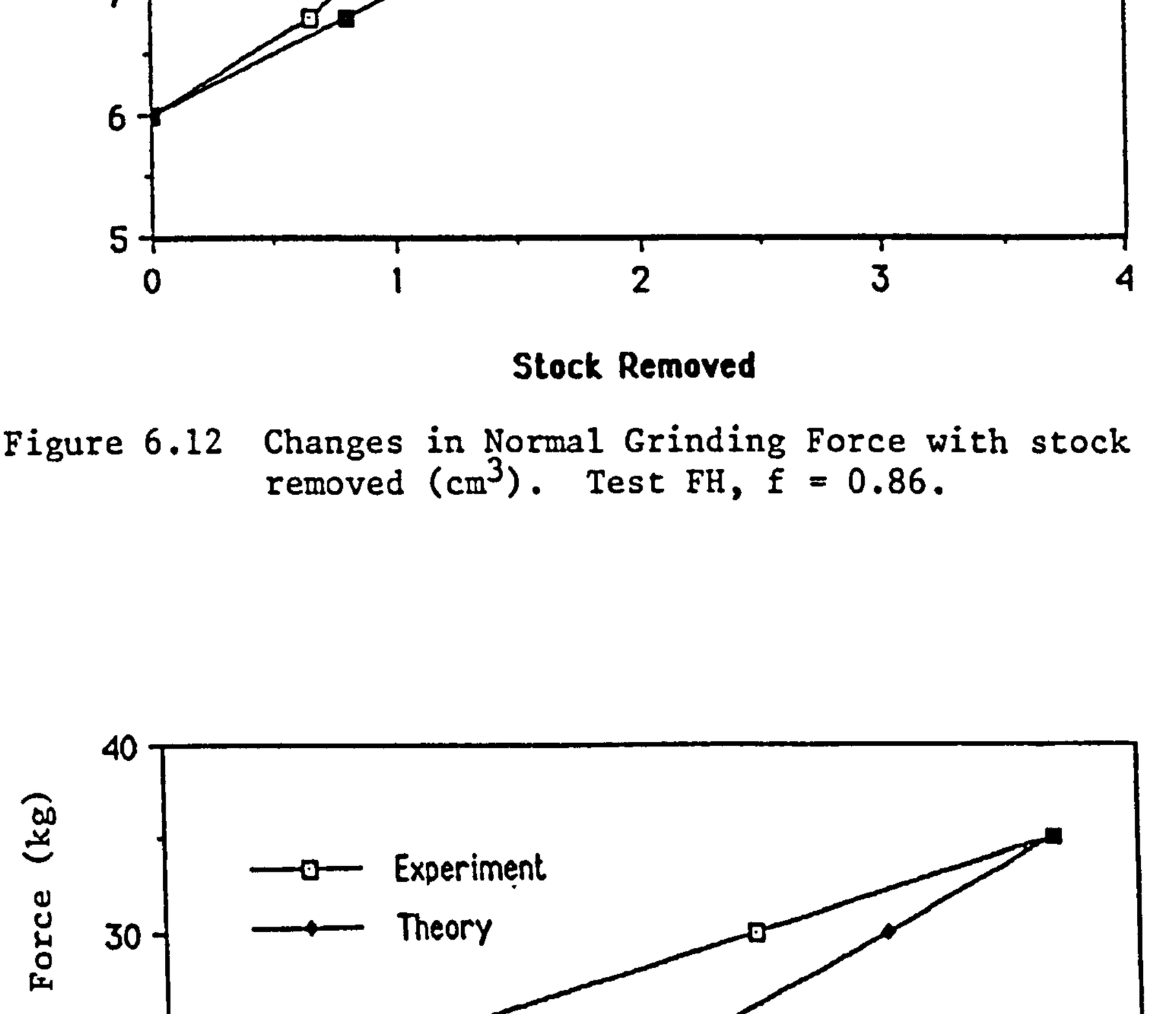

Figure 6.13 Changes in Normal Grinding Force with stock removed (cm^3). Test FS, f = 0.1.

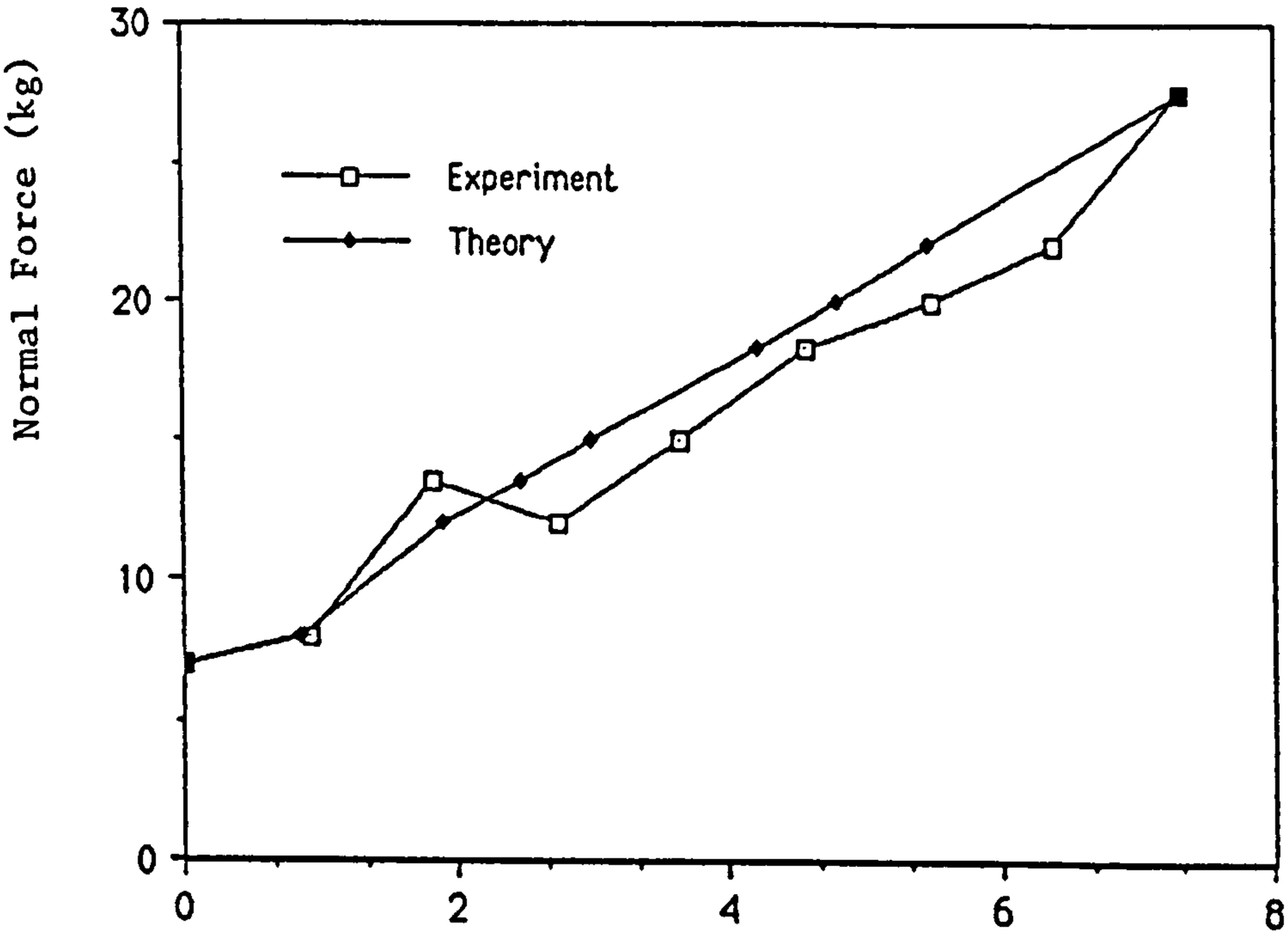

Figure 6.14 Changes in Normal Grinding Force with stock removed (cm^3). Test RS, f = 0.16.

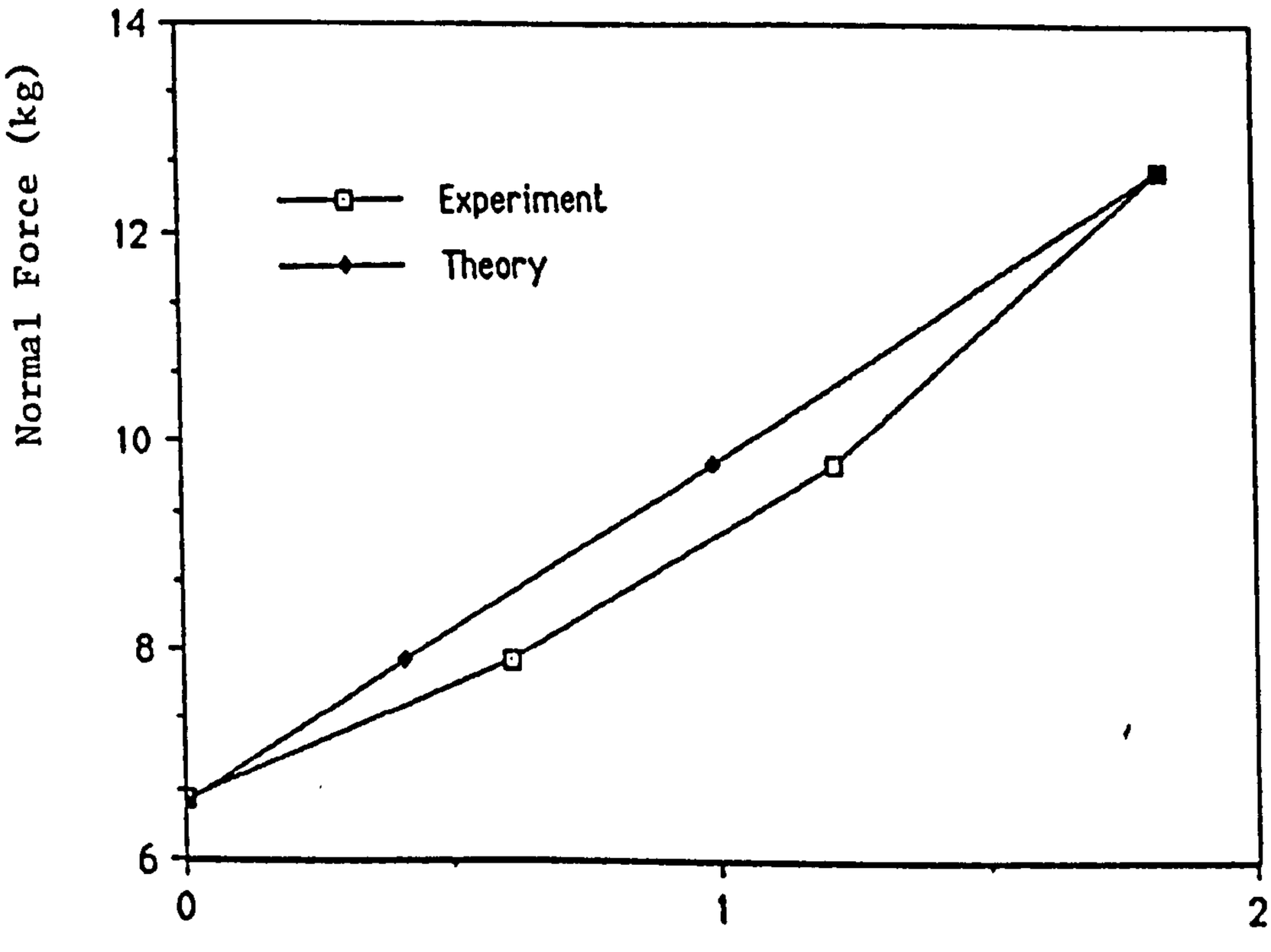

Figure 6.15 Changes in Normal Grinding Force with stock removed (cm^3). Test MS, f = 0.2.

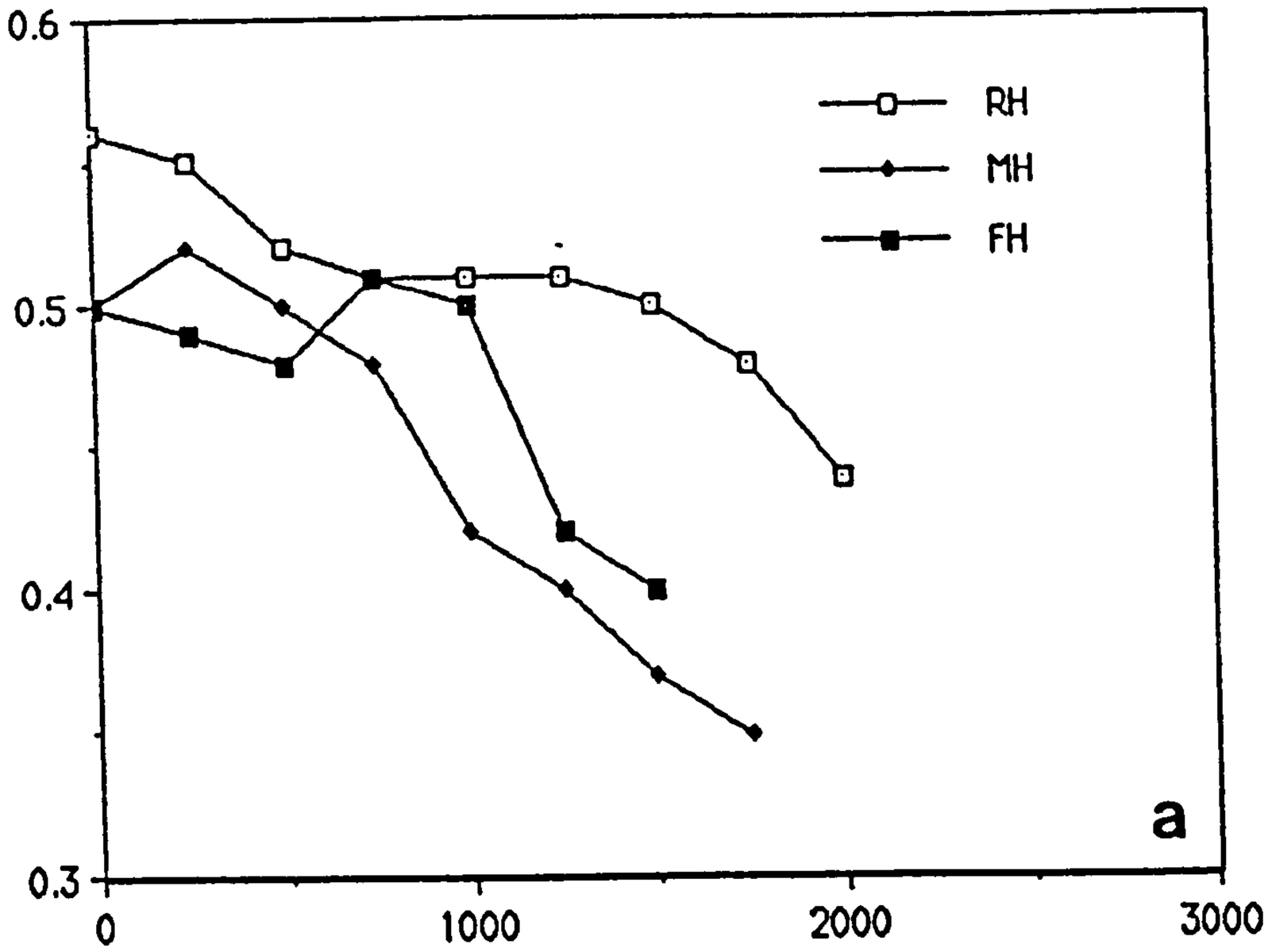

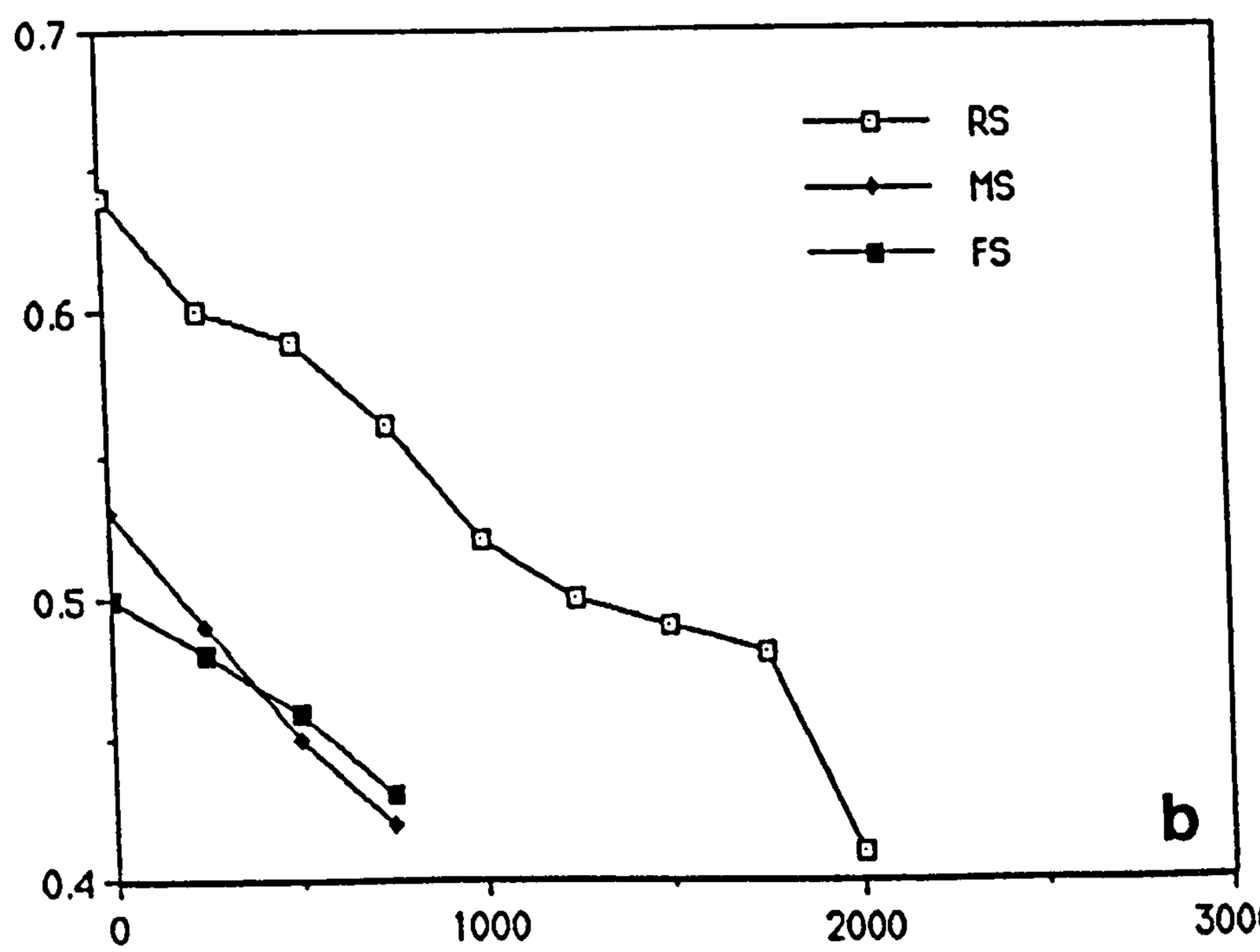

Figure 6.16 Grinding coefficient against number of passes.
(a) Hard specimen, (b) Soft specimen.

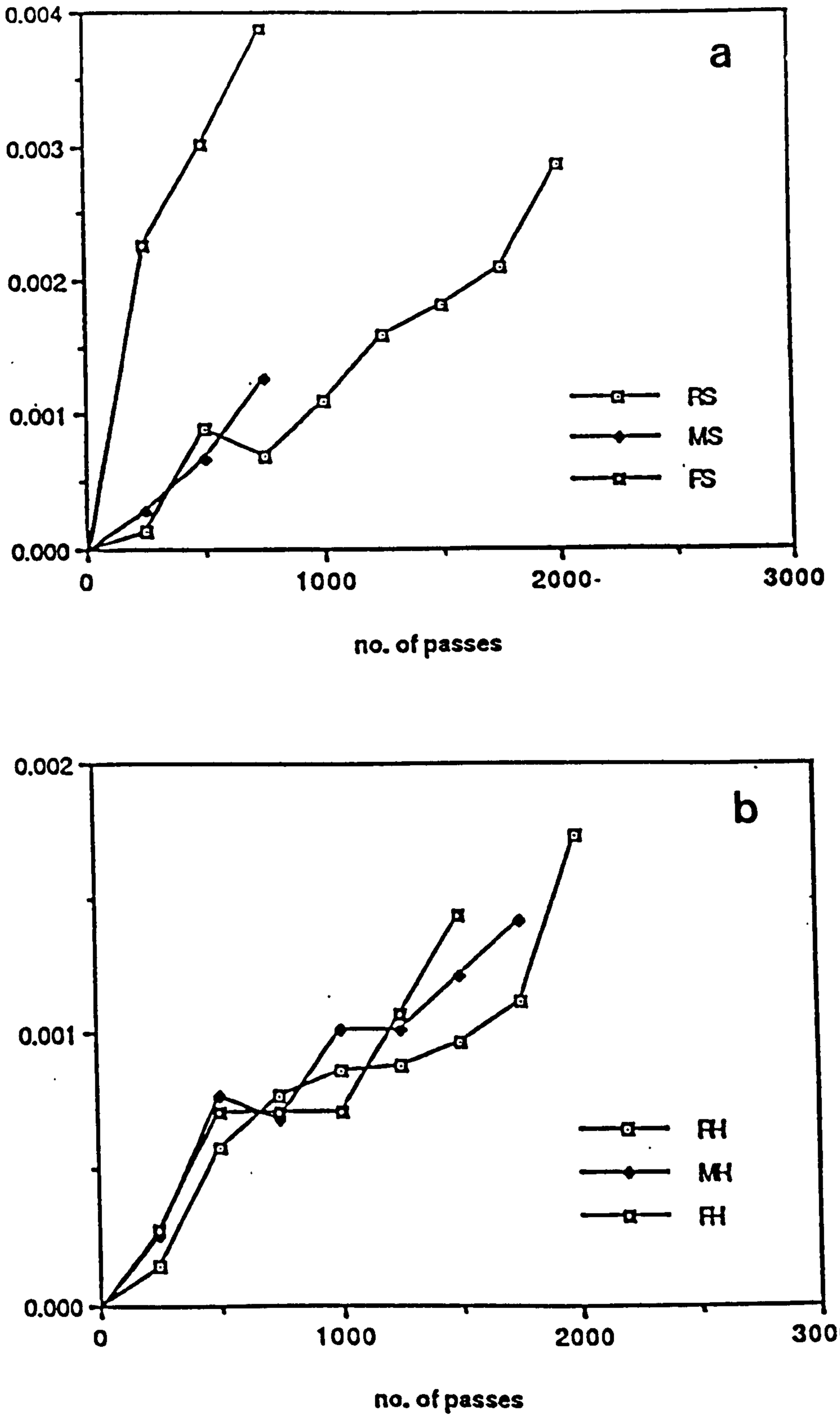

Figure 6.17 Area of flats (mm^2) on the wheel per square millimetre of the wheel-work interface against number of passes. (a) Hard, (b) Soft specimen.

CHAPTER SEVEN

RUNNING - IN

Chapter 7 - Running-in

7.1 Surface Topography and Wear

An important contribution was made by Holm in the understanding of contacting surfaces. Holm (1946) reached the following conclusions:

1. The real area of contact is formed by plastic deformation of contacting asperities.
2. Wear is caused by atomic interaction between two surfaces.

According to Holm the wear quantity V is given by

$$V = \frac{ZP}{H} \tag{7.1}$$

where P = load

H = hardness

Z = probability of removal of an atom from the surface when it encounters another atom or, the number of atoms which are removed on encountering all the other atoms within a unit area per unit distance of sliding.

By assuming that wear occurs by removal of particles rather than of individual atoms, Burwell and Strang (1952) translated Holm's theory into macroscopic terms. A more detailed relationship between wear V, sliding distance L, load W and hardness P_m is due to Archard (1953).

$$\frac{V}{L} = K\frac{W}{3P_m} \tag{7.2}$$

In this equation $\frac{V}{L}$ is proportional to the load because the true area of contact is proportional to the load. The equation is therefore valid for plastic contacts. In the experiments performed by Archard and Hirst (1957) the value of K was shown to vary within 10^{-2} to 10^{-7}. Rabinowicz (1958) gives values of K = 0.1 for a blunt file, K = 0.01 for a new emery paper and K = 0.001 for rounded abrasive particles in the case of abrasive wear conditions.

As Archard explains, in this theory surface topography plays a significant, but not a crucial role. Surface topography is only important in that it ensures that deformation of asperities is plastic rather than elastic. Otherwise the details of the surface finish seems unimportant since it plays no part in determining the severity of the deformation conditions.

The considerably small values of K (10^{-2} - 10^{-7}) suggest that only a very small proportion of contact between asperities results in worn particles. Alternatively this means that in continuous rubbing each point on the rubbing surface is rubbed many times without damage. This suggests an elastic deformation between the asperities of the surfaces which is not the condition on which the theory is based, Archard (1957). It is, in resolving this apparent contradiction by Archard that we see an example of the inevitable involvement of surface details in the analysis of tribological regimes of wear and contact. Archard solved the problem by showing that, even if the deformation were entirely elastic, the area of contact would be proportional to the load for a rough surface; the crucial point is the consideration of multiple contact condition as it happens between rough surface asperities.

In a single elastic contact according to the Hertz equation the true area of contact is proportional to $W^{2/3}$. For two elastically contacting spherical asperities R_1 and R_2, we can write

$$A = \pi \left[\frac{3W\ R_1\ R_2}{4E'(R_1+R_2)}\right]^{2/3} \qquad (7.3)$$

Where W is the load, R_1 and R_2 the radii of the asperities and E' is the composite elastic modulus.

$$\frac{1}{E'} = \frac{1-v_1^2}{E_1} + \frac{1-v_2^2}{E_2}$$

E_1 and E_2 are the elastic modulii of the materials and v_1 and v_2 their poisson's ratios.

By using a series of deterministic models of varying complexity, Archard showed that the relationship for a single elastic contact is greatly modified as the number of contact points increased. Asperities of progressively smaller radii were superimposed on one another and it was demonstrated both analytically and practically that as the complexity of the model increased the power of the load in the relationship tended towards unity. It was shown that increase in the load was mainly to cause new contacts rather than the enlargement of existing ones. The Archard idea was later verified further by Bush et al (1975) when they developed similar results for a two dimensional, isotropic, Gaussian rough surface.

It has now been established that in order to understand and be able to explain phenomena which occurs when solid surfaces are

in contact - either stationary or moving - it is necessary to know the geometry of the surfaces, and equally important is to be able to describe them in a useful fashion. Greenwood and Williamson (1966), for instance, have shown that static contact is controlled by two material properties: the plain-stress elastic modulous and hardness; and three topographic properties: the density of asperities on the surface, the standard deviation of their height distribution, and the mean radius of their summits. The nature of deformation of contacting asperities (plastic or elastic) which strongly influence the wear of sliding surfaces, is controlled by a dimensionless parameter which depends on these material and topographic parameters. The plasticity index, which is, in effect, a generalized surface texture parameter is defined as

$$\Psi = \frac{E'}{H} \left(\frac{\sigma}{\beta}\right)^{\frac{1}{2}} \qquad (7.4)$$

where

E' is the composite elastic modulous

H, hardness

σ, standard deviation of the height distribution of the summits

β, the mean radius of the summits curvature.

Contact is shown to be plastic only when the index exceeds unity. The mode of deformation is therefore not determined by load only, but is determined by material and topographic parameters and has only minor dependence on load.

Although this theory discusses static contact only, however it seems clear that the topographic parameters will be important in

sliding contact. A similar criterion for the mode of asperity deformation is due to Mikic and Roca (1974).

$$\Psi = \frac{E'}{H}\tan\theta \qquad (7.5)$$

where θ is the mean absolute slope of the surface. For this criterion at least 2% of the asperities deform plastically if $\Psi > 0.25$ while at lower values of Ψ contact is predominantly elastic.

7.2 Wear

Wear is generally defined as progressive loss of substance from the operating surface of a body occurring as a result of relative motion at the surface. This definition, however, involves a diversity of processes, such as adhesion, abrasion, fatigue and corrosion. One or a combination of these processes may be in operation in any particular instance of wear.

Burwell (1957) classified five types of wear namely adhesion or galling, abrasion or cutting, corrosion, surface fatigue and minor types. A different approach was adopted by Archard and Hirst (1956). The wear of metals was divided into mild wear and severe wear.

The first quantitative relationship between wear, the properties of the material and the external condition of sliding was obtained in 1937 by Tonn for abrasive wear. Tonn introduced the concept of relative wear resistance and obtained a linear relationship between the relative wear resistance and the hardness of the material.

$$\frac{B_2}{B_1} = aH + b \qquad (7.6)$$

This idea was developed further by Kruschov and Babichev (1960). For commercially pure and annealed metals they established the relationship

$$\frac{B_2}{B_1} = K\frac{H}{q_n} \qquad (7.7)$$

where

$\frac{B_2}{B_1}$ = ratio of the wear resistance of the material B_2 to that of a reference sample B_1.

K = constant of proportionality

q_n = nominal pressure

Bowden and Tabor (1954) used the ideas of plastic deformation of asperities first introduced by Holm. They assumed friction to be due to necessity of shearing these contacts before relative motion can take place; the frictional force should therefore be proportional to the load and in accordance with Amonton's laws of friction.

An equation for the adhesive wear regime due to Burwell (1957) can be written as he suggested for the volumetric wear V.

$$V = k\ A\ L \qquad (7.8)$$

where

A is the real area of contact

L, the sliding distance

K, a wear coefficient

Burwell noted that K coefficient remained reasonably constant over a range of speeds and loads up to an average pressure of approximately one-third of the indentation hardness. Above this the wear coefficient rises sharply and with further increase in pressure, large scale welding and seizure occurred.

Archard (1953, 6 & 7) presented a model of adhesive wear in which wear, similar to the Burwell equation is proportional to the real area of contact, equation (7.1). He discussed the wear factor K, and suggested two alternative interpretation. Wear could be considered as a result of accidents such as chance encounters of exceptional severity and that K was the probability of such encounters or alternatively that each asperity needed K encounters to produce a wear fragment. Archard model of wear, equation (7.1), can be applied to abrasive wear as well.

Abrasive wear is frequently subdivided into two body and three body forms. In two body abrasive wear (sometimes also termed cutting wear) the softer material is ploughed and/or cut by the harder surface. The three body situation occurs when hard, loose particles (of grit or oxide for example) are present, and these are able to abrade the surfaces.

7.3 Running-In

The phase of wear occurring in the early stages of sliding is

usually referred to as running-in. The classic concept of running -in is a condition known as boundary or marginal lubrication where the asperities on the mating surfaces break through the lubricating film and wear. The running-in period may be considered as the point when the mating surfaces can accept full load conditions (load and speed) without excessive distress to the surfaces in relative motion, i.e. when friction and wear characteristics reach a steady state following a higher initial rate.

Examination of cylinder bores before and after this period by Campbell (1972) indicated that the surface depth was reduced to give a plateau area of between 20% and 40%. Furthermore, he showed that the amount of wear volume and the reduction in surface height of the original surfaces to achieve run-in condition vary with the type of bore finish. Campbell suggested that the unworn surface must have only a minimal plateau crest roughness which is just sufficient to allow bedding to take place, in the desired running-in time.

In the experiments by Ostvik and Christensen (1969) similar conclusion were reached. They performed tests in conditions of combined rolling and sliding and pure sliding using a pin-on-ring machine to examine the effect of running-in on surface topography. Surface finish measurements were made with a talysurf coupled direct to a digital computer. They showed that run-in surfaces achieved greater load bearing capacity and could be safely run at much lower film thicknesses than their newly machined counterparts. Ostvik and Christensen confirmed the compliance of the softer surface to the roughness of the harder surface.

Kragel'skii and Kombalov (1969) showed that surface roughness reaches a stable value during running-in and this situation corresponds to a minimal friction coefficient.

The influence of surface topography on running-in has been subject of many investigations. Rowe (1974) and Rowe et al (1975) have studied the topographic changes during running-in by the stylus measurement. They pointed out that the initial surface roughness seemed to have a dominant effect on the results. They concluded that the slider surface roughness (hard component) is the governing factor and that the softer bearing surface acquired the slider surface characteristics.

The dependence of the wear history during running-in on the initial surface roughness was also observed by Sreenath and Raman (1976) for the friction of piston rings on cylinder liners. The authors tried to describe the functional behaviour of the moving parts during running-in in terms of C.L.A. parameter.

Masouros et al (1977) developed a model of wear to show quantitatively that in systems working in the boundary lubrication regime, such as journal bearings, gears and cams running-in is greatly influenced by the initial surface roughness of the harder component. Masouros deduced his model by correlating wear rates with surface roughness and concluded that high surface roughnesses give high values of wear during the initial transient stage of wear curve before the steady condition is reached. The value of R_a if high enough, may lead to deterioration and stopping of the process.

Bayer and Sirico (1975) performed a series of tests in which brass spheres were reciprocated across a soft steel plane (of known roughness) under boundary lubricated conditions. Their aim was to investigate the magnitude and anisotropic properties of surface roughness on wear. They determined that higher wear could occur with a smooth surface than with a surface of greater roughness. Directional effects of surface roughness were found also to be highly significant in wear tests. With the surface lay oriented perpendicular to the direction of sliding, wear of brass spheres was much greater.

King et al (1977) have modelled the running-in process for a soft material (having a Gaussian amplitude distribution) whose original surface topography was gradually worn away or truncated by a straight line. For the more realistic case in which two surfaces (each having Gaussian or near Gaussian distribution) are slid over one another, a computer simulation was performed. They determined that the measurements of skewness of the amplitude distribution provided useful numeric information as to the extent of wear when the wear is confined within the original surface topography. Kurtosis values were considered to be unsuitable for monitoring running-in wear since, in the early stages the rate of change of Kurtosis is almost zero, whilst in the latter stages of wear its rate of change is excessive.

In the experiment by Chowdry (1979), a six station wear machine were used to study the running-in of grease lubricated (bronze on steel) bearings. Compression tests were also carried

out on a surface to see if a deformation process could account for the changes in amplitude distribution. Although the compressed surface topography took the appearance of a run-in surface, they concluded that the process of running-in wear is partially due to the loss of material by abrasion, while small amount of plastic deformation is likely throughout the smoothing process.

More recently, Yinjie et al (1985) studied the characteristics of selected wear debries by testing five materials on five abrasives, some abrasives softer than the material. The results suggested three wear mechanisms : microcutting, ploughing and brittle fragmentation. They concluded that hard materials can be worn by softer abrasive. Microcutting chips can form, although this constitute a minor part of wear process.

There is now a growing realisation that in order to reduce the oil consumption and blowby in engines the running-in process should be reduced to a minimum. This has created a need for development in manufacturing processes which allow better initial geometrical conformity between the piston ring and cylinder and therefore reduces the time taken to achieve the required run-in profile for optimum performance. This minimum initial wear is also important in bearings and other applications where a very small tolerance is allowed. It might appear that the use of a polished surface would achieve this end, however, this would only be true in the case of an engine for example, if both bore and piston rings, for instance, could be machined exactly to their run-in form and if no distortion of these parts occurred during assembly or when the

engine was run. Since these conditions are impossible to achieve it is more satisfactory to obtain mating of rubbing surfaces by allowing a certain amount of wear to take place during the running-in process. Experiments have shown that a smooth surface finish does not give the shortest running-in period and in some cases may lead to seizure of the parts.

7.4 Experiments

7.4.1 Introduction

The experiments carried out in this part are concerned with the functional behaviour of precision surfaces run-in under marginally lubricated conditions. Most new pieces of machinery incorporating sliding surfaces require a period of running-in before they can be subjected to full load. It is generally accepted that the time and care taken at the running-in stage will be repaid with an extension in the useful life of the component. From a study of the literature there appears to be at least two classic types of running-in:

Mode I

Running-in between precision surfaces where both components are of a similar hardness; the wear necessary to achieve running-in being contained within the original surface topography of the components. Analysis of such surfaces shows that the running-in process is associated with progressive truncation of the surface and the formation of an increasing number of plateau. Kaliszer et al (1973) used the concept of "zero wear", which was considered to be wear

within the original surface topography, when discussing the role of surface metrology in Tribology. It was suggested that such wear would have little effect on the physical dimensions of a component and therefore the term zero wear could be applied. A significant parameter for predicting this type of wear is the bearing area curve despite its sensitivity to freak observations.

Some of the topographical changes produced by mode I running-in can be simulated by the progressive micropolishing of a ground surface, Buttery et al (1985). The results obtained show a steady improvement in surface roughness (R_a) and a reduction in average slope Δ_a (figure 7.1) the surface becoming negatively skewed. Eventually a new random surface is established at a lower level of surface roughness. The bearing area curves (figure 7.2) show a similar trend, starting from a random surface progressing to a run-in surface and finishing as a random surface at a lower level of surface roughness.

Mode II

This type of behaviour occurs when one of the surfaces is relatively soft (bearing metal) and changes its surface topography during running-in to conform with that of the harder material (shaft). Once the bearing material has conformed with the shaft the wear rate falls dramatically. Further changes in surface topography (running-in) will proceed very slowly and will normally involve slow progressive changes in the surface topography of the harder material (shaft) by a mode I mechanism.

7.4.2 Experimental Considerations

A number of stylised wear arrangements such as pin-on-disc,

pin-on-ring, and cross-cylinders have been developed to monitor the wear process. A stylised wear arrangement can offer significant advantages if surface finish is to be monitored. This is because surface measurement can be arranged with minimum disturbance to the wear process.

In the experiments described in this part a pin-on-ring test rig incorporating stylised surface measurement facilities was used. The experiments were designed to study the effect of the ring's surface finish on the running-in process. Flat end pins were used to ensure that the pin would wear to conform with the ring's topography (Mode II running-in). Under similar conditions Rowe et al (1975) concluded that surface finish of the softer material is of relatively little importance. A flat pin configuration allows accurate measurement of wear by observing the scar formed on the pin. Since the initial condition gives line contact the consequent high pressure ensure some metal to metal contact at the start of each experiment. As the pin wears the specific pressure falls and eventually a stable oil film will form giving hydrodynamic lubrication and a dramatic fall in wear rate. Although accurate alignment of pin in both lateral directions is essential in this type of experiment it is not as critical as that required when using a preformed pin. Preformed pins have the advantage of giving a better simulation of running-in within the original surface although quantitative assessment of wear is more difficult to obtain.

7.5 Experimental Procedure

7.5.1 Test Rig

Experiments were carried out using a pin-on-ring wear tester designed by T.G. King and a complete description is given elsewhere, King (1980). Essentially the test rig consists of an aerostatic spindle (Westwind Model 125A) mounted on a large cast iron bed. To reduce vibration to a minimum the motor variator drive is mounted independently and connected to the spindle through a rubber bush coupling. The original flexible bellows was replaced by a more robust flexible coupling (Fenner). This arrangement ensured a low level of drive induced noise which might otherwise affect the wear mechanism. Shaft speeds could be reliably controlled between 100-800 rpm giving speeds of 0.47 to 3.8 m/s with a ring of 90 mm diameter. Appropriate instrumentation was used to monitor shaft speed and to record the cumulative number of revolutions completed.

The pin was mounted on a pivoted support arm and was loaded against the ring using masses suspended below the bed by a loading frame and wire. The load could be applied smoothly by means of an elevating and lowering platform operated by a double acting pneumatic cylinder.

An important consideration in the design of the rig has been the location of the line of action between pin and ring once they are brought into contact. The tangent to the ring at the point of contact passes through the pivot axes of the pin support arm so that the effective applied load is in principle independent of the friction

force, figure (7.3). Complete details of the pin and ring arrangement are shown in figure (7.4). A unique feature of the rig was the facility to monitor the surface topography of both pin and ring without removing them from the rig and with accurate relocation. This was achieved by building a Talysurf 3 gearbox and stylus into the wear tester. The output from the surface measuring equipment was digitised and then processed through a PDP11 computer to give a range of surface parameters including surface roughness, bearing area curve, slope distribution and average wavelength. A plotter interface allowed the use of the graphical output software routines to drive the plotter. An example of the graphical output of the system is shown in figure (7.5). The existing version of a data acquisition programme (King, 1980) was used for this purpose. This programme was later extended to include a bearing ratio curve and percent zero slopes. The programme is written in BASAC IV a listing of which is given in the appendix (1).

7.5.2 Specimen Materials and Preparation

A series of pin-on-ring wear tests were undertaken using a combination of both bronze and steel pins and rings. The bronze pins and rings were made from phosphor bronze (BS 1400 PB-1C) and had a nominal hardness of 140 VPN. The steel pin and ring specimens were made from SKF hardened steel after being heat treated to a hardness of about 850-900 VPN.

The pins were nominally of 6 mm square by 30 mm long. After

their contact faces had been traverse ground to a fine finish they were micropolished using a 1 μm diamond paste. Micropolishing enabled the wear scar to be measured accurately and ensured that only the surface finish of the ring would influence the running-in process. Great care had to be taken during micropolishing to keep the contact face of the pin flat.

The rings were of 90 mm diameter and 20 mm wide. They were plunge ground on a Jones and Shipman 1300 series cylindrical grinder using an A46 grit wheel running at a surface speed of 23.5 m/s and a work speed of 0.24 m/s. By altering the grinding conditions, in particular the wheel dressing, three different surface finishes were obtained corresponding to coarse, medium and fine dressing.

A drip feed lubrication system was used delivering Mobile DTE light oil at a rate of approximately 0.005 ml/min. The oil was spread over the ring by means of a pair of felt pads which also helped to remove wear debries. The pads were renewed at the beginning of each test.

7.5.3 Running-In Tests

Using different combinations of bronze and steel pins and rings four series of tests were undertaken:

Steel ring/Steel pin (SS)

Steel ring/Bronze pin (SB)

Bronze ring/Steel pin (BS)

Bronze ring/Bronze pin (BB)

Each of these combinations were repeated three times using rings of different roughness measured by their R_a values; namely Rough, Medium and Fine. The steel ring/bronze pin combination (SB) for instance was repeated three times with rough ring (SBR), medium ring (SBM) and fine ring (SBF). A total of twelve tests were performed in this way.

Tests were carried out at a sliding speed of 1.43 m/s (300 rpm) and under a load of 40N. Since the pin-on-ring arrangement used was not self-aligning, considerable care was expended in the initial setting of the specimen. A very light film of engineering blue was applied to the ring surface and the pin rested against this under the weight of the specimen holder arm. Gentle rotation of the ring through a small angle allowed the compound to be transferred to the contacting regions of the pin. If necessary, the projection of the pin from its holder was adjusted to bring the contact line central to the pin and of even width. After cleaning the surfaces of the pin and ring surface traces were taken from both pin and ring. The pin was then brought into contact with the ring and the load was applied. The test run was then started after presetting the number of the revolutions on the counter; the grinding direction on the ring being parallel to the direction of sliding.

The wear scar formed on the pin was measured at appropriate intervals and the volume loss calculated. At the same time Talysurf traces from both pin and ring were processed through the computer. The pin profiles were taken using a straight datum, the glass straight line datum was set parallel to the pin surface before profile being taken. The ring profile traces were taken using a

skid nosepiece. Relocation of the ring profiles in the circumferential direction was made using a radius arm with a ball end kept attached to the ring. For profile measurement the ball was brought into contact with a datum formed by a gauge block placed on the machine bed. No filtering was used for either pin or ring profile measurement.

Composite Test:

Considerations of some preliminary tests showed that when a ring from previous test was used with a new pin running-in stage could happen at a shorter time and with smaller amount of wear. This can offer a guideline to preparation methods to be used for producing tribological surfaces. A further test was designed in which the peaks of the rough steel ring was removed using a very fine emery paper to produce a composite surface on the ring similar to the run-in surfaces within the original topography. The ring was then used in a test with a steel pin at conditions similar to the previous tests to observe any change in the wear behaviour, (test CSSR).

7.6 Results

The total volume of pin wear as a function of sliding distance is shown in figures (7.6) and (7.7) for different test combinations. Pin wear volume was calculated from the width of the scar on the pin surface. The initial surface roughness of the rings are indicated in these figures for each case. Rougher surfaces can be seen to produce greater wear to run-in in general but some exceptions were

also present, BBR and BBM.

Examination of the ring profiles before and after running-in show that when running-in was successful the ring profile remained almost unchanged; a small degree of wear within the original surface topography was observed, however, in some cases. This can be seen for test SSM in figure (7.8) which shows the ring profiles at the start and after the running-in is completed (40957 metres of sliding). The corresponding pin profile at the end of the running-in process is also shown and it can be seen that the pin surface roughness is much smaller than that of the ring. Some indication of the ring wear within the original surface topography can be seen even in the case of bronze pin rubbing against the steel ring, test SBM in figure (7.9). Similar changes are shown in figure (7.10) for test BSF where the ring profiles before and after running-in are shown with their amplitude and slope distributions.

Where running-in did not occur, BBR for example, the original ring profile was completely removed and the ring acquired a new random profile. This is shown in figure (7.11) where the computer analysis of the new and the old ring profiles are shown with their profiles.

Examination of the p in profiles suggests that the peaks profile of the ring was transformed on to the pin surface. This can best be seen in test BSR, figure (7.12). Computer analysis of the pin profiles at the start and after 90957 metres of sliding for this test are shown in figure (7.13); corresponding ring profiles can be seen in figure (7.14). The transition of the ring profile to the pin surface was, however, much faster in other test combinations. For steel ring bronze pin combination (SB) for instance,

the ring's peaks profile was transformed on to the pin surface almost immediately after test run was commenced and further change in the pin profile was very small and gradual.

Statistical distributions: the amplitude distribution of different ring profiles before and after running-in remained almost unchanged. The R_a value dropped slightly and the distribution, to a small extent, became negatively skewed. The bearing area response to the ring wear was weak, its shape altered slightly from an ogival or S-shaped representative of a random surface at the beginning of the test run to become slightly truncated at the top, figure (7.10). This change, however, was not noticeable in every case. In test BBR, for which running-in did not happen, the range of the ring amplitude distribution was increased as a new random profile was formed on the ring whilst the shape of the bearing area curve did not change, figure (7.11).

The ring slope distribution changed little with wear, the significant change being an increase in the value of the percentage of zero slopes resulting in an increase in the kurtosis value, figure (7.14). For pins the general behaviour was an increase in the range of both amplitude and slope distributions. The amplitude distribution and the bearing area curve at the completion of running-in suggested an almost normal distribution. The pin's slope distribution changed with wear from a 'pulse' at zero to a symmetrical 'bell', the percentage of zero slope being dropped with an increase in range. These changes can be seen from figure (7.13) where the pin surface has acquired a composite nature consisting of two random profiles at different levels.

Variation of profile parameters: In general all the surface parameters for both pin and ring reached a steady value when running-in was complete. The changes in R_a with sliding distance are shown in figure (7.15) for both pin and ring. Ring surface roughness decreased slightly in general while a sharp increase followed by a gradual change to reach a steady value was associated with the pin. The RMS parameter followed similar pattern. Figure (7.16) shows the variation of average wavelength of the pin and ring for some of the test combinations. The R_a and the average wavelength from these figures can be seen to be greater for the ring in general, exceptions being BBF for R_a and SBF for average wavelength. The general pattern of average slope variation with sliding distance is shown in figure (7.17); figure (7.18) is the percentage of zero slope against sliding distance for both pin and ring for the same tests combinations.

Composite test (CSSR): Figure (7.19) shows the computer analysis of the steel ring profile after the peaks have been truncated. It can be seen from the amplitude distribution and the bearing area curve that a composite surface is produced. The profile analysis of the ring before truncation is shown in figure (7.20). The steel pin wear volume against sliding distance is shown in figure (7.21) for the composite test and the same ring before being truncated (test SSR); wear characteristic of the test SSF is also shown for comparison.

The variations of pin and ring surface profile parameters with sliding distance are shown in figures (7.22) to (7.25).

7.7 Discussion

The wear results obtained showed in general a rapid fall in wear rate with sliding distance, at long sliding distances the wear rate was hardly measureable. The total wear consisted of two components; a minimum steady wear plus an additional "running-in" wear which is a function of surface topography. From figures (7.6) and (7.7) it is clear that surface topography plays a major role in the wear process; the final amount of wear and the wear rate depend on the component surface topography. Rougher surfaces produced higher initial wear rate in general and at the end of the experiments the rank order remained the same. No clear relation could be obtained, however, between the R_a of the ring and the total wear to reach the running-in stage. Despite some degree of correlation, it was found that there was not always a one to one relationship between R_a and the wear volume for any test condition. In test BSR, for instance, after 637m of sliding the wear scar covered the whole pin surface and the test had to be stopped before running-in being reached whereas in a series of preliminary tests running-in had been achieved under similar conditions; the scar width reached a stable value of 3.28mm after 6000m of sliding, Buttery et al (1985). Comparison of the results from the composite test (CSSR) with the test (SSR) provides further evidence that the observed correlation between R_a and the amount of wear when running-in is reached does not hold in general and can only apply under certain circumstances. This can be seen from figure (7.21) which gives the volume of wear for tests (CSSR), (SSR) and (SSF) against sliding distance. It is clear that although the roughness of the ring for tests (SSR) and (CSSR) are almost identical, the total

wear to run-in differs drastically in these two cases. The composite test produced much smaller wear to run-in compared with the test (SSR) which used a ring of similar roughness the degree of reduction being of the order of eight.

A consequence of the use of a flat ended pin is the progressive reduction in specific pressure with sliding distance provided the wear scar does not cover the whole surface of the pin. The variation of specific pressure with sliding distance is shown in figure (7.26) for the (SS) test series. As running-in is reached at different scar widths it is clear that the specific pressure between the pin and ring at running-in stage varies with different tests. Some rings therefore can support a much higher value of specific pressure when run-in. It is suggested that the common factor for each specimen when run-in is the area of zero slope. This can be given by

$$A = XYZ \qquad (7.9)$$

where A = area of zero slope

X = width of pin

Y = width of scar

Z = % zero slope.

The above formula was used to calculate the area of zero slope for both pin and ring surfaces. When the values obtained for area of zero slope of corresponding pins and rings are added together the resulting values are very close for each series of tests. These are shown graphically in figures (7.27) and (7.28) where the sum of the area of zero slopes for each pin and ring pair is plotted at different sliding distances and it can be seen that it acquires

almost the same value when the surfaces are run-in. It appears that the running-in process can be explained at least in part as a smoothing operation associated with changes in slope and percentage in zero slopes.

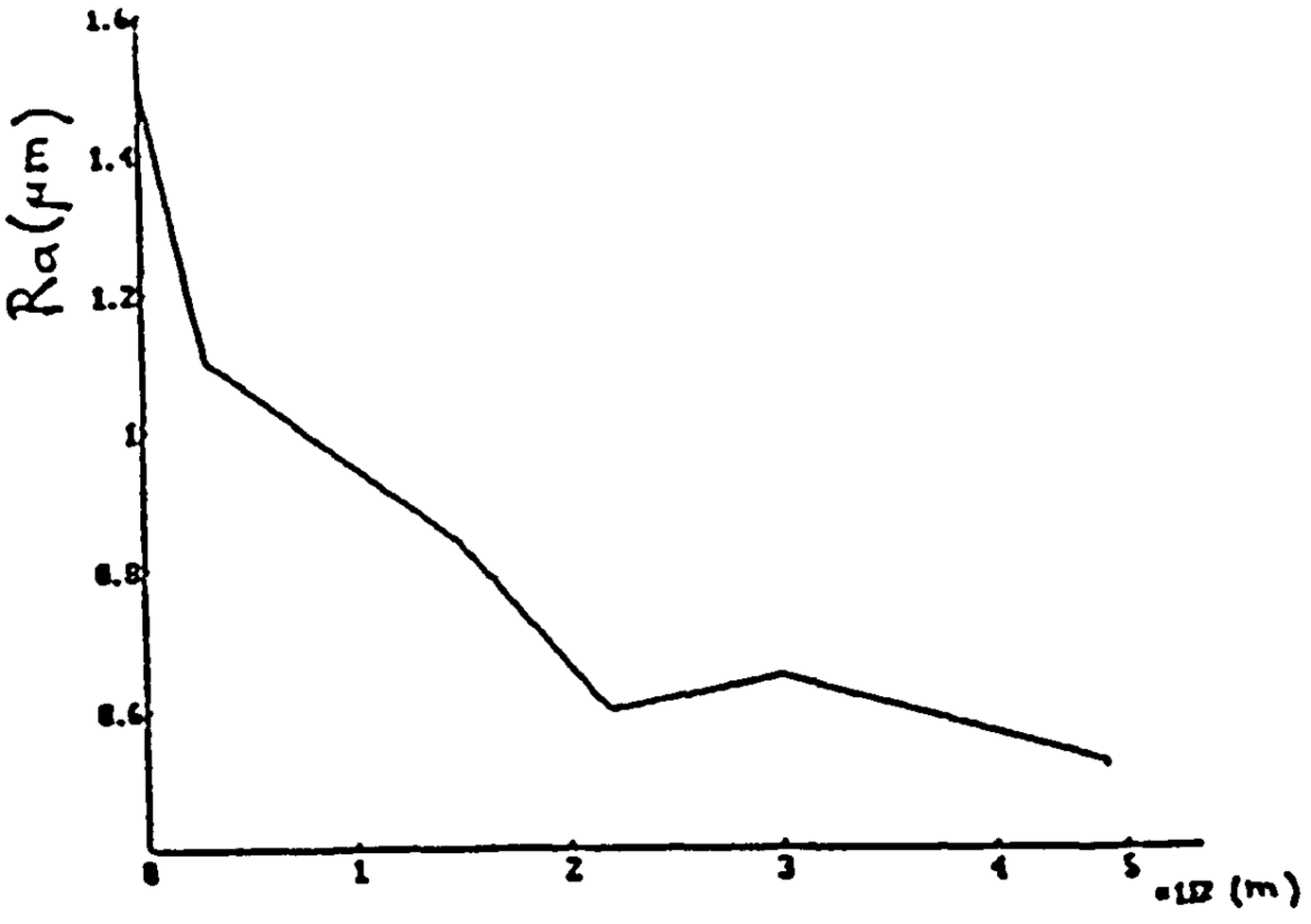

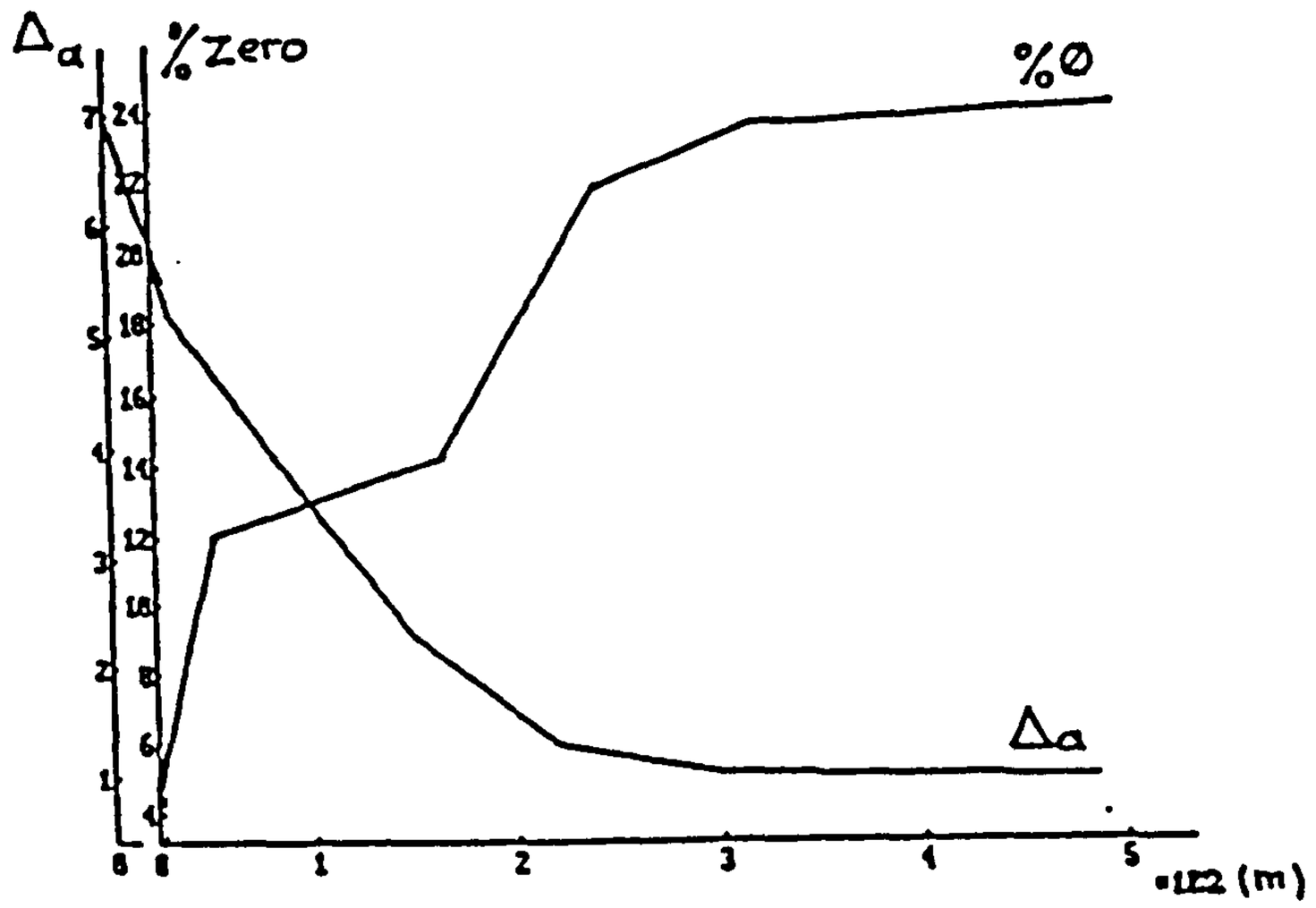

Figure 7.1 Changes of R_a, Average slope and Percentage zero slope in a simulated running-in.

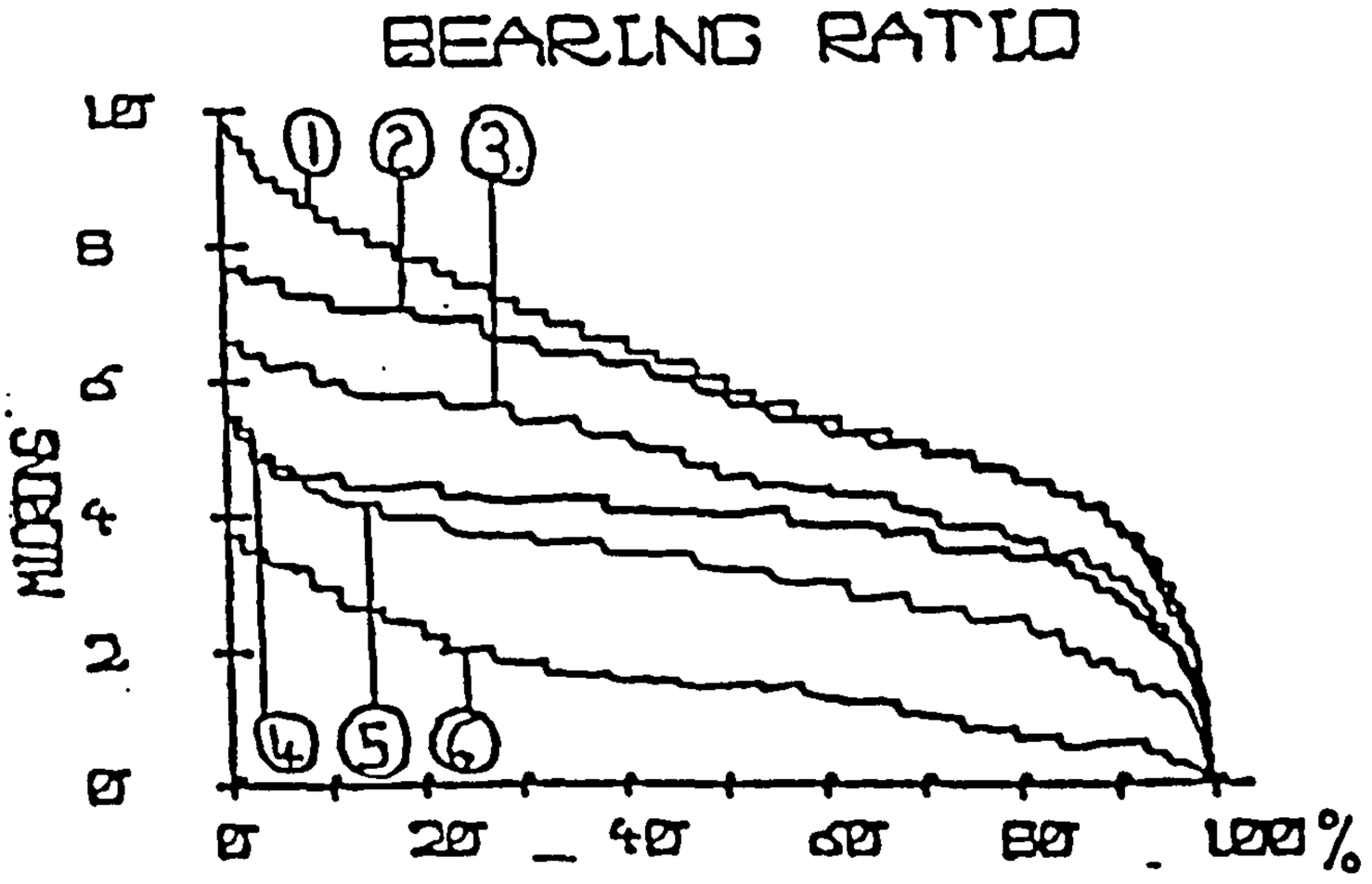

Figure 7.2 Running-in simulation: Changes of Bearing ratio with progressive micropolishing of a ground surface.

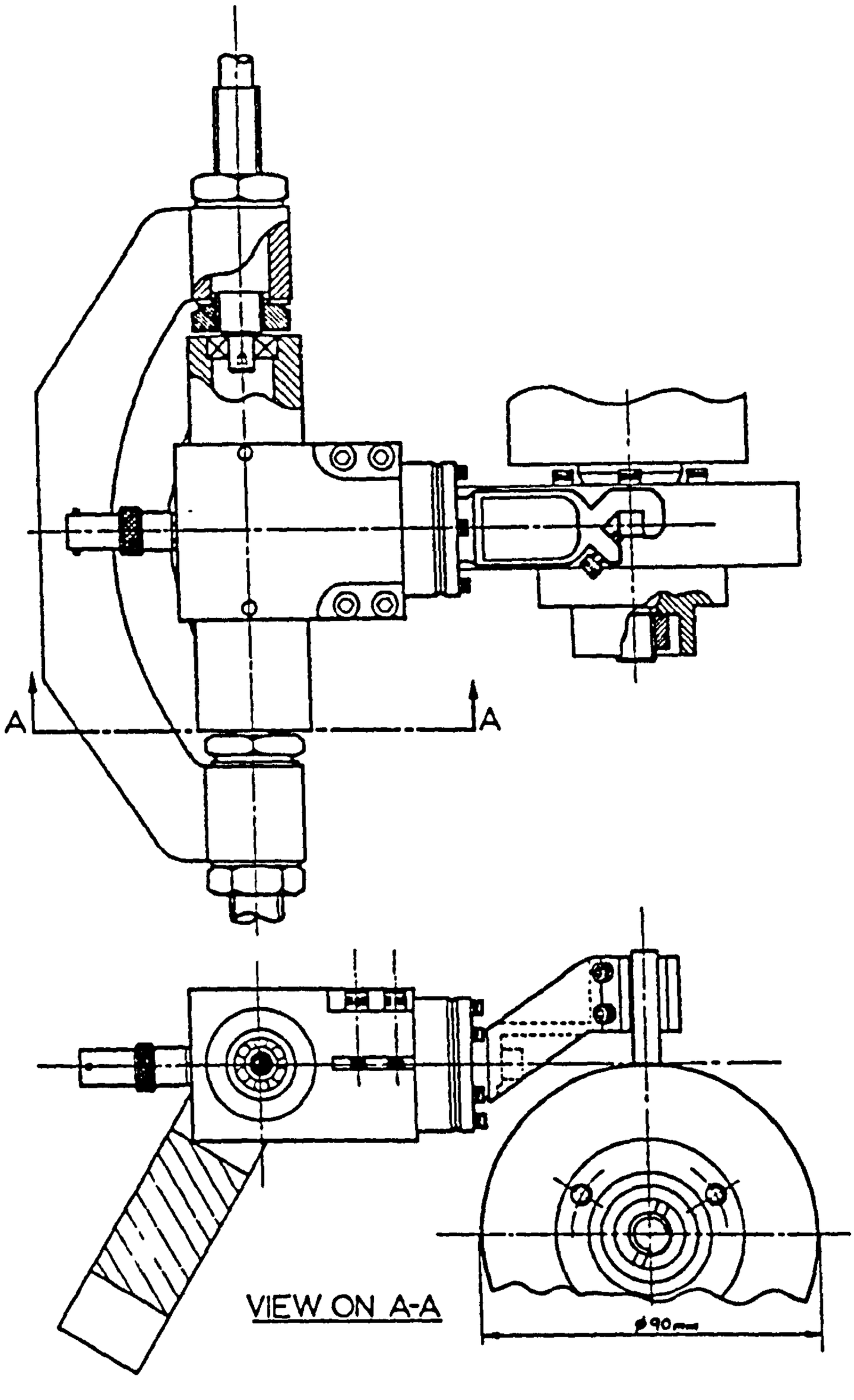

Figure 7.3 Geometric arrangement of pin and ring (King, 1980).

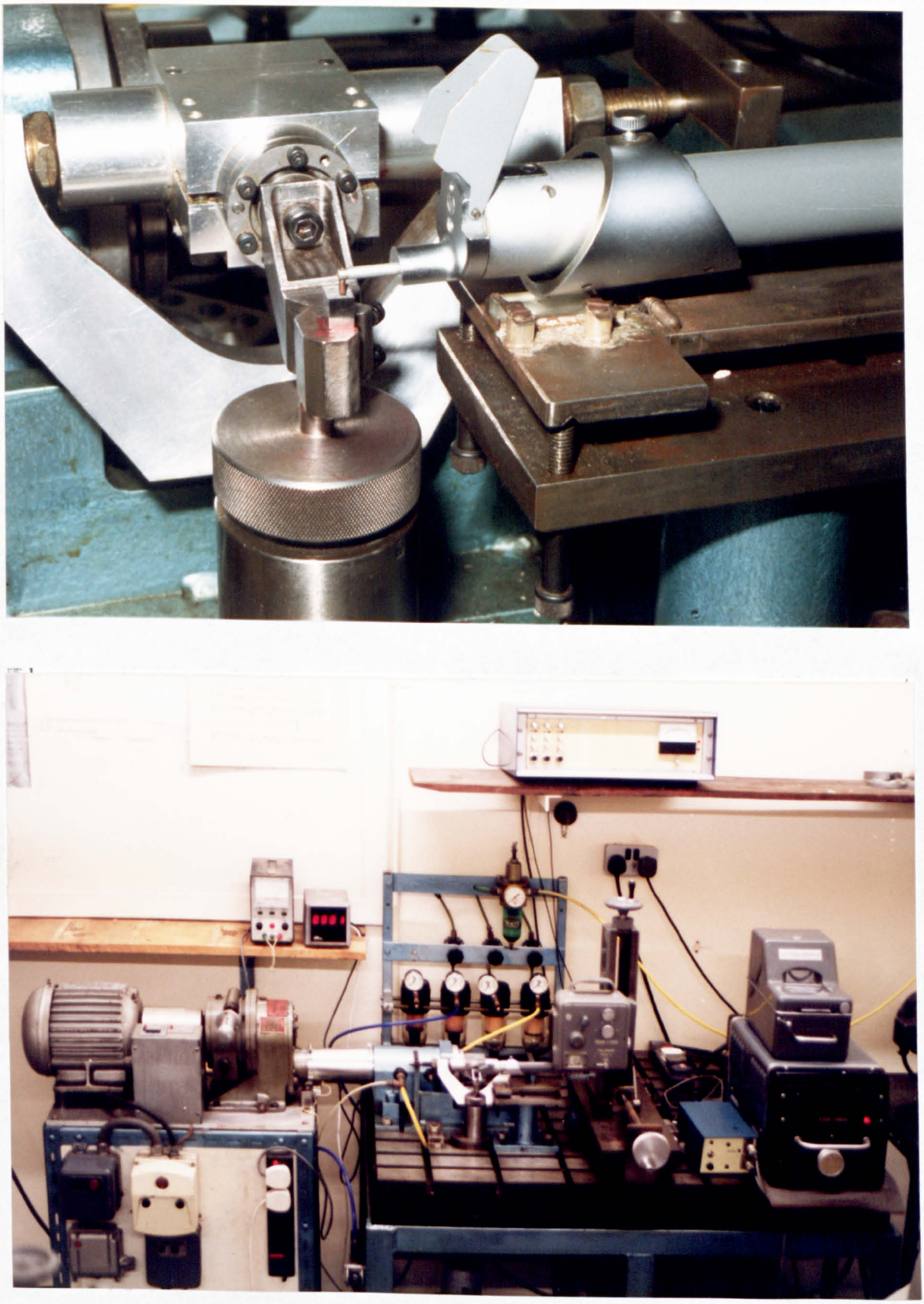

Figure 7.4 Details of the pin on ring test rig.

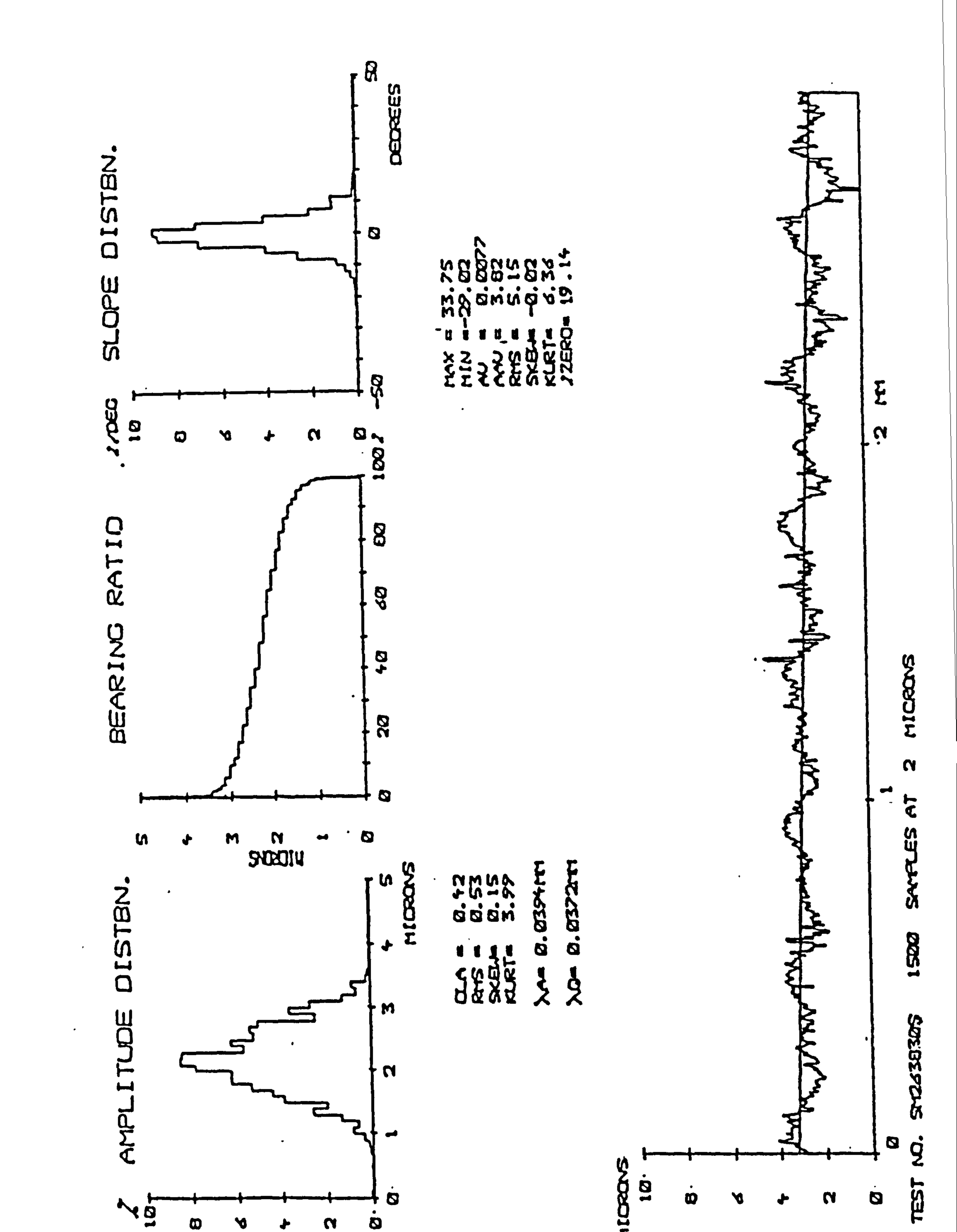

Figure 7.5 Computer analysis of a typical profile.

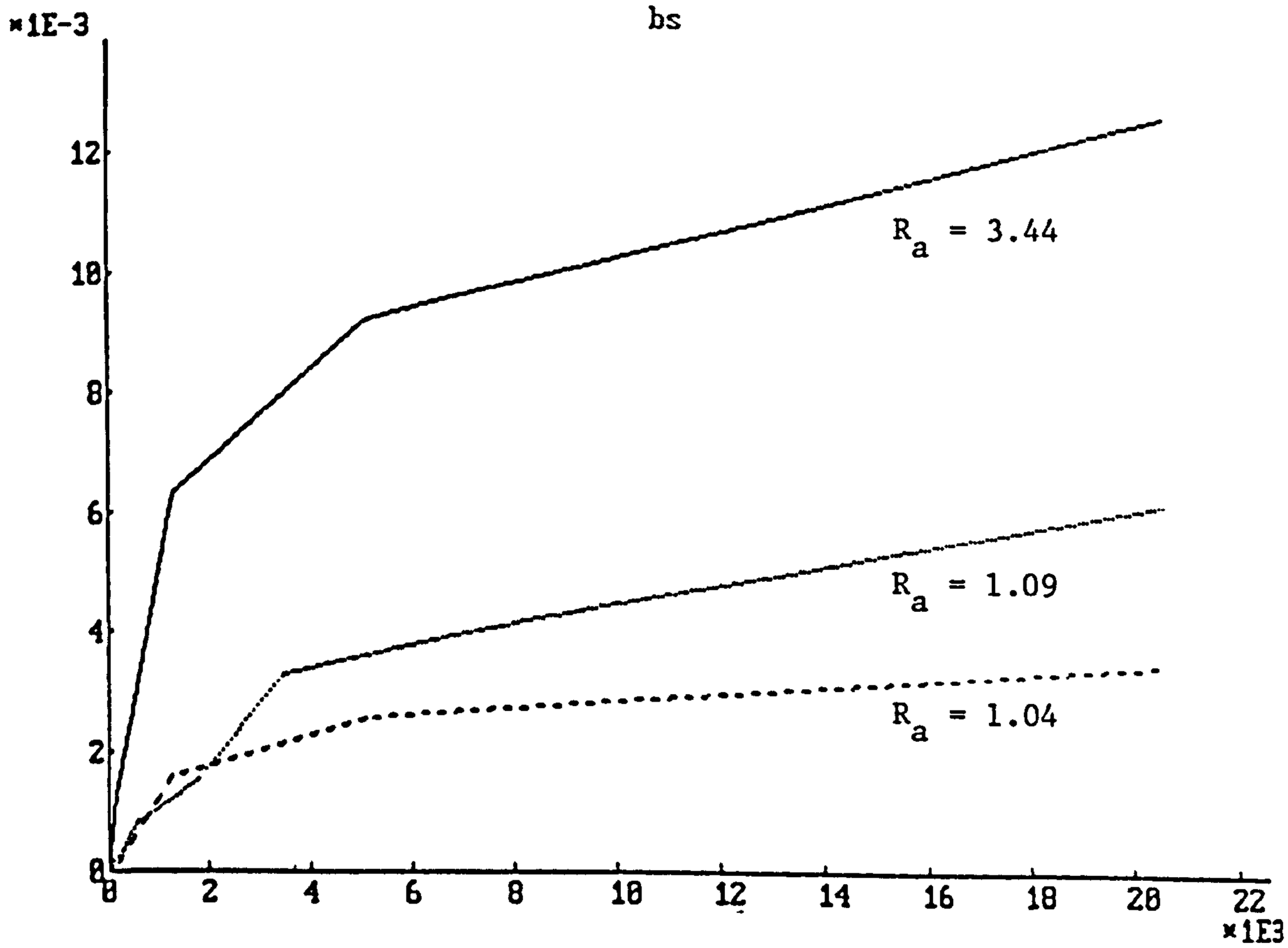

Figure 7.6 Pin wear (mm^3) against sliding distance (m) for bronze ring steel pin (bs) and bronze ring bronze pin (bb) combinations.

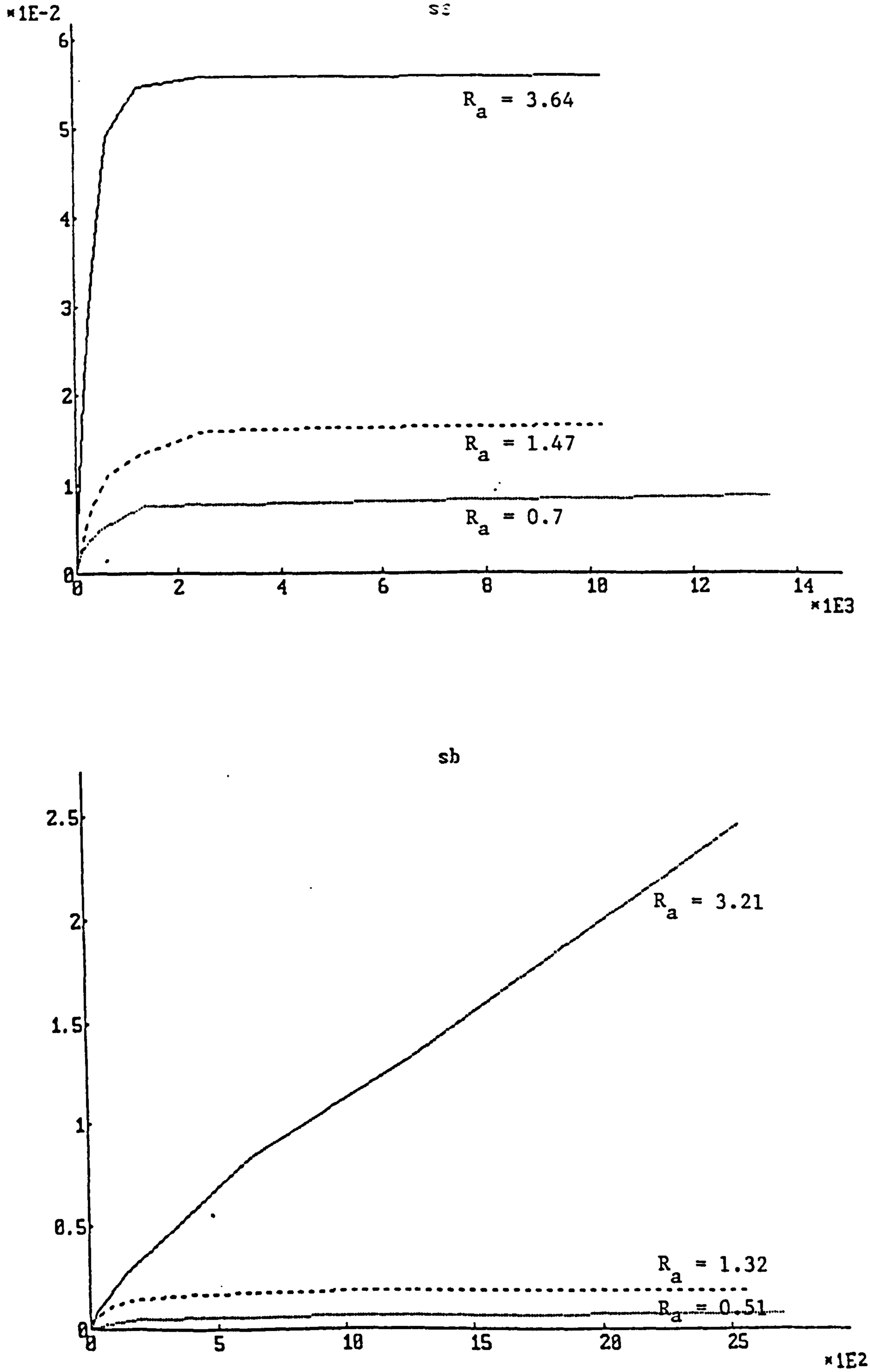

Figure 7.7 Pin wear (mm^3) against sliding distance (m) for steel ring steel pin (SS) and steel ring bronze pin (Sb) combinations.

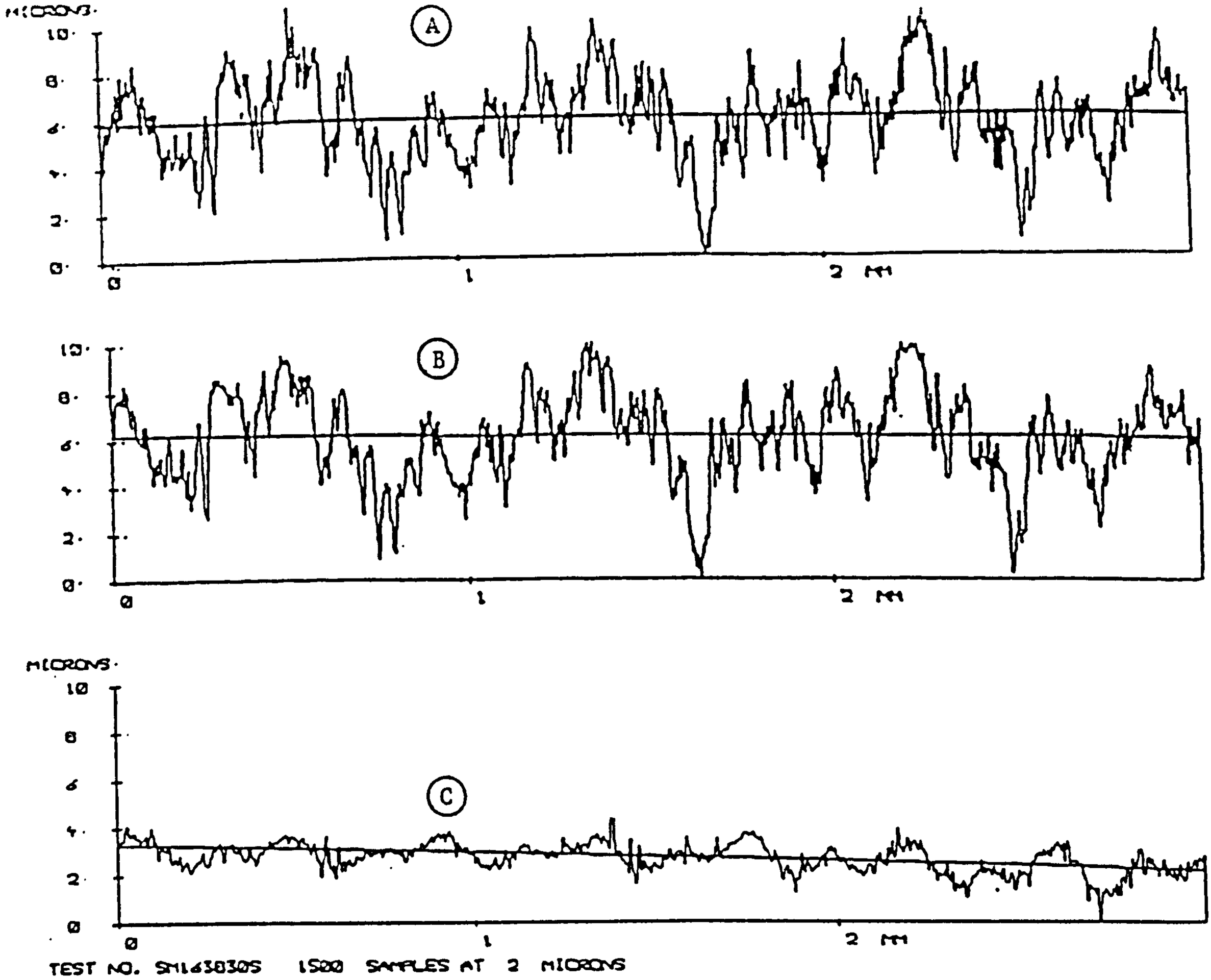

Figure 7.8 Wheel profiles for test SSM. A: before, B: after running-in C: pin profile after running-in (Vertical Magnification 5000).

Figure 7.9 Wheel profile before and after running-in,test SBM (Vertical Magnification 2000) showing running-in within original surface topography, marked X.

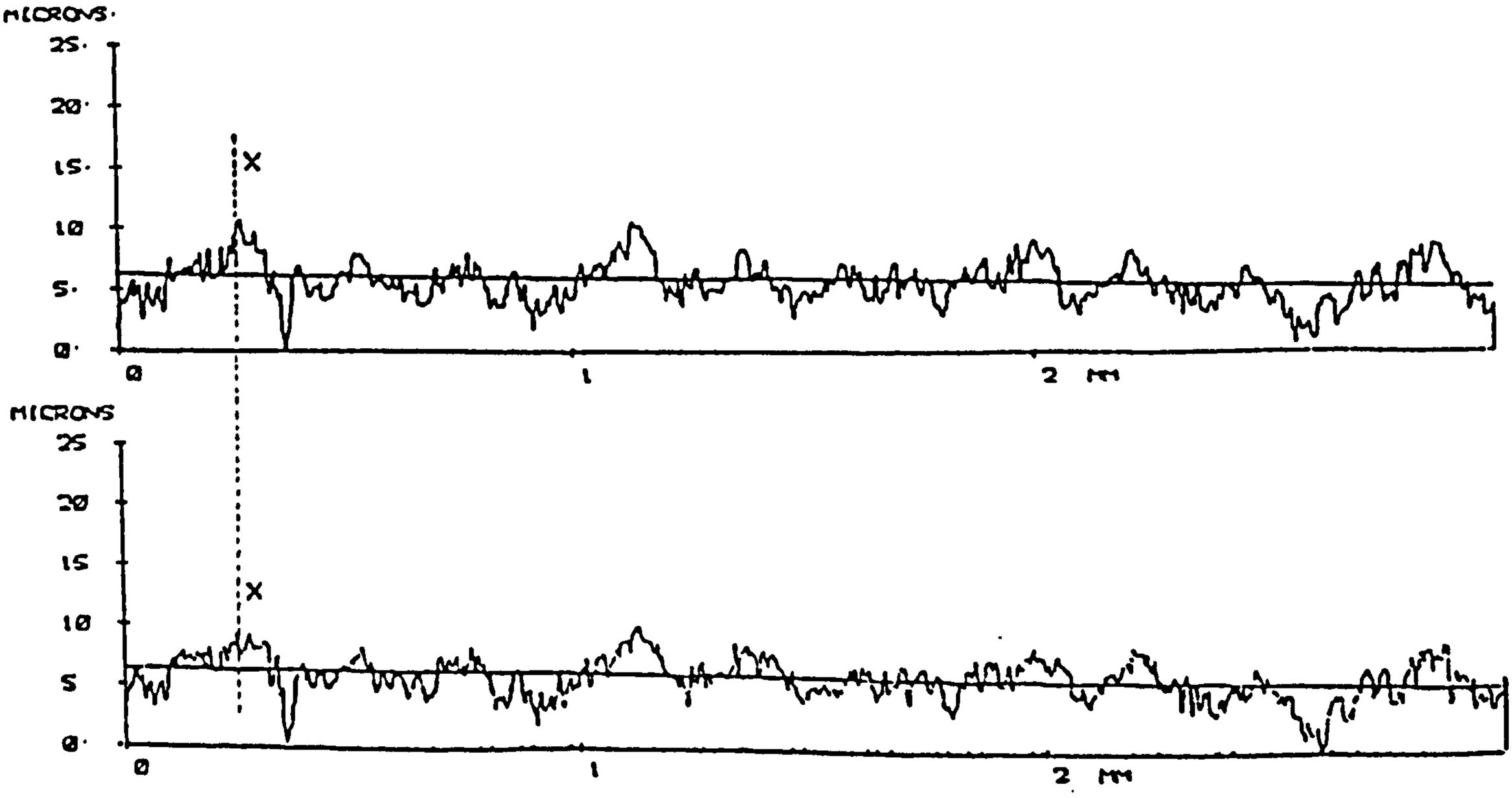

Figure 7.10 Ring profile analysis before (A) and after (B) running-in. Test BSF (Vertical Magnification 2000).

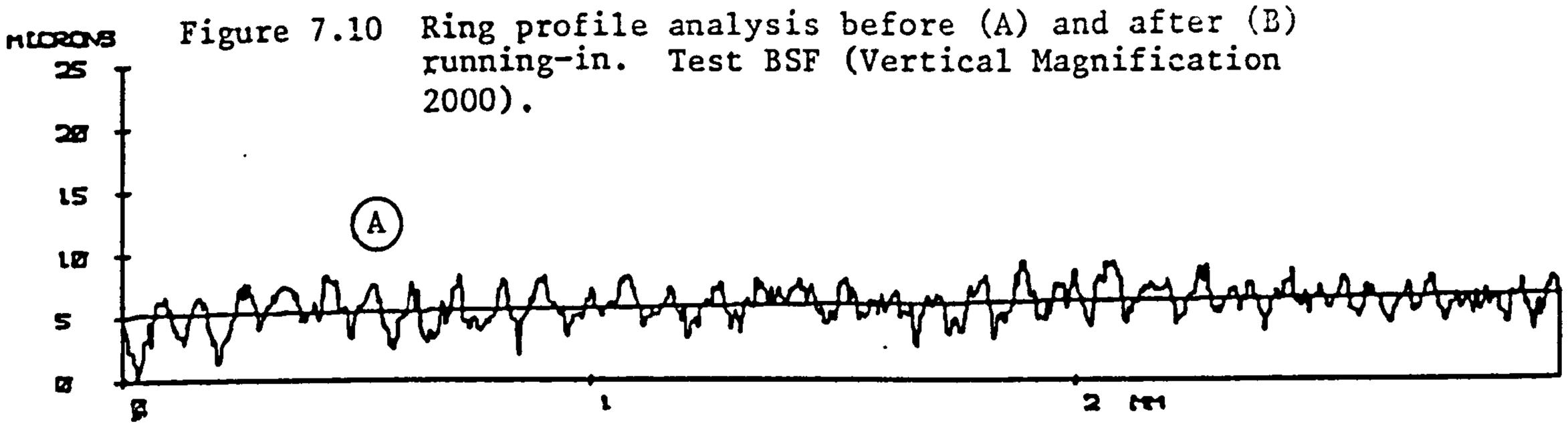

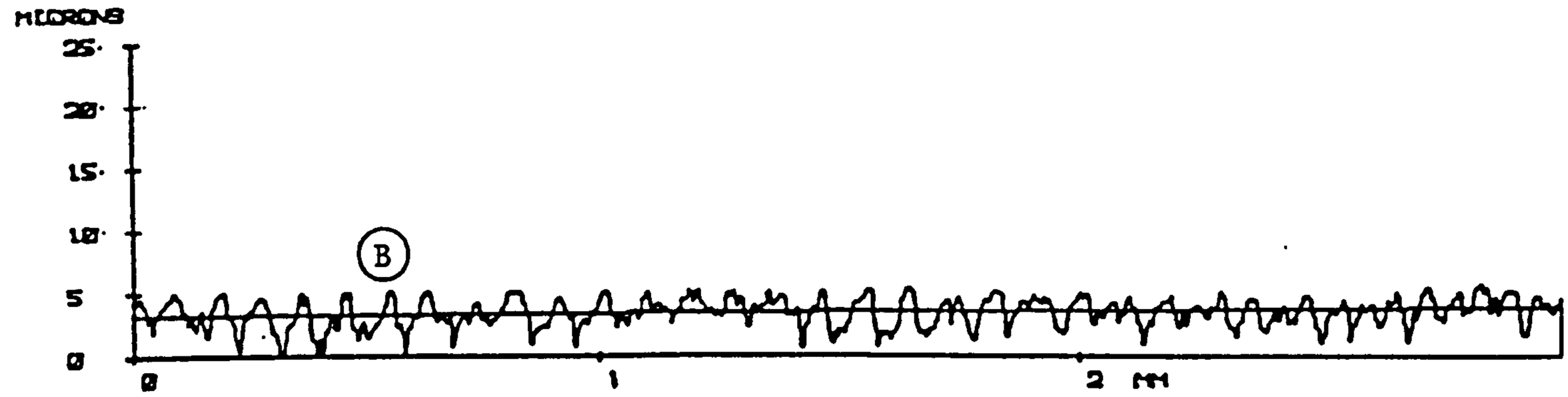

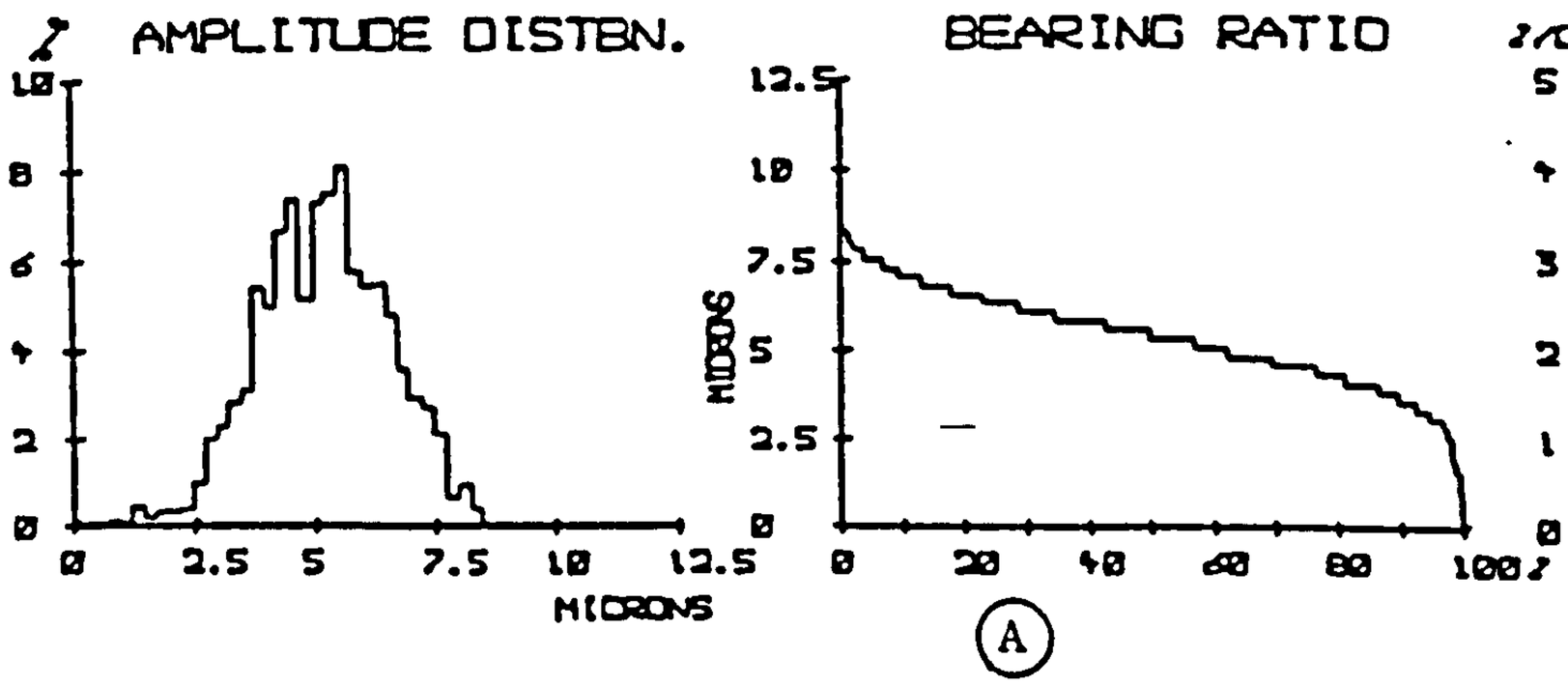

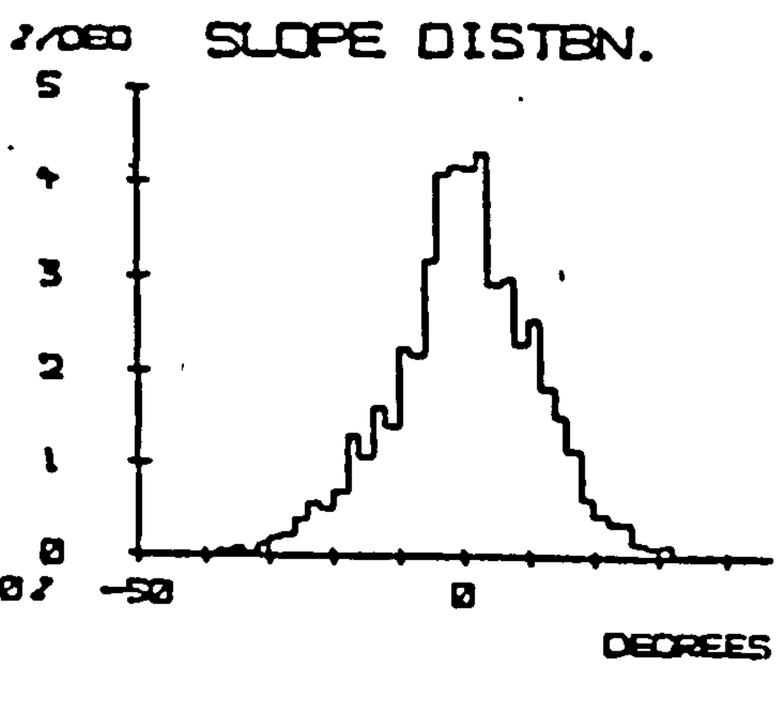

CLA = 1.09
RMS = 1.35
SKEW= -0.22
KURT= 3.01

λA= 0.0151MM

λQ= 0.0131MM

MAX = 40.10
MIN = -39.96
AV = 0.05809
AAV = 8.61
RMS = 11.14
SKEW= -0.21
KURT= 3.43

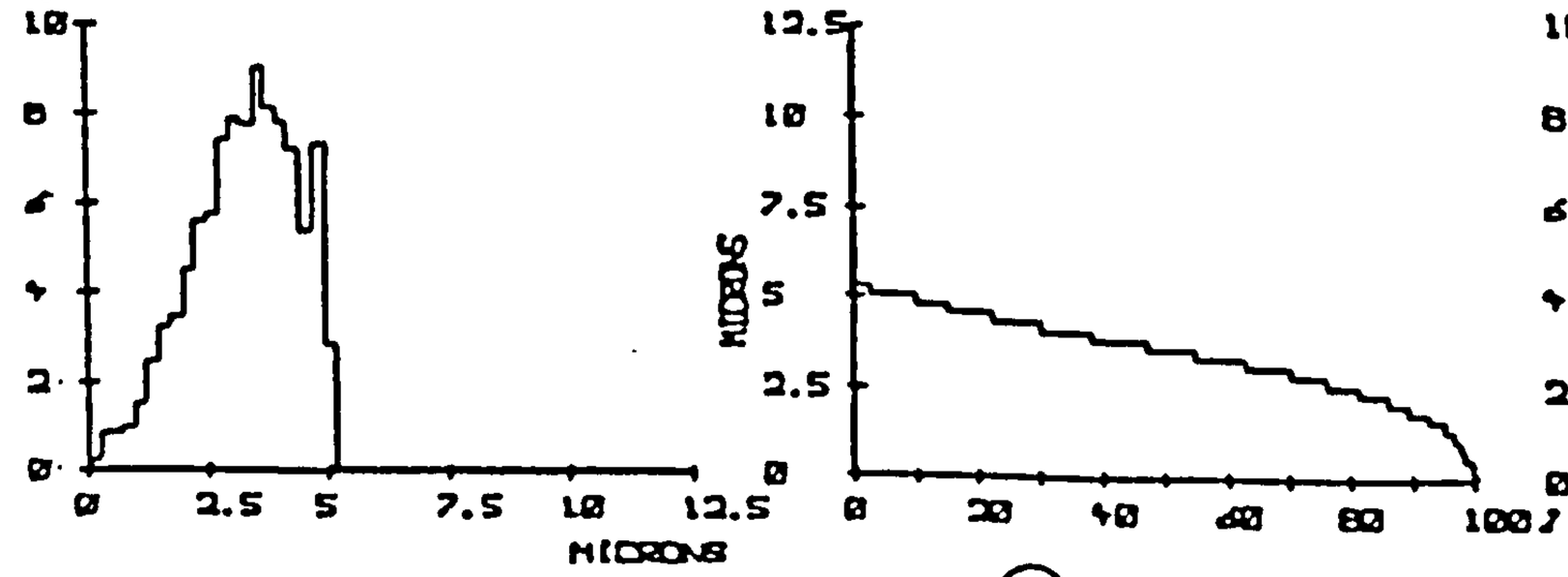

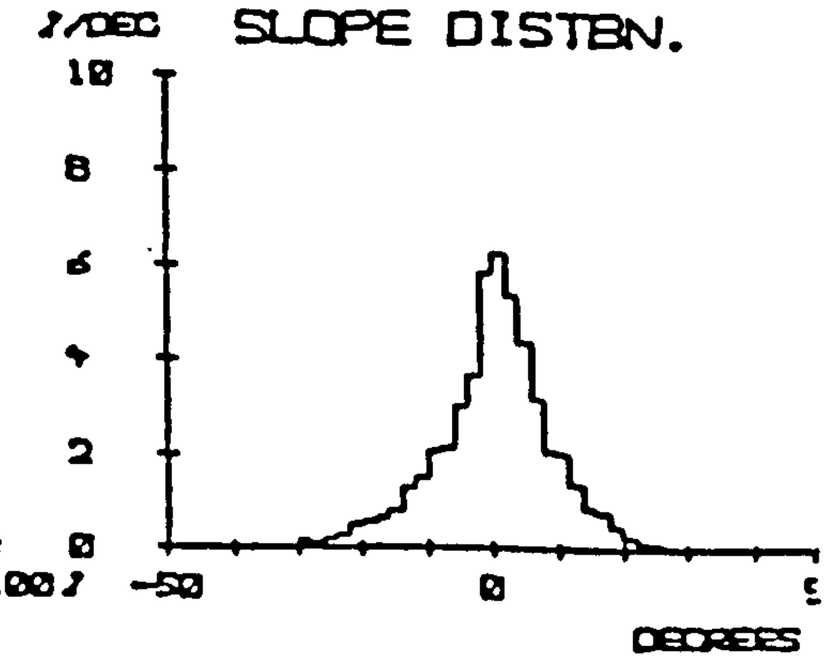

CLA = 0.91
RMS = 1.11
SKEW= -0.45
KURT= 2.80

λA= 0.0103MM

λQ= 0.0138MM

MAX = 30.01
MIN = -38.18
AV = 0.01113
AAV = 6.78
RMS = 9.07
SKEW= -0.46
KURT= 4.09

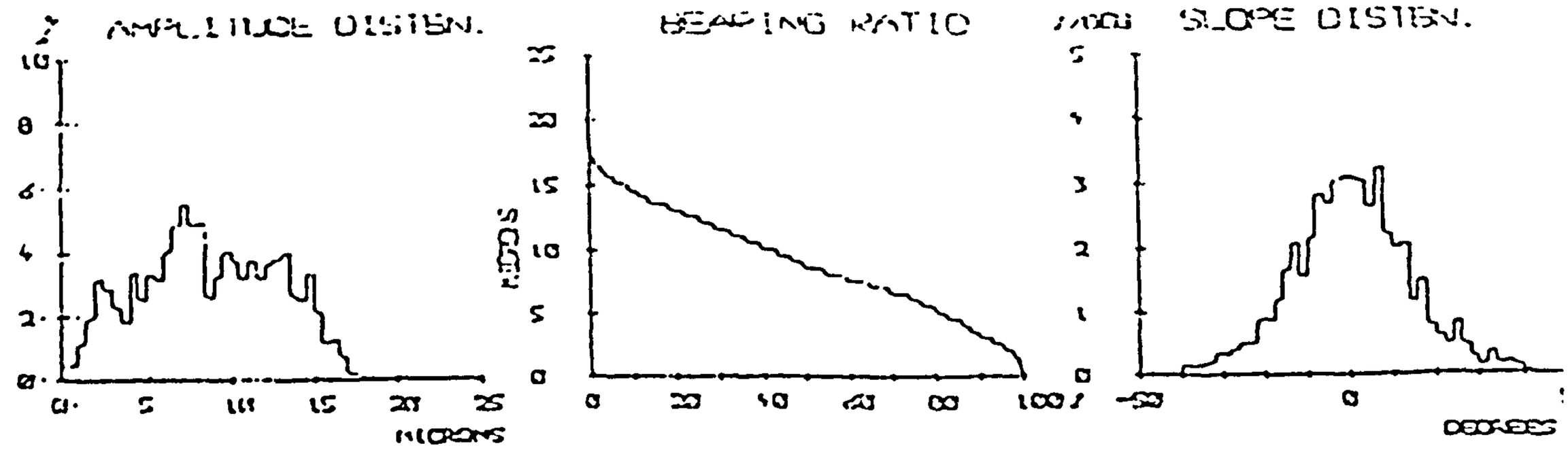

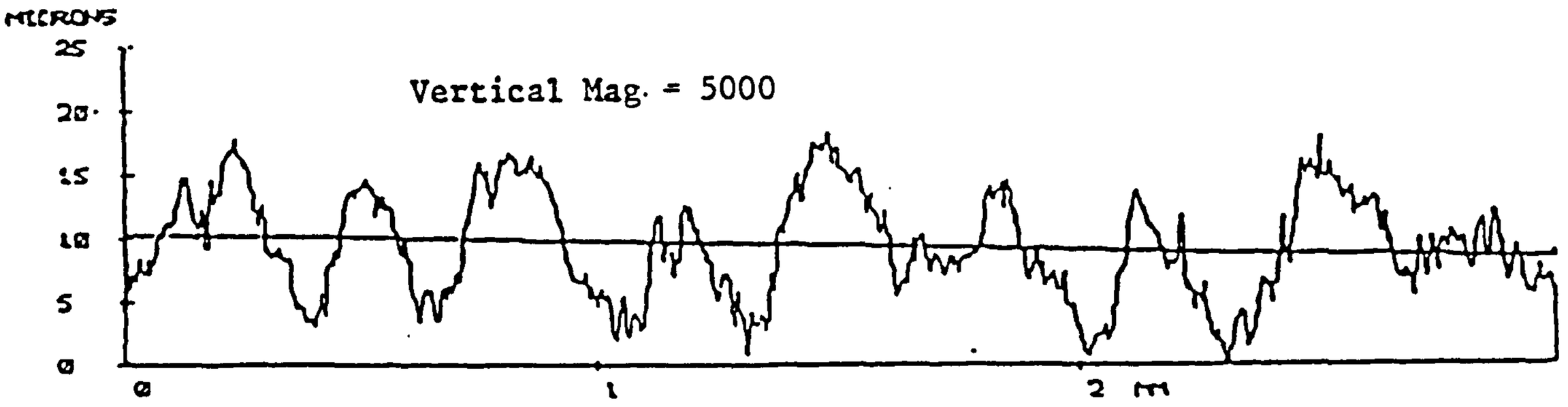

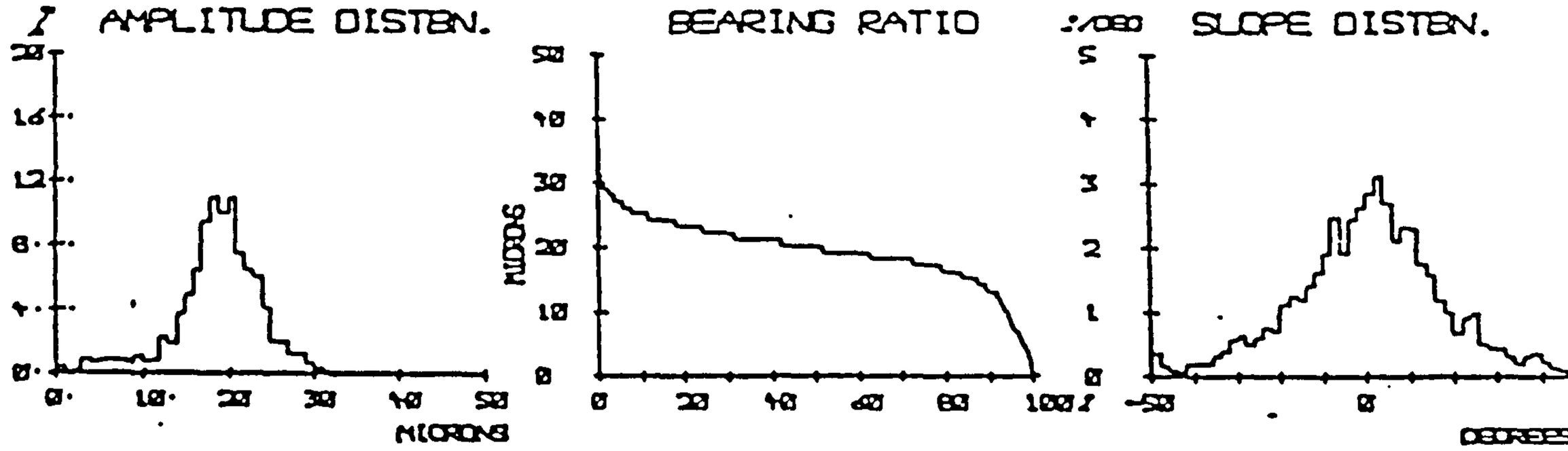

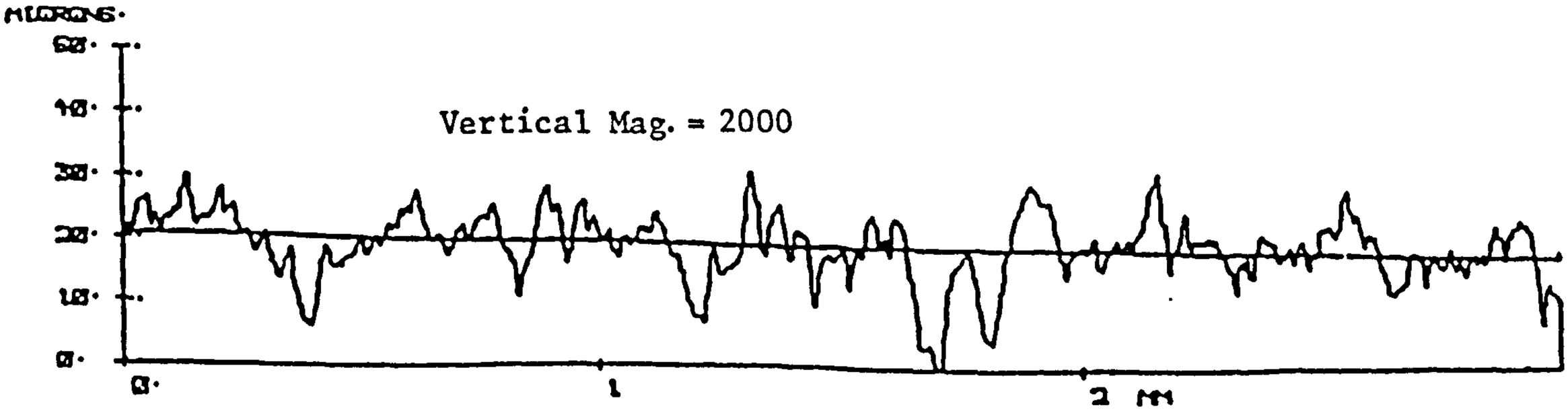

Figure 7.11 Computer analysis of the new and old (after wear) ring profiles. Test BBR.

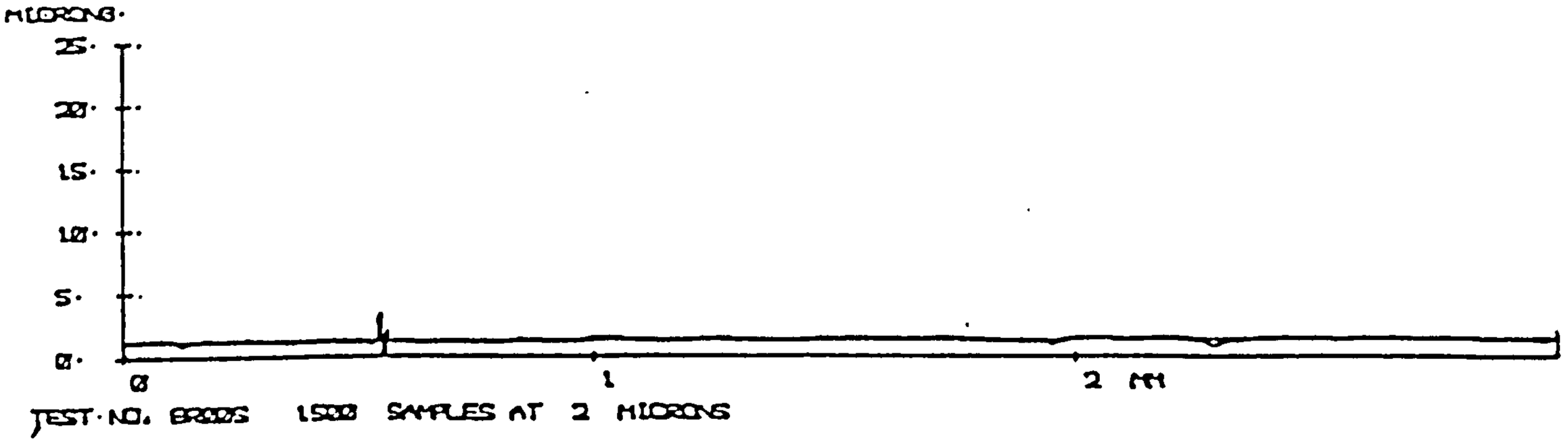

Figure 7.12 Traces of pin surface after 0, 1277, 20470 and 90957 metre of sliding showing the progressive transition of ring profile onto the pin surface. Test BSR (VM = 5000).

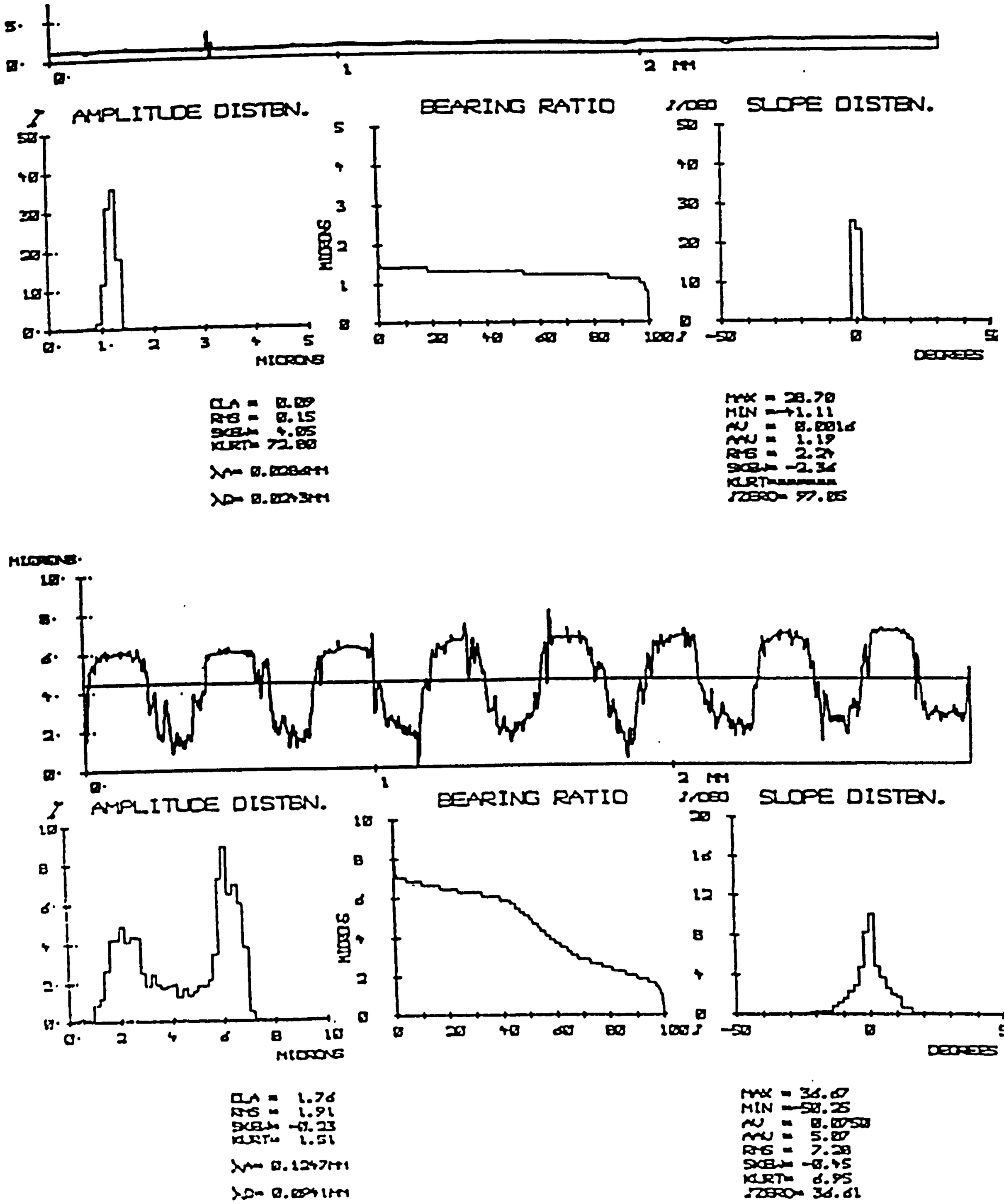

Figure 7.13 Pin profile analysis after 0 and 90957 metre of sliding. Test BSR (VM = 5000).

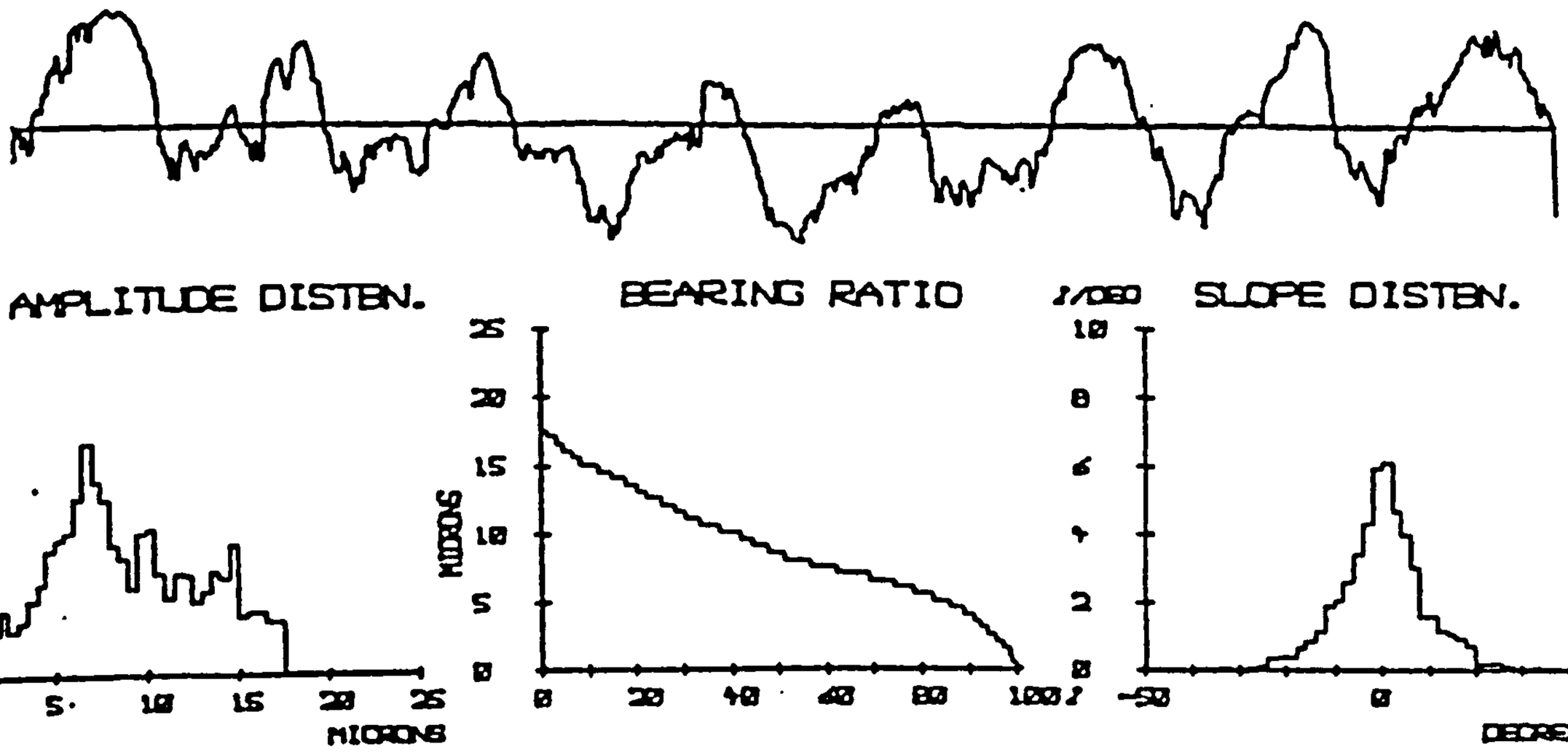

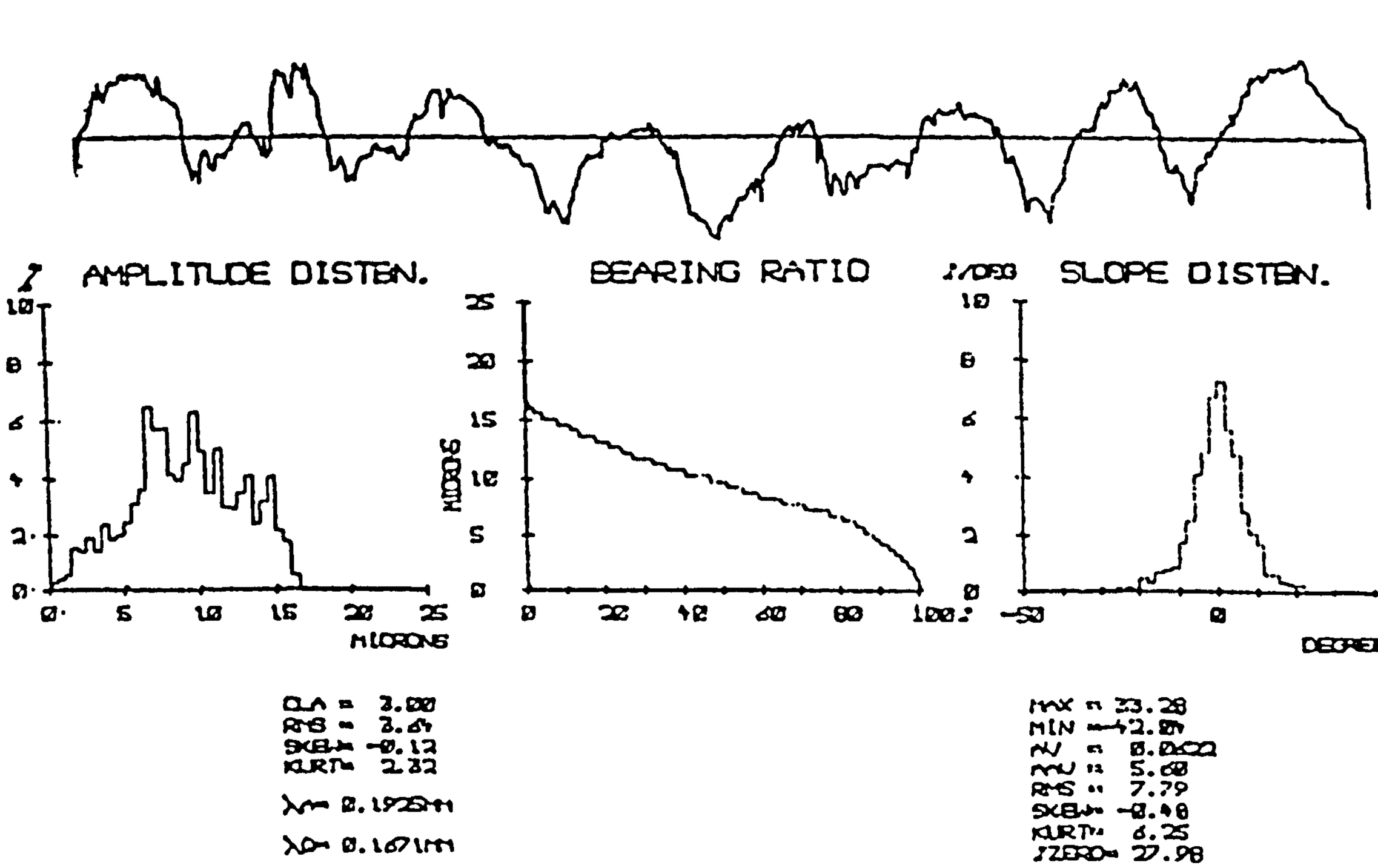

Figure 7.14 Ring profile analysis at 0 and 90957 metre of sliding. Test BSR (VM = 2000).

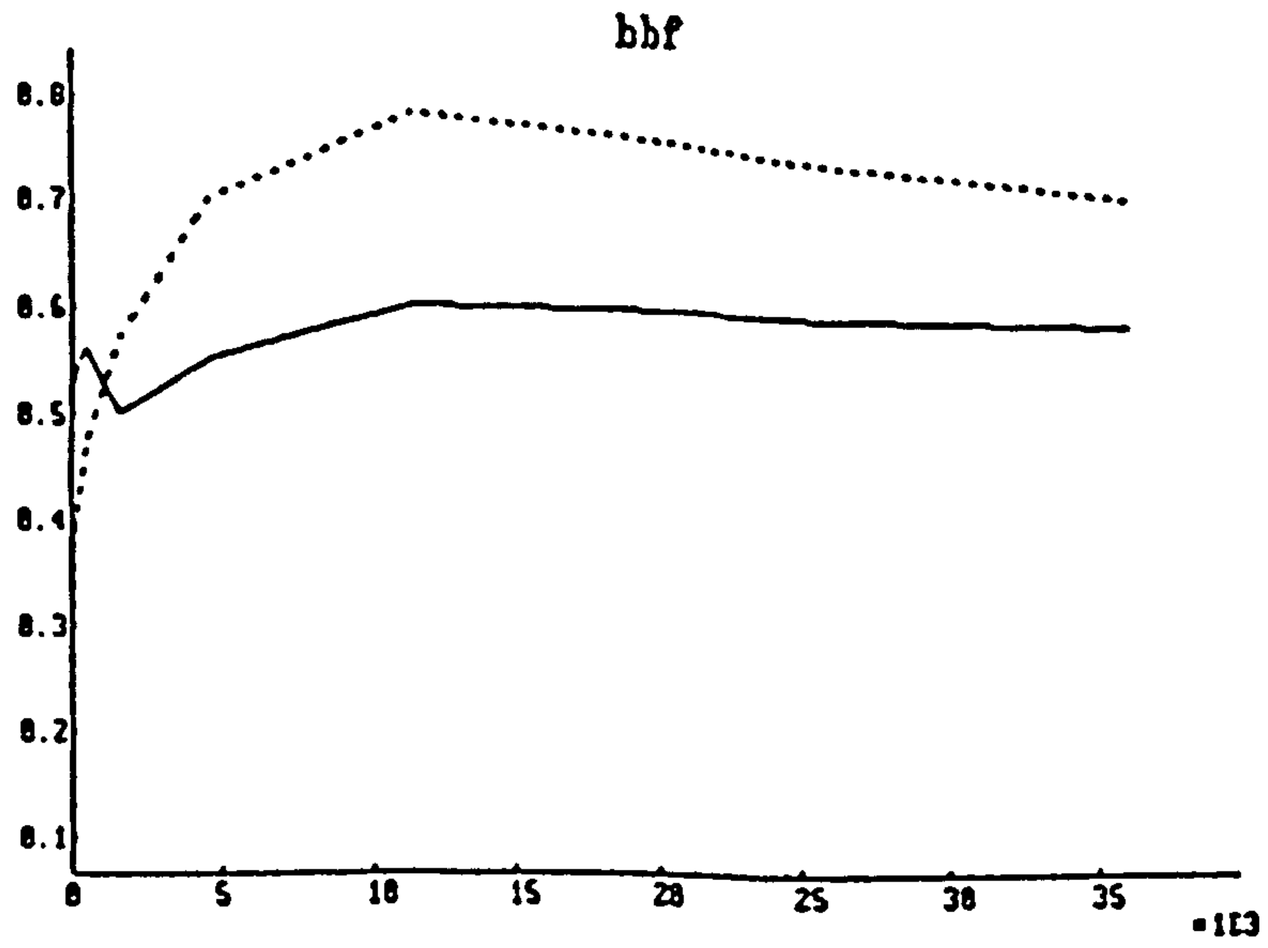

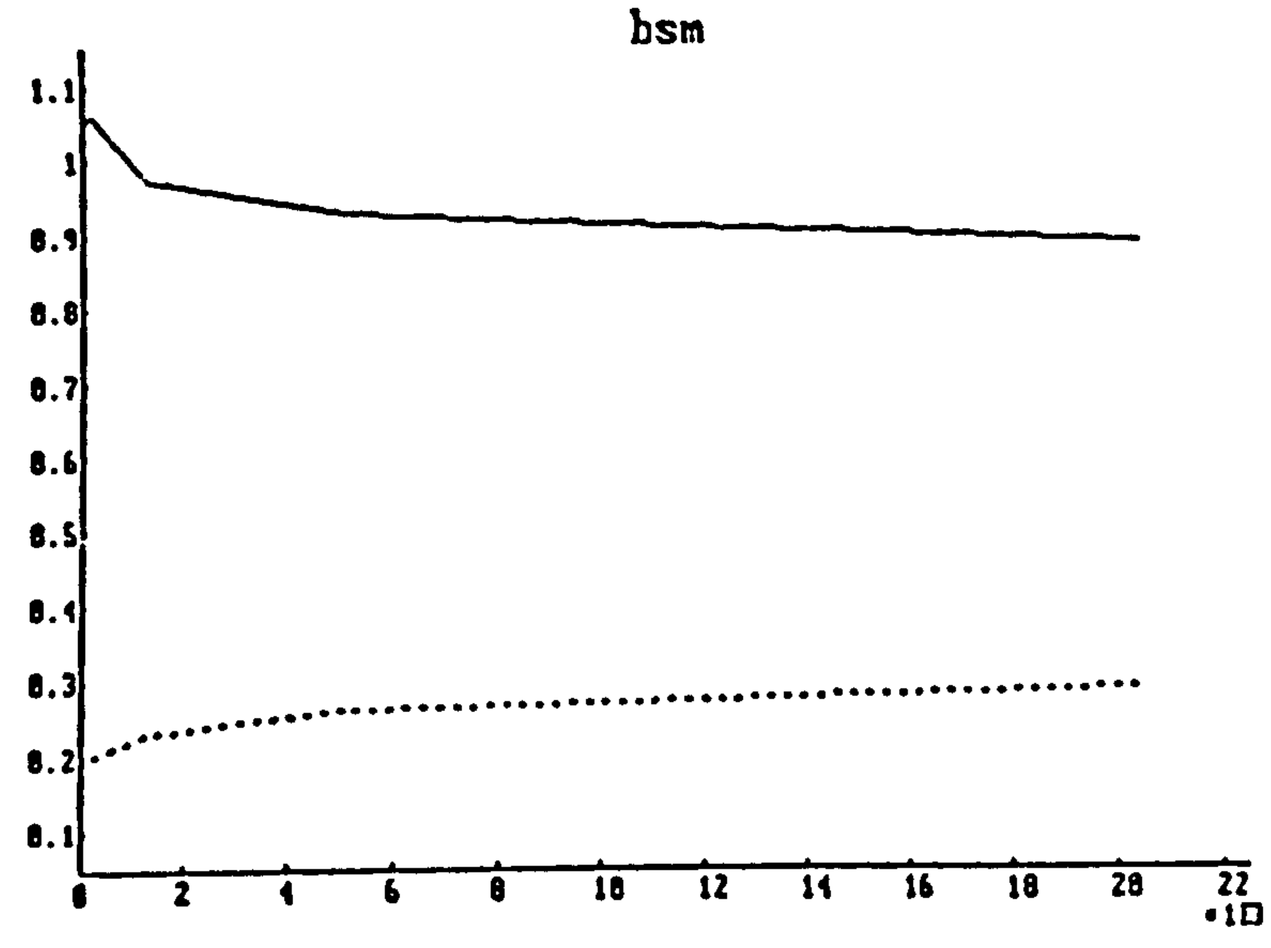

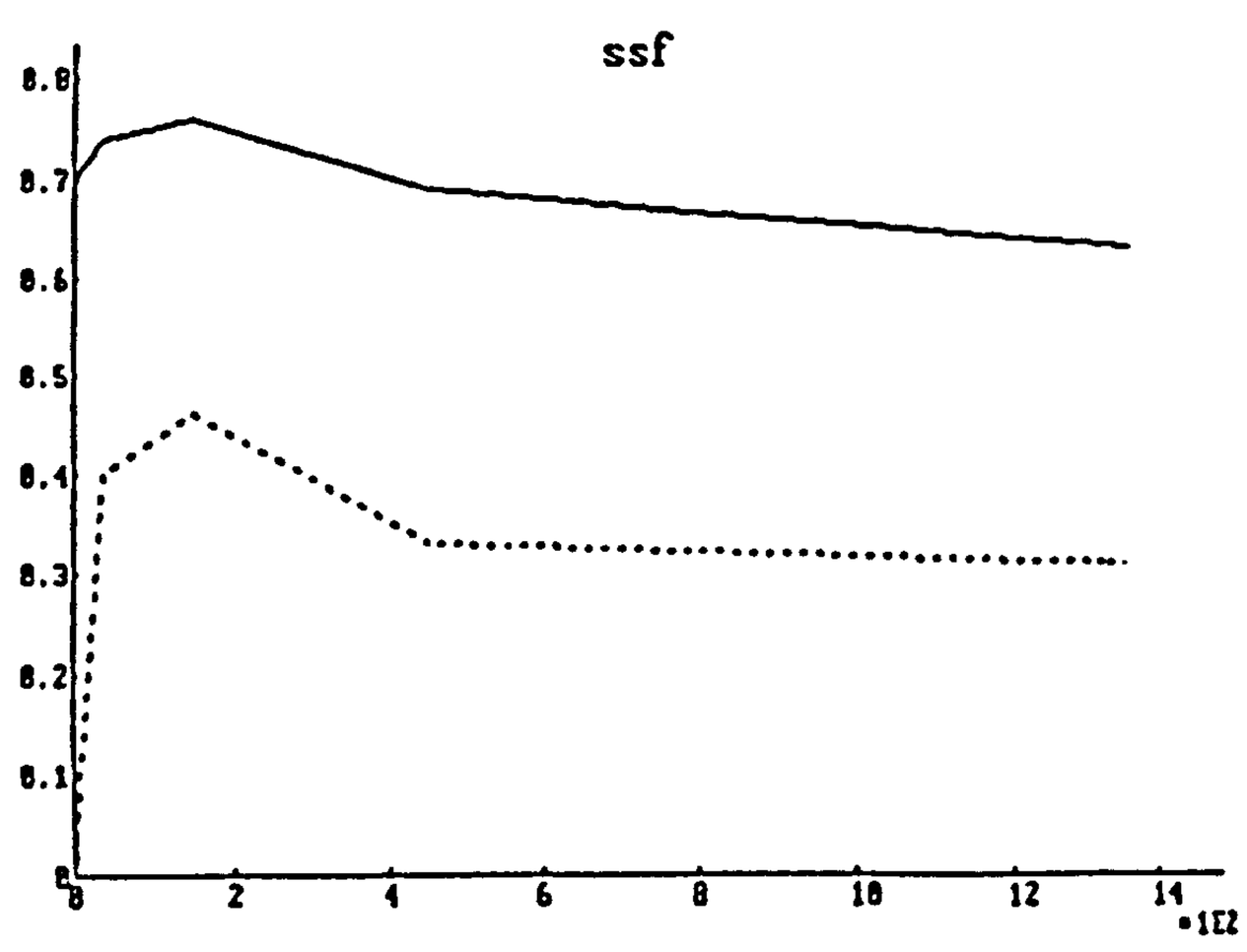

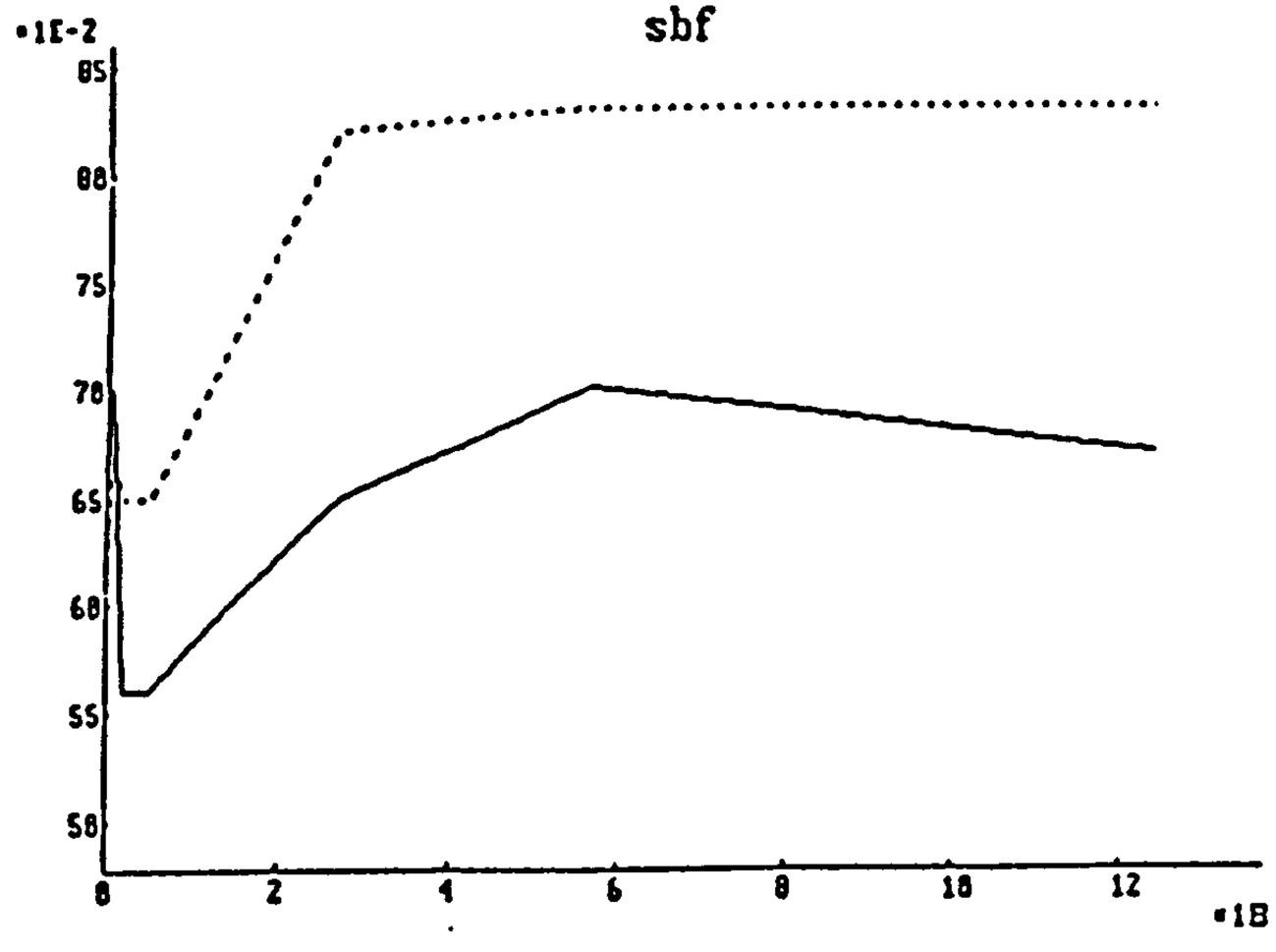

Figure 7.15 Changes of R_a (μm) with sliding distance (m). ———Ring ……Pin.

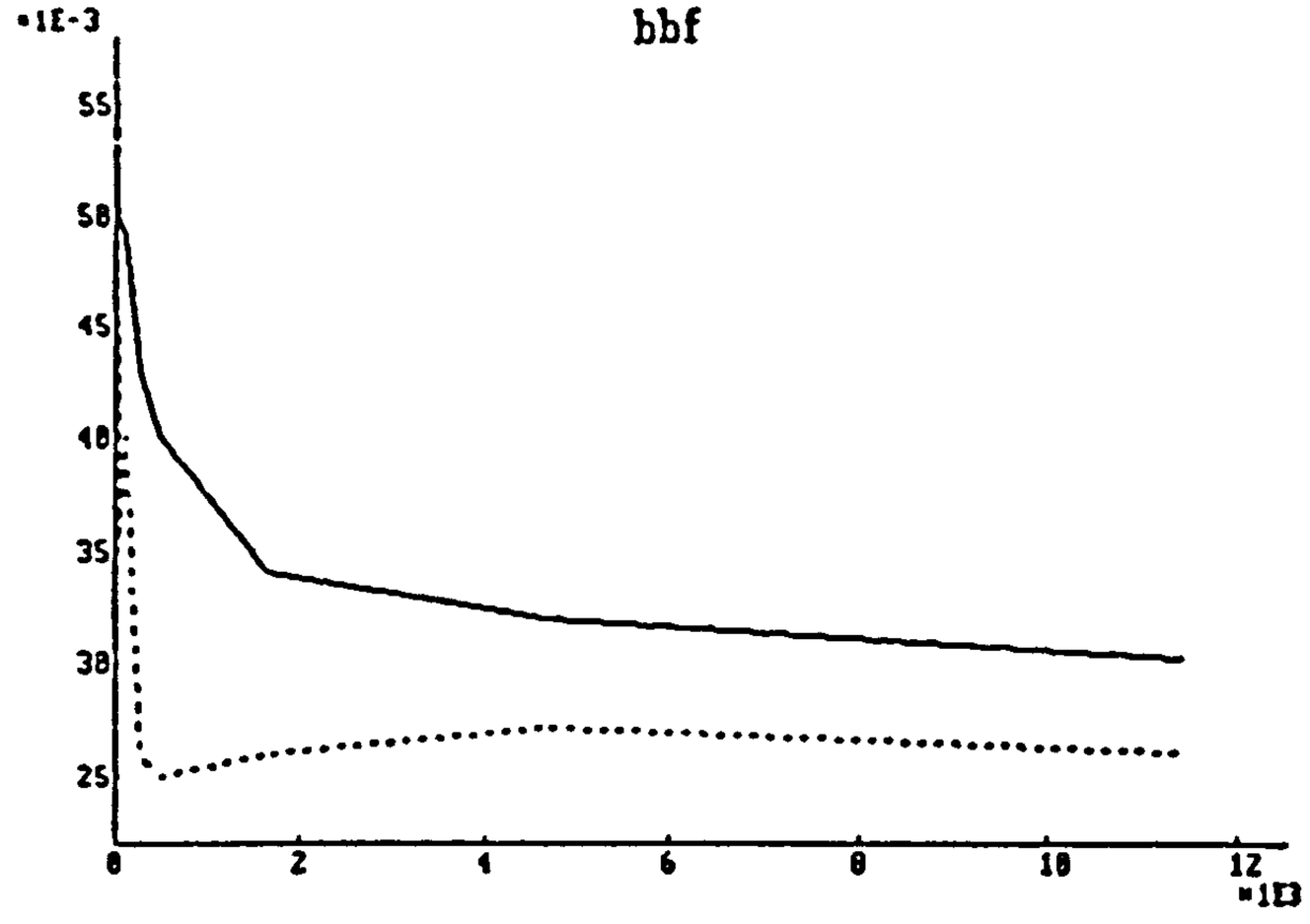

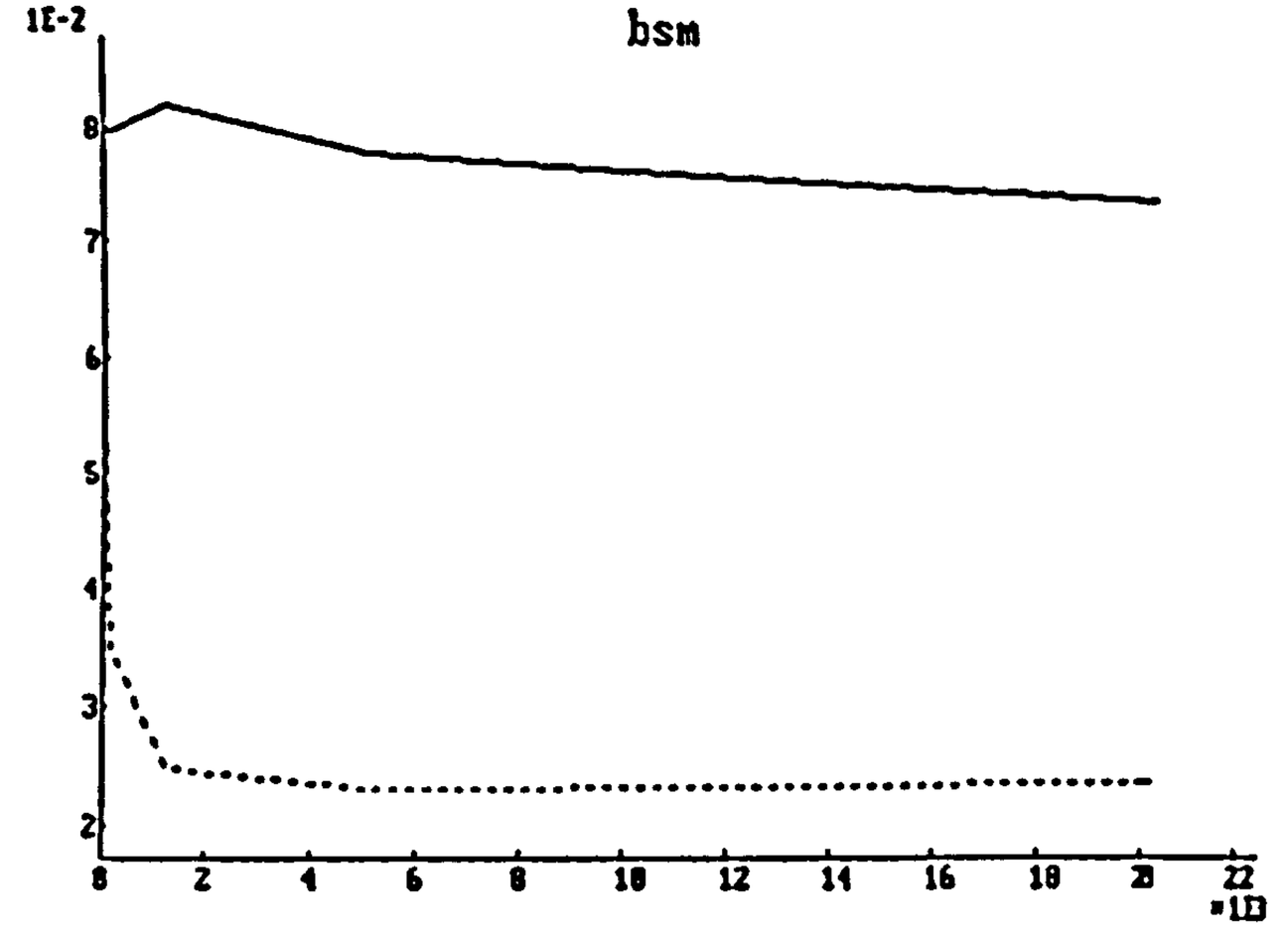

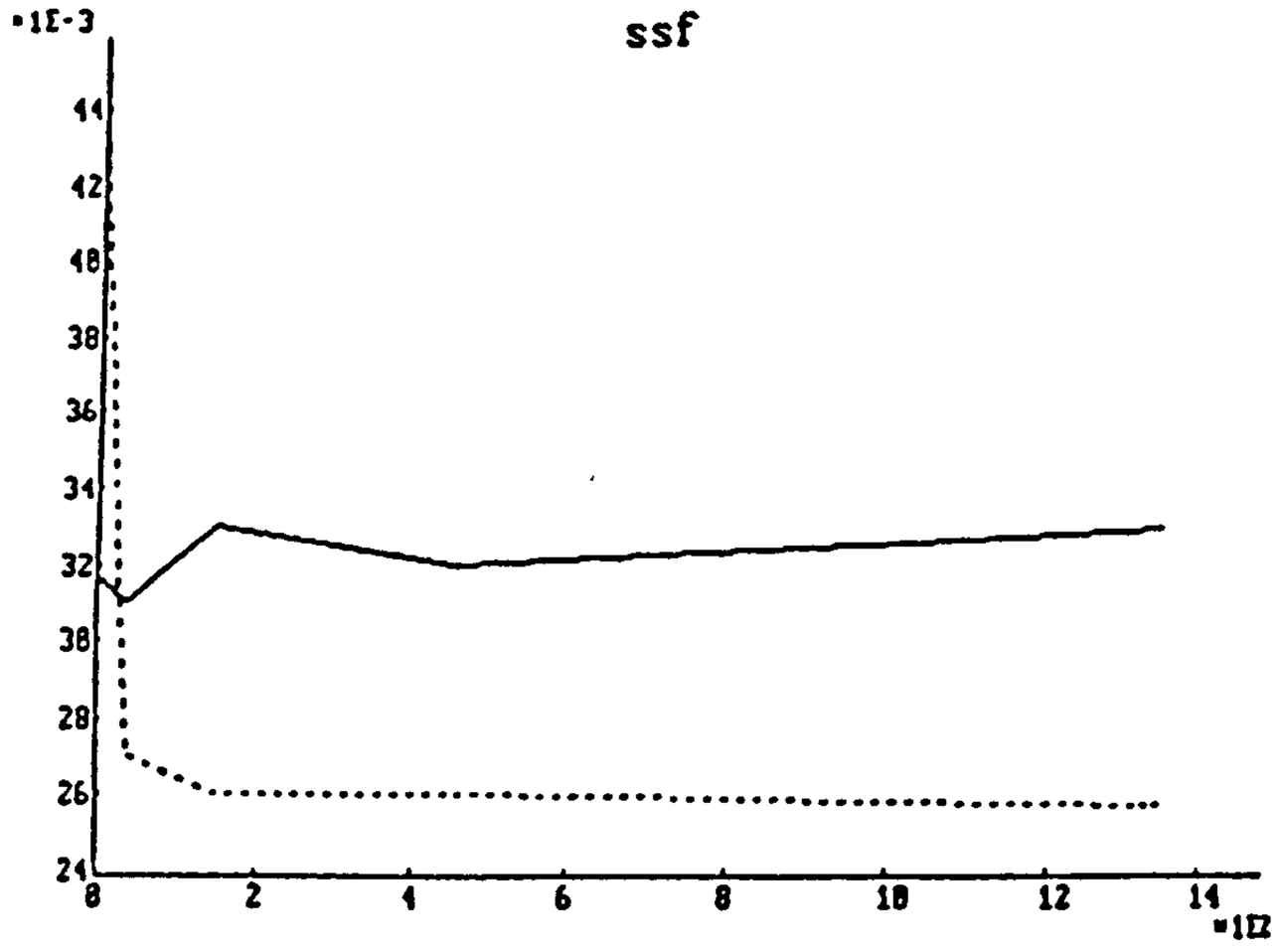

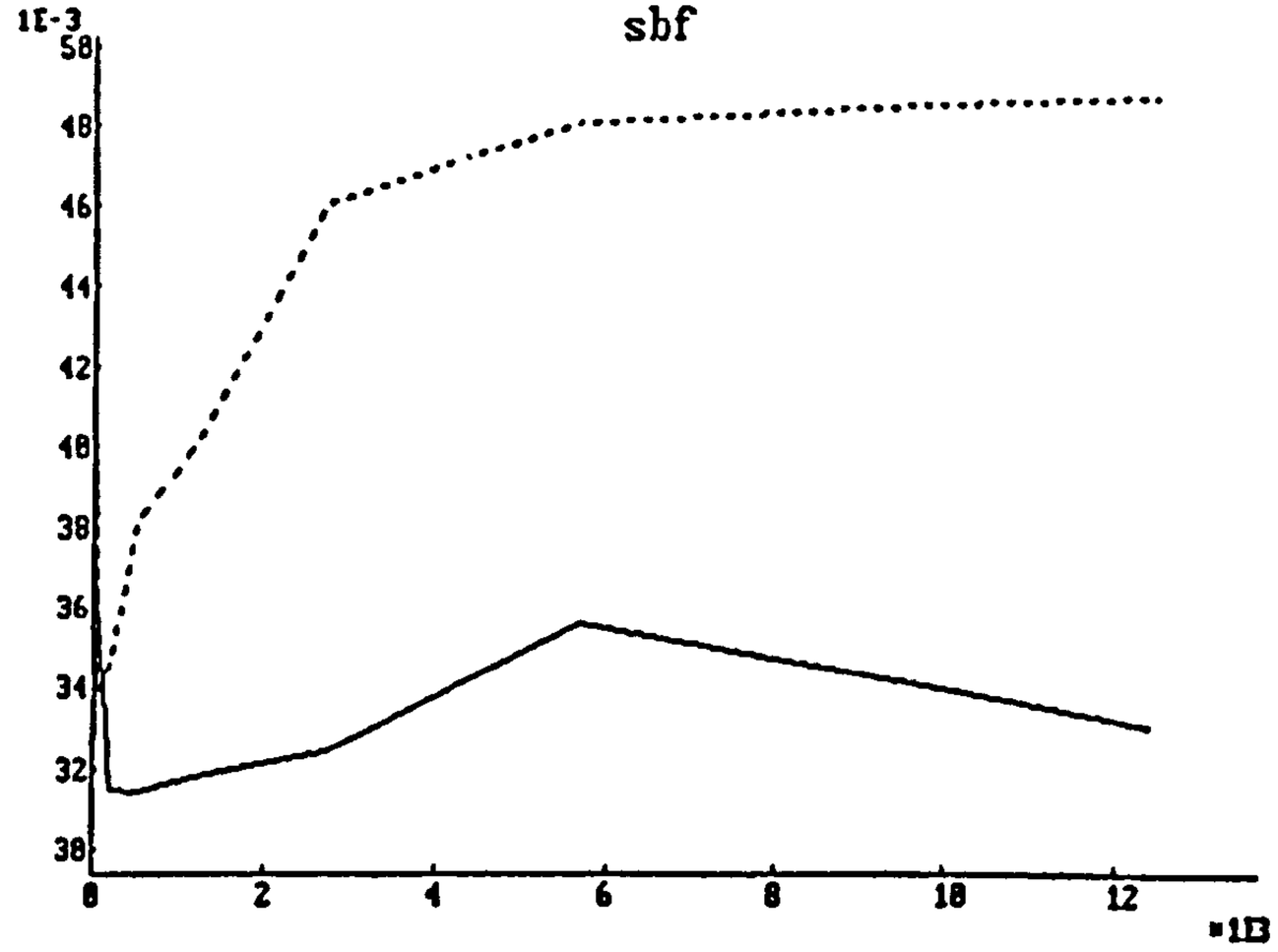

Figure 7.16 Changes of average λ (mm) with sliding distance (m). ——— Ring ..... Pin

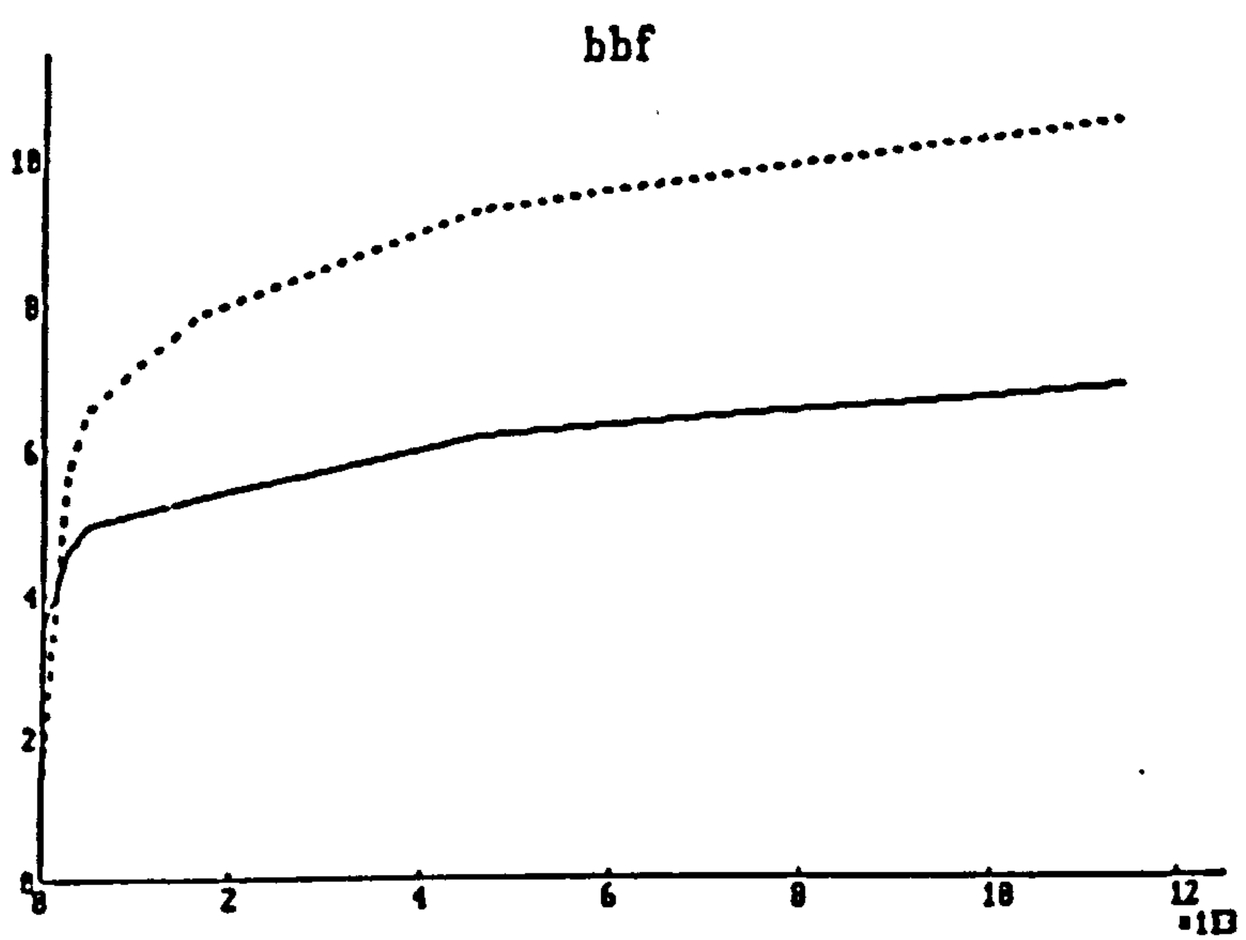

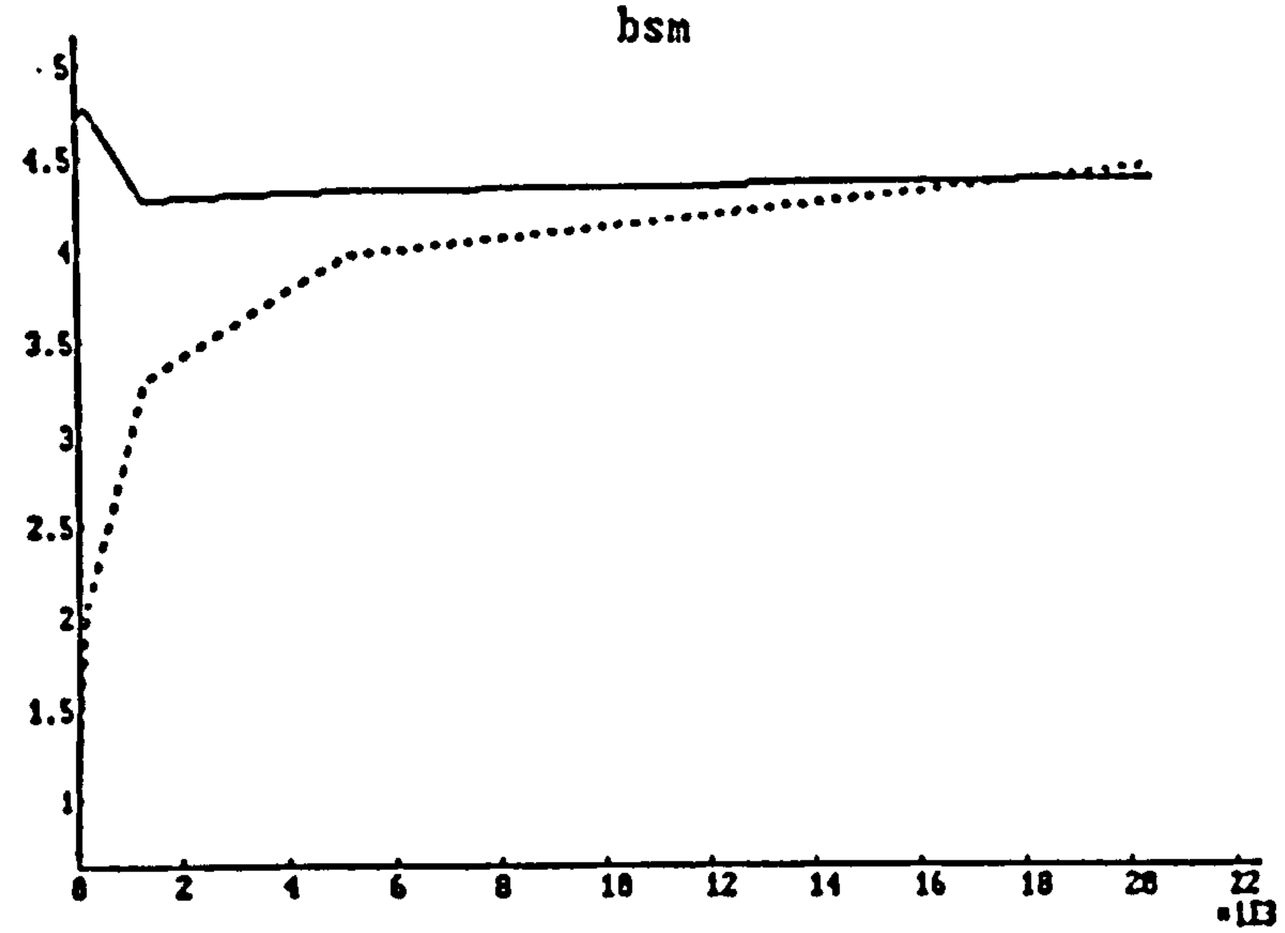

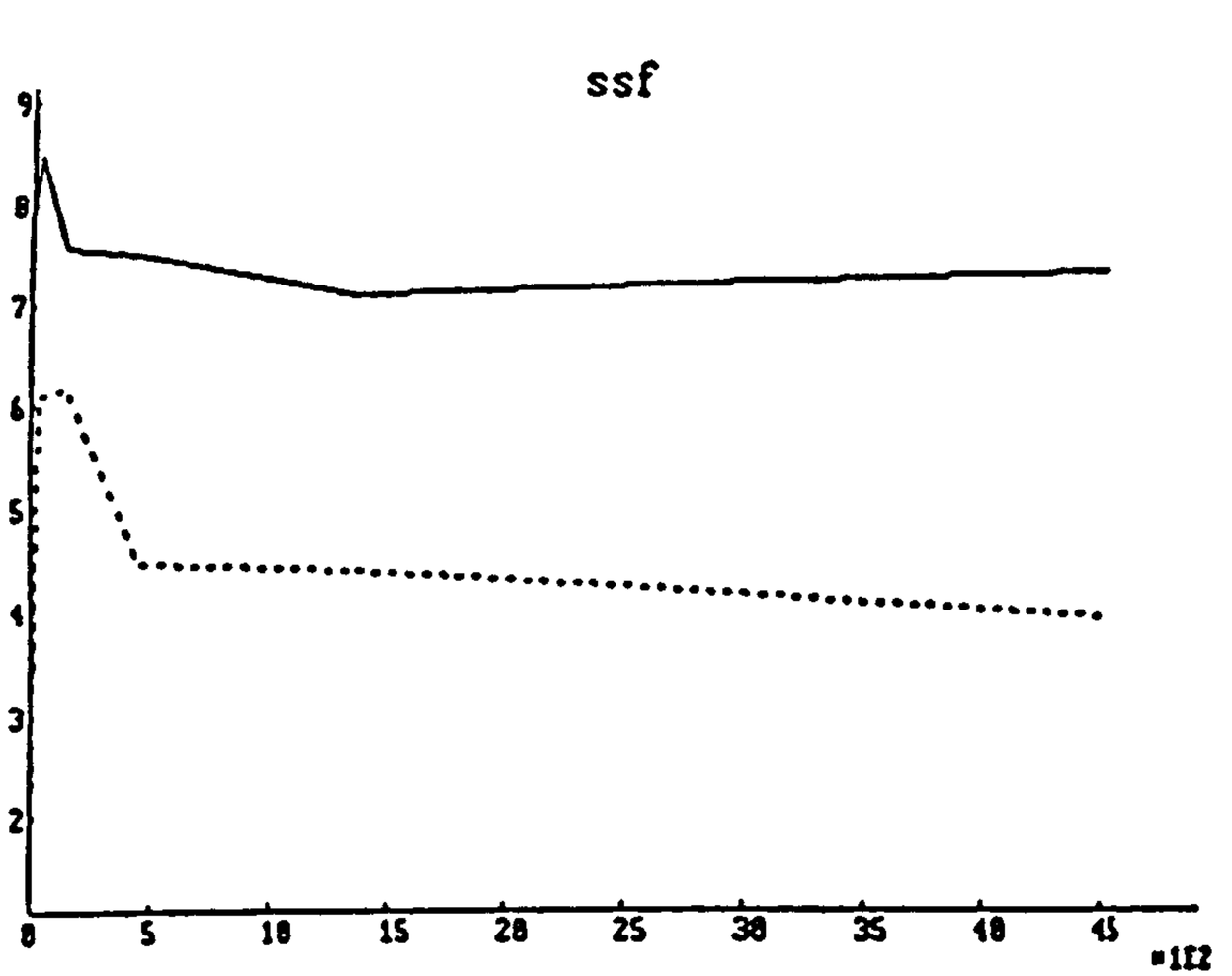

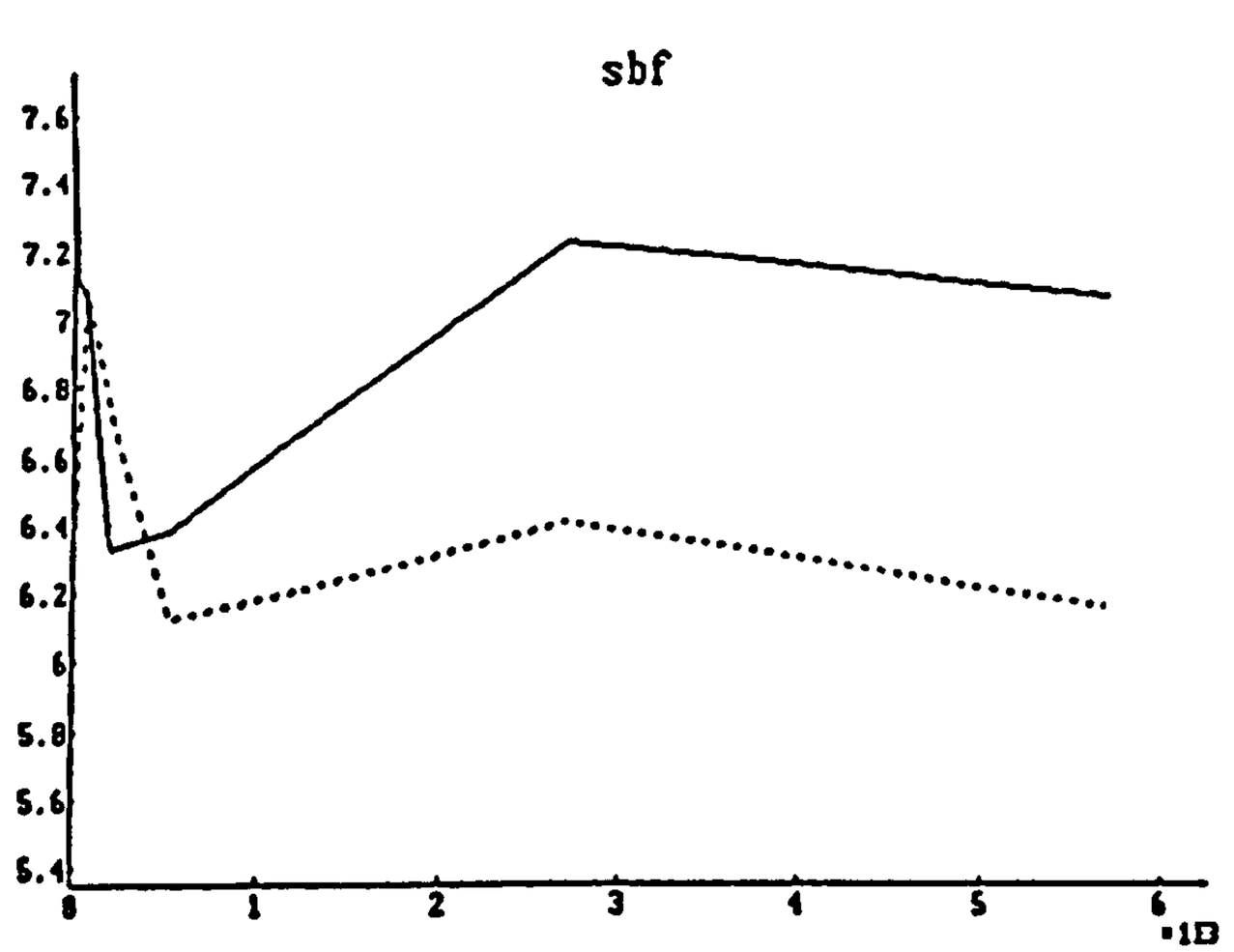

Figure 7.17 Variation of average slope with sliding distance. ——— Ring .....Pin.

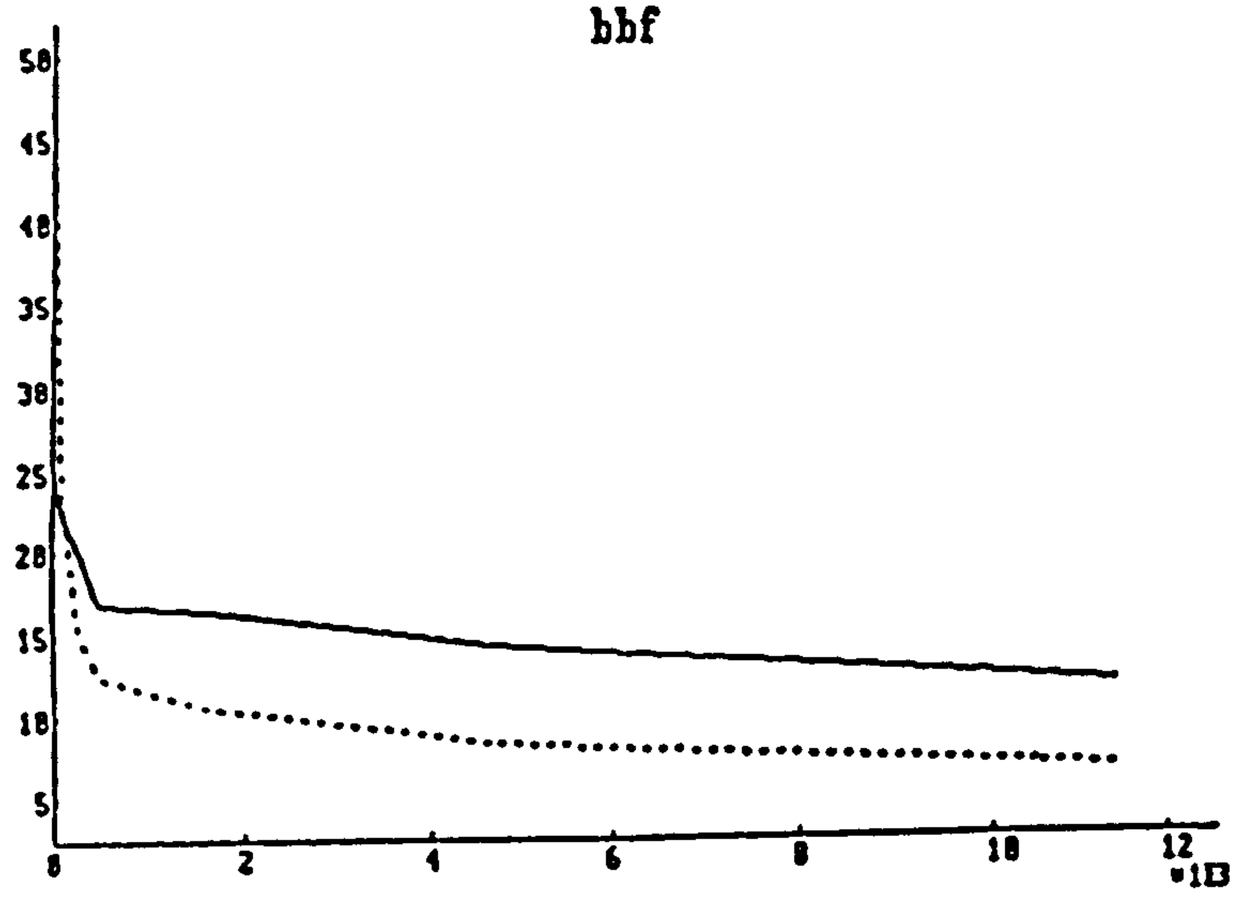

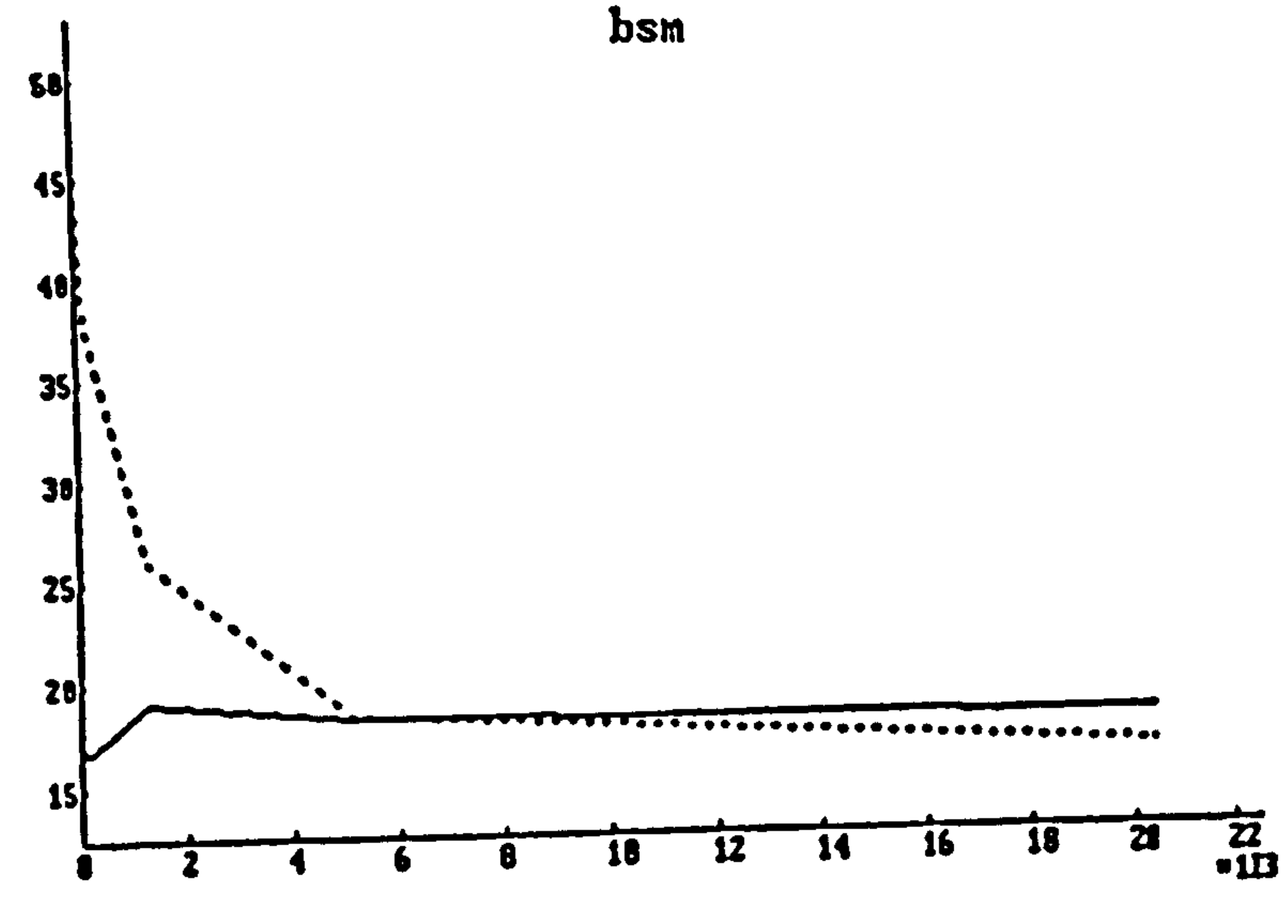

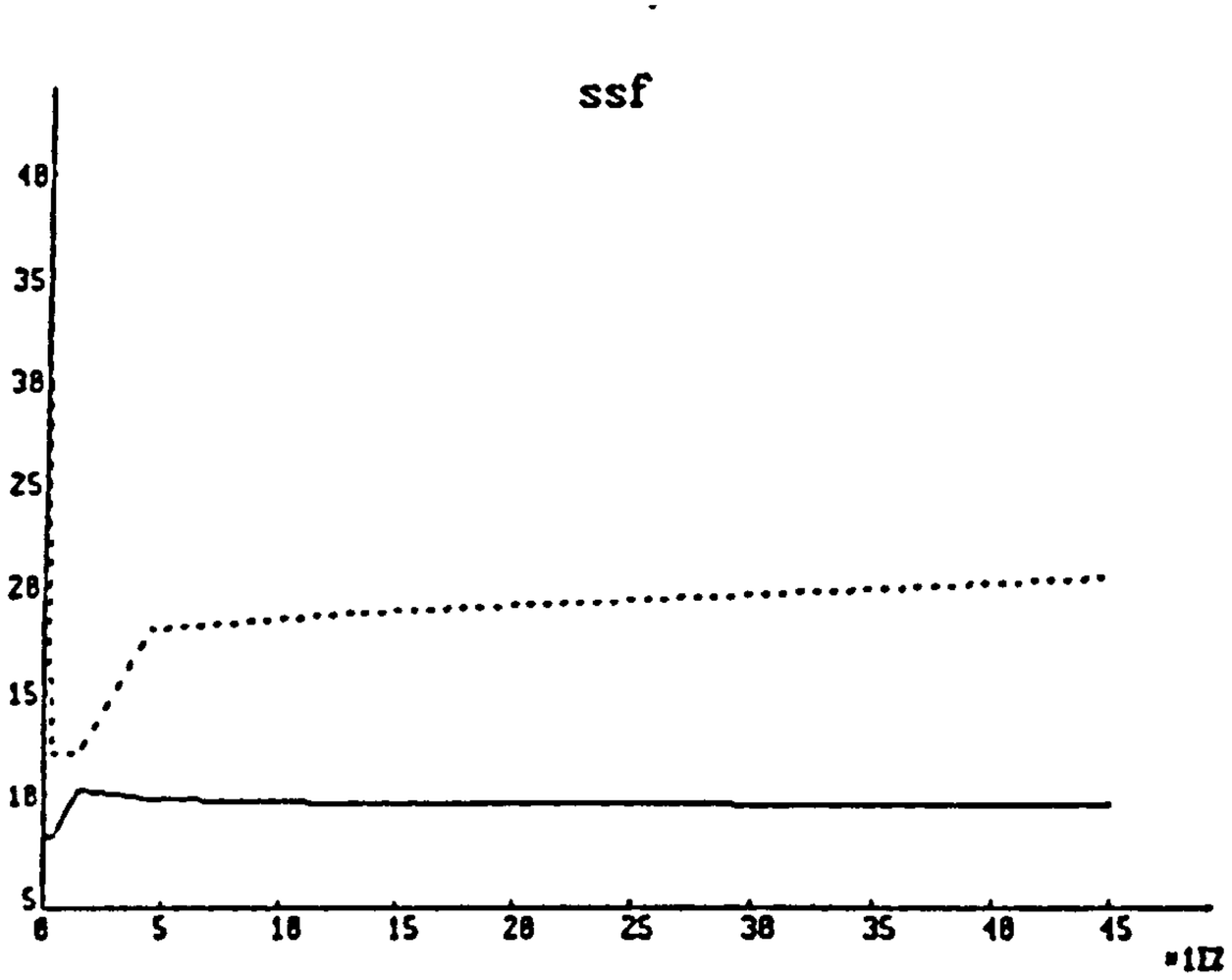

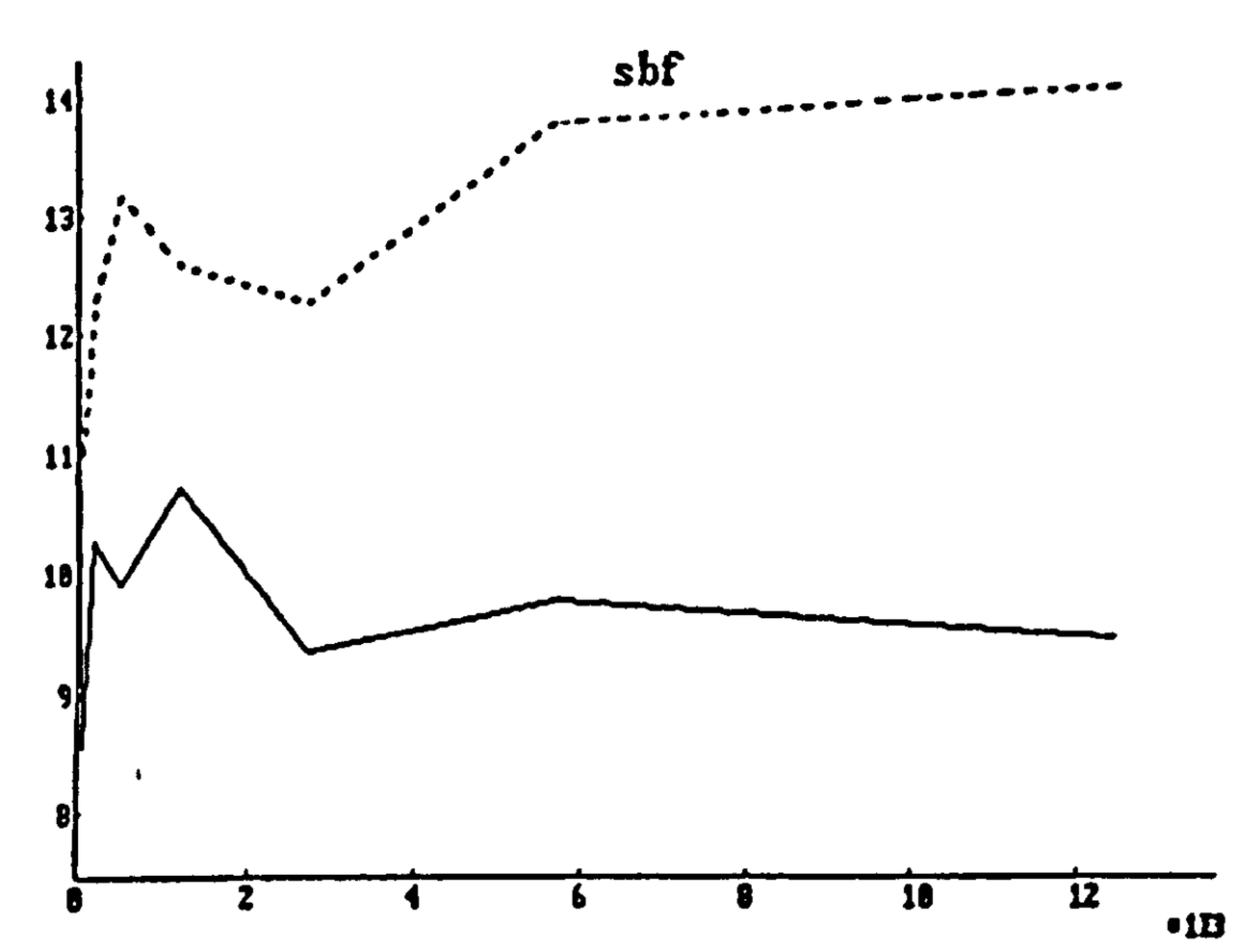

Figure 7.18 Percentage of zero slope against sliding distance. ——— Ring .....Pin.

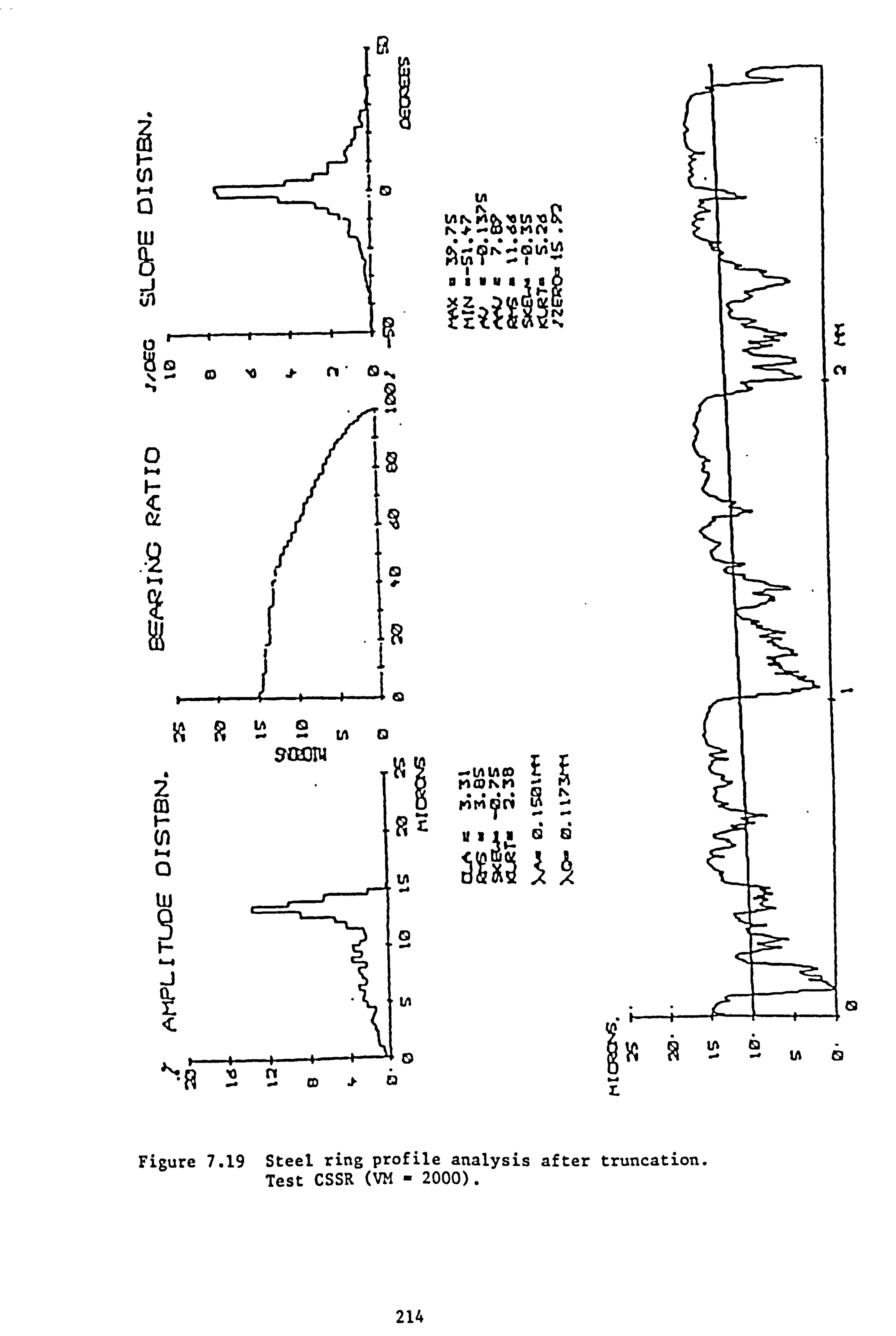

Figure 7.19 Steel ring profile analysis after truncation.
Test CSSR (VM = 2000).

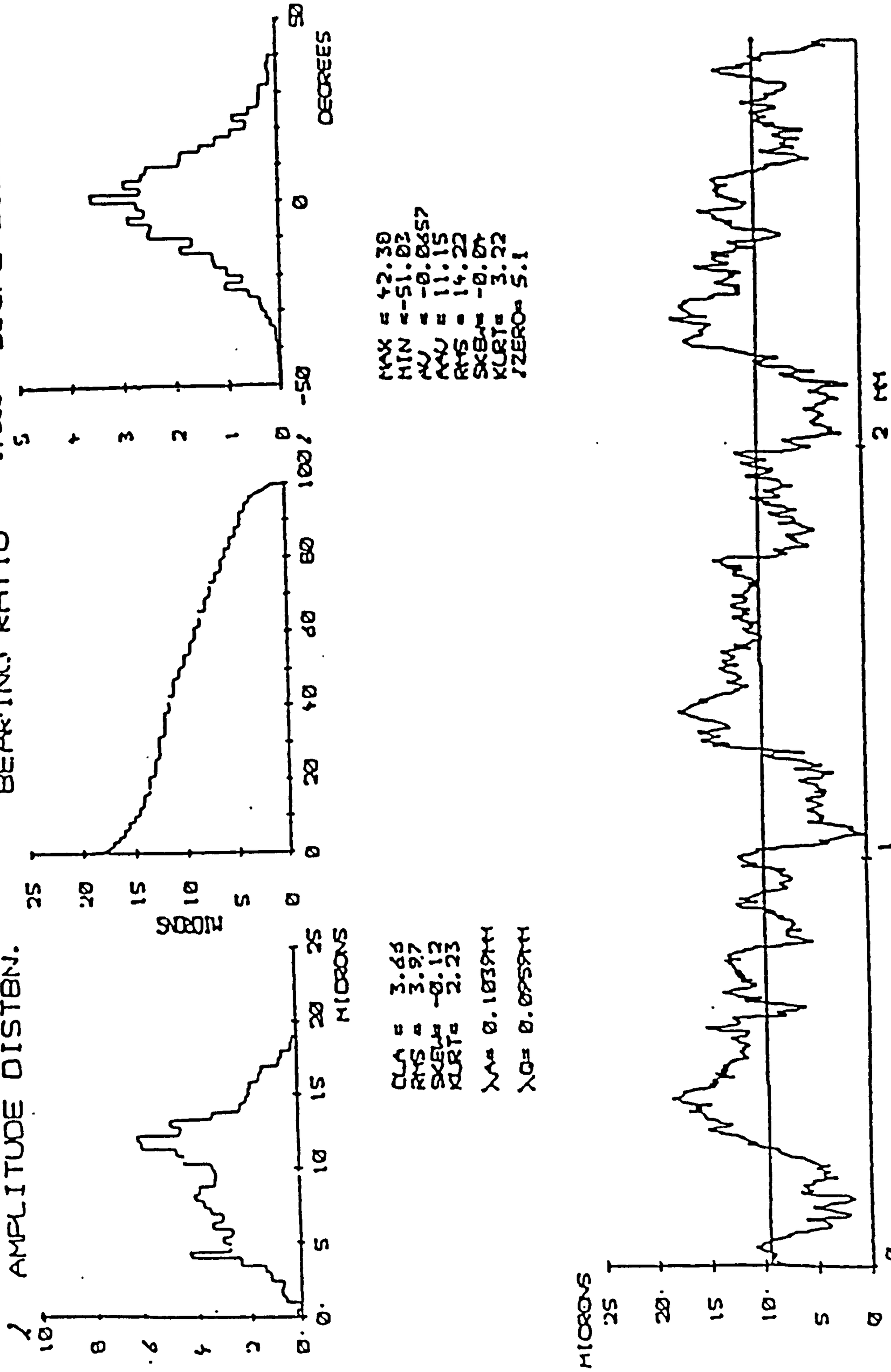

Figure 7.20 Steel ring profile analysis before truncation.
Test CSSR (VM = 2000).

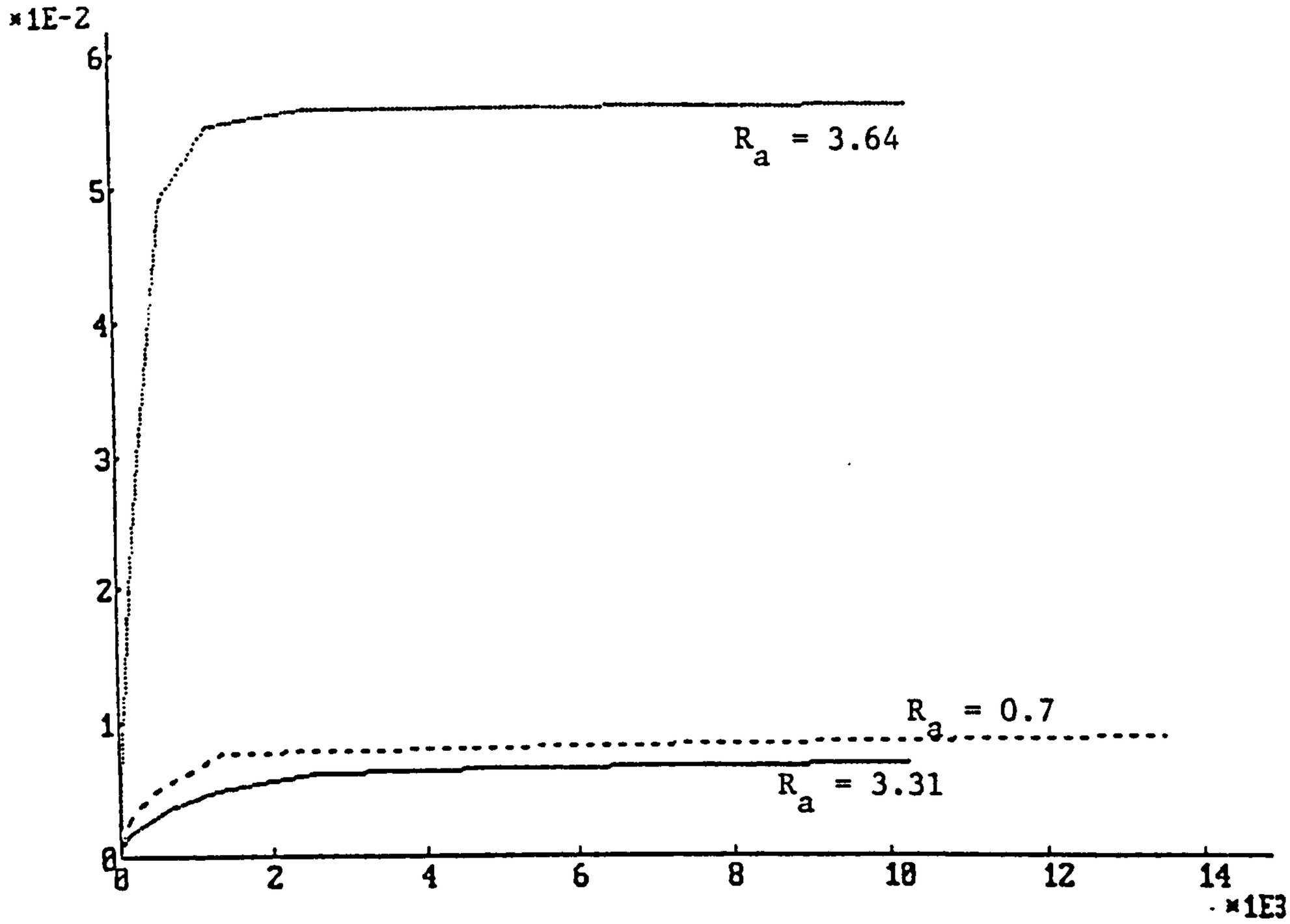

Figure 7.21 Wear volume against sliding distance for tests.
——— CSSR ------SSF ——.—SSR

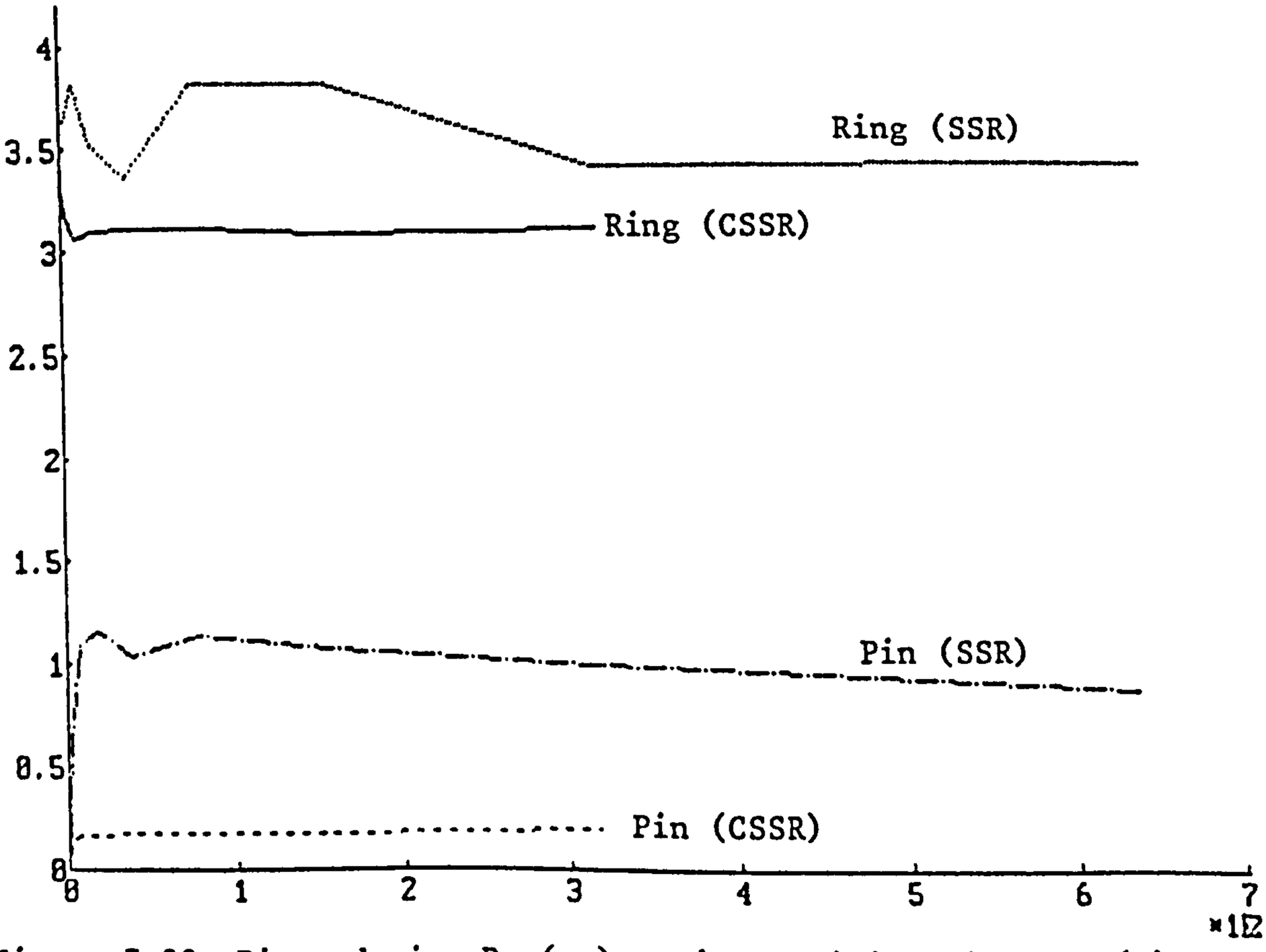

Figure 7.22 Pin and ring R_a (μm) against sliding distance (m) for tests CSSR and SSR.

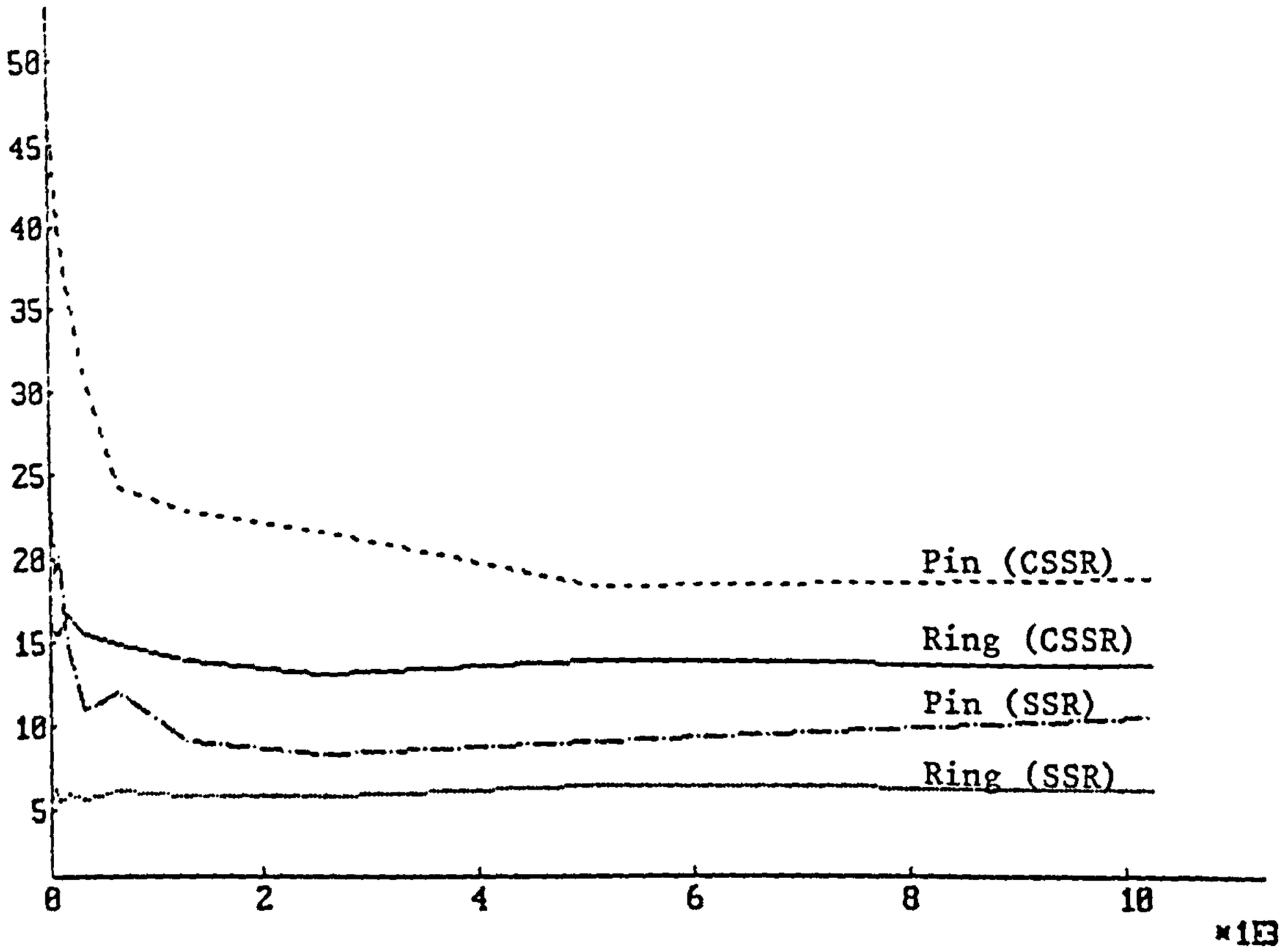

Figure 7.23 Percentage zero slope against sliding distance for tests CSSR and SSR.

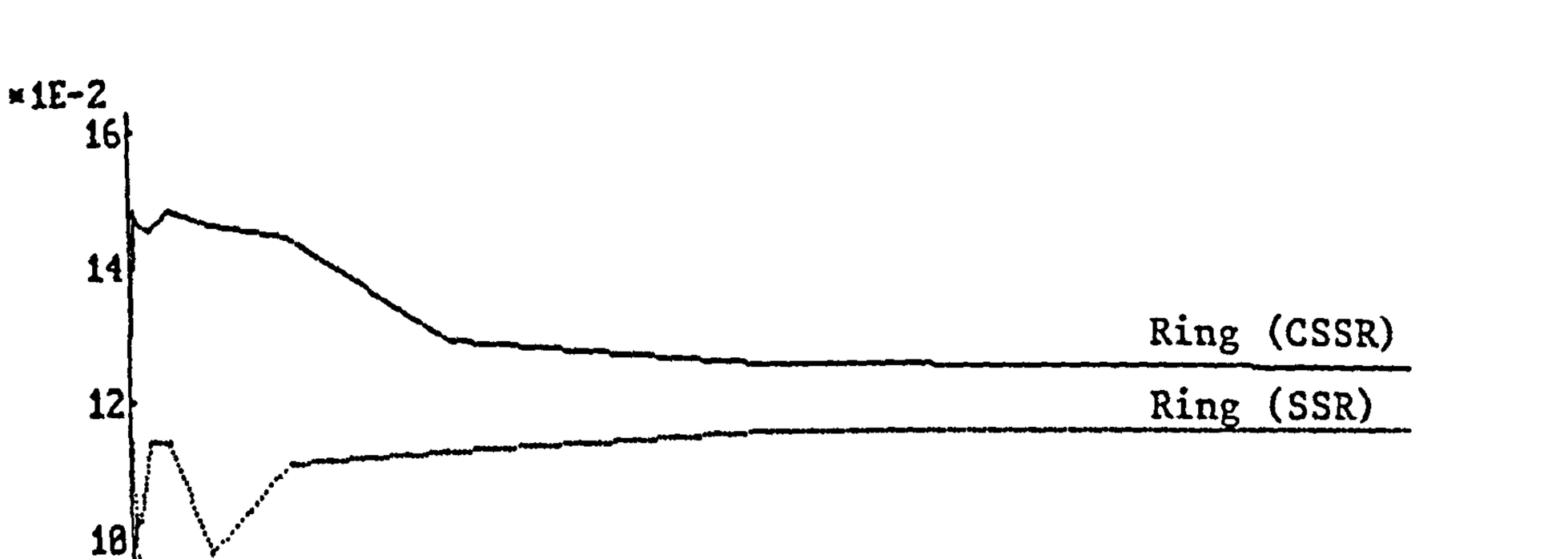

Figure 7.24 Average wavelength (mm) against sliding distance for tests CSSR and SSR.

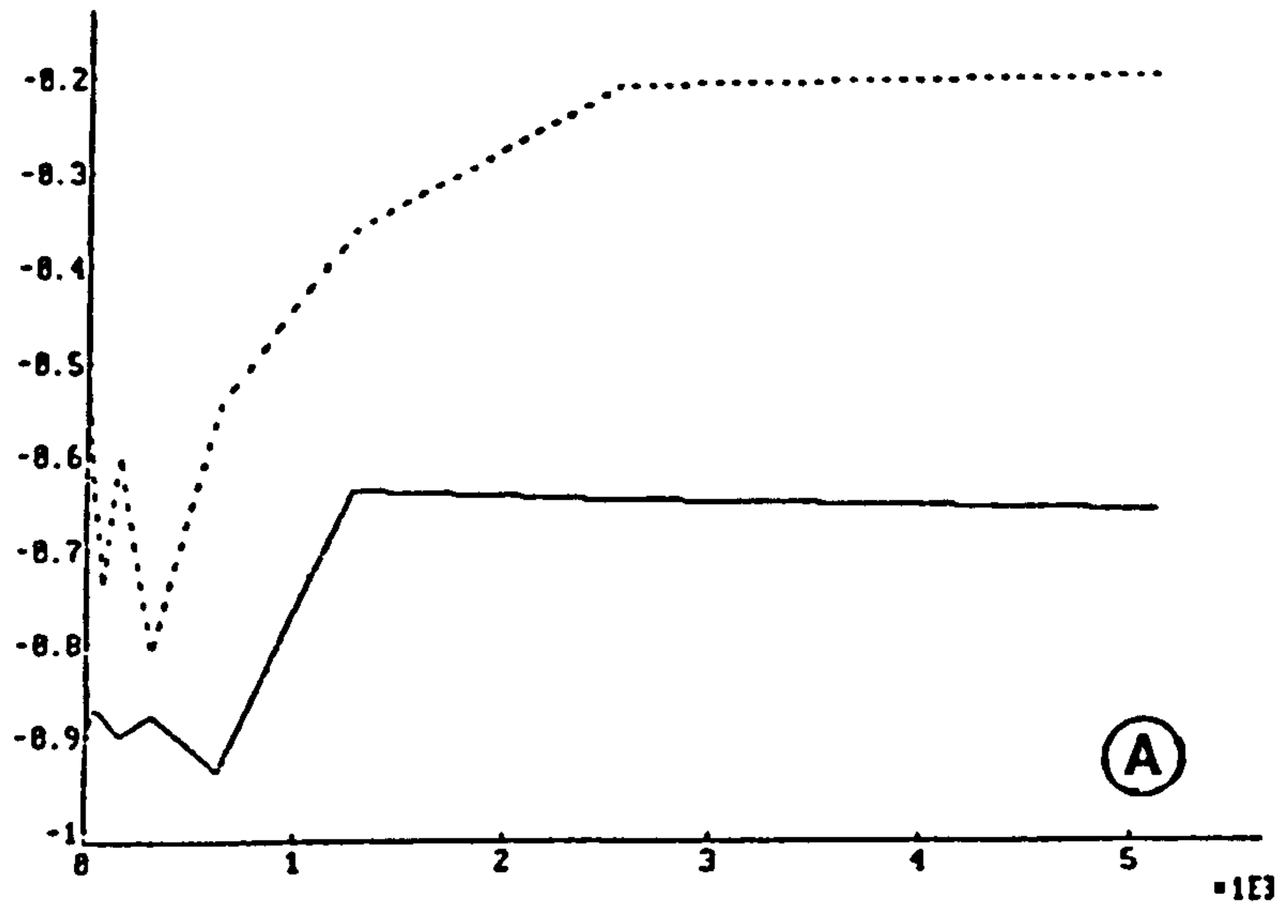

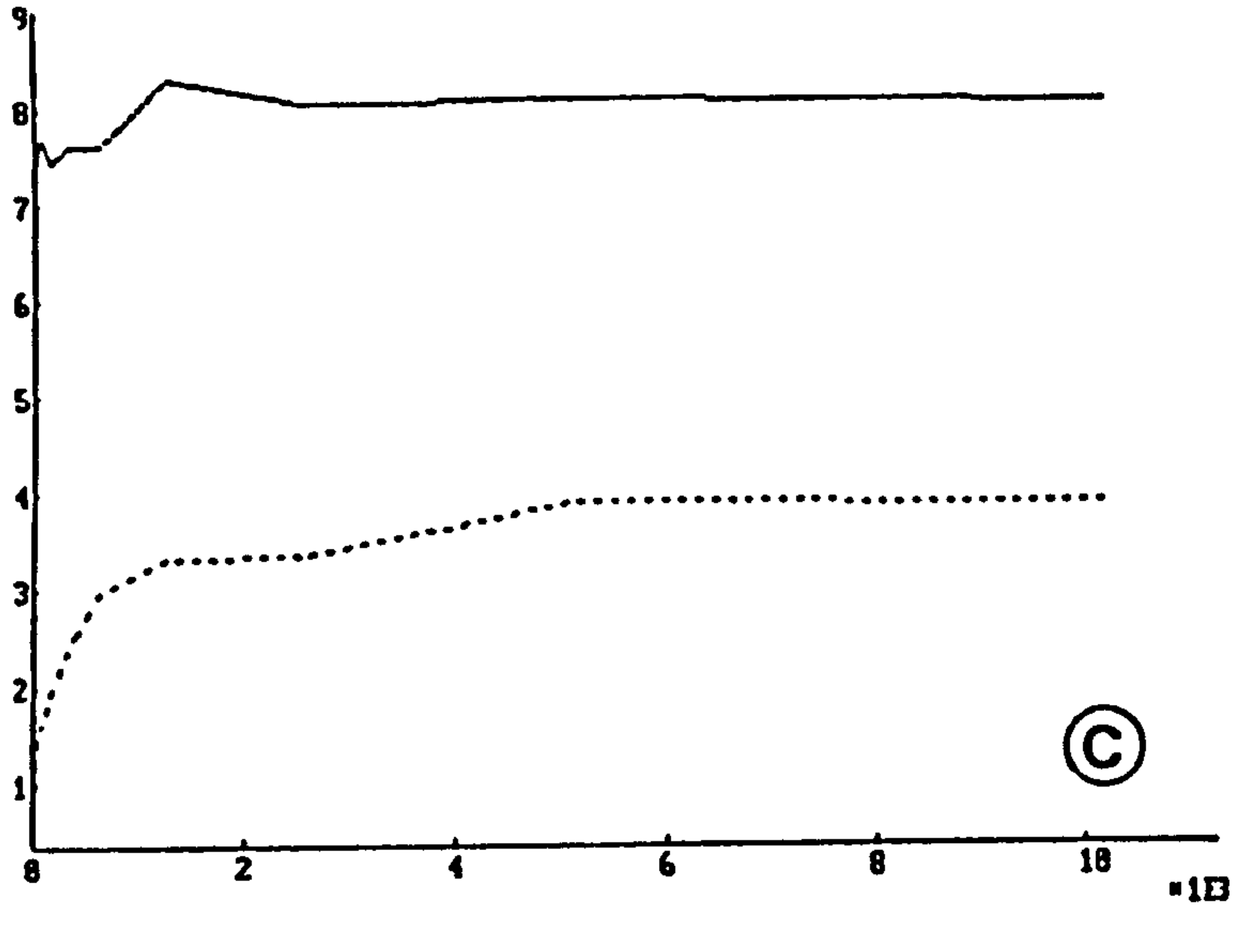

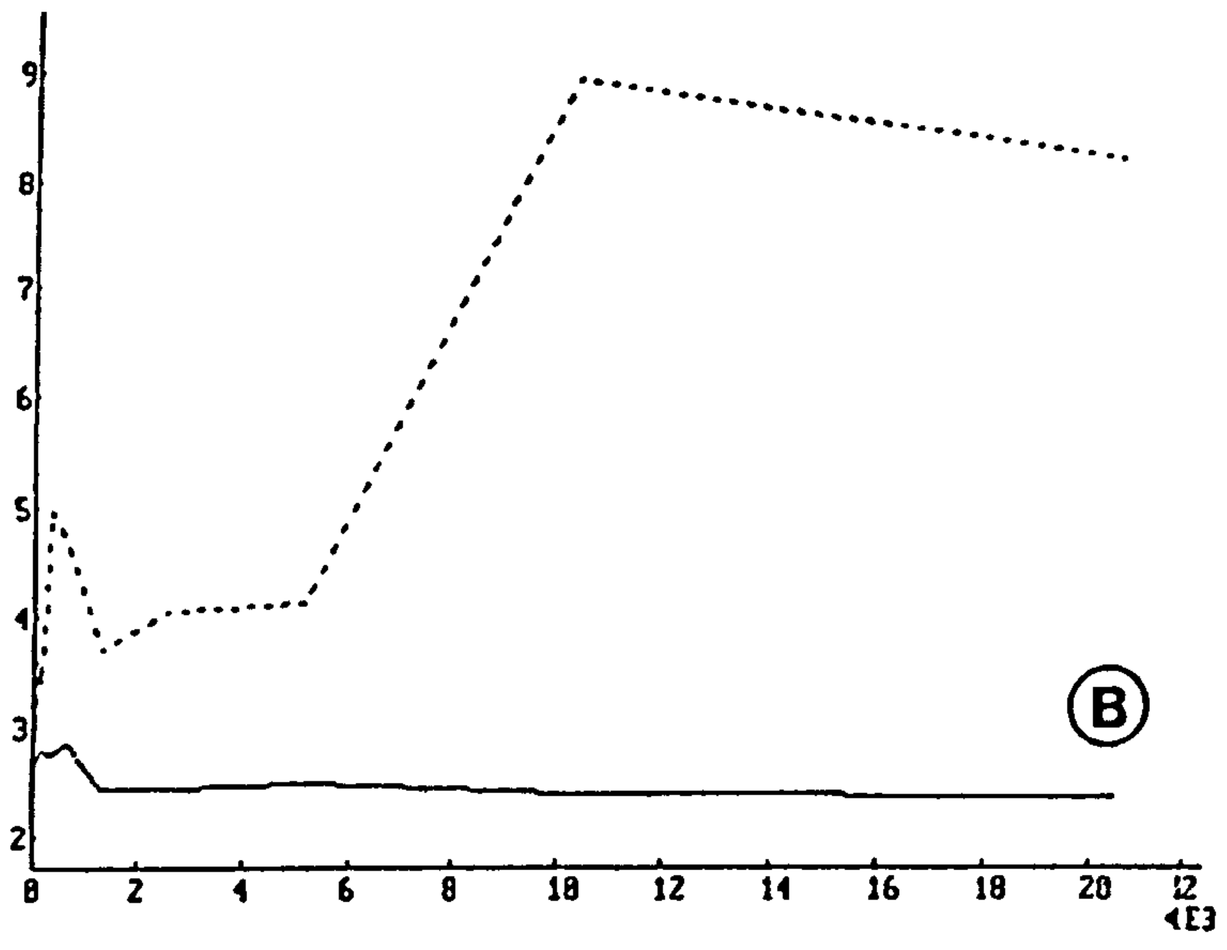

Figure 7.25 (A) Skewness, (B) Kurtosis parameters for pin and ring profile amplitude distributions. Test CSSR.

(C) Average slope of pin and ring profiles against sliding distance. Test CSSR.

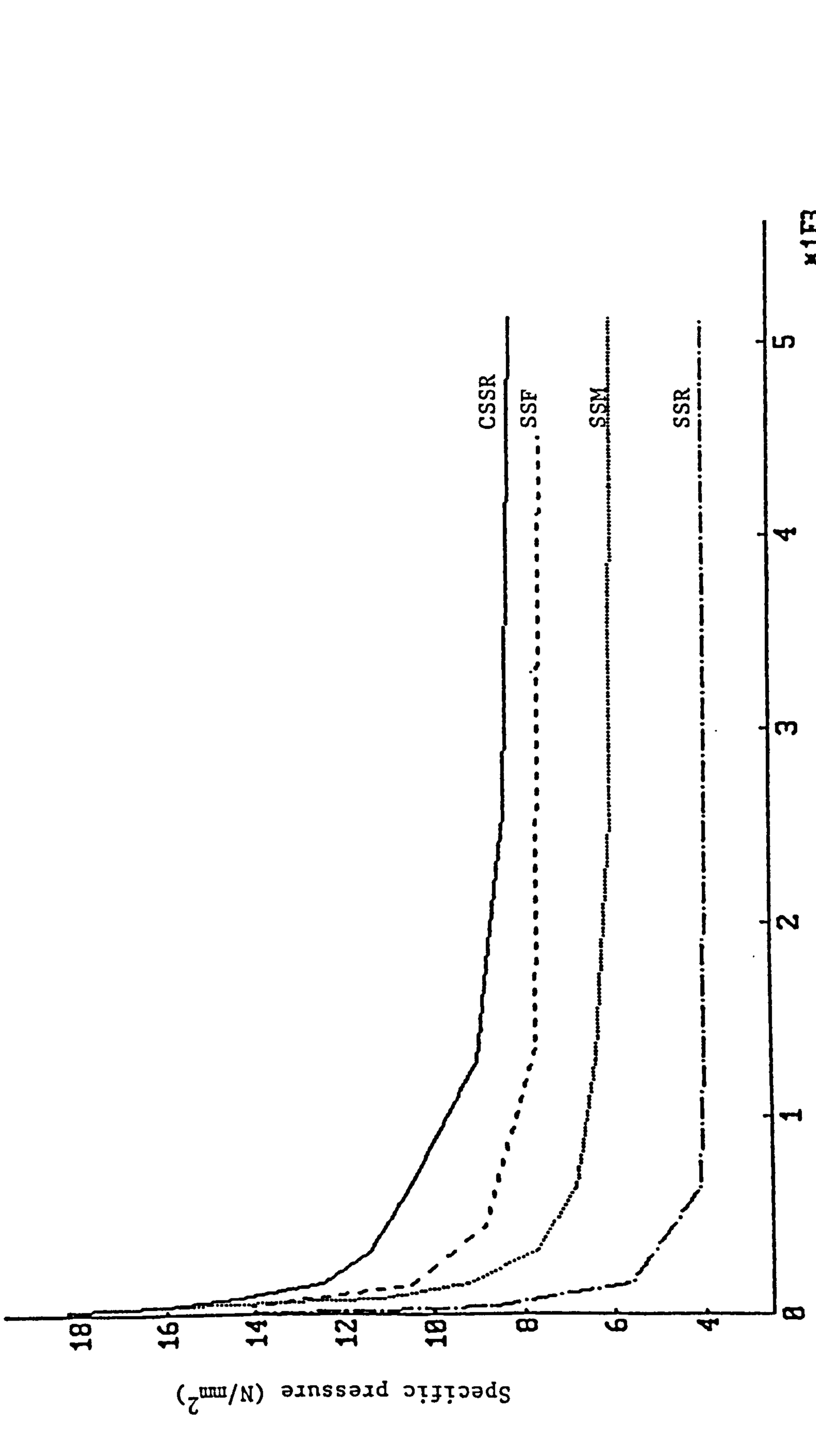

Figure 7.26 Specific pressure as a function of sliding distance for a range of ring surface finishes of the SS test combination.

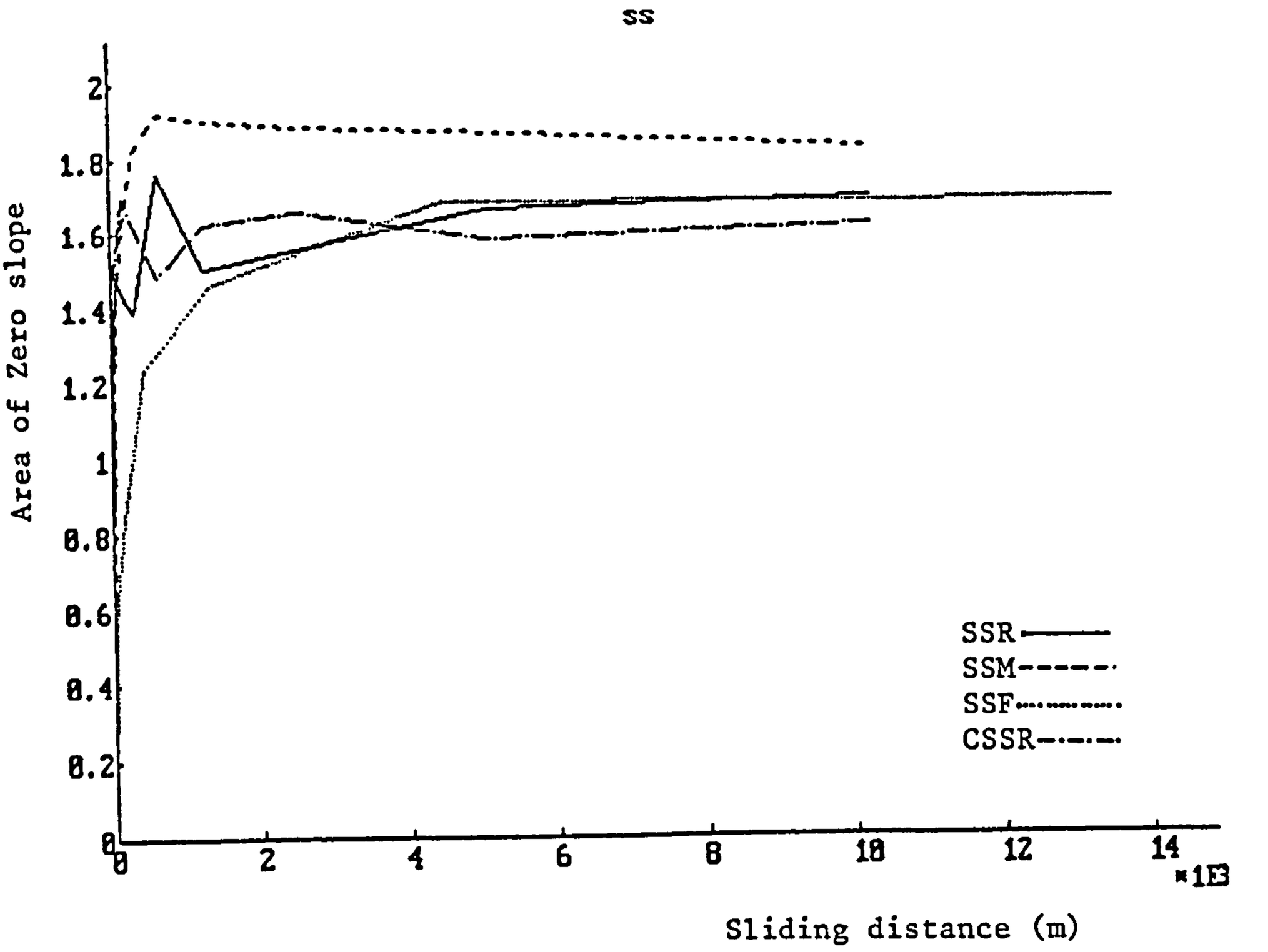

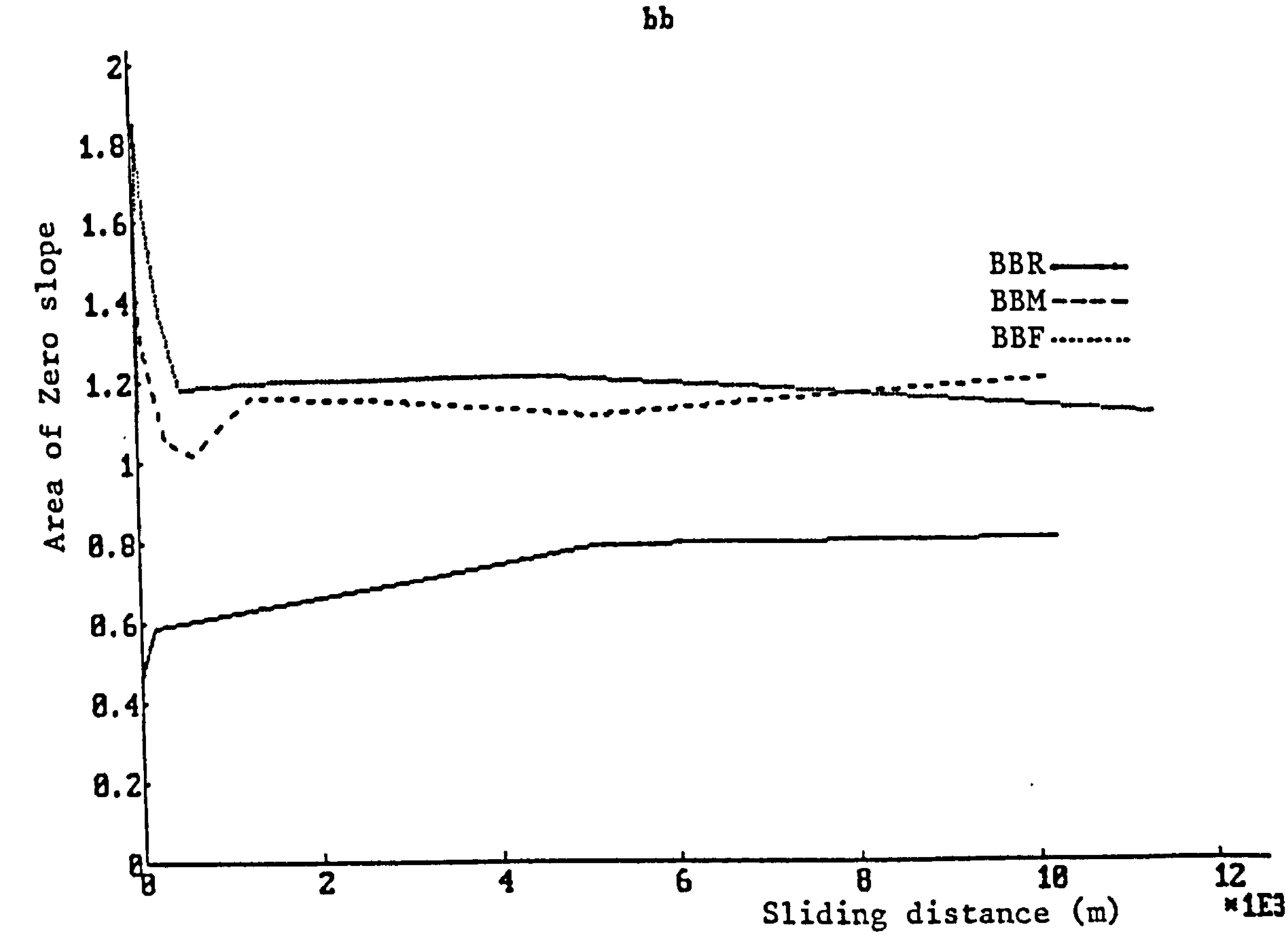

Figure 7.27 Area of zero slope as function of sliding distance (m) for SS and BB test combinations.

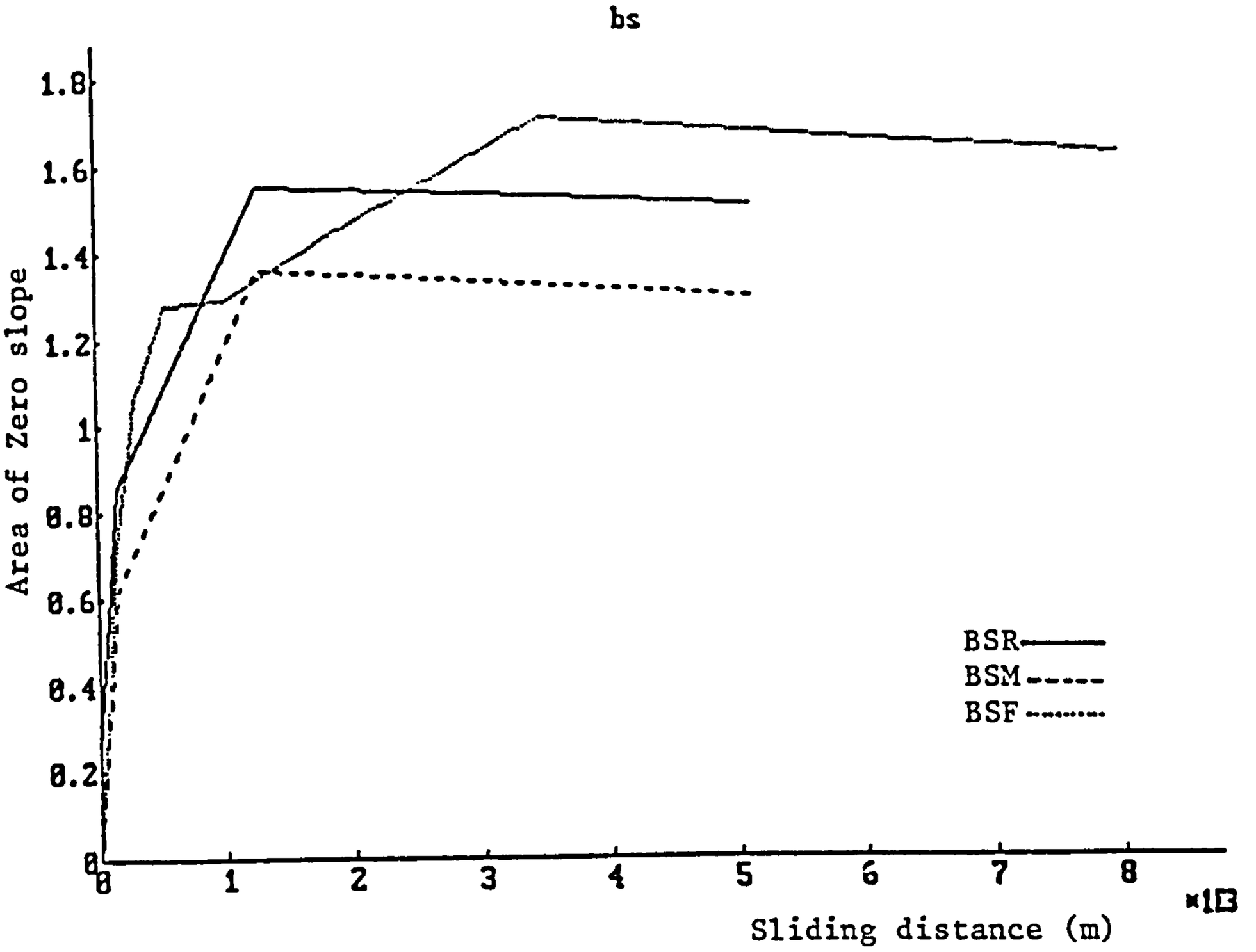

Figure 7.28 Area of zero slope as a function of sliding distance (m) for BS and SB test combinations.

CHAPTER EIGHT

LEVELLING

Chapter 8 - Levelling

8.1 Introduction

In many metal finishing processes, particularly electroplating, the initial surface preparation involves mechanical polishing using progressively finer abrasives. The amount of polishing can be reduced, with consequent economic advantages, by utilising the fact that during electroplating there is frequently an improvement in the surface finish of the workpiece. Mayer (1935, 36) was the first to report on this phenomenon which is now known as levelling. By levelling is meant a decrease in the initial surface roughness of a part through deposition of the electrolytic coating. Recently reported work has shown that the effectiveness of the levelling process is a function of workpiece surface topography as well as plating conditions, Buttery and Hamed (1979). The characteristics of the surface have a marked influence on the changes produced by electroplating.

Levelling effects arise from two fundamental mechanisms (i) geometric levelling and (ii) true levelling. Assessment of percentage of levelling using surface profilometry (R_a) is well established, Denis and Such (1972). This work concentrates on the mathematical modelling of progressive formation of a surface by electroplating and the influence of the initial surface characteristics on the levelling effect. It should be emphasized that the computer modelling described in this work is based on geometric changes rather than chemical processes which have been studied by Oldfield (1973).

8.2 Electroplating

Electroplating is a widely used metal finishing process which changes the surface topography of the workpiece by addition of material at different rates at the peaks to the valleys, giving a progressive improvement in surface finish. Other applications of electroplating are decorative and resistance to wear, corrosion and heat. Electroplating is used to provide a variety of special surface effects, these include:

- low coefficient of friction (chromium).
- high electrical conductivity (silver).
- solderability as in tin or lead alloy.
- suitability in contact with food stuff (tin).

Important commercial deposits are nickel, chromium, cadmium, gold, silver, zinc, copper and alloy deposits. Among the alloys which are electrodeposited on a commercial scale are brass (copper and zinc), bronze (copper and tin) and tin alloys as tin-lead, tin-nickel and tin-zinc. Nickel is the most important commercial deposit having wide industrial applications.

In general, the plating thickness is not uniform over the part serving as cathode. The local thickness differences depends on a large number of factors, and are more pronounced when the profile of the part is irregular. Sometimes no noticeable deposition takes place in recesses, the interior of tubes, etc. The term "throwing power" is used to denote the local thickness differences in electrolytic coating on an object. The throwing power of an electrolyte bath is good when the distribution of the deposite is uniform, Raub and Muller (1967). This is particularly important in view of the minimum plating

thickness required at the critical points of the part. The critical points are those which are subject to particularly intense mechanical or chemical stresses during use or which are particularly important for the functioning of the part. "Microthrowing power" is given by the difference in deposit thickness at two particular points of a microprofile (grooves and surface or the peaks). As the transition from the "macro-" to the micro-profile is continuous, it is important to know the factors which determine the microthrowing power and those which are important in larger scale "macrothrowing power". The cause of the macroscopic variation is the "primary current" distribution. Inadequate convection at the microlevel, however, can give rise to effective differences in the thickness of the cathodic diffusion layer within the range of the microthrowing power. A primary current distribution does not occur within the range of microthrowing power. Microthrowing power, in contrast to the behaviour of macrothrowing power, is improved in the stirred electrolyte.

8.3 Levelling Definitions

Levelling is a decrease in the initial surface roughness of a part through deposition of the electrolytic coating. The microscopic profile of a surface is levelled by an electrodeposit when the coating thickness in the recesses of the profile is greater than the coating thickness on the flat surface (or peaks). This effect can arise in two ways.

1) Geometrical levelling: when a uniform layer is applied to the whole surface, valleys are gradually filled in as plating proceeds due to purely geometric effects. Groove angle remains constant

throughout the process and levelling is directly proportional to the plating thickness, figure (8.1a). A solution with a good microthrowing power therefore can give some improvement in surface finish even in the absence of true levelling.

2) True Levelling: valleys are filled in preferrentially, but at a more rapid rate than with simple geometric levelling. Groove angle declines at a reducing rate as plating proceeds and the rate of levelling also declines with the plating thickness, figure (8.1b). True levelling is generally more effective than geometric levelling and it has been suggested that it consists of geometric levelling with an additional factor, Buttery et al (1983).

True levelling is brought about by the so called levelling additives or "levellers". Organic compounds, and also certain metal ions, can act as levellers. A characteristics of levelling additives is that they are always incorporated into the electrolytic deposit and that the quantity incorporated decrease with increasing current density.

Several methods are available for assessing the extent to which levelling has been achieved from a given plating solution. Probably the most convenient is surface profilometry; the surface finish (R_a) of the component is determined before and after plating and the results are substituted in the following equation of levelling, Dennis and Such (1972):

$$\% \text{ levelling} = \frac{\text{Original } R_a - \text{Final } R_a}{\text{Original } R_a} \times 100\% \qquad (8.1)$$

Alternatively, the characteristics of plating solution can be assessed by plating specimens containing idealised profiles. For example Foulke and Karados (1956) used gramophone record grooves as microprofiles as did Watson and Edwards (1957). After plating, the specimens were sectioned and micropolished or, alternatively, Talysurf traces are taken at stages throughout the process using the relocation techniques, Buttery et al (1982). The percentage levelling has been calculated using expressions of the form:

$$\text{percentage levelling} = \frac{H_o - H_1}{H_o} \times 100\% \qquad (8.2)$$

or

$$\text{percentage levelling} = \frac{T_N - T_S}{H_o} \times 100\% \qquad (8.3)$$

Where H_o, H_1, T_N and T_S are defined in figure (8.2).

These expressions gives 100% levelling when:

$H_1 = 0$ equation (8.2)

$T_N - T_S = H_o$ equation (8.3)

Nakamura (1961) calculated the levelling of simple surface profiles by means of formula

$$E = \frac{T_n}{H_o + T_S} \qquad (8.4)$$

which also takes the groove depth into account. At 100% levelling $E = 1$.

Alternatively it has been suggested, Buttery et al (1983), that the average slope (Δa) of the surface could give a more

meaningful indication of levelling/smoothing since the process seeks to produce a smooth surface rather than a geometrically flat surface. Percentage levelling being calculated as:

$$\text{percentage Levelling/Smoothing} = \frac{\text{Original } \Delta_a - \text{Final } \Delta_a}{\text{Original } \Delta_a} \times 100\% \qquad (8.5)$$

8.4 Modelling

8.4.1 Geometric Levelling

With geometric levelling the whole surface is coated to a uniform thickness T_S, figure (8.3). At the bottom of the groove and at any point on the slope the vertical thickness through the plating T_x is given by

$$T_X = \frac{T_S}{\text{Cos}\theta} \qquad (8.6)$$

Buttery and Hemmaty (1986). Obviously with increasing values of θ (sharper scratches) T_X increases and levelling is more rapid. If $\theta = 0$ (flat surface) $T_X = T_S$.

At 100% levelling

$$T_X = T_S + H_o \qquad (8.7)$$

Combining (8.6) and (8.7) gives T_S for 100% levelling:

$$T_S = \frac{H_o}{\frac{1}{\text{Cos}\theta} - 1} \qquad (8.8)$$

This equation demonstrates the profound influence which surface characteristics exert on levelling process. Levelling is achieved purely due to geometrical effects.

Using equations (8.6) and (8.3) computer programmes were developed to give graphic simulations of geometric levelling and the influence of average slope (Δ_a) and scratch depth on plating thickness at 100% levelling. Using equations (8.6) and (8.8) computer programmes were developed to give graphic simulations of geometric levelling and predict the effect of groove angle and groove depth on levelling performance.

The computer graphics shows (1) that for a given groove angle the deeper the groove the greater the thickness of plating to produce 100% levelling (figure 8.4a) and (2) for the same groove depth reducing groove angle (θ) increases the thickness of plating to give 100% levelling (figure 8.4b). Figure (8.5) shows the same details presented in graphical form for a wide range of conditions. Since the grooves are symmetrical, it can be assumed that the effective R_a of a groove is 0.25 H_o.

An expression for the prediction of R_a can be developed. Assuming successive layers of plating each of thickness T_S are applied the groove depth H_o would change to H_1, H_2, ... H_n. Then

$$R_{a_o} = \frac{H_o}{4}$$

Referring to figure (8.3) we can write

$$H_1 = H_o + T_S - T_X \qquad (8.9)$$

Replacing for T_X from equation (8.6), we have

$$H_1 = H_o + T_S(1 - \frac{1}{Cos\theta})$$

Or since $R_a = 0.25H$

$$R_{a_1} = R_{a_o} + \frac{T_S}{4}(1 - \frac{1}{Cos\theta}) \qquad (8.10)$$

Similarly

$$R_{a_2} = R_{a_1} + \frac{T_S}{4}(1 - \frac{1}{Cos\theta})$$

or

$$R_{a_2} = R_{a_o} + 2 \times \frac{T_S}{4}(1 - \frac{1}{Cos\theta})$$

In general we can write

$$R_{a_n} = R_{a_o} + n \times \frac{T_S}{4}(1 - \frac{1}{Cos\theta}) \qquad (8.11)$$

Or, since total thickness is given by $n\ T_S$, we have, in general

$$R_a = R_{a_o} + \frac{T_S}{4}(1 - \frac{1}{Cos\theta}) \qquad (8.12)$$

If θ remains constant, as it is expected in geometrical levelling, surface roughness will fall linearly with increase in T_S since $1/Cos\theta$ is greater than one. The rate of decline however depends on the scratch angle.

It is important to realise that real surfaces have very low values of average slope (large θ) and to level such surfaces by geometric

levelling will require unrealistic thicknesses of plating. The ideal surface for geometric levelling should have a low value of R_a and a high average slope; for the examples shown in figure (8.6) the surface with the sharper grooves will have the better levelling characteristics. Unfortunately, as a material is progressively polished on finer grades of emery paper, the R_a will fall making levelling easier, but this will be offset by the reduction in average slope (Δ_a) which makes levelling more difficult.

8.4.2 True Levelling

Unlike geometric levelling which can be defined mathematically, true levelling relies on experimental observations for model development. With true levelling, valleys are filled preferrentially at a rate exceeding that for geometric levelling. Mathematical models have been developed to simulate true levelling but the underlying physical mechanism associated with the process have not been explored in this work.

If proportionally more material is added at the bottom of the groove and this mechanism is continued as each successive layer is applied the groove will fill preferentially. The thickness at the bottom of the groove T_n, for example, could be given by

$$T_n = T_S \times m \qquad (8.13)$$

Where m is the plating or levelling coefficient. Figure (8.7) shows examples of the same idealised groove levelled with different values of m for this model. As m increases the groove levels more rapidly.

However, the changes observed with this model show marked deviations from practical results. The results of Elze (1961), figure (8.8), and others show that groove angle changes at a decelerating rate, not accelerating and the rate of levelling declines with plating thickness, whereas the model levels at a constant rate.

The second model which gives better agreement with practical observations assumes that:

1) plating thickness is a function of groove depth H.

2) m is a function of plating layer thickness, but is independent of groove angle and groove depth. Computer simulations were based therefore on an equation of the form:

$$T_X = T_S(1 + mH) \qquad (8.14)$$

Where H is the instantaneous groove depth and m is the plating/levelling coefficient. For successive layers of plating of thickness Ts, we can write :

$$T_{X_1} = T_S(1 + mH_o)$$

$$T_{X_2} = T_S(1 + mH_1)$$

.
.
.
.

$$T_{X_n} = T_S(1 + mH_{n-1}) \qquad (8.15)$$

Total thickness T_X is given by

$$T_X = T_{X_1} + T_{X_2} + \ldots\ldots\ldots + T_{X_n} \qquad (8.16)$$

When H = 0, surface is levelled, $T_X = T_S$. Using a combination of equations (8.15) and (8.16) enables graphic simulations of practically observed results by adjusting to value of m. The value of m is related to the thickness of the successive layers of plating. For example, if the plating thickness is 5μm, the plating/levelling coefficient is written m_5. Different layer thicknesses will give different values of m related by the following expression:

$$m_{10} = \frac{m_5(H_o + H_1)}{2H_o} \qquad (8.17)$$

where

m_{10} = value of m for layers 10μm thickness.

m_5 = value of m for layers 5μm thickness.

H_o = original groove depth.

H = groove depth after the first layer of 5μm thickness.

Figure (8.9) shows a computer simulation of the results reported by Elze; the rate of levelling and the rate of decline in groove angle are in reasonable agreement with the practical results when using the appropriate value of m calculated from the first layer. The computer model was developed to simulate the behaviour of a real surface under the true levelling conditions. The surface was stored in the computer in digital form and each height adjusted as layers of equal thickness were added. Typical results are shown in figure (8.10) for a range of values of m, the R_a and average slope of the surface change in the expected manner. The greater the value of m the more rapidly the surface levels.

8.5 Discussion of the Model

In general, the true levelling coefficient m_n (equation 8.14) for a plating thickness $n.T_S$ is given by

$$m_n = \frac{m_1(H_o + H_1 + . . . + H_{n-1})}{nH_o} \qquad (8.18)$$

where m_1 is the coefficient of a plating with thickness T_S and H_1, H_2, ... are groove depths after successive layers of plating each having a thickness T_S. Consideration of the above equation reveals more information about the nature of the model.

For n = 4 we have

$$m_4 = \frac{m_1(H_o + H_1 + H_2 + H_3)}{4H_o}$$

But m_4 can be written as

$$m_4 = \frac{m_2(H_o + H_2)}{2H_o}$$

Therefore, by equating these two expressions for m_4 we get:

$$\frac{m_1(H_o + H_1 + H_2 + H_3)}{4H_o} = \frac{m_2(H_o + H_2)}{2H_o}$$

or

$$m_2 = \frac{m_1(H_o + H_1 + H_2 + H_3)}{2(H_o + H_2)}$$

m_2 can also be written from equation (8.18) as

$$m_2 = \frac{m_1(H_o + H_1)}{2H_o}$$

Comparing the expressions for m_2 we get:

$$\frac{H_3}{H_2} = \frac{H_1}{H_o} = \ldots\ldots = \text{constant}$$

or

$$\frac{H_3 - H_2}{H_2} = \frac{H_1 - H_o}{H_o} = \ldots\ldots = \frac{\Delta H}{H} = \text{constant}$$

Therefore the model behaves in such a way that for a very small change of the groove height dH brought about by a thickness dT_S of plating we have

$$\frac{dH}{H} = -K \qquad (8.19)$$

Integrating the above equation results in

$$\text{Log}_e H = -KT_S + L$$

or

$$H = Ae^{-KT_s}$$

When $T_S = 0$, $H = H_o$ and therefore:

$$A = H_o$$

And we have:

$$H = H_o \, e^{-KT_S} \tag{8.20}$$

and

$$T_n = T_S + H_o \, (1 - e^{-KT_S}) \tag{8.21}$$

For an idealised scratch R_a can be written as

$$R_a = R_{a_o} \, e^{-KT_S} \tag{8.22}$$

Where K is a constant. The model, therefore, predicts a decaying rate of levelling and theoretically only at $T_S = \infty$ gives 100% levelling. This is to be expected since the levelling process by definition contradicts itself; levelling mechanism is such that it covers valleys more than peaks and by doing so the valleys are less and less distinct from the rest of the surface and therefore there is less ground for levelling. This observation has been confirmed by experiment. Figure (8.11) shows the changes in R_a versus plating thickness with geometric and true levelling for an idealised scratch, Buttery and Hamed (1979). The rate of improvement in surface finish for true levelling can be seen to fall as plating continues; the levelling models for geometric levelling, equation (8.12) and true levelling, equation (8.22) are also shown in this figure.

The relation between K and m coefficients is made clear by referring to figure (8.2).

$$T_n + H = H_o + T_S$$

Replacing for T_n from equation (8.15) results in

$$H = H_o(1 - mT_S)$$

Comparison of the above equation with (8.20) yields:

$$1 - mT_S = e^{-KT_S}$$

But $e^{-KT_S} = 1 - KT_S + \frac{K^2}{2!} T_S^2 - \ldots\ldots\ldots\ldots$

Therefore

$$1 - mT_S = 1 - KT_S + \frac{K^2}{2!} T_S^2 - \ldots\ldots\ldots\ldots \qquad (8.23)$$

The above equation suggests that as $T_S \rightarrow 0$ the coefficient m tends towards K; only at very small values of T_S the two coefficients are identical. While m changes in steps according to the values of T_S, K remains unchanged and does not depend on T_S. The exponential expression for the model, therefore, is a more general and finer representation of true levelling than the special case of equation (8.15).

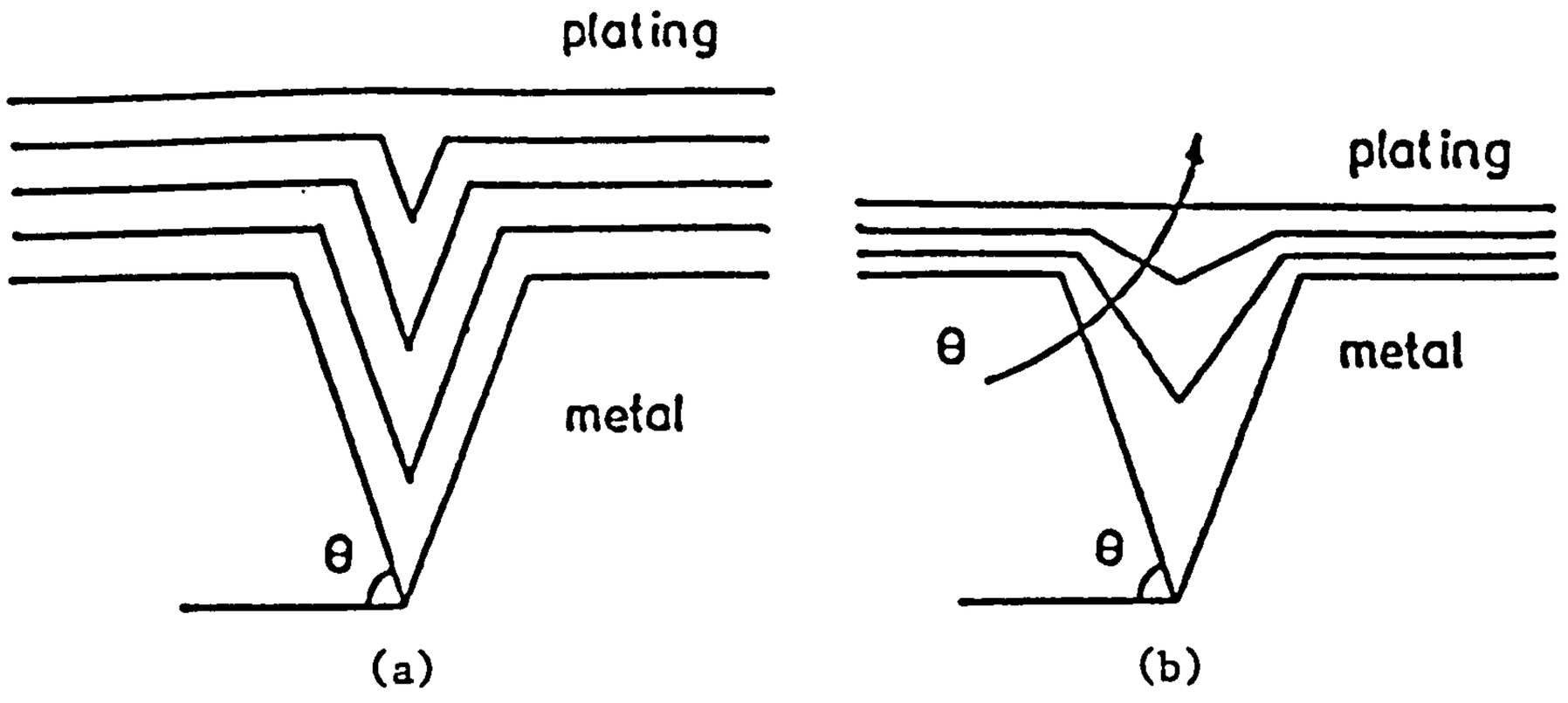

Figure 8.1 Levelling processes.
(a) geometric.
(b) true.

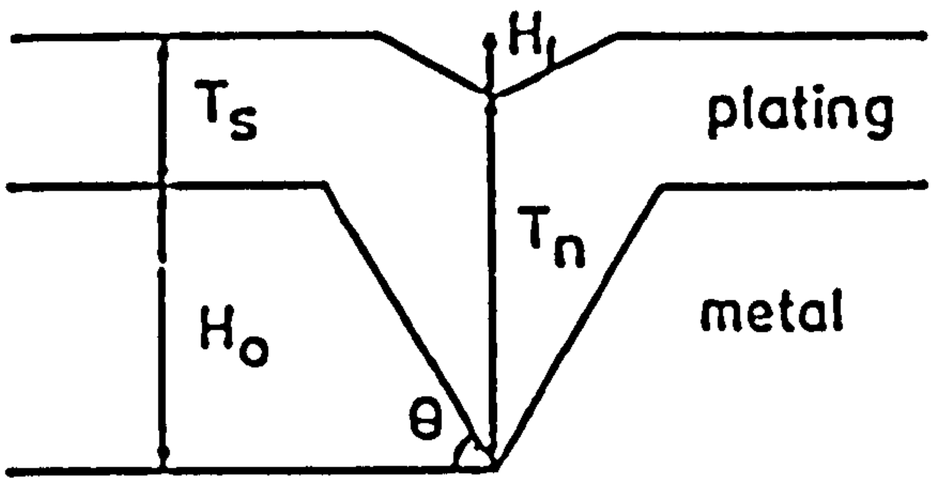

Figure 8.2 Groove details for levelling calculation equations 8.2, 8.3.

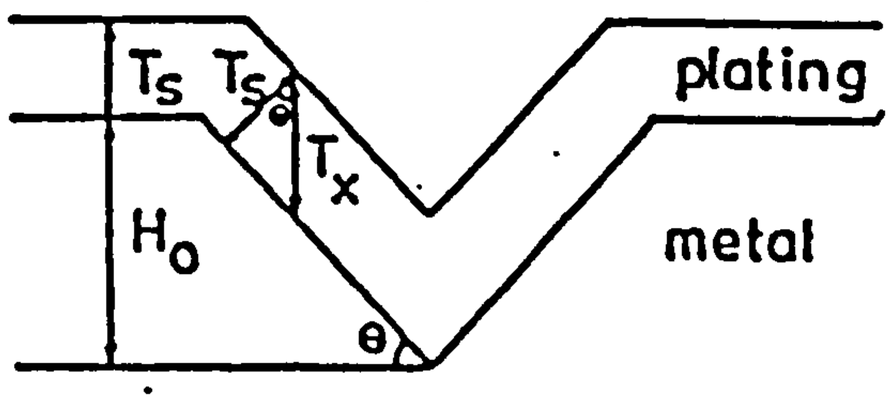

Figure 8.3 Groove details for geometric levelling model.

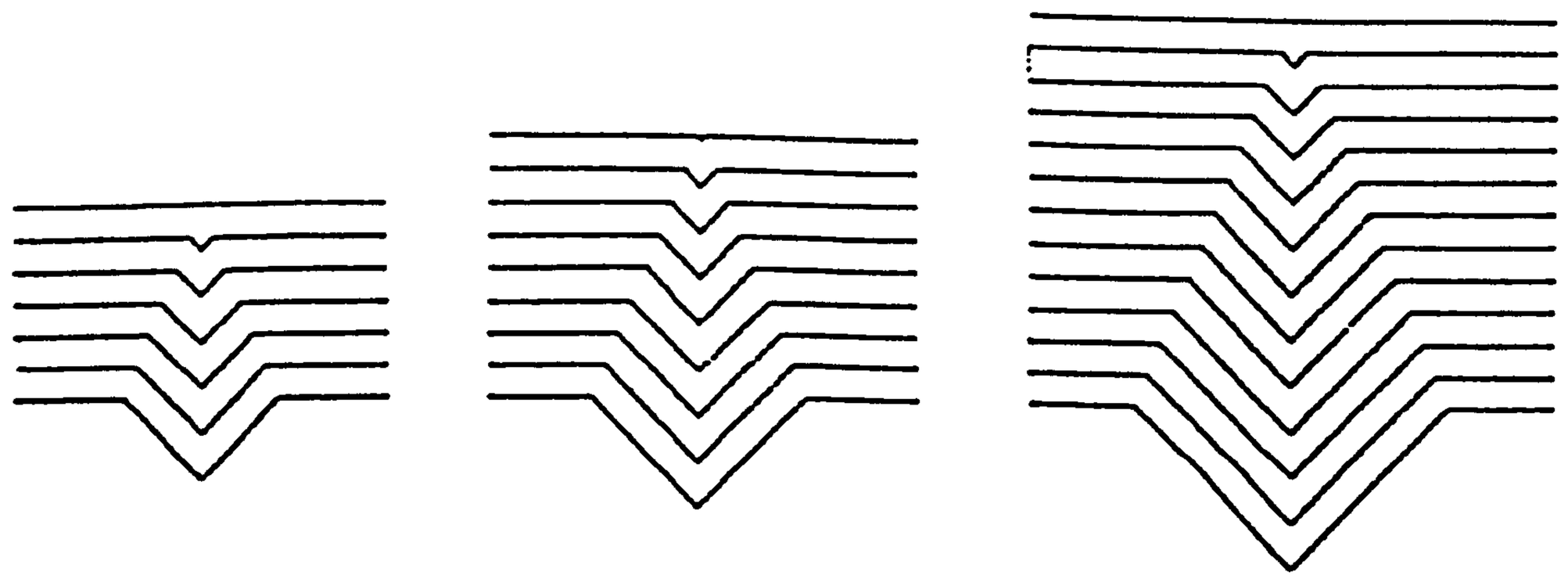

(a) Effect of groove depth on plating thickness for 100% levelling for a 45° groove.

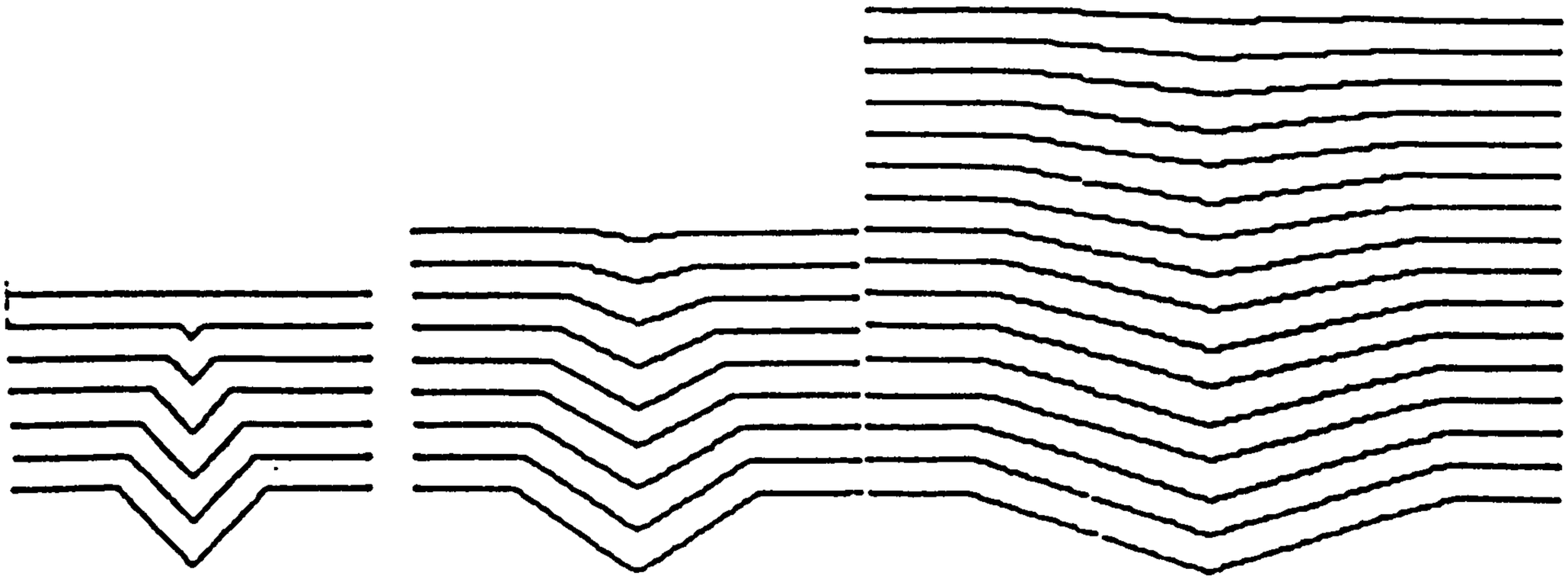

(b) Effect of groove angle on levelling performance.

Figure 8.4 Computer graphic of geometric levelling.

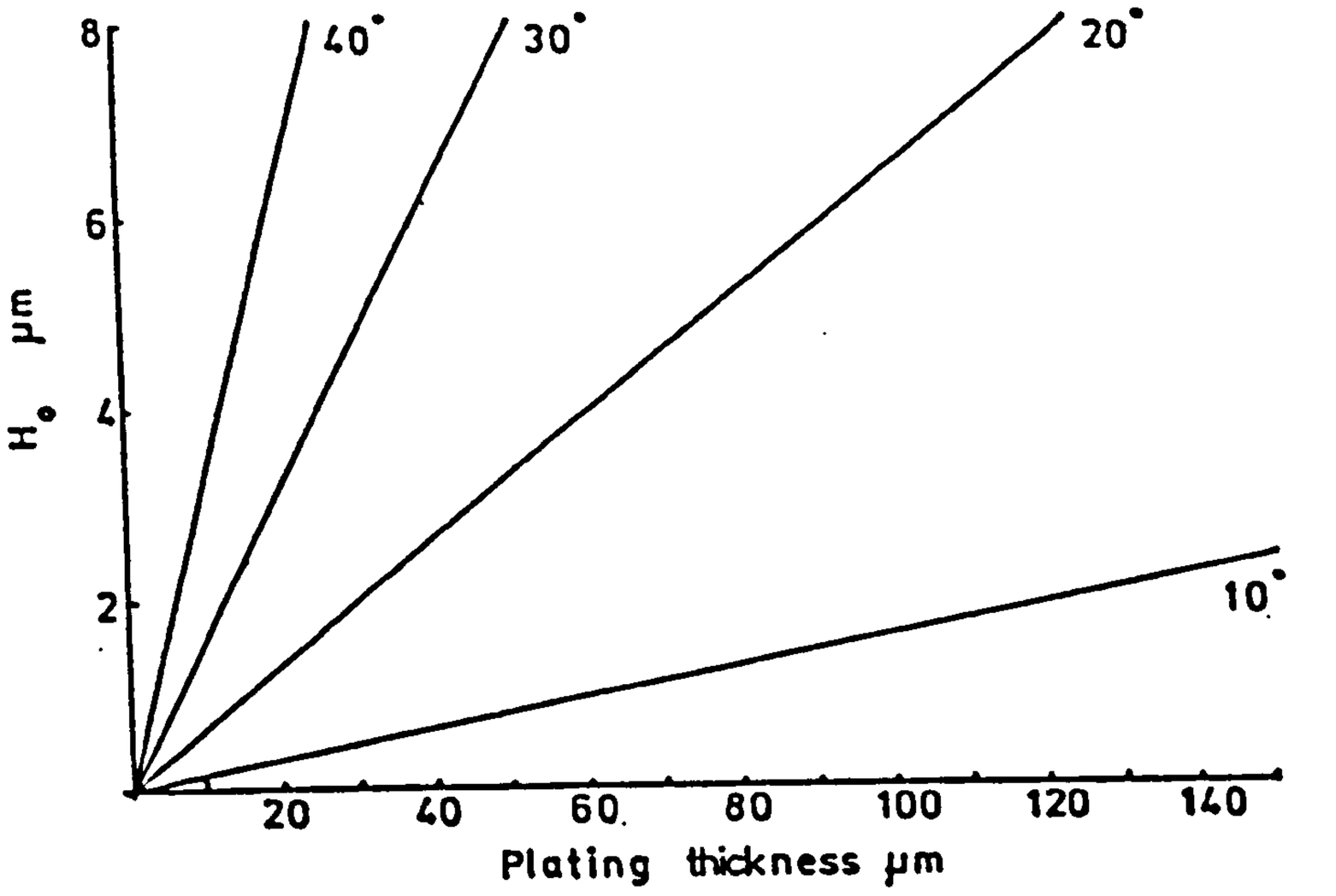

(a)

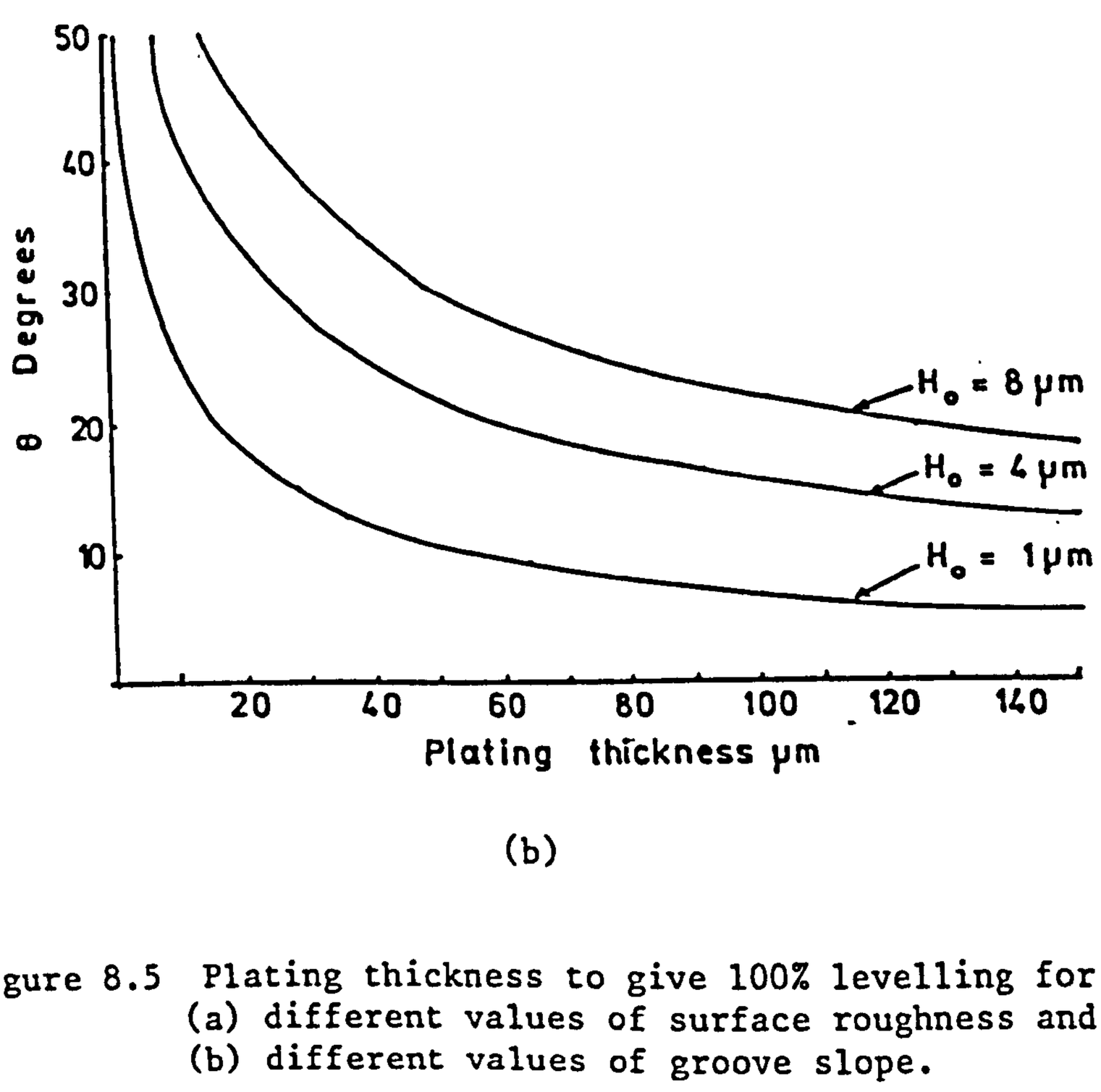

(b)

Figure 8.5 Plating thickness to give 100% levelling for (a) different values of surface roughness and (b) different values of groove slope.

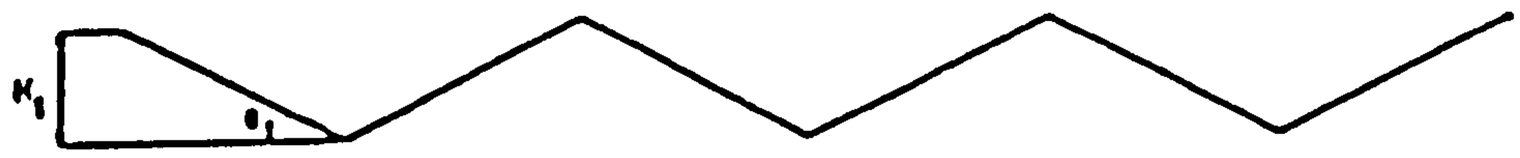

Figure 8.6 Two surfaces having the same value of surface roughness but different surface slopes.

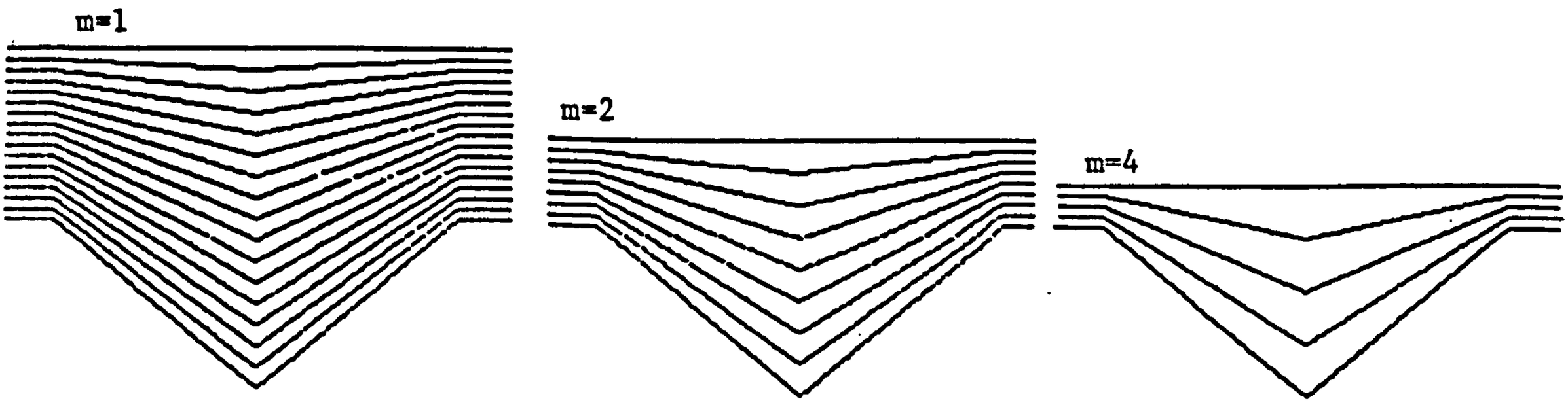

Figure 8.7 100% levelling for a range of values of plating coefficient (m) equation (8.13).

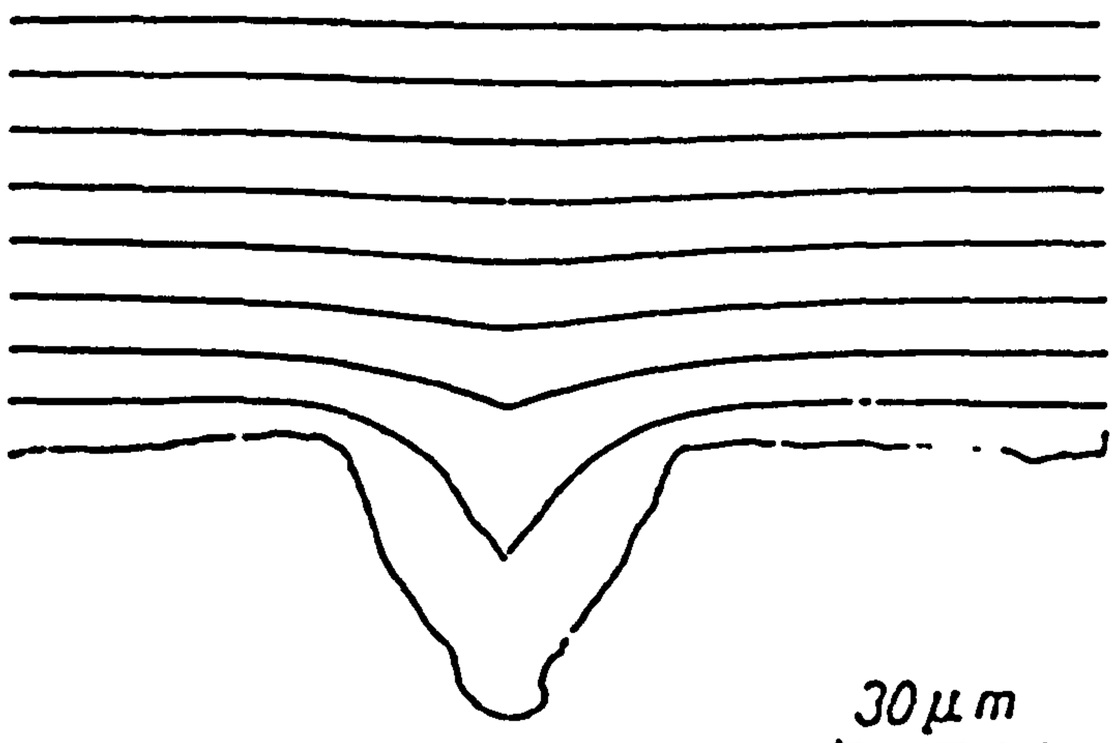

Figure 8.8 Section through plated layer. Elze (1961).

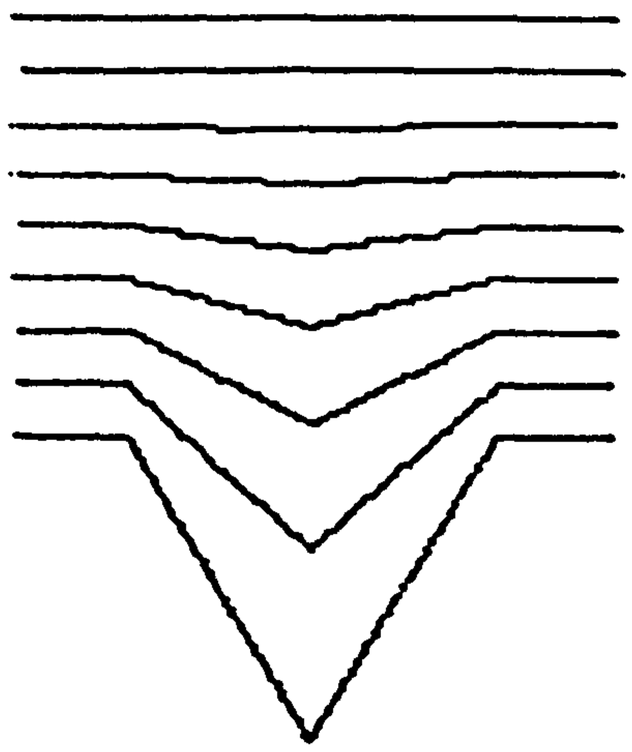

Figure 8.9 Simulation of figure 8.8 using equation (8.14).

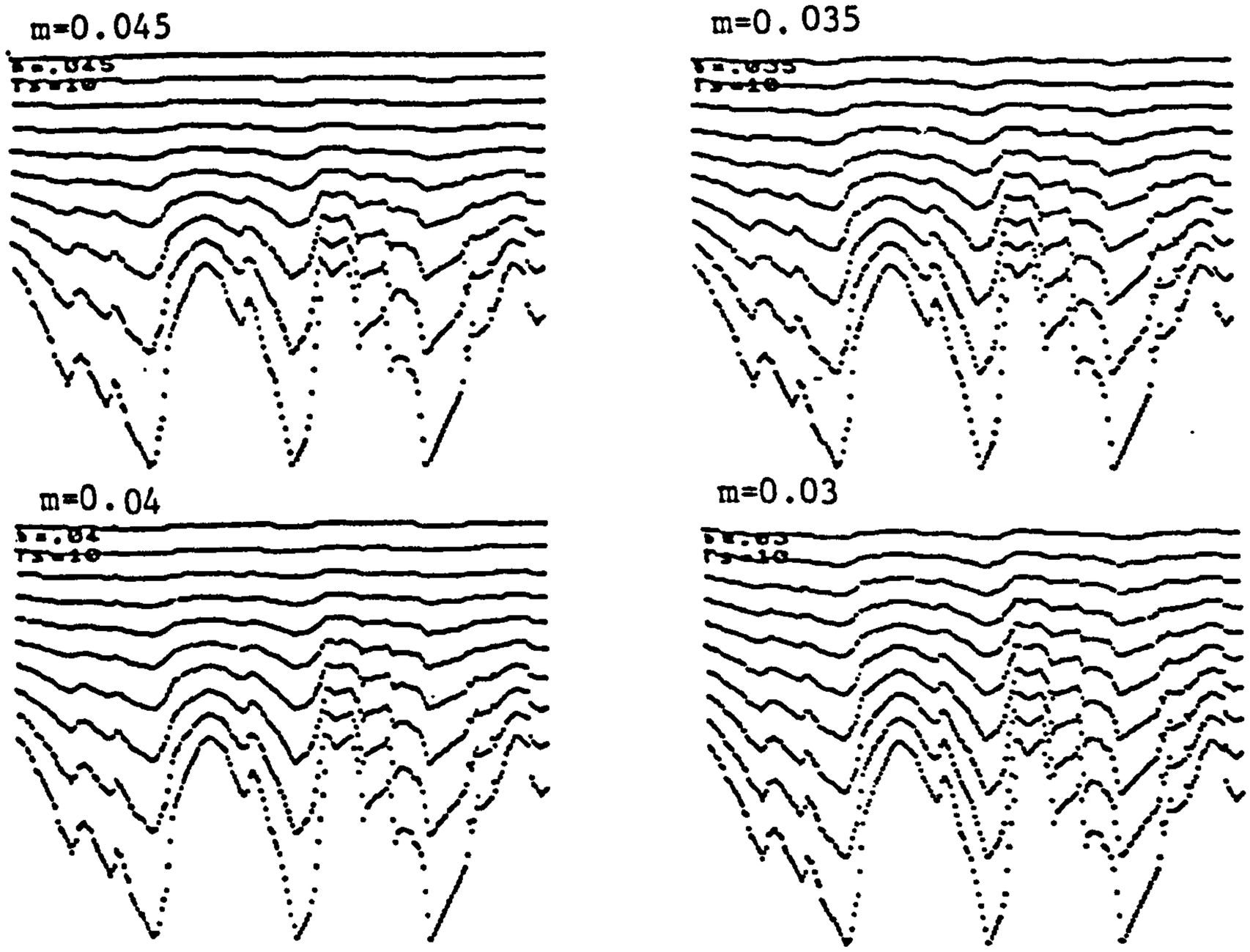

Figure 8.10 Effect of variation in plating/levelling coefficient on the levelling of a real surface.

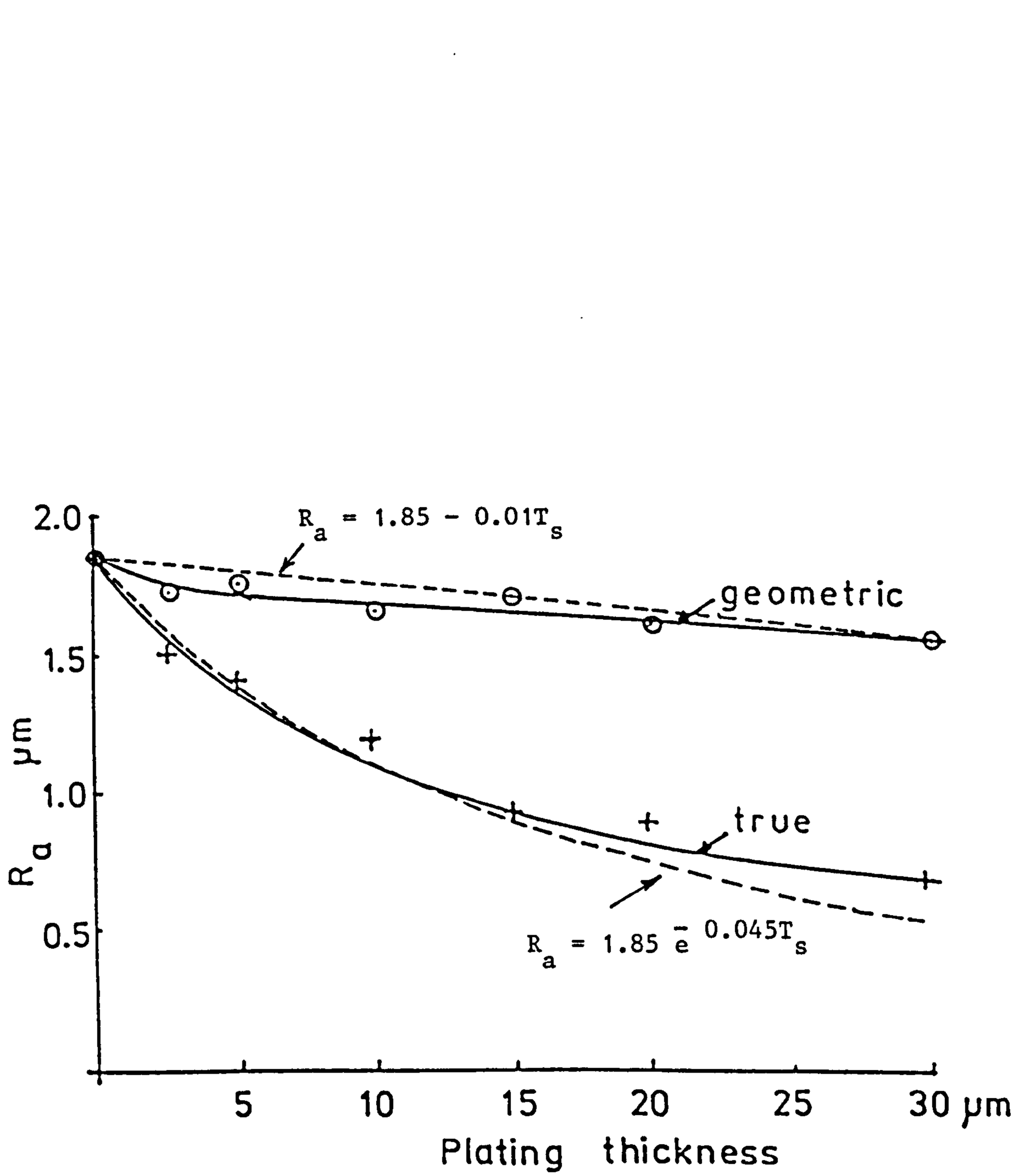

Figure 8.11 Changes in R_a against plating thickness with geometric and true levelling (Buttery and Hamed, 1979) and the corresponding predictions by the models equation (8.12) and (8.22).

Experimental ——

Theory - - - - -

CHAPTER NINE

GENERAL DISCUSSION AND CONCLUSIONS

The processes investigated in this work show specific examples of the importance of surface topography in both manufacture and function of precision surfaces. Surface characteristics were used not only to define but also to detect the changes which could occur in these processes. Analytical theories such as that developed in chapter 3 using geometric surface characteristics provide a more exact model of the assumed mechanism of wear and also provide a basis for comparison between theory and experiment. From such comparison the value of the constant factor in the theory can be deduced. The blunt grit model above has been developed based on the conformity of the grit and scratch geometry. This assumes a 100% plastic material and ignores elasticity. In applying the single grit model to practical situation, further assumptions were made. In particular, an arithmetic average was used for the distribution of load on grits and grit heights. Despite these simplifications, considerable improvement in predicting wear rate was achieved compared with the sharp grit model. This prediction emphasises the importance of flat lands formed during the abrasive wear process.

When the wear theory was applied to a grinding situation, a convenient model was obtained to predict the changes in normal grinding force with attricious wheel wear as a function of the material being removed. The close agreement between the theory and the results which were obtained assuming flat lands being the only variable in the model further underlines the significance of this parameter in abrasive processes. An interesting result from the grinding experiments was the observed correlation between

grinding forces and percentage of zero slope obtained at different dressing conditions. Higher values of forces were accompanied by higher percentages of zero slopes. This correlation provides experimental support for using percentage of zero slope to represent blunting of the grits and hence a method of monitoring the condition of the grinding wheel/abrasive paper.

Unlike the force based predictions where the theory requires reliable values of Δ_a surface finish predictions reqiare reliable values of both Δ_a and C and consequently correlation with the experimental data is less satisfactory. It has been shown, Hamed (1977), that the topography of the surface is determined by the shape and the number of a few prominent grits. This suggests that R_a prediction is strongly dependent on the exact statistical distribution of grit heights. A more detailed knowledge of the number of active grits, which is very difficult to measure and its value depends on a number of factors such as dressing, wheel wear and grit depth of cut is also required. The effect of grit blunting on R_a for a single scratch has been shown by the R_a model to be small compared with pile-up, and to reduce with increase in plateaux area. In practice any improvement in R_a by blunting of the grits is always smaller than that for a single scratch due to process effects, such as overlapping of the profiles, ploughing and the likely masking by process noise. It seems therefore that much of the improvement in R_a which was observed at the initial stages of the pin on disc results, is due to levelling of the abrasive paper rather than blunting of the grits which happens at the later stage of the process.

Some recognition for the R_a model and validity of the basic

assumptions in the theory were found, however, when the model was compared with the expression for the maximum chip thickness developed by Marshall and Shaw (1952). By drawing two separate and distinct approaches to grinding together it was shown that two completely different theories which start from different points, converge on the same result. It is significant that both treatments use two parameters which are particularly difficult to measure reliably; namely the width to depth ratio of an average scratch and C the number of grits per unit area. One outcome of this comparison has been the introduction of average slope as a replacement for width to depth ratio. When combining the two techniques it is possible to express R_a in terms of grinding parameters which are entirely controllable. This could be very useful in optimisation of the grinding process, considering most of the time the surface roughness of the product is one of the main concerns.

A number of authors, many of them quoted in this work have emphasised the importance of initial R_a on the history of the running-in wear. It has been suggested, Masoures (1977) for instance, that higher surface roughness results in higher values of wear during the initial transient stage of the wear curve before the completion of running-in. The pin on ring tests carried out to simulate the running-in process showed some support for this view. The results from these tests and in particular the composite test, however, suggests that the importance of R_a in this respect is only relative. It was established that there was not always a one to one relation between R_a and the amount of wear prior to

running-in. Further confirmation for this came from the comparison of the results of some repeated tests. With test SBR, for instance, the initial wear was so high that after a short running distance the wear scar covered the entire width of the pin surface and the test run had to be stopped. Nevertheless, in a series of preliminary tests at identical conditions and using rings of similar R_a, running-in was achieved; wear scar reached a steady value confined within the width of the pin surface. It should be mentioned that in these two series of experiments the rings had been ground to the desired R_a value with no specific dressing procedure being observed. This could result in rings being produced with similar roughness but having different surface characteristics. In the light of the composite test results it is suggested that the percentage of zero slope plays an important role in determining the running-in stage. The Masoures statement can only be true, therefore, in the case of surfaces being produced under exactly similar conditions. Adoption of a different dressing procedure in grinding or the changes which happen during grinding wheel life with attricious wear of the grits, could for instance result in surfaces with similar R_a which behave differently during the running-in stage. This view seems to be supported by the findings of other authors, Bayer and Sirico (1975) for instance found that higher wear could occur with a smooth surface than with a surface of greater roughness. Directional effects of surface roughness were found also to be highly significant in wear tests. Although the area of zero slope has been shown to give satisfactory indication of the running-in stage, care must be taken if this is to be applied to the real situation. For example, since any waviness is automatically

excluded by the nature of the design in the pin on ring tests the area of zero slopes can only be valid as a criteria for running-in in the absence of any waviness.

It appears from these discussions in general that slope distribution and its derivatives in particular average slope and percentage of zero slope are useful parameters which have been highly neglected. They have been shown to provide convenient measures for defining the abrasive process and the functional behaviour of parts during running-in. Geometric levelling was also found to be highly dependent on slope and a complete solution for the process can be obtained using average slope. The conclusions from the computer models are in close agreement with practical observations and show that geometric levelling is ineffective with real surfaces. True levelling, on the other hand, is a more complex process. It appears from the reported data that average slope is not highly important and this form of levelling can be regarded as being mainly a function of groove depth. An exact solution for the process was derived on this basis which shows that the initial form of levelling is greater for deeper grooves, but declines exponentially as plating continues. An important factor in the theory for true levelling is the plating or levelling coefficient which controls the rate of levelling and is a convenient way of defining the performance. Its value can be found experimentally and then used to predict the subsequent behaviour as plating proceeds. When values of plating coefficient determined in this way were used to predict the plating behaviour, some deviation was observed as levelling approached 90-95%; the theory predicting the better

surface. This may mean that the plating coefficient is not independent of groove angle. To define this relationship and further refine the theory, however, will require considerably more experimental data. It is worth mentioning that the models developed to simulate electroplating are equally applicable to any coating process and also to electropolishing by employing the appropriate levelling coefficients.

BIBLIOGRAPHY

Abbot, E.J. and Firestone, F.A. (1933) Specifying surface quality. Mechanical Engineering, 55, 509 - 572.

Abbot, E.J. and Goldschmidt, E. (1937) Surface quality. Mech. Engineering, 59, 813 - 25.

Agullo, J.B. and Pages-Fita, J. (1974) Performance analysis of the stylus technique of surface roughness assessment : A random field approach. Proc. 15th int. Mach. Tool Des. and Res. Conf., 349 - 62, Macmillan, London.

Alden, G.I. (1914) Operation of the grinding wheel in machine grinding. A.S.M.E. Vol. 36, p 451.

Al Salihi, T. (1967) Investigation of surface roughness as a random process in regard to surface formation while grinding. Ph.D. Thesis, University of Birmingham, U.K.

Archard, J.F. (1953) Contact and rubbing of flat surfaces. J. App. phys. Vol. 24, No.8, 981 - 988.

Archard, J.F. and Hirst, W. (1956) The wear of metals under unlubricated conditions. Proc. Roy. Soc. (London), A236, 397 - 410.

Archard, J.F. (1957) Proc. Roy. Soc., A243, 190.

Archard, J.F. and Hirst, W. (1957) An examination of a mild wear process. Proc. Roy. Soc. (London), A238, 515 - 528.

Archard, J.F. (1961) J. Appl. Phys. 32, 1420.

Avient, B.W.E., Goddard, J. and Wilman, H. (1960) An experimental study of friction and wear during abrasive of metals. Proc. Roy. Soc. (London), 258A, 159 - 179.

Backer, W.R., Shaw, M.C. and Marshall, E.R., (1952) A.S.M.E. Vol.74, p.61.

Bayer, R.G. and Sirico, J.L. (1975) The influence of surface roughness on wear. Wear 35, 251 - 260.

Bhateja, C.P. (1971) A computer aided study of the working surface of grinding wheels. Proc. 12th Int.1 M.T.D.R. Conference, Manchester, pp 535 - 541.

Bhateja, C.P. (1974) On the mechanism of the diamond dressing of grinding wheels. Proc. Int. 1 Prod. Eng. Res. Conf., Tokyo, pp 733 - 739.

Bowden, F.P. and Tabor, D. (1954) Friction and lubrication of solids. Oxford Univ. Press.

Burwell, J.T. and Strang, C.D. (1952) On the empirical law of adhesive wear. J. App. Phys., 23, 1952, pp 18 - 28.

Burwell, J.T. (1957) A survey of possible wear mechanisms. Wear 1, 119.

Bush, A.W., Gibson, R.D. and Thomas, T.R. (1975) The elastic contact of rough surfaces. Wear 35, 87 - 111.

Buttery, T.C. (1969) Grinding and abrasive wear. PhD thesis, University of Leicester.

Buttery, T.C. and Archard, J.F. (1971) Some microscopical investigations of grinding and abrasive wear. Journal of microscopy, Vol. 94, Pt. 1, August, pp 13 - 24.

Buttery, T.C. and Archard, J.F. (1971) Grinding and abrasive wear. Proc. Inst. Mech. Engrs. Vol. 153, p 537.

Buttery, T.C., Hamed, M.S., Mackie, W.H. and Statham, A. (1977) Some effects of deterioration in abrasive wheels on cutting efficiency and surface finish. 1st Poly. Sym. on Man. Eng. Leicester Polytechnic, 14 - 15 June.

Buttery, T.C. and Hamed, M.S. (1979) Study of Geometric and True leveling in electroplating using stylus methods. Wear 57, p 207 - 215.

Buttery, T.C. (1981) The way ahead. School of Mechanical and Production Engineering, Leicester Polytechnic, U.K.

Buttery, T.C., Mackie, W.H., Salib, N.R.I. and Hamed, M.S. (1982) Some applications of surface profilometry to the study of surfaces formed by electrochemical processes. Current advances in Mechanical design and production. Second Cairo University MDP Conf. Cairo, Egypt.

Buttery, T.C., Mackie, W.H., Salib, N.R.I. and Hamed, M.S. (1983) The optimisation of component surfaces for electroplating using coated abrasives. 2nd joint Int. Conf. on Prod. Eng., Leicester.

Buttery, T.C., Fancourt, H.G., Hemmaty, G.H. (1984) Some effects of Surface Topography in the functional behaviour of cylindrically ground components in simulated bearing experiments. 4th Polytechnics Symposium on Manufacturing Engineering, 23 - 24 May, City of Birmingham Polytechnic.

Buttery, T.C. and Hemmaty, G.H. (1986) Computer modelling of changes in surface topography by electrochemical processes. 5th Polytechnics Symposium on Manufacturing Engineering, Eastbourne, England.

Campbell, C. (1972) Cylinder bore surface roughness in internal combustion engines : its application and control. Wear 19, 163 - 168.

Chetwynd, D.G. (1978) Slope measurement in surface texture analysis. Journal of Mechanical Engineering Science, Vol. 20, No.3, 115 - 119.

Chetwynd, D.G., McKee, F.A. and Rakels, J.H. (1982) Machined surfaces : Final texture and underlying structure. Wear 83, 233 - 240.

Chowdry, S.K.R., Kaliszer, H. and Rowe, G.W. (1979) An analysis of changes in surface topography during running-in of plain bearings. Int. Conf. on Metrology and properties of engineering surfaces. Leicester (1979). Reprinted in Wear.

Church, E.L. (1979) Measurement of surface texture and topography by differential light scattering. Wear 57, 93 - 105.

Crisp, J., Seidel, J. and Stokey,W. (1968) Measurement of forces during cutting with a single abrasive grain. Int. J. Prod. Res., Vol. 7 (2), p 159.

Dennis, J.K. and Such, T.E. (1972) Nickel and Chromium plating. Newness-Butterworths, London.

Dickinson, S.R. (1967 - 68) Survey of factors affecting surface finish. Proc. I. Mech. E., 182 (3K), 135 - 147.

Eberhardt, H.W. (1965) How rough the surface. Prod. Engineering, August 16, p 105 - 107.

Elze, J. (1961) Geometric der Mikros treuuing und Einebnung durch Electrolytisch abgeschiedene Metallniedershlage. Metal 15, 542.

Foulke, D.G. and Karados, O. (1956) Current distribution in microprofiles, I. Proc. Am. Electroplates Soc. 43, 172.

Fromson, R.E., Brecker, J.N. and Shum, L.Y. (1976) A universal surface texture measuring system. S.M.E. paper IQ76 - 597.

Geary, R.C., (1935) The ratio of the mean deviation to standard deviation as a test of normality. Biometrika, 27, 310 - 332.

Ghabrial, S.R., Saleh, S.M., Kohail, A. and Moisan, A. (1982) Problems associated with Electrodischarge machined, Electrochemically machined and Ultrasonically machined surfaces. Wear 83, 275 - 283.

Goddard, J. and Wilman, H. (1961) A theory of friction and wear during the abrasion of metals. Wear, 5 (1962) 114 - 135.

Graham, D. and Baul, R.M. (1972) An investigation into the mode of metal removal in the grinding process. Wear, 19, p 301.

Graneek, M. and Wunsch, H.L. (1952) Application of pneumatic gauging to the measurement of surface finish. Machinery, 81, 701 - 706.

Greenwood, J.A. and Trip, J.H. (1965) Burndy Res. Rep., No.21.

Greenwood, J.A. and Williamson, J.B.P. (1966) Contact of nominally flat surfaces. Proc. Roy. Soc. (London) A295, 300 - 319.

Grisbrook, H., Moran, H. and Shephered, D. (1965) Metal removal by a single abrasive grit. ISI Inst. Metal. Joint Conf. on machinability, London.

Grisbrook, H. (1960) Precision grinding research. Production Engineer (May - June).

Grisbrook, H. (1962) Cutting points on the surface of a grinding wheel and chips produced. Advances in Machine Tool Design and Research. Proceedings of the 3rd international M.T.D.R. Conf. University of Birmingham.

Grisbrook, H., Hollier, R.H. and Varley, P.G. (1962) Related patterns of grinding forces, wheel wear and surface finish. Int. J. Prod. Res. 1 (3), 57.

Guest, J.I. (1915) The theory of grinding. Proc. Soc. Mech. Engrs.

Hahn, R.S. (1956) A.S.M.E. Vol. 78, p 807.

Hahn, R.S. and Lindsay, R. (1967) On the effects of real area of contact and normal stress in grinding. Annals of C.I.R.P. Vol. XV, pp 197 - 204.

Hahn, R.S. and Lindsay, R.P. (1971) Principles of grinding. Machinery Magazine, July to Nov.

Hamed, M.S. and Buttery, T.C. (1977) Grinding process simulation. Proceedings of the 18th international Machine Tool Design and Research Conference, pp 447 - 459.

Hamed, M.S. (1977) Grinding Mechanics, single grit approach. PhD, Leicester Polytechnic.

Hamed, M.S., Whitehouse, D.J. and Buttery, T.C. (1978) Random surface generation - an integrated approach. CIRP Ann. Vol. 27/1.

Holm, R. (1946) Electrical contacts H. Gerbers, Stockholm.

Hydell, R.R. (1967 - 68) Todays need - Functional surface roughness control. Proc. Inst. Mech. Engrs., 182, pt 3K, 127 - 134.

Ishigaki, H. and Kawaguchi, I. (1981) Effect of skid on the accuracy of measuring surface. Wear, 68, 203 - 211.

Kaliszer, H., Grieve, D.J. and Rowe, G.W. (1972) Digital computation of surface topography. Proc. 12th Inter. M.T.D.R. Conf. The Macmillan Press Ltd.

Kaliszer, H., Rowe, G.W. and Trmal, G. (1973) On the relationship between wear and surface topography. Annals CIRP. Vol.22/2/73, pp 284 - 290.

Keragelskii, I.V. and Kombalov, V.S. (1969) Calculation of value of stable roughness after running-in (elastic contact). Wear 14, 137 - 140.

King, T.G., Watson, W. and Stout, K.J. (1977) Modelling the microgeometry of lubricated wear. Proc. 4th Leeds-Lyon Symposium on lubrication. Inst. Mech. Eng. Sept. (1977).

King, T.G., Whitehouse, D.J. and Stout, K.J. (1978) Some topographical features of the wear process - Theory and experiment. Ann. CIRP, 25 (1), 351 - 356.

King, T.G. (1980) Plain bearings - Aspects of wear and related surface characteristics. PhD thesis, Leicester Polytechnic.

King, T.G. and Spedding, T.A. (1982) On the relationship between surface profile light parameters. Wear 83, 91 - 108.

King, T.G. and Spedding, T.A. (1983) Towards a rational surface profile characterisation system. Precision Engineering, 5, No.4, 153-160. Butterworth & Co.

Koloc, J. (1959) On the wear of grinding wheels. Microtechnic, VXIII, n1.

Krabacher, E.J. (1959) Factors influencing the performance of Grinding Wheels. Trans. A.S.M.E., Series B, August.

Kruschov, M.M. (1957) Paper 46. Proc. Conf. Lubrication and Wear. Institution of Mechanical Engineers, London.

Kruschov, M.M. and Babichev, M.A. (1960) Investigation of the wear of metals. SSSR Acad. Sci. pub. House.

Kubo, M. (1965) Rev. Scient. Instrum. 36, 263.

Larsen - Badse, J. (1968) Influence of grit diameter and specimen size on wear during sliding abrasion. Wear, 12, p35.

Larsen - Badse, J. (1972) Some effects of specimen size on abrasive wear. Wear 19, p 27.

Lindsay, R.P. (1969) ASTME Creative Manufacturing Seminars. Paper MR69 - 568.

Mackie, W.H. (1982) Some aspects of metal removal using coated abrasives. M.Phil., Leicester Polytechnic.

Malkin, S. and Cook, N.H. (1971) The wear of grinding wheels. Part 1 - Attricious wear. Trans. A.S.M., Series B., November.

Marshall, E.R. and Shaw, M.C. (1952) Forces in dry surface grinding. A.S.M.E., p 51.

Mashloosh, K., Akbasoglu, F. and Eyre, T. (1984) Wear of digger teeth. IMechE Conf., Tribology in minding - War on wear. Nottingham 17 - 19, September 1984.

Masouros, G., Dimarogonas, A. and Lefas, K. (1977) A model for wear and surface roughness transients during the running-in of bearings. Wear 45, 375 - 382.

Maycock, K.M. (1987) The assessment of quality in planed and spindle moulded products. PhD. Transfer report, Leicester Polytechnic.

Meyer, W.R. (1935) Proc. Am. Electroplaters Soc. 23, 116, 135.

Meyer, W.R. (1936) Proc. Am. Electroplaters Soc. 24.135.

Mickic, B.B. (1974) Thermal contact conductance - Theoretical considerations. Int. J. Heat Mass transfer, 17, 205 - 214.

Moore, M.A. (1971) A preliminary investigation of frictional heating during abrasive wear. Wear, 17, p 51.

Mulhearn, T.O. and Samuels, L.E. (1962) The abrasion of metals; a model of the process. Wear 5, p 478.

Nakamura, M. (1961) On experimental methods of studying levelling power of plating Batch. Kinzoku Hyomen Gijatsu 12, 215.

Nakamura, T. (1966) On the deformation of surface roughness curves caused by the finite radius of the stylus tip and tilting of stylus holder arm. Bull. Jap. Soc. Prec. Engng., 1, 240 - 8.

Nara, J. (1962) Some analysis of paper finished surfaces. J.S.P.M.J. 28, 120.

Nara, J. (1966) On CLA value obtained with direct reading, surface roughness tester - effect of skid on high pass filter. Bull. Japan Soc. Prec. Engng., 1, 263 - 73.

Nathan, G.K. and Jones, W.J.D. (1966) The empirical relationship between abrasive wear and the applied conditions. Wear 9, p 300.

Ochiai, N. (1975) M.Sc. Thesis, University of Birmingham.

Oldfield, J.W. (1973) The Use of Computer simulations to study the nature of an electrodeposit during the early stages of growth. Cont. Inst. Metal Finishing, Edinburgh.

Ostvik, R. and Christensen, H. (1969) Changes in surface topography with running-in. Proc. I. Mech. E., 183 pt 3, p 57 - 65.

Pahlitzch, G. and Appun, J. (1954) Ind. Diamond Rev. 14, Sept/Oct.

Pahlitzsch,G. and Thoeing, W. (1959) New research into the truing process in grinding. Industrial Diamond Review, Vol.19, May/June/July, 1959.

Pattinson, E.J. and Chisholm, A.J.W. (1967) The effect of dressing techniques on grinding wheel wear. Int. Conf. on Manufacturing Technology, Ann Arbor, Michigan.

Peklenik, J. and Opitz, H. (1962) Testing of grinding wheels. Advances in Machine Tool Design and Research. Proceedings of the 3rd international M.T.D.R. Conference, University of Birmingham.

Peklenik, J. (1963) Grinding fundamentals II. Proceedings of the international conference on Production Engineering Research, pp 201 - 208.

Peklenik, J. (1964) Contribution to the correlation theory for the grinding process. Trans. ASME, J. of Eng. for Indust., May, pp 85.

Peklenik, J. (1965) Contribution to the theory of surface characterisation. CIRP Annalen, Vol. XII, pt. 3.

Peklenik, J. (1967-68) New developments in surface characterisation and measurements by means of random process analysis. Proc. Inst. Mech. Engrs. 182 pt 3K, 108 - 126.

PERA Report 403 (1987) Grinding - the current status in UK manufacturing industry. I. Malcolmson, G.J. Trmal and A. Wagstaff.

Rabinowicz, E. (1950) Taper sectioning, a method for the examination of metal surfaces. Metal industry, 76, 83 - 86.

Rabinowicz, E. (1958) Predicting the wear of metal parts. Prod. Engng, 29, p 71.

Rabinowicz, E. (1965) Friction and wear of materials. John Wiley & Sons, Inc. New York.

Radhakrishnan, V. (1971) Analysis of surface profiles by computational methods. J. Inst. Engrs. India, 51 (ME-6), 272.

Radhakrishnan, V. (1973) Significance of profile length in roughness measurement. Wear 23, 339 - 347.

Raub, E. and Muller, K. (1967) Fundamentals of metal depositions, Elsevier.

Reason, R.E. (1944) Surface finish and its measurement. J. Inst. Prod. Engrs., 23, 347 - 72.

Reason, R.E. (1979) Progress in the appraisal of surface topography during the first half-century of instrument development. Wear 57, 1 - 16.

Rowe, G.W. (1974) Surface topography changes at breakdown of thin-film lubrication. Wear 28, 125 - 130.

Rowe, G.W., Kaliszer, H., Trmal, G. and Cotter, A. (1975) The running-in of plain bearings. Wear 34, pp 1 - 14.

Sato, K. (1955) On the surface roughness in grinding. Tohoku University Tech. Reports 20, 23.

Sayles, R.S. and Thomas, T.R. (1976) The structure function; a practical alternative to auto correlation. Proc. 1st British Conf. on the teaching of correlation and spectral techniques in higher education. Leeds Polytechnic.

Sedriks, A.J. and Mulhearn, T.O. (1963) Wear 6, p 457.

Sedriks, A.J. and Mulhearn, T.O. (1964) Wear 7, p 451.

Sherwood K.K. and Crookall, J.R. (1967 - 68) Surface finish assessment by an electrical capacitance technique. Proc. Inst. Mech. Engrs. 182, pt 3K, 344 - 349.

Sherrington, I. and Smith, E.H. (1986) The significance of surface topography in Engineering. Precision Engineering. Butterworth & Co. Ltd. 79 - 87.

Shonozaki, T. and Shigematu, H. (1966) Mechanism of rubbing and biting of cutting edges on work surface in the grinding process. Bull. JSME, Vol. 2 (1).

Shunmugam, M.S. and Radhakrishnan, V. (1976) Selection and filtering of reference line for surface profiles. Proc. Instn. Mech. Engrs. Vol. 190, 193 - 201.

Spragg, R.C. and Whitehouse, D.J. (1972) An average wavelength parameter for surface metrology. Measurement and Control, Vol. 5, March 1972.

Sreenath, A.V. and Raman, N. (1976) Running-in wear of a compression ignition engine : factors influencing the conformance between cylinder liner and piston rings. Wear 38, 271 - 289.

Stoute, K.J., Whitehouse, D.J. and King, T.G. (1977) Analytical techniques in surface topography and their application to a running-in experiment. Wear, 43, 99 - 115.

Stout, K.J. (1980) Surface measurement and their significance in manufacturing. Prod. Eng. 59 (5), 17 - 22.

Stout, K.J. (1981) Surface roughness - Measurement, Interpretation and significance of data. Materials in Engineering, Vol.2, part I, 260 - 265.

Tadao Tsukada (1986) Evaluation of two and three dimensional surface roughness and their confidence. Wear, 109, 69 - 78.

Thomsen, E.G., Young, C.T. and Kobayashi, S. (1965) Plastic deformation in metal processing. MacMillan Company.

Thomas, T.R. and Sayles, R.S. (1978) Some problems in the tribology of rough surfaces. Tribology Int., 11, 8 - 9.

Tonn, W. (1937) Contribution to the knowledge of the wear process in short-time experiments. Z. Metallk, 29, 196.

Trumpold, H. (1967 - 68) Limits of application of the interface methods for surface measurement. Proc. Inst. Mech. Engrs. 182, pt. 3K, 241 - 254.

Tsuwa, H. (1960) On the behaviour of Abrasive grains in grinding (I). J. Soc. Precision Mechanics, Japan, Vol.26, p 199.

Tsuwa, H. (1961) On the behaviour of Abrasive grains in grinding, II and III. J. Soc. Precision Mechanics, Japan, Vol.27, pp 409 - 414.

Verkerk, J. (1974) The effect of dressing wheel profile on cutting edge density. CIRP group G Bled.

Verkerk, J. (1977) Characterisation of wheel wear in plunge grinding. Annals C.I.R.P. Vol.25/1, pp 127-131.

Vickerstaff, T.J. (1970) On the significance of the wheel dressing operation in the grinding process. MSc Thesis, University of Nottingham.

Vickerstaff, T.J. (1974) A study of some factors which influence surface finish in the grinding process. PhD Thesis, University of Aston in Birmingham.

Vickerstaff, T.J. (1976) Int. J. Mach. Tool Des. Res. Vol. 16, pp 145 - 152.

Von Weingraber, H. (1957) Suitability of the envelope line as a reference standard for measuring roughness, Microtechnic, 11, 6 - 17.

Watson, S.A. and Edwards, J. (1957) An investigation of the mechanism of levelling in electrodeposition. Trans. Inst. Metal Finishing, 34, 167.

Whitehouse, D.J. (1967-68) Improved type of wave filter for use in surface finish measurements. Proc. Inst. Mech. Eng. London, 182 (3K), 306 - 318.

Whitehouse, D.J. and Archard, J.F. (1970) Properties of random surface of significance in their contact. Proc. Roy. Soc. (London) A 316, 97 - 121.

Whitehouse, D.J. (1971) The properties of random surfaces of significance in their contact. PhD. Thesis, Leicester University.

Whitehouse, D.J. (1974) Theoretical analysis of stylus integration. Ann. CIRP, 23, 181 - 2.

Whitehouse, D.J. (1974) The measurement and analysis of surfaces. Tribology International, December 1974, 249 - 259.

Whitehouse, D.J. (1978) Surfaces - a link between manufacture and function. Proc. Instn. Mech. Engrs. Vol. 192, 179 - 188.

Whitehouse, D.J. (1982) The parameter rash - is there a cure? Proceedings of the 2nd Int. Conf. on Metrology and properties of Engineering surfaces. April 14 - 16, Leicester, U.K.

Williamson, J.B.P. (1967 - 68) The microtopography of surfaces. Proc. Instn. of Mech. Engrs., 182, pt 3K, 21 - 30.

Williamson, J.B.P. and Hunt, R.T. (1968) Relocation profilometry, J. Phys. E. : Sci. Instrum. 1, 749 - 52.

Williamson, J.B.P., Pullen, J. and Hunt, R.T. (1969) The shape of solid surfaces. Surface mechanics, A symposium volume, American Society of Mechanical Engrs., p 24 - 35.

Yingjie, L., Xingui, B. and Kegiang, C. (1985) A study of the formation of wear debries during abrasion. Trib. Int. Vol. 18, No.2, p 107.

Yoshikawa, H. (1962) Characteristics of tool life in grinding. J. Soc. Precision Mechanics, Vol.28, 1962, p 562.

APPENDIX 1 - COMPUTER PROGRAM

```
50 PRINT "LSML DATAQ" \ PRINT "GENERAL PURPOSE VERSION"
52 PRINT "UPDATED 17.2.82 PREVIOUS VERSIONS WITHDRAWN" \ PRINT
240 PRINT "? NO. OF SAMPLES = "; \ INPUT N1
250 PRINT "? SAMPLE SPACING (MICRONS)  "; \ INPUT H
260 IF H=2 THEN H5=2 \ GO TO 320
270 IF H=3 THEN H5=20 \ GO TO 320
280 IF H=4 THEN H5=40 \ GO TO 320
290 IF H=5 THEN H5=55 \ GO TO 320
300 IF H=6 THEN H5=70 \ GO TO 320
310 PRINT " 2 3 4 5 OR 6 MICRONS ARE AVAILABLE " \ GO TO 250
320 PRINT "? VERTICAL MAG. = "; \ INPUT V
330 N=N1-1 \ DIMA(50) \ DIMY(2000)
345 PRINT "? TEST NO. = "; \ INPUT I$
346 IF I$="STOP" THEN END
347 IF I$="RESET" THEN 240
350 PRINT "START TRAVERSE" \ SETDVM(2,4) \ T=1.5
380 MEASURE(S,3) \ IF S<T THEN 380
400 SETDVM(2,5) \ STIME(0,0,0)
410 FOR X=0 TO N
420 MEASURE(Y(X),4)
430 FOR S=1 TO H5 \ H=H
440 NEXT S
450 NEXT X
460 RTIME(H1,M1,S1) \ PRINT "LOGGING TIME = ";60*M1+S1;" SECS"
500 SCALE(9,0,28,0,18) \ PLOT(9,0,0,0,0) \ M0=9999 \ P=0 \
    T9=0 \ M9=0
570 FOR X=0 TO N \ IF Y(X)<M0 THEN M0=Y(X)
580 NEXT X
590 TEXT(1,0)FMT("A",5) \ PLOT(9,1+(Y(0)-M0)/2,0,0) \ X1=25/N
635 FOR X=0 TO N \ Y(X)=Y(X)-M0 \ PLOT(9,2+X*X1,1+Y(X)/2,1,0)
640 P=P+Y(X)*X \ T9=T9+Y(X) \ NEXT X
660 PLOT(9,2+N*X1,1,1,0) \ PLOT(9,2,1,1,0) \ T8=0
690 FOR X=2 TO 25 STEP 25000/N/H
700 PLOT(9,X,1,0,7) \ TEXT(1,0) \ TEXT(1,0)T8; \ T8=T8+1 \
    NEXT X
730 TEXT(1,0)" MM" \ PLOT(9,2,1,0,0)
750 FOR X=1 TO 6 \ PLOT(9,2,X,1,8) \ NEXT X
760 FOR X=6 TO 1 STEP -1 \ PLOT(9,.7,X,0,0) \
    TEXT(1,0)(X-1)*10000/V \ NEXT X
780 PLOT(9,0,6.5,0,0) \ TEXT(1,0)"MICRONS"
790 M5=T9/N1 \ P1=N*N1/2 \ P2=P1*(2*N+1)/3 \ P3=N1*M5 \
    P4=P1*P1
820 U1=(P2*P3-P*P1)/(N1*P2-P4) \ U2=(P1*P3-N1*P)/(P4-N1*P2)
831 M9=-9999 \ M0=9999 \ PLOT(9,2,1+U1/2,0,0) \ T9=0 \ T8=0
850 FOR X=0 TO N \ T9=U1+U2*X \ Y(X)=Y(X)-T9 \ T8=T8+Y(X)
852 IF Y(X)<M0 THEN M0=Y(X)
853 IF Y(X)>M9 THEN M9=Y(X)
860 PLOT(9,2+X*X1,1+T9/2,1,0) \ NEXT X
865 M5=T8/N1 \ R=M9-M0 \ IF R>5 THEN R=5 \ GO TO 1019
990F R>2 THEN R=10 \ GO TO 1019
1000 R=25
1019 FOR X=0 TO 50 \ A(X)=0 \ NEXT X
1020 FOR X=0 TO N \ T5=INT((Y(X)-M0)*R)
1041 IF T5>49 THEN T5=49 \ PRINT " OTL=";Y(X)-M0;
```

```
1050 A(T5)=A(T5)+1 \ NEXT X
1080 T5=0
1090 FOR X=0 TO 49 \ IF A(X)>T5 THEN T5=A(X)
1100 NEXT X
1110 T5=T5*100/N1 \ IF T5>50 THEN T5=20 \ GO TO 1170
1130 IF T5>20 THEN T5=10 \ GO TO 1170
1140 IF T5>10 THEN T5=4 \ GO TO 1170
1150 IF T5>5 THEN T5=2 \ GO TO 1170
1160 T5=1
1170 PLOT(9,1,12,0,0)
1175 FOR X=12 TO 17 \ PLOT(9,1,X,1,8) \ NEXT X
1180 PLOT(9,.1,17.5,0,0) \ TEXT(3,0)" %"
1185 FOR X=17 TO 12 STEP -1 \ PLOT(9,.1,X,0,0) \
     TEXT(1,0)(X-12)*T5 \ NEXT X
1195 PLOT(9,1,12,0,0) \ T5=T5*N1/100 \ C3=0 \ R3=0 \ S3=0 \
     K3=0
1210 M6=(M5-M0)*R-.5 \ X1=6.66666
1215 FOR X=0 TO 49 \ PLOT(9,1+X/X1,A(X)/T5+12,1,0) \ D3=X-M6 \
     D4=D3*D3
1220 PLOT(9,1+(X+1)/X1,A(X)/T5+12,1,0) \ C3=C3+A(X)*ABS(D3)
1230 R3=R3+A(X)*D4 \ S3=S3+A(X)*D4*D3 \ K3=K3+A(X)*D4*D4 \
     NEXT X
1260 R3=R3/N1 \ K3=K3/N1/R3/R3 \ RSQR(R3) \ S3=S3/N1/R3/R3/R3
1285 C3=C3*5000/V/R/N1 \ R3=R3*5000/V/R \ PLOT(9,8.5,12,1,0)
1305 FOR X=8.5 TO 1 STEP -1.5 \ PLOT(9,X,12,1,7) \ NEXT X
1315 FOR X=.7 TO 8.2001 STEP 1.5 \ PLOT(9,X,11.6,0,0)
1325 TEXT(1,0)(X-.7)/7.5/R*25*10000/V; \ NEXT X
1332 PLOT(9,7.1,11.1,0,0) \ TEXT(1,0)"MICRONS"
1340 PLOT(9,5.7,10,0,0) \ TEXT(1,0)FMT("F",6,2)"CLA =";C3
1345 TEXT(1,0)"RMS =";R3 \ TEXT(1,0)"SKEW=";S3 \
     TEXT(1,0)"KURT=";K3
1360 PLOT(9,2,17.5,0,0) \ TEXT(2,0)"AMPLITUDE DISTBN."
1370 PLOT(9,10.5,17,0,0)
1375 FOR X=17 TO 12 STEP -1 \ PLOT(9,10.5,X,1,8) \ NEXT X
1380 FOR X=10.5 TO 18 STEP .75 \ PLOT(9,X,12,1,7) \ NEXT X
1385 PLOT(9,18.9,11.6,0,0) \ TEXT(1,0)FMT("A",8)"%"
1390 FOR X=100 TO 0 STEP -20 \ PLOT(9,10.2+X*.075,11.6,0,0) \
     TEXT(1,0)X \ NEXT X
1400 FOR X=12 TO 17 \ PLOT(9,9.2,X,0,0) \
     TEXT(1,0)(X-12)/5/R5*10000/V; \ NEXT X
1407 PLOT(9,12,17.5,0,0) \ TEXT(2,0)"BEARING RATIO"
1408 PLOT(9,9,13.5,0,0) \ TEXT(1,1)"MICRONS";
1430 PLOT(9,10.5,17,0,0) \ X1=0
1435 FOR X=0 TO 49 \ X1=X1+A(49-X) \
     PLOT(9,10.5+X1/N*7.5,17-X/10,1,0)
1450 PLOT(9,10.5+X1/N*7.5,17-(X+1)/10,1,0) \ NEXT X
1560 PLOT(9,20,12,0,0) \ G1=5000/V/H \ G=180/PI \ S0=999 \
     S9=-999 \ T9=0
1600 FOR X=3 TO N-3
1610 T5=(Y(X+3)-9*Y(X+2)+45*Y(X+1)-45*Y(X-1)+9*Y(X-2)-
     Y(X-3))/60
```

```
1620 T5=ATN(T5*G1)*G \ IF T5>S9 THEN S9=T5 \ GO TO 1650
1640 IF T5<S0 THEN S0=T5
1650 T9=T9+T5 \ Y(X-3)=T5 \ NEXT X
1660 FOR X=0 TO 10 \ PLOT(9,20+X*.75,12,1,7) \ NEXT X
1670 PLOT(9,25.5,11.1,0,0) \ TEXT(1,0)"DEGREES"
1680 FOR X=2 TO 0 STEP -1 \ PLOT(9,19.7+X*3.75,11.6,0,0)
1700 TEXT(1,0)FMT("A",8)(X-1)*50 \ NEXT X
1720 PLOT(9,20,12,0,0)
1730 FOR X=0 TO 5 \ PLOT(9,20,12+X,1,8) \ NEXT X
1740 PLOT(9,18.7,17.5,0,0) \ TEXT(1,0)"%/DEG"
1750 PLOT(9,21,17.5,0,0) \ TT(2,0)"SLOPE DISTBN."
1760 PLOT(9,20.2,10,0,0) \ TEXT(1,0)FMT("F",6,2)"MAX ="S9
1780 TEXT(1,0)"MIN ="S0 \ TEXT(1,0)FMT("F",8,4)"AV  =";
     T9/(N1-6);FMT("A",8)
1800 FOR X=0 TO 50 \ A(X)=0 \ NEXT X
1810 FOR X=0 TO N-6 \ T5=INT(Y(X)/2+25)
1822 IF T5>49 THEN T5=49 \ PRINT " STL=";Y(X);
1823 IF T5<0 THEN T5=0 \ PRINT " STS=";Y(X);
1830 A(T5)=A(T5)+1 \ NEXT X
1850 T5=0
1860 FOR X=0 TO 49 \ IF A(X)>T5 THEN T5=A(X)
1880 NEXT X
1890 T5=T5*100/2/(N1-6) \ IF T5>20 THEN T5=10 \ GO TO 1950
1910 IF T5>10 THEN T5=4 \ GO TO 1950
1920 IF T5>5 THEN T5=2 \ GO TO 1950
1930 IF T5>2 THEN T5=1 \ GO TO 1950
1940 T5=.5
1950 FOR X=5 TO 0 STEP -1 \ PLOT(9,18.7,12+X,0,0) \
     TEXT(1,0)X*T5 \ NEXT X
1970 PLOT(9,20,12,0,0) \ R4=0 \ C4=0 \ S3=0 \ K3=0 \ X1=6.66667
1990 FOR X=0 TO 49 \ A=A(X)/(N1-6)*100/2
2010 PLOT(9,20+X/X1,12+A/T5,1,0) \
     PLOT(9,20+(X+1)/X1,12+A/T5,1,0)
2030 D3=(X-24.5)*2-(T9/(N1-6)) \ D4=D3*D3 \ C4=C4+A(X)BS(D3)
2060 R4=R4+A(X)*D4 \ S3=S3+A(X)*D4*D3 \ K3=K3+A(X)*D4*D4 \
     NEXT X
2100 R4=R4/(N1-6) \ K3=K3/R4/R4/(N1-6) \ R4=SQR(R4)
2130 S3=S3/(N1-6)/R4/R4/R4 \ C4=C4/(N1-6)
2150 PLOT(9,20.2,10,0,0) \ TEXT(1,0) \ TEXT(1,0) \ TEXT(1,0)
2160 TEXT(1,0)FMT("F",6,2)"AAV =";C4 \ TEXT(1,0)"RMS =";R4
2180 TEXT(1,0)"SKEW=";S3 \ TEXT(1,0)"KURT=";K3
2185 TEXT(1,0)"%ZERO=";(A(24)+A(25))/2/(N1-6)*100
2200 C4=C4*PI/180 \ R4=R4*PI/180 \ C4=SIN(C4)/COS(C4) \
     R4=SIN(R4)/COS(R4)
2240 C4=C3/C4*2*PI/1000 \ R4=R3/R4*2*PI/1000
2260 PLOT(9,5.7,8.2,0,0) \ TEXT(2,0)"\"
2270 PLOT(9,5.7,8.2,0,0) \ PLOT(9,5.55,8.05,1,0)
2280 PLOT(9,6,8.2,0,0) \ TEXT(1,0)FMT("F",7,4)"A=";C4;"MM"
2290 PLOT(9,5.7,7.5,0,0) \ TEXT(2,0)"\"
2300 PLOT(9,5.7,7.5,0,0) \ PLOT(9,5.55,7.35,1,0)
2310 PLOT(9,6,7.5,0,0) \ TEXT(1,0)"Q=";R4;"MM"
```

```
2320 PLOT(9,.5,0,0,0) \ TEXT(1,0)FMT("A",8)"TEST NO. ";
2340 TEXT(1,0)I$;"  ";N1;" SAMPLES AT ";H;MICRONS  "
2359 PRINT  \ PRINT  \ GO TO 345
```

APPENDIX 2 - RELATED PUBLICATIONS

SOME EFFECTS OF SURFACE TOPOGRAPHY ON THE FUNCTIONAL BEHAVIOUR OF CYLINDRICALLY GROUND COMPONENTS IN SIMULATED BEARING EXPERIMENTS.

T.C. Buttery, H.G. Fancourt and G.H. Hemmaty.
School of Mechanical and Production Engineering, Leicester Polytechnic.

In this preliminary investigation, the running-in of plain bearings has been simulated using a pin on ring machine. Cylindrically ground case hardened steel rings having a range of surface finishes were run against phosphor bronze pins under marginally lubricated conditions.
The results show that both the initial wear during running-in and the equilibrium bearing pressure are a function of the surface topography of the steel ring. Smoother surfaces can carry higher specific pressures and require less running-in.

INTRODUCTION.

Most new pieces of machinery incorporating sliding surfaces require a period of running-in before they can be subjected to full load. It is generally accepted that the time and care taken at the running-in stage will be repaid with an extension in the useful life of the equipment. Certainly the owner of a new car hopes this to be true.

From a study of the literature there appears to be at least two classic types of running-in.

Mode I

Running-in between precision surfaces where both components are of a similar hardness; the wear necessary to achieve running-in being contained within the original surface topography of the components. Analysis of such surfaces shows that the running-in process is associated with progressive truncation of the surface and the formation of an increasing number of plateau. Kaliszer et al(1) used the concept of "zero wear", which was considered to be wear within the original surface topography, when discussing the role of surface metrology in Tribology. It was suggested that such wear would have little effect on the physical dimensions of a component and therefore the term zero wear could be applied. A significant parameter for predicting this type of wear is the bearing area curve despite its sensitivity to freak observations.

Mode II

This type of behaviour occurs when one of the surfaces is relatively soft(bearing material) and changes its surface topography during running-in to conform with that of the harder material(shaft). Once the bearing material has conformed with the shaft the wear rate falls dramatically

Further changes in surface topography (running-in) will proceed very slowly and will normally involve slow progressive changes in the surface topography of the harder material(shaft) by a mode I mechanism.

In the work described in this paper, using a pin on ring machine, the experimental conditions were arranged to ensure that the pin would wear to conform with the harder ring(mode II running-in). The experiments were designed to study the effects of the ring's surface finish on the running-in process. Under similar conditions Rowe et al(2) concluded that the surface finish of the softer,member is of relatively little importance.

EXPERIMENTAL PROCEDURE

Test Rig.

Experiments were carried out using a pin on ring wear tester designed by T.G. King and a complete description is given eleswhere(3).

Essentially the wear tester consists of an aerostatic spindle(Westwind Model 125A) mounted on a large cast iron bed. To reduce vibration to a minimum the motor variator drive was mounted independently and connected to the spindle through a rubber bush coupling. Shaft speeds could be reliably controlled between 100 - 800 rpm giving surface speeds of 0.47 to 3.8 m/s with a ring 90 mm diameter.

Appropriate instrumentation was used to monitor shaft speed and to record the cumulative number of revolutions completed.

The pin was mounted on a pivoted support arm and was loaded against the ring using masses suspended below the bed by a loading frame and wire. The load could be applied smoothly by means of an elevating and lowering platform operated by a double acting pneumatic cylinder. Complete details of the pin and ring arrangement are shown in figure 1.

A unique feature of the rig was the facility to monitor the surface topography of both the pin and ring without removing them from the rig and with accurate relocation. This was achieved by building a Talysurf 3 gearbox and stylus into the wear tester. The output from the surface measuring equipment was digitised and then processed through a PDP 11 computer to give a range of surface parameters including surface roughness, height distribution, average slope, slope distribution, bearing area curve and average wavelength.

Specimen materials and preparation.

The pins were made from phosphor bronze (BS 1400 PB-1C) and were 6 mm square by 30 mm long. The material had a nominal hardness of 140 VPN.

After the contact faces had been surface ground they were micropolished using 1 um diamond paste. Micropolishing enabled the wear scar to be measured accurately and ensured that only the surface finish of the ring would influence the running-in process. Great care had to be taken during micropolishing to keep the contact face of the pin flat.

The rings were case hardened mild steel(EN 32B) 90 mm diameter and

20 mm wide; nominal hardness 760 VPN. They were traverse ground on a Jones and Shipman 1300 series cylindrical grinder using an A46 grit wheel running at a surface speed of 23.5 m/s and a work speed of 0.24 m/s. By altering the grinding conditions, in particular the wheel dressing, three widely differing surface finishes were obtained corresponding to coarse, medium and fine dressing. Finally one of the fine finish rings was micropolished in-situ on the rig using 800 grit silicon carbide paper followed by 6 um and 1 um diamond paste. Some of the major surface parameters of the ring specimens are shown in table I.

Grinding Condition	R_a um	Δ_a degrees	λ_a mm	%zero slopes
Coarse	4.30	14.0	0.1091	2.5
Medium	1:09	9.9	0.0392	4.0
Fine	0.42	6.5	0.0231	5.0
Fine + Micropolishing	0.13	1.02	0.0447	25.0

Table I.

Experimental method.

Tests were carried out using flat ended pins rather than preformed. This configuration allows accurate measurement of wear by observing the scar formed on the pin. Since the initial conditions give line contact the consequent high pressures ensure some metal to metal contact at the start of each experiment. As the pin wears the specific pressure falls and eventually a stable oil film will form giving hydro-dynamic lubrication and a dramatic fall in wear rate. Although accurate alignment in both lateral directions is essential in this type of experiment it is not as critical as that required with preformed pins. Preformed pins have the advantage of giving a better simulation of running-in within the original surface although quantitative assessement of wear is more difficult to obtain.

A drip feed lubrication system was used delivering Mobil DTE light oil at a rate of approximately 0.005 ml/m. The oil was spread out over the ring by means of a felt pad which also removed any wear debris which formed. The pads were renewed at the beginning of each test.

Test were carried out for a sliding distance of 6000 m at a speed of 300 rpm(sliding speed of 1.43 m/s) and a load of 40 N. The wear scar formed on the pin was measured at appropriate intervals and the volume loss calculated. At the same time Talysurf traces from both the pin and ring were processed through the computer.

RESULTS

All the tests showed a rapid fall in wear rate with sliding distance(fig 2)

and after a sliding distance of about 6000 m the wear rate was hardly measureable. The rougher the surface the greater the initial wear rate and at the end of the experiments the rank order remained the same; the micropolished ring giving the lowest wear rate.

When the results are replotted to show the cumulative volume loss with sliding distance (fig 3) the significance of variations in surface become more evident. To run-in rough surfaces requires progressively longer sliding distances and involves more wear. To run in the roughest surface (4.3 um) involved a volume loss of 0.3853 mm^3 compared with 0.00229 mm^3 with the micropolished surface(0.12 um); a factor of just over two orders of magnitude. The practical significance of this would be a marked reduction in the over-all life of a component.

A consequence of the use of a flat ended pin is the progressive reduction in specific pressure with sliding distance provided the wear scar does not cover the whole surface of the pin. The variations in specific pressure with sliding distance is shown in figure 4. With the ground specimens the soother the surface the higher the specific pressure when run-in; 3.27 N/ mm^2 for the fine ring and 2.03N/ mm^2 for the rough ring. The micropolished ring ran-in at a significantly higher pressure than the ground specimens(10.8N/ mm^2).

Talsurf traces of the rings at the beginning and end of each experiment showed no detectable change in surface topography although a wear track was visible.

Due to their size, the Talysurf traces of the pins were taken using a reference flat. It was found that a new surface was rapidly established on the pins and that once stable conditions occured further running gave no significant change in the topography of the pins. The Talysurf traces of the pins showed that they had worn to conform with the rings; the surface parmeters of both pins and rings are shown in table II.

Grinding Condition		R_a um	Δ_a degrees	λ_a mm	% zero slopes
Coarse	ring	4.16	14.4	0.100	2.7
	pin	0.90	7.2	0.46	6.0
Medium	ring	1.06	9.4	0.039	4.0
	pin	0.30	5.3	0.042	8.0
Fine	ring	0.40	6.5	0.027	5.1
	pin	0.36	3.8	0.034	10.0
Fine + micro.	ring	0.13	1.2	0.042	26.0
	pin	0.35	3.9	0.029	12.0

Table II.

After 6000 m of sliding the surface profiles of the pins exhibited none of the characteristics associated with a run-in surface such as truncation.

DISCUSSION AND CONCLUSIONS

The results show that the total wear consists of two components; a minimum steady state wear plus an additional "running-in" wear which is a function of surface roughness. This result is similar to that reported by other workers in particular Masouros et al[4](fig 5). For the range of conditions studied both the Masouros results and those reported in this paper show an approximately linear relationship between the surface roughness of the harder component and the total wear to reach steady state conditions(fig 6).

The volume of material removed to run-in the roughest surface (4.3 um) was over one hundred times greater than that required with the smoother surface(0.12 um). Specific pressure was similar for the three ground specimens whilst the micropolished specimen could support a much higher specific pressure when run-in. The surface profiles of the pins showed that they had conformed with the rings rather than run-in in the classic sense; there was no evidence of truncation for example.

It is suggested that the common factor for each specimen when run-in is the area of zero slopes. For an isotropic surface this would be given by formula (1).

$$A = X\ Y\ Z^2 \qquad (1)$$

where A = area of zero slopes
X = width of pin
Y = width of scar
Z = % zero slopes

Since the surfaces being studied are anisotropic and highly directional a second formula was also used(2).

$$A = X\ Y\ Z \qquad (2)$$

Formulas (1 and 2) were used to calculate the area of zero slope on both the pins and the rings; the results are shown in table III.

Area of zero slope mm^2.	Rough ground	Medium ground	Fine ground	Polished
Formula (1)				
(a) pin	0.071	0.092	0.108	0.054
(b) ring	0.014	0.023	0.031	0.256
(a + b)	0.085	0.115	0.139	0.310
Formula (2)				
(a) pin	1.188	1.152	1.140	0.453
(b) ring	0.534	0.576	0.612	0.982
(a + b)	1.722	1.728	1.752	1.435

Table III.

Formula (2) shows very similar results for the pins run against the ground specimens and if the calculations for pin and ring are added

together the resulting values are very close. It appears that the running-in process can be explained at least in part as a smoothing operation associated with changes in slope and % zero slopes. Unlike the bearing area curve the slope data is relatively insensitive to freak events in the profile.

Talysurf traces and the parameters derived from them showed the surfaces of both pin(fig 7) and ring(fig 8) to be random; increasing the sliding distance by a factor of ten produced no significant change in the profile of either pin or ring. Features formed on the pin in the early stages on running-in often persisted throughout the run.

Conclusions

1. Running-in took place by a mode II mechanism; the phosphor bronze pins wearing to conform with the steel rings.

2. The total wear of the pin consisted of steady state wear plus the wear to run-in;the later was directly related to the surface roughness of the ring.

3. When run-in smoother surfaces supported a higher specific pressure.

4. Neither the pins or rings exhibited the classic characteristics of a run-in surface.

5. The results suggest that the area of zero slopes on the surface of both pin and ring are an early indicator of running-in.

6. By controlling the manufacturing process to give a transitional or composite surface bearing performance could be optimised. Although processes such as plateau honing and super-finishing (fig 9) give a partially run-in surface the same benefits might be obtained more simply. It is suggested that this could form the basis for further work.

REFERENCES

1. H, Kaliszer, G.W. Rowe and G. Trmal. " On the relationship between wear and surface topography" Annals CIRP Vol. 22/2/73 pp 284 - 290.

2. G.W. Rowe, H.Kaliszer, G. Trmal and A. Cotter. "The running-in of plain bearings" Wear, 34(1975) pp 1 - 14.

3. T.G. King. "Plain Bearings - Aspects of Wear and Related Surface Characteristics" PhD Thesis (CNAA)Leicester Polytechnic 1980.

4. G. Masouros, A. Dimarogonas and K. Lefas."A model for wear and surface roughness transients during the running-in of bearings." Wear, 45(1977) pp 375 - 382.

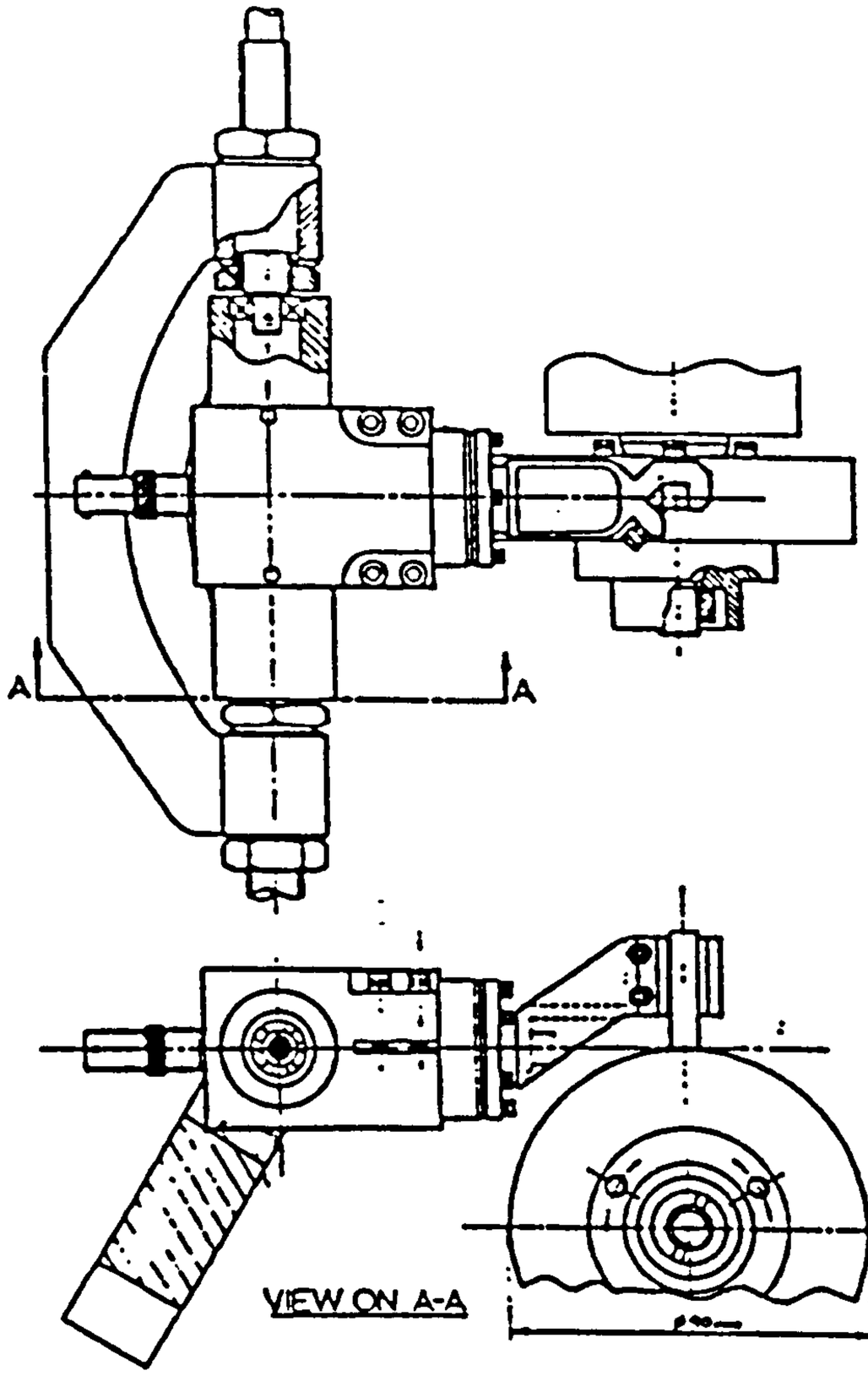

Figure 1. Geometric arrangement of pin and ring(King[3]).

Figure 2. Wear rate of phosphor bronze pins as a function of sliding distance.

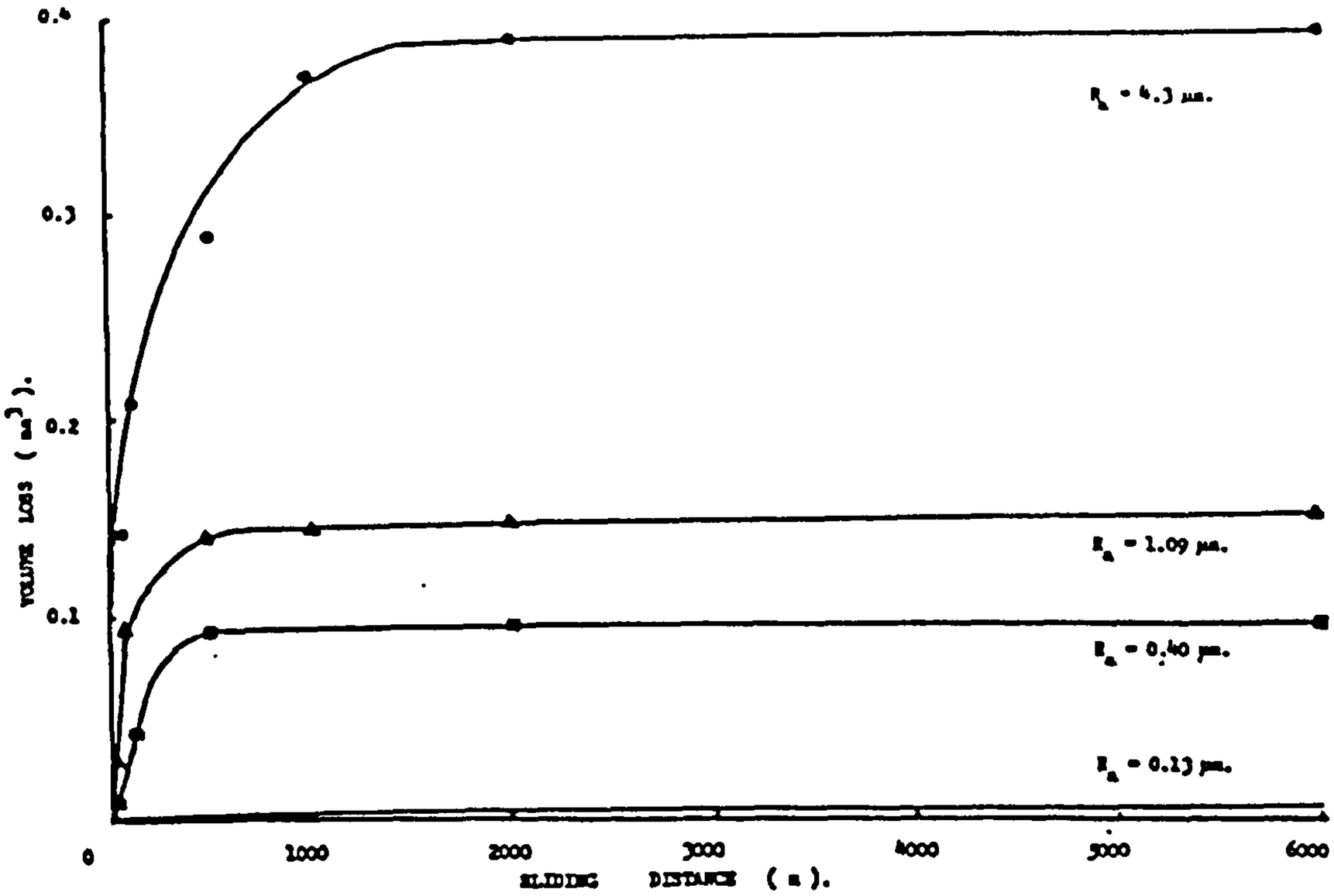

Figure 3. Cumulative wear of phosphor bronze pins showing the effect of ring surface finish on pin wear.

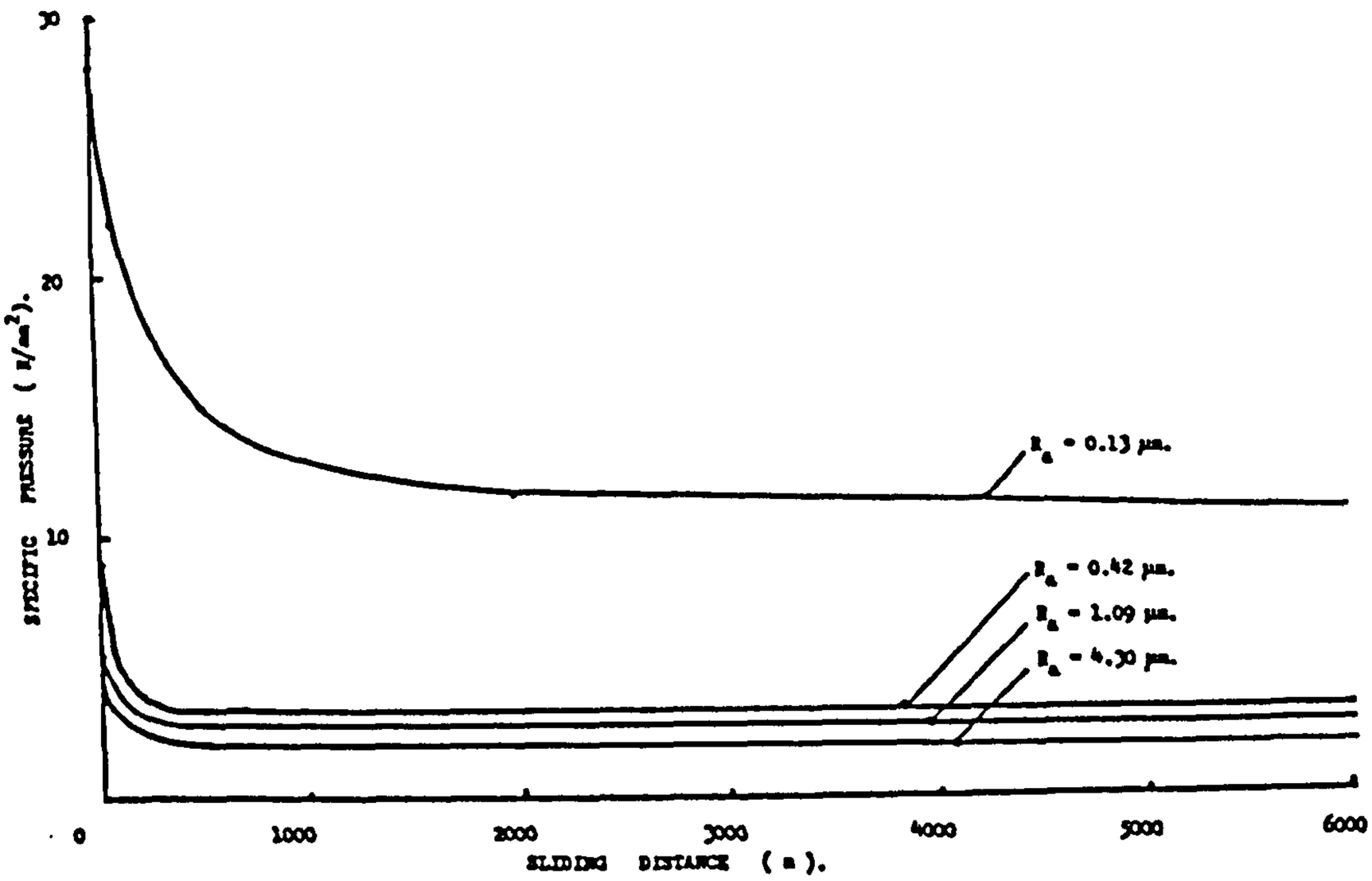

Figure 4. Specific pressure as a function of sliding distance for a range of ring surface finishes.

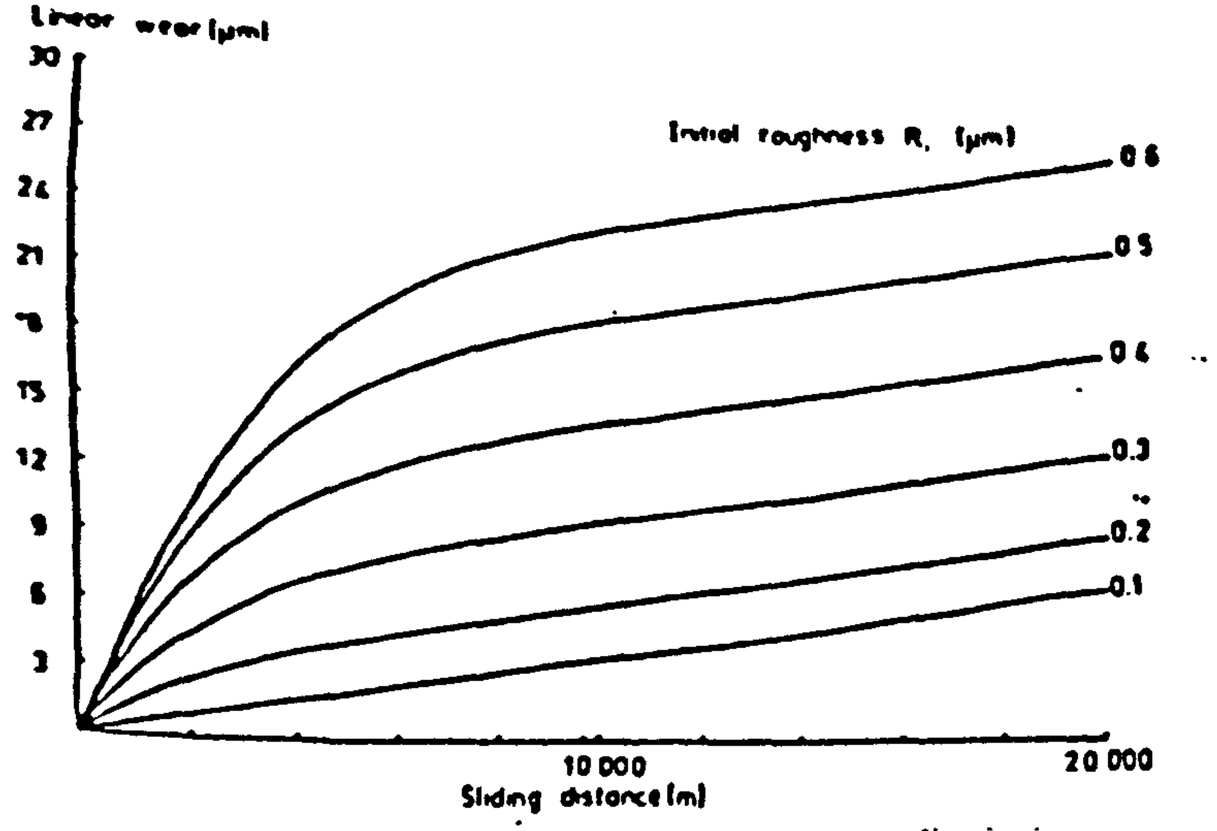

Figure 5. Wear during running-in (Masouros et al[4]).

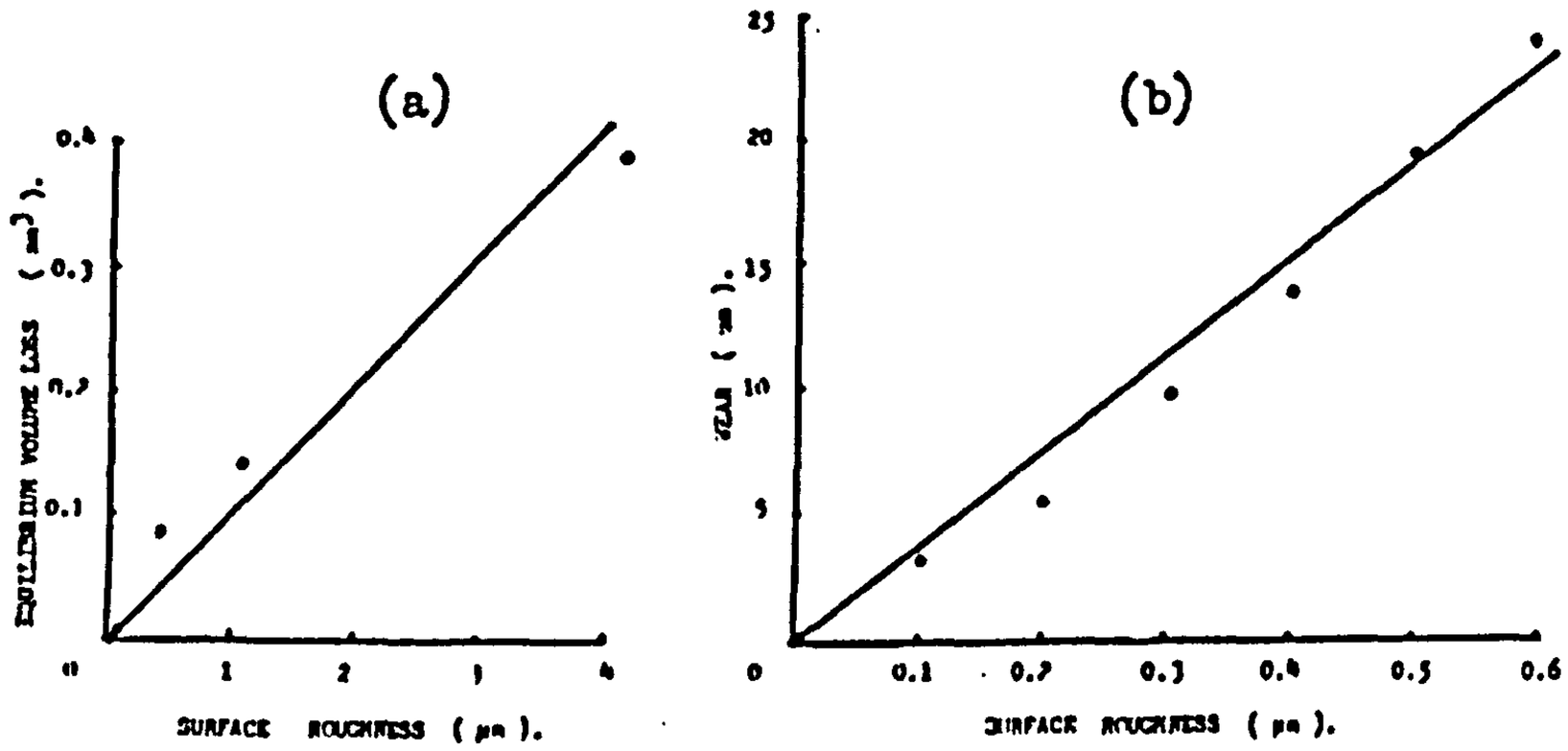

Figure 6. (a) Equilibrium volume loss versus surface roughness.
(b) Masouros results replotted as in (a).

Figure 7. Surface profile and other parameters for phosphor bronze ring run against rough ring (R_a = 4.30 um).

Figure 8. Surface profile and other parameters for steel ring orignal surface roughness (R_a = 4.30 um).

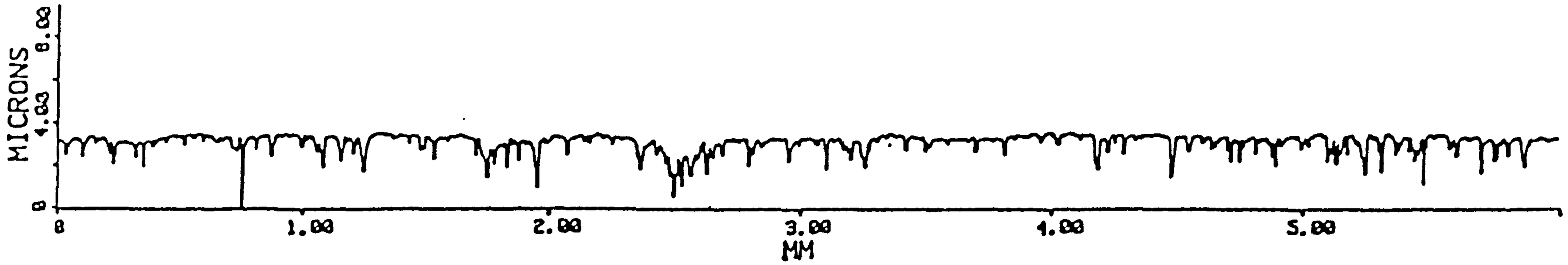

Figure 9a. Worn Portion of the Cylinder Liner of Figure

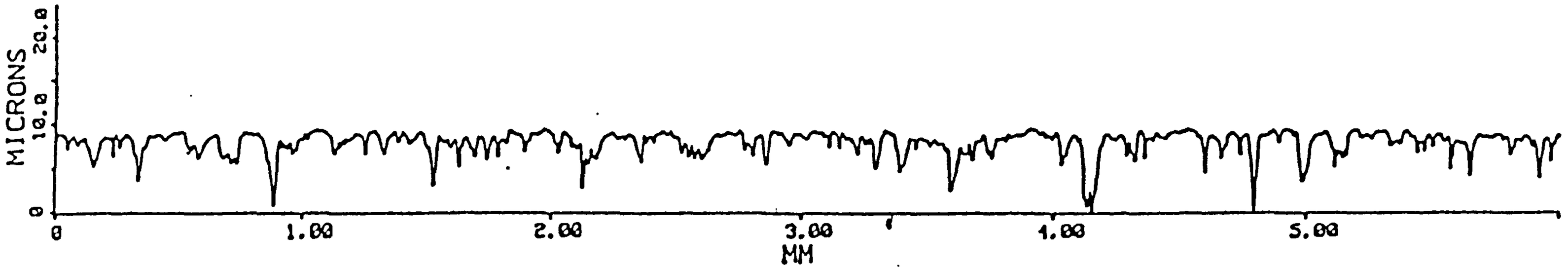

Figure 9b. Plateau Honed Cylinder Bore Finish of a Six Cylinder Petrol Engine.

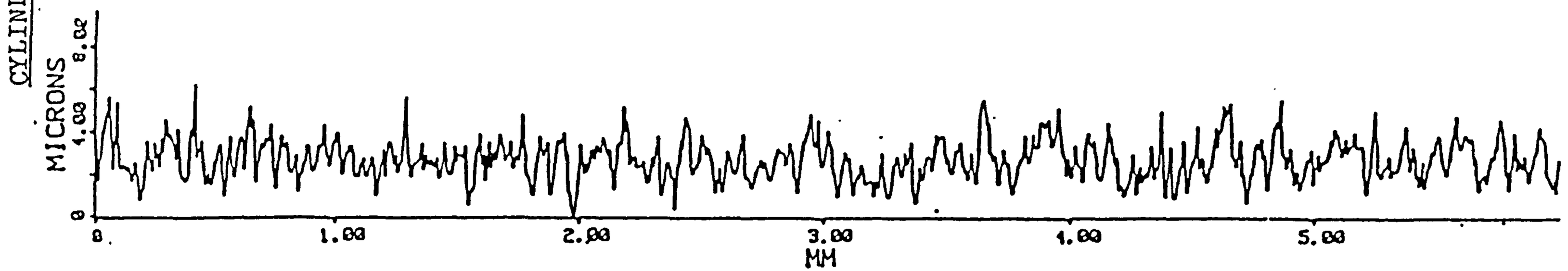

Figure 9c. Honed (Unworn) Surface Finish of a Diesel Engine Cylinder Liner.

COMPUTER MODELLING OF CHANGES IN SURFACE TOPOGRAPHY PRODUCED BY ELECTROCHEMICAL PROCESSES

Buttery, T.C. and Hemmaty, G.H.
School of Mechanical and Production Engineering,
Leicester Polytechnic, P.O. Box 143, Leicester. LE1 9BH

ABSTRACT

Electrochemical processes such as electroplating and electropolishing change the surface topography of the workpiece by either the addition or removal of material at different rates at the peaks to the valleys, giving a progressive improvement in surface finish. This paper details a number of computer models which have been developed to give a graphic simulation of the changes in surface topography associated with electrochemical processes. These models have been tested against experimental data and that reported in the literature. In true levelling processes, it is suggested that variations in plating/polishing performance can be explained in terms of a plating/polishing coefficient (m).

INTRODUCTION

In many metal finishing processes, particularly electroplating, the initial surface preparation involves mechanical polishing using progressively fine abrasives. The amount of polishing can be reduced, with consequent economic advantages, by utilising the fact that during electroplating there is frequently an improvement in the surface finish of the workpiece. Meyer [1+2] was the first to report on this phenomenon which is called levelling. It is also possible to reduce the amount of mechanical polishing, in certain circumstances, by using electropolishing.

Recently reported work [3] has shown that the effectiveness of the levelling process is a function of workpiece topography as well as plating conditions.

This paper reports on the development of computer graphic simulations of levelling processes using both new and established models of geometric and true levelling.

Levelling Mechanisms and Assessment

When a coating is applied to a surface, by electroplating or other means, it may fill in the valleys preferentially, giving a progressive improvement in surface finish (Ra). The effect is called levelling and can arise in two ways.

1) Geometric levelling: when a uniform layer is applied to the whole surface, valleys are gradually filled in as plating proceeds due to purely geometric effects. Groove angle remains constant throughout the process and levelling is directly proportional to plating thickness (Fig. 1a).

2) True levelling: valleys are filled in preferentially, but at a more rapid rate than with simple geometric levelling. Groove angle declines at a reducing rate as plating proceeds and the rate of levelling also declines wth plating thickness (Fig. 1b).

True levelling is generally more effective than geometric levelling and it has been suggested that it consists of geometric levelling with an additional factor.[4]

Several workers[4,5,6&7] have reported on the levelling of ideal profiles (gramophone record grooves, wire and idealised scratches) subject to electroplating. After plating the profiles were either sectioned and micropolished or, alternatively, Talysurf traces were taken at stages throughout the process using relocation techniques; the percentage levelling was then calculated using expressions of the form:-

$$\text{percentage levelling} = \frac{H_o - H_1}{H_o} \times 100 \qquad [1]$$

or

$$\text{percentage levelling} = \frac{T_N - T_S}{H_o} \times 100 \qquad [2]$$

where H_o, H_1, T_N and T_S are defined in Figure 2.

These expressions give 100% levelling when:

$$H_1 = 0 \text{ (eqn [1]) or } T_N - T_S = H_0 \text{ (eqn [2])}$$

For real surfaces the most convenient method of assessing levelling is surface profilometry, the surface roughness (Ra) and other parameters being measured before and after plating. The percentage levelling is then given by the expression:

$$\text{percentage levelling} = \frac{\text{Ra original} - \text{Ra final}}{\text{Ra original}} \times 100 \qquad [3]$$

Alternatively it has been suggested [4] that the average slope (Δ_a) of the surface could give a more meaningful indication of levelling/smoothing. Percentage levelling being calculated as follows:

$$\text{percentage levelling (smoothing)} = \frac{\Delta_a \text{ original} - \Delta_a \text{ final}}{\Delta_a \text{ original}} \times 100 \qquad [4]$$

Obviously levelling is of considerable economic and technical value. In order to produce computer models of the changes in surface topography associated with levelling the two basic mechanisms will be dealt with separately.

GEOMETRIC LEVELLING

With geometric levelling; the whole surface is coated to a uniform thickness T_S (Fig. 3) at the bottom of the groove and at any point on the slope the vertical thickness through the plating T_X is given by:

$$T_X = \frac{T_S}{\cos \theta} \qquad [5]$$

Obviously with increasing values of θ (sharper scratches) T_X increases and levelling is more rapid. If θ is zero (surface flat) $T_X = T_S$.

At 100% levelling: $T_X = T_S + H_O$ [6]

combining [5] and [6] gives 100% levelling

$$T_S = \frac{H_O}{\left(\frac{1}{\cos\theta} - 1\right)} \quad [7]$$

Using equations [5] and [2] computer programs were developed to give graphic simulations of geometric levelling and the influence of average slope (Δ_a) and scratch depth on plating thickness at 100% levelling. Using equations [5] and [7] computer programs were developed to give graphic simulations of geometric levelling and predict the effect of groove angle and groove depth on levelling performance.

The computer graphics show (1) that for a given groove angle the deeper the groove the greater the thickness of plating to produce 100% levelling (Fig. 4a) and (2) for the same groove depth reducing groove angle (0) increases the thickness of plating to give 100% levelling (Fig. 4b). Figure 5 shows the same details presented in graphical form for a wide range of conditions. Since the grooves are symmetrical it has been assumed that the effective Ra of a groove is 0.25 H_O. It is important to realise that real surfaces have very low values of average slope Δ_a and to level such surfaces by geometric levelling will require unrealistic thicknesses of plating.

The ideal surface for geometric levelling should have a low value of Ra and a high average slope; for the examples shown in Figure 6 the surface with the sharper grooves will have the better levelling characteristics. Unfortunately, as a material is progressively polished on finer grades of emery paper, the Ra will fall making levelling easier, but this will be offset by the reduction in average slope (Δ_a) which makes levelling more difficult.

TRUE LEVELLING

Unlike geometric levelling, which can be defined mathematically, true levelling relies on experimental observations for model development. With true levelling, valleys are filled preferentially at a rate exceeding that for geometric levelling. Mathematical models have been developed to simulate true levelling but the underlying physical mechanisms associated with the process have not been explored.

If proportionally more material is added at the bottom of the groove and this mechanism is continued as each successive layer is applied the groove will fill preferentially.

For example the thickness at the bottom of the groove T_X could be given by the equation:

$$T_X = T_S \times m \quad [8]$$

where m is the plating or levelling coefficient.

Figure 6 shows examples of the same idealised groove levelled with different values of m. As m increases, the groove levels more rapidly. However the changes observed with this model show meshed deviations from practical results. The results of Elze (Fig. 8 and others) show that groove angle changes at a decelerating rate, not accelerating and the rate of levelling declines with plating thickness, whereas the model levels at a constant rate.

The second model which gives better agreement with practical observations assumes that:

1) Plating thickness is a function of groove depth (H).

2) m is a function of plating layer thickness, but is independent of groove angle and groove depth.

Computer simulations were based on an equation of the form:

$$T_{X_0} = T_S (1 + mH_0) \qquad [9]$$

where H_0 is the instantaneous groove depth and m is the plating/levelling coefficient.

$$T_{X_1} = T_S (1 + mH_1)$$

$$T_{X_2} = T_S (1 + mH_2)$$

$$T_{X_n} = T_S (1 + mH_{n-1}) \qquad [10]$$

$$\text{Total thickness} \quad T_X = T_{X_0} + T_{X_1} + T_{X_2} \cdots T_{X_n} \qquad [11]$$

When $H = 0$ surface is level $T_X = T_S$.

Using a combination of equations [10] and [11] enables graphic simulations of practically observed results by adjusting to value of m. The value of m is related to the thickness of the successive layers of plating, for example if the plating thickness is 5 um, the plating/levelling coefficient is written m_5. Different layer thicknesses will give different values of m, related by the following expression:

$$m_{10} = \frac{m_5 (H_0 + H_1)}{2H_0} \qquad [12]$$

where m_{10} = value of m for layers 10 um thick
m_5 = value of m for layers 5 um thick
H_o = original groove depth
H_1 = groove depth after the first layer has been applied

Figure 9 shows a computer simulation of the results reported by Elze[7]; the rate of levelling and the rate of decline in groove angle are in reasonable agreement with the practical results when using the appropriate value of m calculated from the first layer.in the expected results.

Finally, the computer model was developed to simulate the behaviour of a real surface under true levelling conditions. The surface was stored in the computer in digital form and each height adjusted as layers of equal thickness were added. Typical results are shown in Figure 10 for a range of values of m, the Ra and average slope of the surface change in the expected manner. The greater the value of m the more rapidly the surface levels. Electropolishing can be simulated in the same way, except material is removed more rapidly from the peaks than the valleys.

DISCUSSION AND CONCLUSIONS

Since the mechanism of geometric levelling can be precisely defined, computer modelling is relatively straightforward. The conclusions from such models are in close agreement with practical observations and show that geometric levelling is ineffective with real surfaces.

True levelling is a more complex process and both the computer simulations and reported data suggest that this form of levelling is mainly a function of groove depth. The initial rate of levelling is greater for deeper grooves but declines as the groove fills. An important factor in the theory for true levelling is the plating or levelling coefficient (m) which controls the rate of levelling. The better the levelling characteristics of a plating solution, the larger the value of m. A value of m can be found experimentally and then used to predict the subsequent behaviour as plating proceeds. When values of m determined in this way were used to predict plating behaviour, some deviation was observed as levelling approached 90-95%; the theory predicting the better surface. This may mean that m is not independent of groove depth and groove angle. It should be remembered that geometric levelling is very dependent on groove angle (θ).

It is concluded that geometric and true levelling can be successfully modelled using the following expressions:

Geometric levelling:

$$T_X = \frac{T_S}{\cos \theta} \qquad [13]$$

True levelling:

$$T_X = T_S \ (1 + mH) \qquad [14]$$

T_S = plating thickness on a smooth surface.
T_X = plating thickness at point X when a layer T_S is applied.
H = depth of groove at point X .
m = plating/levelling coefficient for plating thick T_S .

To further refine the theory will require considerably more experimental Data. The methods reported in this paper are equally applicable to any coating process and also to electropolishing.

REFERENCES:

1. W.R. Meyer (1935) Proc.Am. Electroplaters Society, 23,116,135.
2. W.R. Meyer (1936) Proc.Am. Electroplaters Society, 24,135
3. T.C. Buttery & M.S. Hamed (1979). "Study of Geometric & True Levelling in Electroplating using Stylus Methods", Wear 57, p207-215.
4. T.C. Buttery, W.H. Mackie, N.R.I. Salib & M.S. Hamed. "The Optimisation of Component Surfaces for Electroplating Using Coated Abrasives", 2nd Joint Int.Conf. on Prod.Eng., Leicester 1983.
5. D.G. Foulke & O. Kardos. "Current Distribution in Microprofiles", Proc.Am. Electroplaters Society, 43 (1956) 172 & 181.
6. S.A. Watson & J. Edwards. "An Investigation of the Mechanism of Levelling in Electrodeposition". Trans.Inst. Metal Finishing, 34 (1957) 167.
7. J. Elze. "Geometrie der Mikrostrewing und Einebnung durch Electrolytisch abgeschiedene Metallniedershlage". Metall (1961), 15, 542.

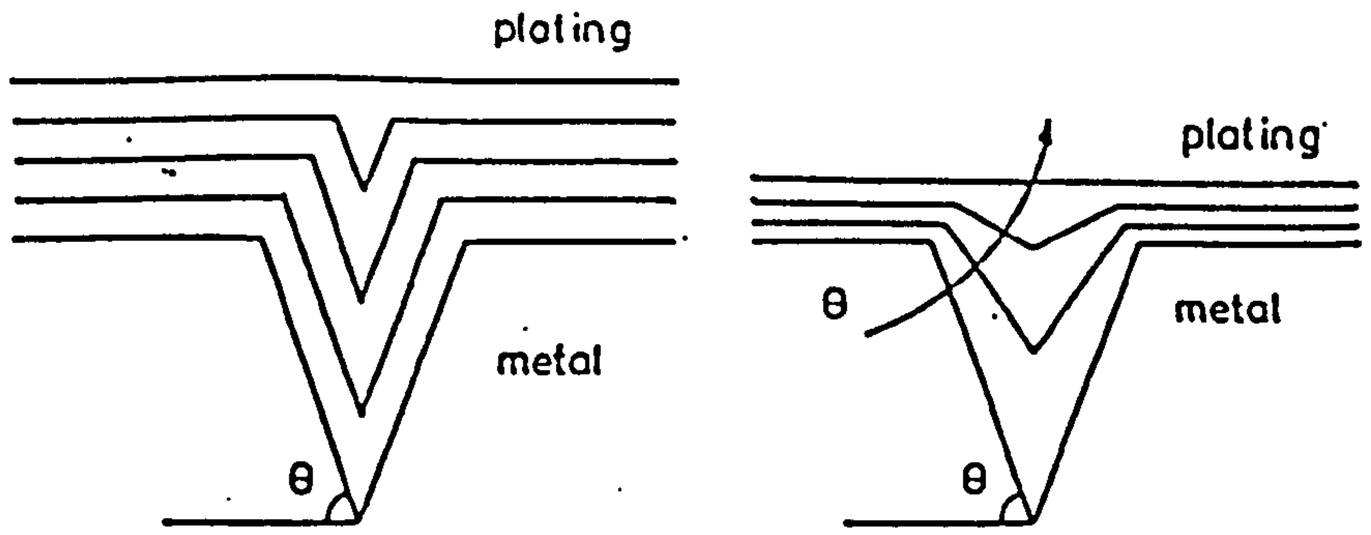

fig 1. (a) geometric levelling (b) true levelling.

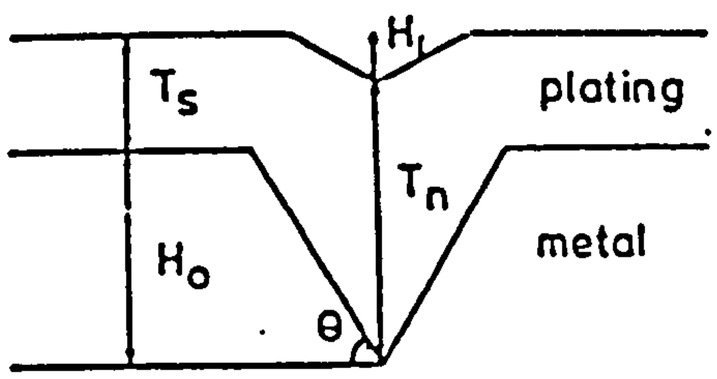

fig 2. Groove detail for levelling calculation equation (2)

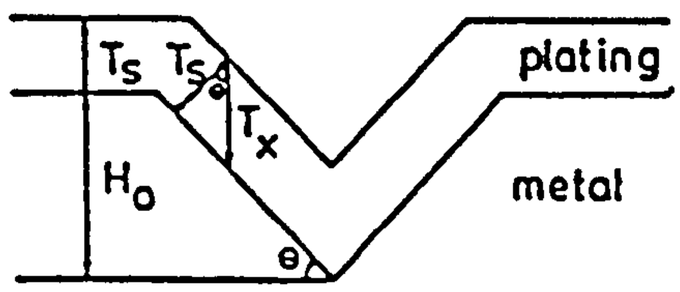

fig 3. Groove detail for calculation of T_x equation (5)

fig 4.

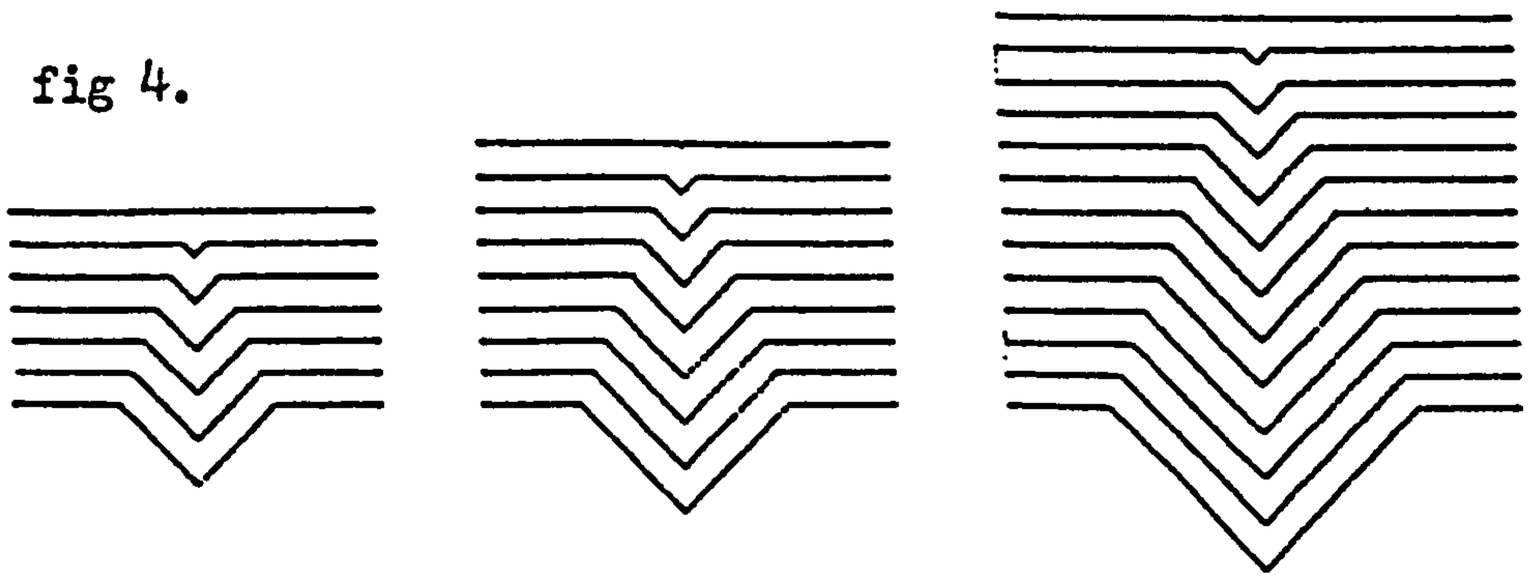

(a) Effect of groove depth on plating thickness for 100% levelling for a 45^{o} groove

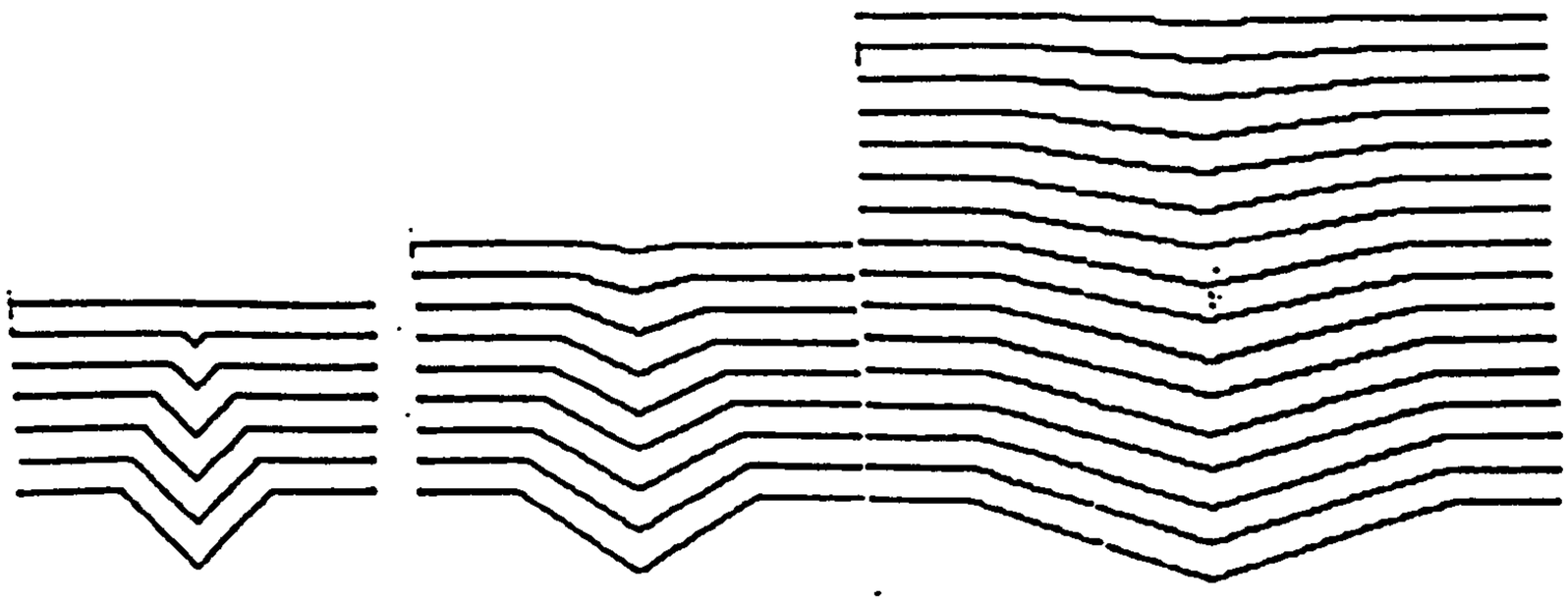

(b) Effect of groove angle on levelling performance.

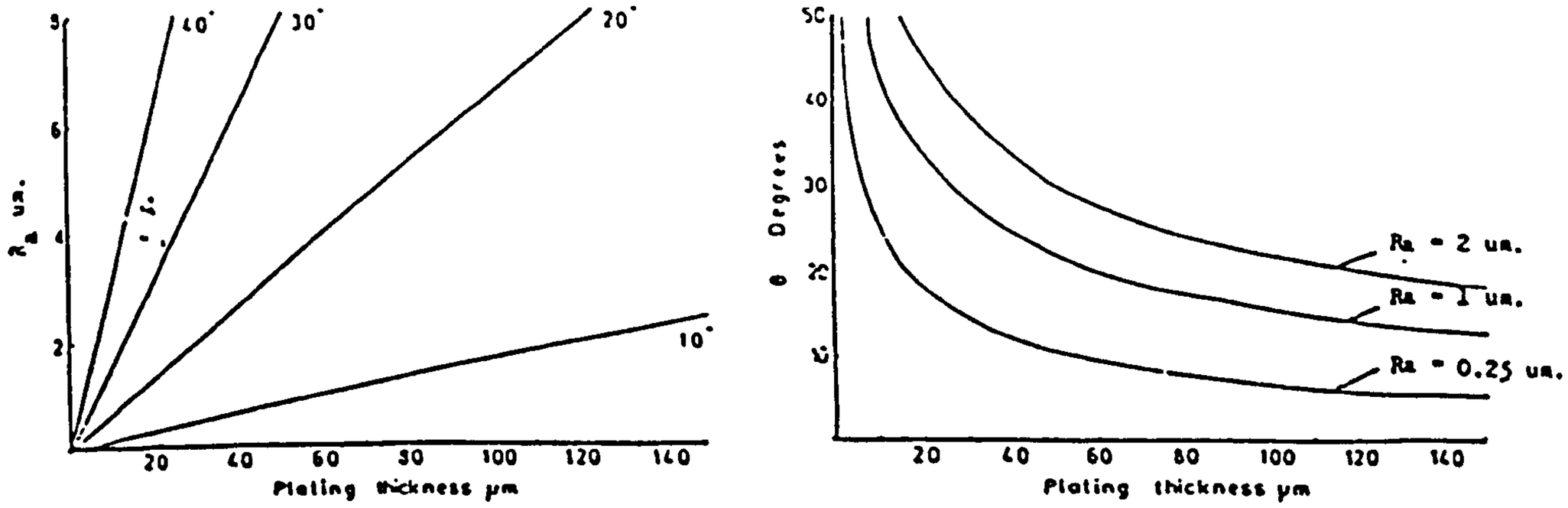

(a) (b)

fig 5. Plating thickness to give 100% levelling for (a) different values of surface roughness and (b) different values of groove slope.

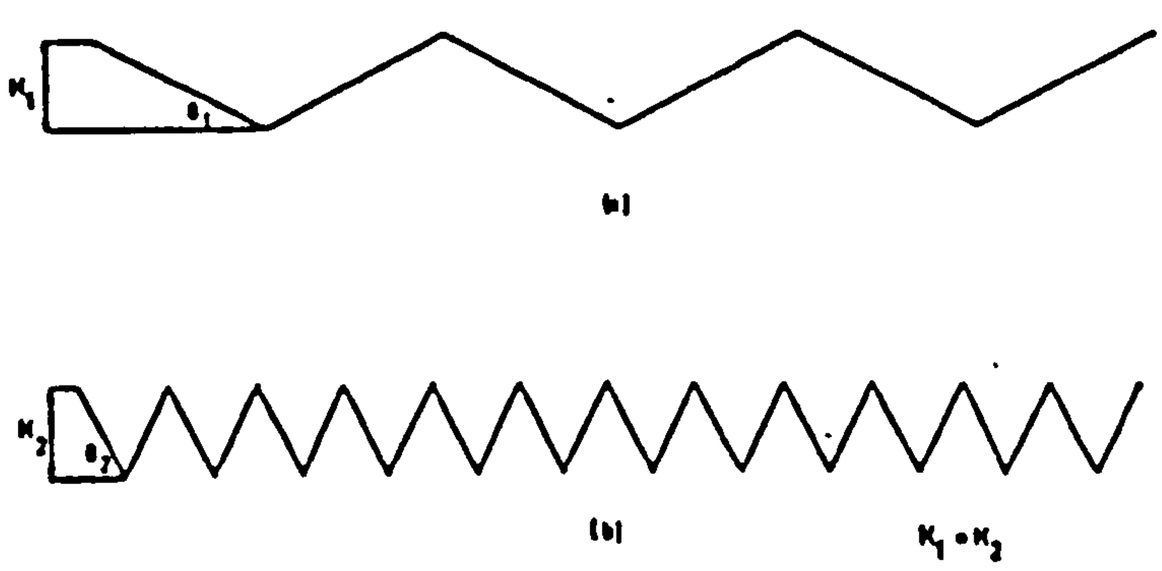

fig 6. Two surfaces having the same value of surface roughness but different surface slopes.

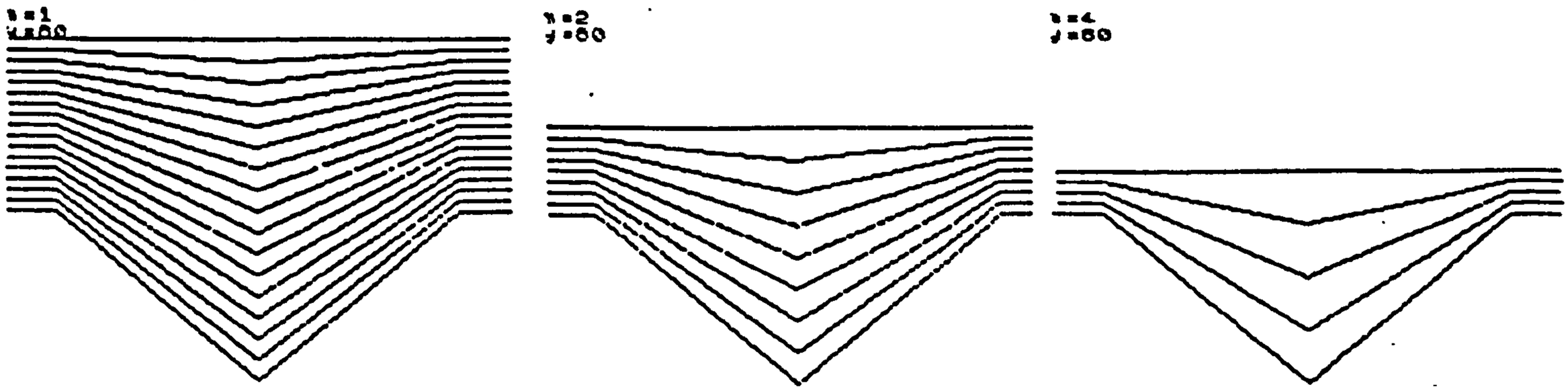

Fig 7. 100% levelling for a range of values of plating coefficient (m) equation (8).

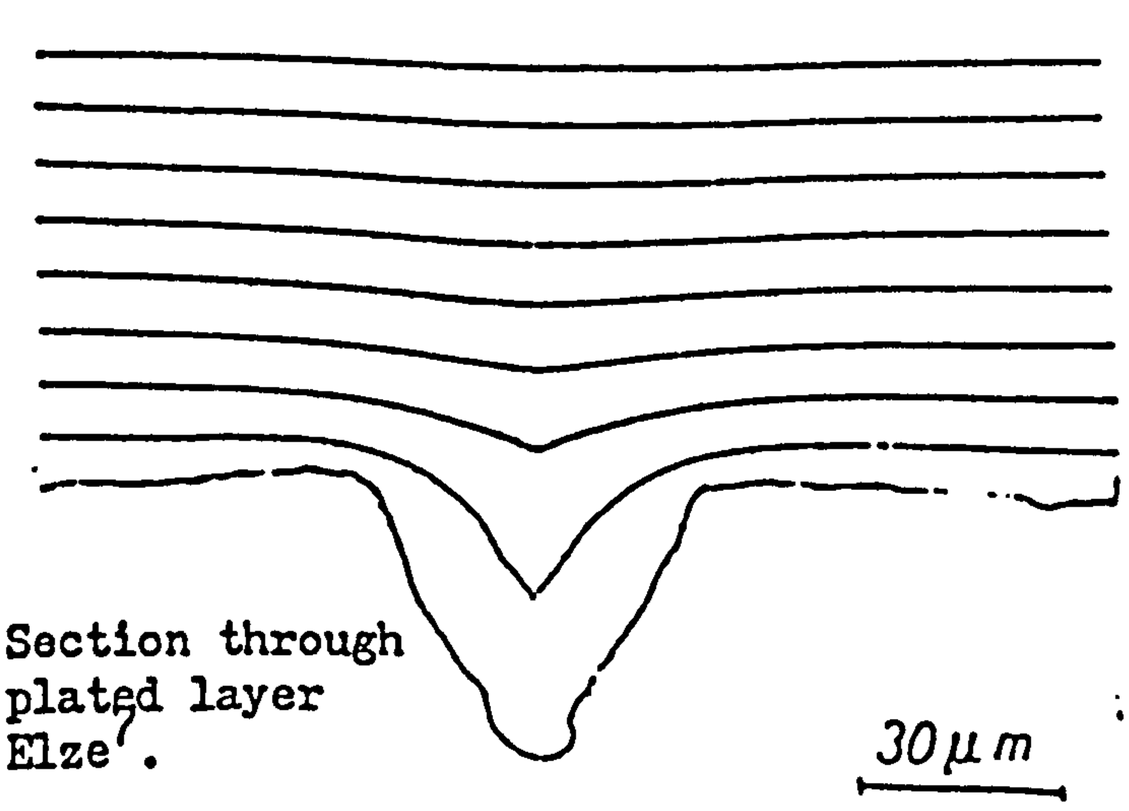

fig 8. Section through plated layer Elze'.

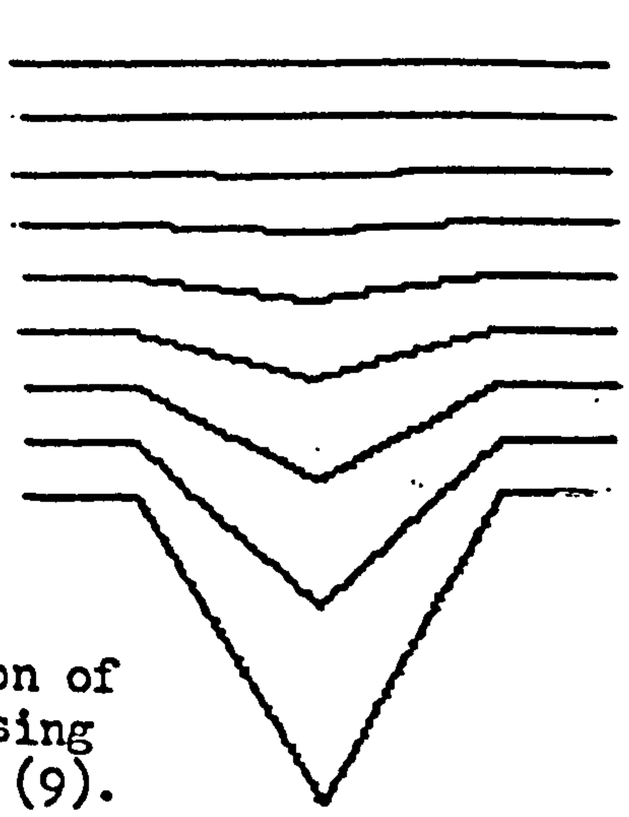

fig 9. Simulation of fig 8. using equation (9).

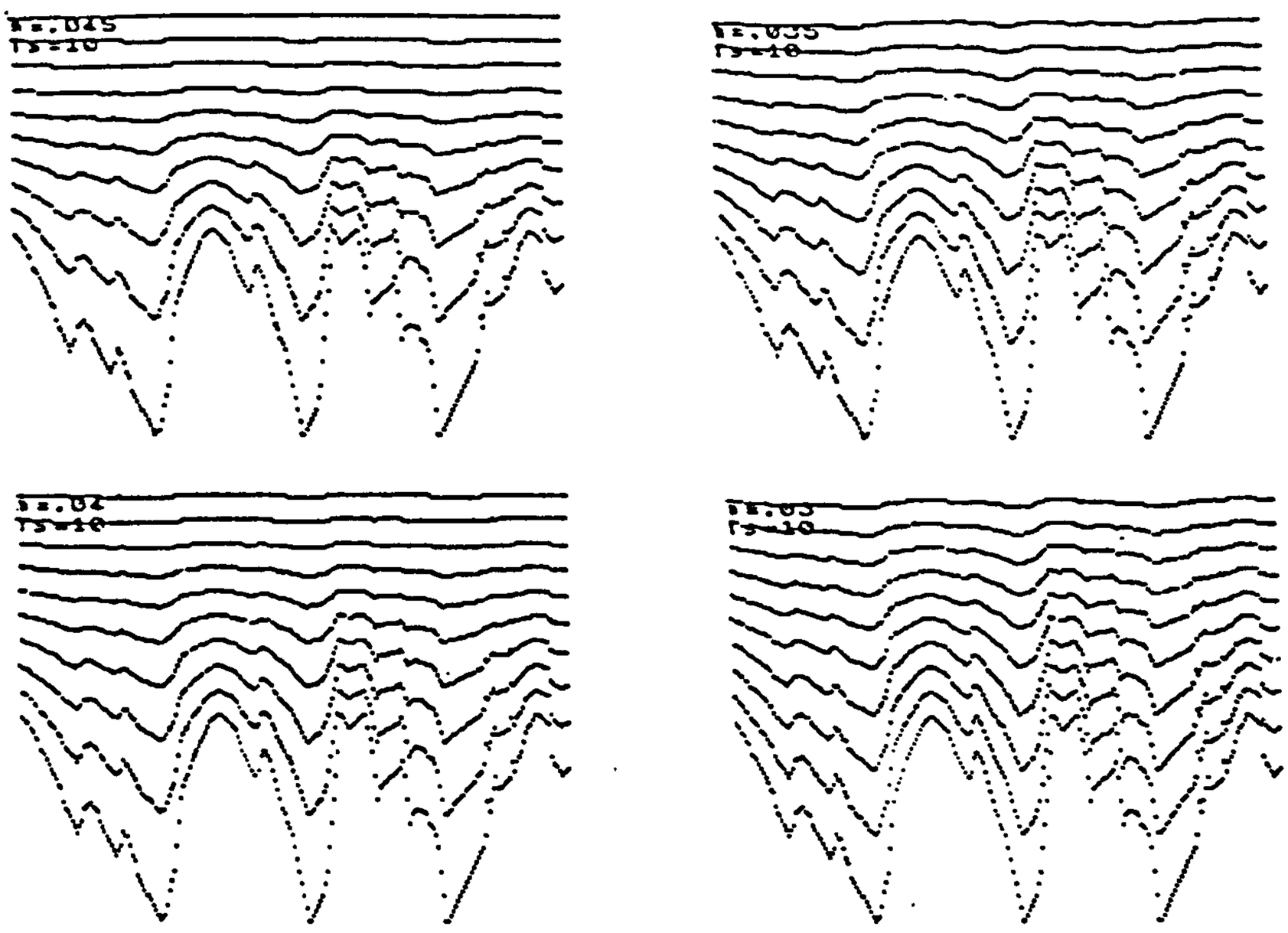

(a)

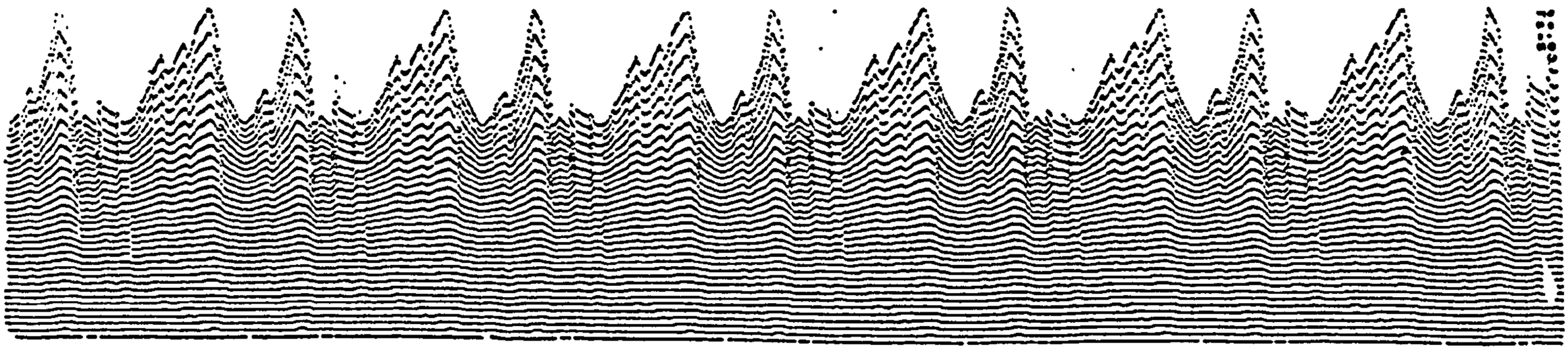

(b)

fig 10. Effect of variations in plating/levelling coefficient on the levelling of a "real " surface is shown in (a) whilst electropolishing is simulated in (b).